Thermal Behaviour Model Identification for Three Different Office Buildings

A thesis submitted for the degree of Doctor of Philosophy

by

Giorgio Mustafaraj

Mechanical Engineering

School of Engineering and Design

Brunel University

July 2008

Table of Contents

Abstract

The thermal behaviour was investigated of three offices positioned in three buildings built in different periods, one academic institute built in 1920 and two modern commercial buildings in London. The buildings chosen for this study are the Rockefeller Building, which is part of University College London (UCL), Portman House in Oxford Street and the Visa Building in Paddington. Due to the lack of specific information related to the structure of the buildings such as windows, doors, building dimensions and other information that would allow the use of physical models, in this project black-box linear and non-linear mathematical models were used. Data relating to room temperature, hot and chilled water temperature, air flow and temperature from air handling units and outside temperature were collected for one year, from the actual building management systems (BMSs) installed in these buildings. The main assumption of the model development in the three buildings was that although occupancy, computers, printers etc cause an additional internal heat gain, their impact is in part indirectly included in the model.

The primary objective of the analysis was to identify the inputs (independent variables) that gave good models for the prediction of room temperature for a certain period. Consequently, the process of input selection and period of validity in obtaining models that give good thermal prediction (within the same period) were the key points in season subdivision. The first part of the analysis applied the following linear parametric mathematical models to the three office buildings selected: Box Jenkins (BJ), autoregressive moving average with exogenous input (ARMAX) and output error (OE) structure. The project then deals with non-linear mathematical models. The same inputs selected and assumptions made with linear analysis were used to build, in turn, models with feedforward backpropagation (FFBP), non-linear autoregressive mathematical models with parallel arrangement (NARX) and series-parallel arrangement (NARXSP).

The research presented in this project is related to developing models for three real offices positioned in three different buildings whereas previous researchers have applied these models mainly to experimental rooms and HVAC plants, with the purpose of fault detection and diagnostics.

Furthermore, in the past, research on thermal model development has been related to one office or HVAC plant, and for a limited period of time (a few weeks or months). In contrast, this study undertakes an overall analysis of thermal model development for three offices and for a period of one year, where the process of input selection is given priority to obtain good models. Thus, previous studies have not utilized these two types of models for such a long period of data collection nor related them to three different buildings.

Finally, model development and then validation were pursued utilizing the same week, different weeks and different days (where the first part of the data in each case was used for model estimation and the following part for model validation). This was done within the period that the models gave good results for the prediction of room temperature. The best mathematical models (linear and non-linear) that predict the room temperature, in terms of the inputs selected, has been determined for each season. The procedures for how to choose the best models are based on the following techniques: final prediction error (FPE for linear models), mean squared error (mse for non-linear models), and model fits and errors between measurements and simulated model output. Overall, the results related for the prediction of room temperature with non-linear models, are better than those obtained with linear models, as a result of comparison between models' errors, FPE and mse obtained with linear and non-linear models.

Acknowledgements

I cannot fully express my gratitude to Dr. Jie Chen, for his unfailing patience in being ready at any time to give me help and guidance throughout his time as my supervisor.

I also wish to extend my gratitude to my previous supervisor, Dr. Gordon Lowry, for giving me support and advice during the first year I spent on this project.

Special thanks are due to Mr. James Thackrah, Mr. Ian Preston and Mr. Jim Huggins of TAC Satchwell Company who helped and supported me throughout the years 2005 and 2006 during the period of data collection.

I am very grateful for the financial support given to me by the Department of Mechanical Engineering, Brunel University.

I would like to acknowledge all other persons who have supported me throughout the accomplishment of this project; to name just a few: Dr. Duc Nhim Ha, Mr. Khariul Kamaludin, Dr. Yusuke Iida, Dr. Vincent Anjorin and Mrs. Layla Buzinin.

Finally, I would especially like to thank my wife, Evelise; my parents; my brother, Altin; my sister, Angelina; and my aunt, Ilira, for their constant support and encouragement.

List of Ligures

List of Tables

Nomenclature

$A(q)$	$A(q) = I_{ny} + a_1 q^{-1} + .. + a_{na} q^{-na}$ matrix that contain the coefficient $a_{na}(q)$
A_{NN}	matrix that contain the coefficient $a(i, j)$ (NARX network)
$A(q)^{-1}$	inverse of the matrix $A(q)$
$a(i,j)$	coefficient of the nonlinear exogenous terms (NARX network)
$b(i,j)$	coefficient of the nonlinear autoregressive terms (NARX network)
$c(i,j)$	coefficient of the non linear cross term (NARX network)
$\arg\min f(x)$	value of x that minimizes $f(x)$
$B(q)$	$B(q) = b_0 + b_1 q^{-1} + b_2 q^{-2} + ... + b_{nb} q^{-nb}$ matrix that contain the coefficient $b_{nb}(q)$
B_{NN}	matrix that contain the coefficient $b(i, j)$ (NARX network)
$C(q)$	$C(q) = 1 + c_1 q^{-1} + c_2 q^{-2} + ... + c_{nc} q^{-nc}$ matrix that contain the coefficient $c_{nc}(q)$
C_{NN}	matrix that contain the coefficient $c(i, j)$ (NARX network)
$D(q)$	$D(q) = 1 + d_1 q^{-1} + ... + d_{nd} q^{-nd}$ matrix that contain the coefficient $d_{nd}(q)$
$Cov\hat{\theta}_N$	covariace matrix of the random vector $\hat{\theta}_N$
d	is the total number of estimated parameters
D_M	set of values over which θ in a model structure
$e(t)$	disturbance signals or noise linear models
e	is the linear combiner input in neural network
$e(n)$	is the error NARX network
$e_o(t)$	"true" noise acting on a given system linear models

$E\psi(t,\theta_o)$	mathematical expectation of the the random vector $\psi(t,\theta_o)$
$\overline{E}\psi(t,\theta_o)$	is equal to: $\lim_{N\to\infty}\frac{1}{N}\sum_{t=1}^{N}E\psi(t,\theta_o)$
$F(q)$	$F(q)=1+f_1q^{-1}+..+f_{nf}q^{-nf}$ matrix that contain the coefficient $f_{nf}(q)$
f_e	probability density function of the random variable e
$f_k(e)$	transfer function (artificial neural network)
FPE	$FPE=\frac{1+\frac{d}{N}}{1-\frac{d}{N}}V$ Final Prediction Error
$G(q)$	transfer function from u to y
$G(q,\theta)$	transfer function in a model structure, corresponding to the parameter value (see section 3.6)
M	model structure (a mapping from a parameter space to a set of models)
$M^*(\theta)$	set of models (usually generated as the range of a model structure)
$M(\theta)$	particular model corresponding to the parameter value θ
mean(y)	correspond to the mean value of the measured output
mse	mean square error
N	is the length of the data record
P, Q	represents the model order of the exogenous (linear and nonlinear) and the autoregressive terms, respectively
norm $(y_h - y)$	is the Euclidean length of a vector $(y_h - y)$
q	Forward shift operator ($q\ u(t) = u\ (t+1)$)
q^{-1}	backward shift operator ($q^{-1}u(t) = u\ (t-1)$)
$L(q)$	prefilter for the prediction errors
$l(\cdot)$	is a scalar-valued (typically positive) function
R^N	Euclidian N-dimensional space

t	sampling interval of time units
$t(p)$	target at time $t = p$ (neural network)
$u(t)$	input signals
V	dimensionless loss function
$V_N(\theta, Z^N)$	criterion function to be minimized (see equation 3.24)
$v(t)$	disturbance variable at time t
$v_o(t)$	"true" value of disturbance variable at time t
$u(n)$	is the input signal neural network
x_j	are input signals for neural network
$y(t)$	output signals
y_h	the output that results when the model is simulated with the input u
$y_k(p)$	simulated model output at time $t = p$ (neural network)
y	corresponding measured output
y^N	$y^N = (y(1), y(2), ..., y(N))$ random varible that takes values in R^N
$\hat{y}(t/\theta)$	predicted output at time t using a model $M(\theta)$
y_k	outputs for neural network
z	desired output value (the target)
θ	$\theta = [b_1 b_2 .... b_{nb} c_1 c_2 ..... c_{nc} d_1 d_2 ..... d_{nd} f_1 f_2 .... f_{nf}]^T$, vector used to parameterize models (see section 3.6)
$\hat{\theta}_N$	estimate of θ based on Z^N
θ_o	"true" value of θ
$\hat{\theta}_N^{LS}$	estimate of $\hat{\theta}_N$ with least square criterion
$\hat{\theta}_{ML}$	estimate of $\hat{\theta}(y^N)$ with maximum likelihood method
θ_k	is the threshold or bias for neural network

$H(q,\theta)$	disturbance model (see section 3.6)
$\varepsilon(t,\vartheta)$	prediction error
$\varepsilon_f(t,\theta)$	$\varepsilon_f(t,\theta) = L(q)\varepsilon(t,\theta)$ the filtered error $\varepsilon(t,\vartheta)$
Z^N	$Z^N = [y(1), u(1), y(2), u(2), ..., y(n), u(n)]$, collected batch of data
$\varphi(t)$	regression vector at time t (for the ARX structure $\varphi(t)$ is $\varphi(t) = [-y(t-1) - y(t-2)... - y(t-n_a)u(t-1)...u(t-n_b)]^T$)
δ_{kj}	Kronecker's delta: zero unless $k = j$
δ	error signal backpropagation algorithm
λ	the variance of the signal
λ_o	the variance of the "true" disturbance $e_o(t)$
$\psi(t,\theta_o)$	$\psi(t,\theta_o) = \frac{d}{d\theta}\hat{y}(t \setminus \theta)\|_{\theta=\theta_o}$ is the gradient of $\hat{y}(t/\theta)$ with respect to θ
$\psi^T(t,\theta_o)$	traspose of the $\psi(t,\theta_o)$
$w_{k1}.....,w_{kp}$	are synaptic weights of the neuron k
$w_{(xm)n}$	weights of connections between network input x_m and neuron n
η	coefficient affects the network teaching speed (backpropagation algorithm)

CHAPTER 1 Introduction

1.1 Background

A Building Management System (BMS) is a "stand-alone" computer system that can calculate the pre-set requirements of a building and control the connected plant to meet those needs. Its inputs, such as temperature sensors, and outputs, like on/off signals, are connected to outstations around the building. Programs within these outstations use this information to decide the necessary level of applied control. The outstations are linked together and information can be passed from one to another. In addition, a modem is connected to the system to allow remote access.

Conventionally, in almost all BMSs, a cascaded, multi-loop proportional-integral-differential (PID) control structure is used to control the internal air temperature in the heating ventilating and air conditioning (HVAC) system of the building. The underlying principle is the closed loop feedback control of the setting and operating schedules of the HVAC system. In fact, PID control is considered a successful implementation in HVAC control since this conventional approach is employed by most practical systems available nowadays. Albert et al. (1995) have shown that a PID controller is favourable only on the assumption that the system model parameters do not change much, but, in practice, the system parameters do change over time. Consequently, the PID controller response becomes poor and energy consumption increases unless the parameters are re-commissioned from time to time.

Increased energy cost and strict environmental standards mean that more intelligent control over HVAC systems is required based on self-adaptive and predictive methods. To enable intelligence control, a model is needed and the system model is dependent not only on internal changes but also external conditions.

A model is the way we describe the salient features of the system under study. Modelling requires mathematical description to be created, for example, of the physical and chemical phenomena that appear in reality.

The essence of modelling is to select only those characteristics, from among the many available that are necessary and sufficient to describe the process accurately enough to suit the objective of the modeller (inputs and outputs). An important decision in deriving models is the selection of the system's boundaries. These determine which parts of reality, that is, the process, will be taken into account (Bosch and van den Klauw, 1994).

Much effort has been devoted to model buildings' thermal response (Penman, 1990; Jian et al., 2004; Gaudaa et al., 2002; Gilles et al., 2002; Andersen et al., 2000; Madsen and Holst, 1993; Dewson et al., 1993). Some very detailed computer simulations have emerged to describe the dynamics of the temperature and heat supply in buildings. Yet, relatively low-order linear systems can capture the essential elements of observed behaviour. Simplified or reduced order thermal models are, therefore, of interest.

There are a number of techniques available for researchers to model the thermal response of a building. One such technique is physical modelling in which the properties of the system are broken down into subsystems whose behaviours are known. For technical systems this means that the laws of nature that describe the sub-systems are used in general. What happens when the capacitor and resistor are connected follows Ohm's law and the relationship between charge and current for a capacitor. Most researchers (Goudaa et al., 2002; Gilles et al., 2002) have used this analogy to model buildings' thermal response.

Another technique is identification in which the observations of the system are used to fit the model's properties to those of the system. For technical systems the laws of nature themselves are mathematical models, which are based on observations of small systems. This is sound, since models of systems ultimately have to be based on experience.

A building is a collection of different objects, such as walls, windows, internal fabrics and occupants. Therefore, a building is a system in which variables of different kinds interact and produce observable signals. The observable signals of interest to us are the air temperature inside the building, CO_2 and humidity.

Kontoleon et al. (2002) have shown the influence of the glazed openings percentage and type of glazing on the maximum and minimum indoor temperatures, during and after solar hours. Andresen et al. (2000) also consider that the most important heat transfer, which influences the room's air temperature, is the heat input from solar radiation. Therefore, based on the above-mentioned literature, it is clear that the solar heat gained through glazed windows directly contributes to the variation of internal air temperature. An accurate modelling approach for predicting the behaviour of the internal air temperature, therefore, requires consideration of parameters that influence its behaviour.

1.2 Objectives of the Research

In this project, the thermal behaviour of three different buildings built in different periods, one academic institute built in 1920 and two modern commercial buildings in London are investigated. The buildings chosen for this study are the Rockefeller Building that is part of University College London (UCL), Portman House in Oxford Street and the Visa Building in Paddington. Black-box linear (parametric mathematical models) and non-linear mathematical models (neural networks) are used to obtain the models from the data collected.

The main objectives of this research are:

1) To identify the most important variables (inputs and outputs) that can be used in the mathematical models.

2) To apply different modelling techniques to the three selected buildings and to identify the most efficient models for each building.

3) To arrange the data elaborately so that the model can be built without additional sensors or other units.

4) Finally, if changes are detected inside the buildings the models should be sufficiently flexible to predict their new thermal behaviour. As a result they will be useful and reliable in the long term.

1.3 Contributions

- The modelling of three real offices

  The research presented in this project is related to developing models of three real offices positioned in three different buildings in London. This is achieved, by applying black box parametric mathematical models and neural networks to the data collected. Previous researchers have applied these models mainly to experimental rooms (many sensors are installed) and HVAC plants, with the purpose of fault detection and diagnostics.

- Comparison between the models for the three buildings

  In the past, research on thermal model development was related to one office or HVAC plant. In contrast, this study undertakes an overall analysis of thermal model development for three offices positioned in three different buildings in London. The thermal behaviour of the three buildings, one academic institute built in 1920 and two modern commercial buildings are very different, consequently, comparisons are made between them.

- Modelling with an extended period of data (one year)

  Previous research has been related to the study of thermal behaviour for a limited period of time, from a few weeks to a few months. The relatively short periods of data collection and widespread use of experimental rooms resulted in thermal models being developed for the same inputs throughout the analyses. In contrast, in this work, the thermal behaviour of real offices is examined for a period of one year, and the process of input selection is given priority to obtain good models.

- Modelling with black-box linear parametric and non-linear models

  This research is also unique in its model development for the three offices, is that it applies two different mathematical models, parametric mathematical models (linear-models) and neural networks (non-linear models). A comparison of these models is also provided. Conversely, previous studies have not utilized of these two types of models for such a long period of data collection nor related them to three different buildings.

1.4 Achievements

The achievements of this project were:

- It identified the most important inputs affecting thermal behaviour, throughout one year for three different offices based in three different buildings in London. It was found that some inputs gave good models for a limited period of time (several weeks). Consequently, the process of input selection and the period of validity for the models obtained that gave good thermal prediction (within the same period) were the reasons for the subdivision of each season into three parts: beginning, middle and end.

- It developed thermal models utilizing black box linear and non-linear mathematical models based on inputs selected throughout the seasons for the different offices. For parametric linear models the general choices were ARX, OE, ARMAX and BJ, while for non-linear models the FFBP, NARXSP and NARX were the general choices.

- It compared linear parametric mathematical models (through the final prediction error criteria, model errors and fits between measurements and simulated model output) developed throughout the seasons within the selected office for each building. From the analysis of the results obtained with linear models, the BJ models (bj [1 1 1 1 2], bj [1 1 1 1 3], bj [1 1 1 1 4] and bj [1 1 1 1 5]), OE models (oe [1 1 2], oe [1 1 3], oe [1 1 4] and oe [1 1 5]) and ARMAX models (amx [2 2 2 1], amx [2 2 2 2], amx [2 2 2 3], amx [2 2 2 4] and amx [2 2 2 5]) gave good results for periods, ranging from four to twelve weeks.

- It compared non-linear models (through the mean squared error criteria and model errors between measurements and simulated model output) developed throughout the seasons within the selected office for each building. NARX, FFBP and NARXSP networks were applied to the three buildings for one year. NARX, FFBP and NARXSP networks, with the same properties (section 7.3), gave good results for Portman House and the Visa building throughout the year. However, in the Rockefeller building due to the lack of data collected by the BMS, only the NARXSP network produced good results. The NARXSP network had better fits than the FFBP and NARX networks throughout the entire analysis.

- Finally, it compared the linear and non-linear results obtained. The advantages of applying neural networks instead of linear models were:
  - The same networks with the same properties could be used throughout the entire year and for the three buildings, with good results obtained for predicting room temperature.
  - There was no limit on the number of outputs that could be used for model development with non-linear networks.
  - With neural networks, the amount of time required for model development and validation throughout the year was less than that for linear models.
  - The results obtained with non-linear models are better than those obtained with linear models.

1.5 Thesis Outline

This thesis is organized as follows:

Chapter 2 presents the literature review for thermal modelling of buildings and HVAC plants. Black-box, white-box and grey box methods are presented with their advantages and disadvantages.

Chapter 3 provides a detailed description of linear parametric mathematical models and an overview of the methodology used to obtain the results. Furthermore, for parameters estimation, the prediction error estimation method is presented.

Chapters 4, 5 and 6 discuss the results obtained using the linear parametric models for the Visa Building, Portman House and Rockefeller building respectively. A discussion and comparison of the results are also included for one year.

Chapter 7 provides a description of the neural network method used in this study and its application to the three buildings. A comparison of results with the linear models is also undertaken.

Finally, chapter 8 presents the conclusions of the study along with recommendations.

CHAPTER 2 Literature Survey

It is generally accepted that the performance of heating, ventilating, and air-*conditioning (HVAC) systems often falls short of expectation. Thus, modelling the* thermal behaviour of buildings and *plants is very important, because models can be* used for control purposes (faults detection and diagnostics). In this chapter is given an overview of the main techniques used for building the thermal behaviour of buildings and HVAC plants.

The first part of this chapter deals with process history based methods which includes black box models as linear and nonlinear mathematical models. The black box models reflect the fact that no knowledge of the process is used, in which the parameters must all be estimated from measurements of inputs and outputs using an estimating procedure. Finally, fuzzy logic design methodology is presented which allows modelling complex systems using a higher level of abstraction originating from our knowledge and experience.

The second part deals with white-box, grey-box and statistical based methods. White-box assumes complete knowledge of the process (derivation of models from physical knowledge). The grey box modelling derives from the physical models but also use black-box modelling for obtaining the values of some parameters.

The main techniques for modelling the thermal behaviour are:

1. **Black- box based methods**

- Linear Parametric Mathematical Models
- Artificial Neural Networks
- Fuzzy Logic

2. **Other methods**

- White Box Physical-Based Methods
- Grey Box Methods
- Statistical Based Methods

2.1 Black-Box Based Models

When a model's features or parameters have no physical significance, it is referred to as a black box model. Black box models often require less time and effort to develop and apply them compared to grey box approaches. However, the prediction accuracy is generally lower than for grey box models, and they cannot be used to extrapolate beyond the data range for which they were developed (Srinivas and Brambley, 2005).

In contrast to the model-based approaches where a priori knowledge (either quantitative or qualitative) about the process is needed, in process black-box based methods, only the availability of a large amount of historical process data is required. There are different ways in which this data can be transformed and presented as a priori knowledge to a diagnostic system. This is known as feature extraction and it can be either qualitative or quantitative in nature. Two of the major methods that extract qualitative history information are the expert systems and trend modelling methods. Methods that extract quantitative information can be broadly divided into non-statistical and statistical methods. Neural networks are an important class of non-statistical classifiers. Principal component analysis (PCA)/ least squares (LS) and statistical pattern classifiers form a major component of statistical feature extraction methods (Venkatasubramanian et al., 2003c).

In a black-box base (data-driven) model, both inputs and outputs are known and measured. The main objective of a data-driven model is to mathematically relate measured inputs to measured outputs. The input/output data can be transformed and used as a priori knowledge a number of ways in a diagnostic system. This process of transformation is also known as feature extraction or parameter extraction (Srinivas and Brambley, 2005).

The methods based on process history have several advantages and disadvantages are (Srinivas and Brambley, 2005 and Harunori et al., 2001).

Advantages of process history-based models

- These methods are well suited to problems for which theoretical models of behaviour are poorly developed or inadequate to explain observed performance.

- They are suited to situations where training data are plentiful or inexpensive to create or collect.
- Black box models are easy to develop and do not require an understanding of the physics of the system being modelled.
- Computational requirements vary, but they are generally manageable.
- There is a wealth of documented information available on the underlying mathematical methods.

Disadvantages of process history-based models

- Most models cannot be used to extrapolate beyond the range of the training data.
- A large amount of training data is needed, representing both normal and "faulty" operations.
- The models are specific to the system for which they are trained and can rarely be used for other systems of the same class.

2.1.1 Overview of Modelling with Linear Parametric Mathematical Models

The System Identification Toolbox contains different linear parametric mathematical models, and some of these have been used by many researchers. No knowledge of the systems inside structure is considered in these models; namely, the model is categorized as a black box type (Liddament, 1999). The purpose of system identification techniques is to mathematically describe the behaviour between the inputs and outputs of a process. There are numerous techniques available to describe a dynamic process with a mathematical model (Peitsman and Bakker, 1996).

Choosing an appropriate model type and incorporating a good parameter identification method is important. A model that represents the system dynamics well can be used to effective and reliable fault detection (Liddament, 1999).

The procedure to determine a proper linear parametric mathematical model from observed input-output data involves three basic elements (Peitsman and Bakker, 1996):

1. Measurement of input-output data
2. Selection of model structure and estimation of parameters
3. Validation of selected model

Application of the black-box linear parametric mathematical models for model building is widely used technique by many researchers. Penman (1990) used it to model the thermal response in a working school while Dewson et al. (1993) used it to model the thermal response of an experimental building. However, individual researchers have used different techniques such as least squares and maximum likelihood to identify the parameters of their models.

The autoregressive mathematical models, ARMAX and ARX, with both single-input/single-output (SISO) and multi-input/single-output (MISO) will be examined in chapter 3. Furthermore, ARMAX and ARX models have been used for fault detection and diagnostics (Lee et al., 1996).

Peitsman and Soethout (1997) used several different ARX models to predict the performance of an AHU and compared the prediction with measured values to detect faults. The research shows that ARX modelling of the system in combination with a model-based diagnostic tool was able to detect most of the faults that were introduced inside the AHU. Furthermore, the diagnostic tool was able to give a correct indication in these situations of which component of the AHU was defective. Yoshida and Kumar (1999) evaluated the ARX model to identify abrupt faults in AHUs.

Kumar et al. (2001) propose a method based on an autoregressive exogenous model and a recursive parameter estimation algorithm to detect faults in AHUs. Peitsman and Bakker (1996) used two types of black box models (artificial neural networks [ANNs] and auto regressive with exogenous inputs [ARX1]) to detect faults in the system and at the component level of a reciprocating chiller system. Lowry and Lee (2004) applied system identification to the thermal response of an office space using data collected from an existing building management system.

Furthermore, Cunningham (2001) used system identification techniques to develop an autoregressive model (ARX) for allowing room or building ventilation and moisture release rates to be inferred from field psychometric data.

Albert et al. (1995) developed a new controller for a practical air handling system based on the system identification where the input and actuating variables are incorporated into a system identification model which can predict the new system status based on past records and suggest the optimal control action.

In view of the above review literature, system identification is a very useful technique for developing linear parametric models in different fields of research. The System Identification Toolbox is used in this project to develop mathematical models for one year of data collection. Therefore, selection of the system identification method in this project to develop the dynamic thermal model is fully justified.

2.1.2 Overview of Modelling with Artificial Neural Network Methods

Artificial Neural Networks (ANNs) or commonly just Neural Networks (NN) can be viewed as a set of processing units (or neurons, cells or automatons) in which all of the units are in contact with one another or with the outside by means of axonal or synaptic ramifications (IEA Annex 25, 1996).

Guglielmi et al. (1995) state that ANN method is characterized by the following advantages:

- It does not require the run-time use of a system's model, which is often onerous to develop and does not reflect the system's real behaviour accurately;
- It does not exhibit the severe limitation of being based on a linear model. This limitation affects model-based methods due to the mathematical difficulties associated with non linearities which, for instance, prevent the design of effective non linear state estimators.
- It does not require any representative signatures for single types of faults, a tolerance threshold, a hypothesis about the set point values of the plant, a simplifying hypothesis about noise, knowledge of non-parametric signal models, or parametric identification.

The main disadvantages of using an ANN method are IEA (Annex 34, 2001):

- Neural networks require vast amount of training data to model complex processes effectively.

- It is difficult to gain any physical insight into the process being modelled from the parameters of the trained neural network.
- Applying a neural network model to input data that are not well represented in the training data set can lead to erroneous output.

The most popular NN techniques, for modelling the thermal behaviour of buildings and HVAC plants, are presented in the next sections. Successively are presented only the radial basic function, general regression and cerebellar model articulation controller. The network that have been used in this project as multilayer feedforward neural network and nonlinear autoregressive models with exogenous inputs (NARX) models are presented in chapter 7.

Radial Basis Function Network

The Radial Basis Function (RBF) network consists of three layers including input, hidden and output layer (see Fig. 2.1). Such a network is characterized by a set of inputs and a set of outputs. In between the inputs and outputs there is a layer of processing units called hidden units. Each one implements a radial basis function. The input into the RBF network is non linear while the output is linear (Samanta et al., 2006).

In contrast to training a feedforward neural network (FFNN), learning in an RBF network can be done in one, two or three stages (phase learning) (Schwenker et al., 2001). In the one-phase learning procedure, only the output layer weights are adjusted through some kind of supervised optimization, e.g. minimizing the squared difference between the network's output and the desired output value. The two stages of an RBF network are learnt separately. First the parameters of the RBF layer, are adjusted the RBF layer is trained, including the adaptation of centres and scaling parameters, and second the weights of the output layer are adapted. The performance of RBF classifiers trained with two-phase learning has been improved through a third BP-like training phase of the RBF network, adapting the whole set of parameters (RBF centres, scaling parameters and output layer weights) simultaneously.

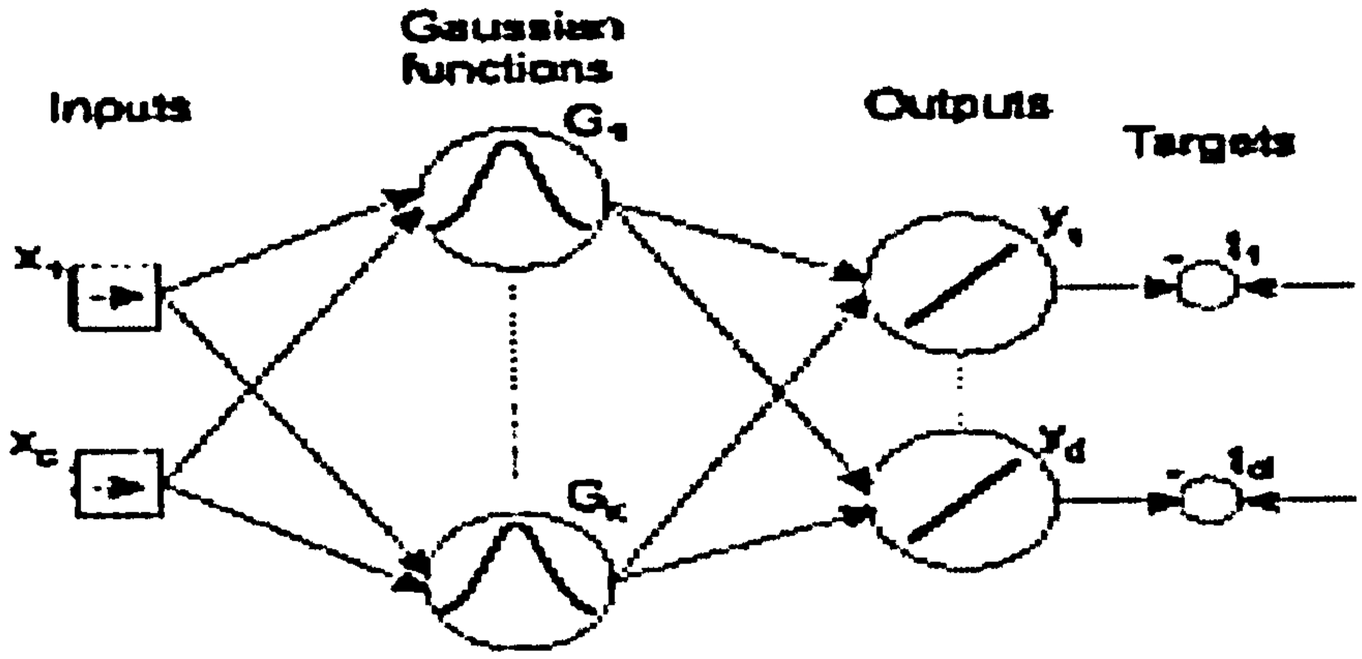

Figure 2.1 Architecture of a high-dimensional input and output RBF network (Samanta et al. 2006)

Advantages of Radial Basis Function network:

- RBF possesses good generalization capability with minimal network structure so that it offers a variety of application (approximation) problems and suits the requirements of the complicated systems (Wang et al., 2005).
- Any continuous function can be uniformly approximated to within an arbitrary accuracy (Bechtler et al., 2001).
- Compared to FFNN, RBF is fast, efficient and needs less computational effort (Bechtler et al., 2001).

A generalised radial basis function (GRBF) network it was used by Swider et al. (2001) to predict chiller performance. Furthermore, Swider (2003) compared different types of black box models to predict chiller performance, while Bechtler et al. (2001) have used general radial basis function for modelling a heat pump under steady state conditions. Finally, Yu and Zhai (2007) used RBF to model the air/fuel ratio control of automotive engines. In this case the RBF network was adapted on-line to model engine parameter uncertainties and extreme non-linear dynamics in different operating regions. They found that RBF modelled the non-linearity of the engine dynamics with a high degree of precision.

General Regression Neural Networks (GRNN)

GRNNs belong to the well-known nonparametric kernel regression models (Hardle, 1989, Fan and Gijbels, 1997) and are theoretically based on the estimation of a probability density function from observed samples using Parzen window estimation (Specht, 1991).

A GRNN is a four-layer feed-forward neural network based on non-linear regression theory consisting of an input layer; pattern layer, summation layer and output layer (see Fig. 2.2). There are no training parameters such as learning rate and momentum as there are in BP networks, but there is a smoothing factor that is applied after the network is trained. The smoothing factor determines how tightly the network matches its predictions to the data in the training patterns. The training of a GRNN is quite different from a training used in other neural networks. It is completed after one presentation of each input-output vector pair from the training data set to the GRNN input layer (Kalogirou et al., 2003).

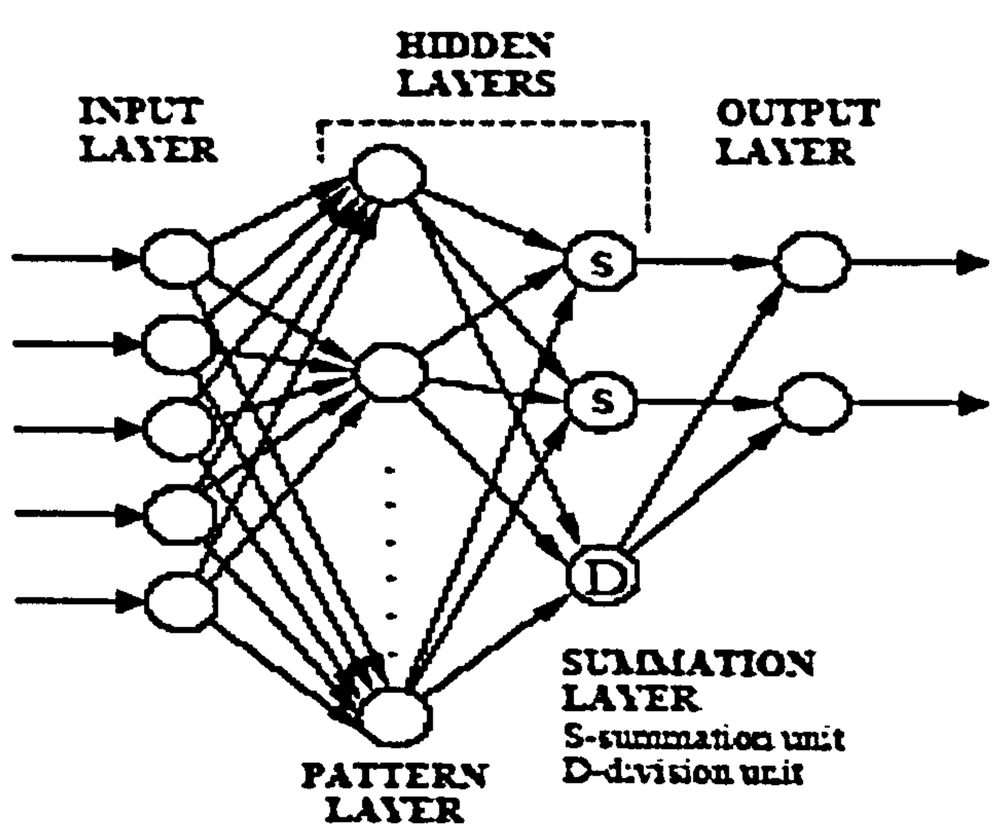

Figure 2.2 Schematic diagram of GRNN architecture (Kalogirou et al., 2003)

GRNN algorithms are characterized by the following advantages:

- They are quick learning (Abdullatif and Mahmoud, 2004).
- There is fast convergence to an optimal regression surface as the number of samples becomes large (Abdullatif and Mahmoud, 2004).

- GRNNs are capable of modelling non-linear relationships without a predetermined functional form (Kalogirou et al., 2003).
- No mathematical model is needed to estimate the system (Lee et al., 2004).
- The inherent one pass learning algorithm and parallel structure make it attractive for real time FDD (Lee et al., 2004).

GRNN algorithms are characterized by the following disadvantages:

- GRNNs require many training samples to adequately span the variation in the data, and require all training samples to be stored for future use (Karri, 2000).
- GRNNs have trouble with irrelevant inputs and there is no intuitive method for selecting the optimal smoothing factor (Karri, 2000).

Abdullatif and Mahmoud (2004) studied the feasibility of using GRNN to estimate the next day cooling load profile before weather conditions are known and Kalogirou et al. (2003) examined the use of GRNN for the prediction of air pressure coefficient across the openings in a light-weight single-sided naturally ventilated test room.

Cerebellar Model Articulation Controller Neural Networks

The Cerebellar Model Articulation Controller (CMAC) is essentially an adaptive, self-calibrating look-up table with continuous inputs and outputs. Unlike ANNs such as FFBP neural networks, the CMAC is based on a sequence of memory and data mappings rather than interconnected neurons. The mapping transforms a real, continuous input vector into a real, continuous output vector (Li et al., 2004).

Fig. 2.3 shows a schematic diagram for CMAC neural network. The CMAC algorithm consists of two mappings and one output computation for determining the value of a complex function as shown in Fig. 2.3.

Mapping S: $X \rightarrow A$ (2.1)

Mapping T: $A \rightarrow W$ (2.2)

Output Computation: $y = \sum_{jactivated} w_j$ (2.3)

Wong and Sideris (1992) show that the CMAC learning algorithm is a Gauss-Seidel iterative scheme for solving linear equations and that the CMAC output learns with an arbitrary accuracy.

CMAC networks are characterized by the following advantages over other types of neural networks:

- CMAC has been adopted widely for the control of complex dynamic systems owing to its fast learning property, good generalization capability, and simple computation compared to the other neural networks (Chiang and Lin, 1996; Kim and Lewis, 2000; Shiraishi et al., 1995).
- Its simple output and gradient-descent weight update calculations and its property of local generalization result in fast learning convergence in comparison to other neural networks for transient control applications (Li et al., 2004).
- CMAC requires minimal a priori knowledge of the system and therefore can be applied to a set of arbitrary systems performing similar tasks (Shiraishi et al., 1995).
- On-line adaptation adjusts CMAC to the unique characteristics of a particular system and likewise modifies the CMAC weights in the event that the system is altered in any way (Shiraishi et al., 1995).

Disadvantages of CMAC Neural Networks compared to other types of neural networks:

- Local generalization means that learning and weight adjustment in one region of the input space does not affect or disrupt what has already been learned in distant regions of the input space (Gordon and Campagna, 1990).

CMAC has been applied primarly to complex robotic systems involving multiple feedback sensors and multiple command variables (Miller, 1989). This type of network has also been used for air-to-fuel ratio control of automotive fuel-injection systems (Majors et al., 1994).

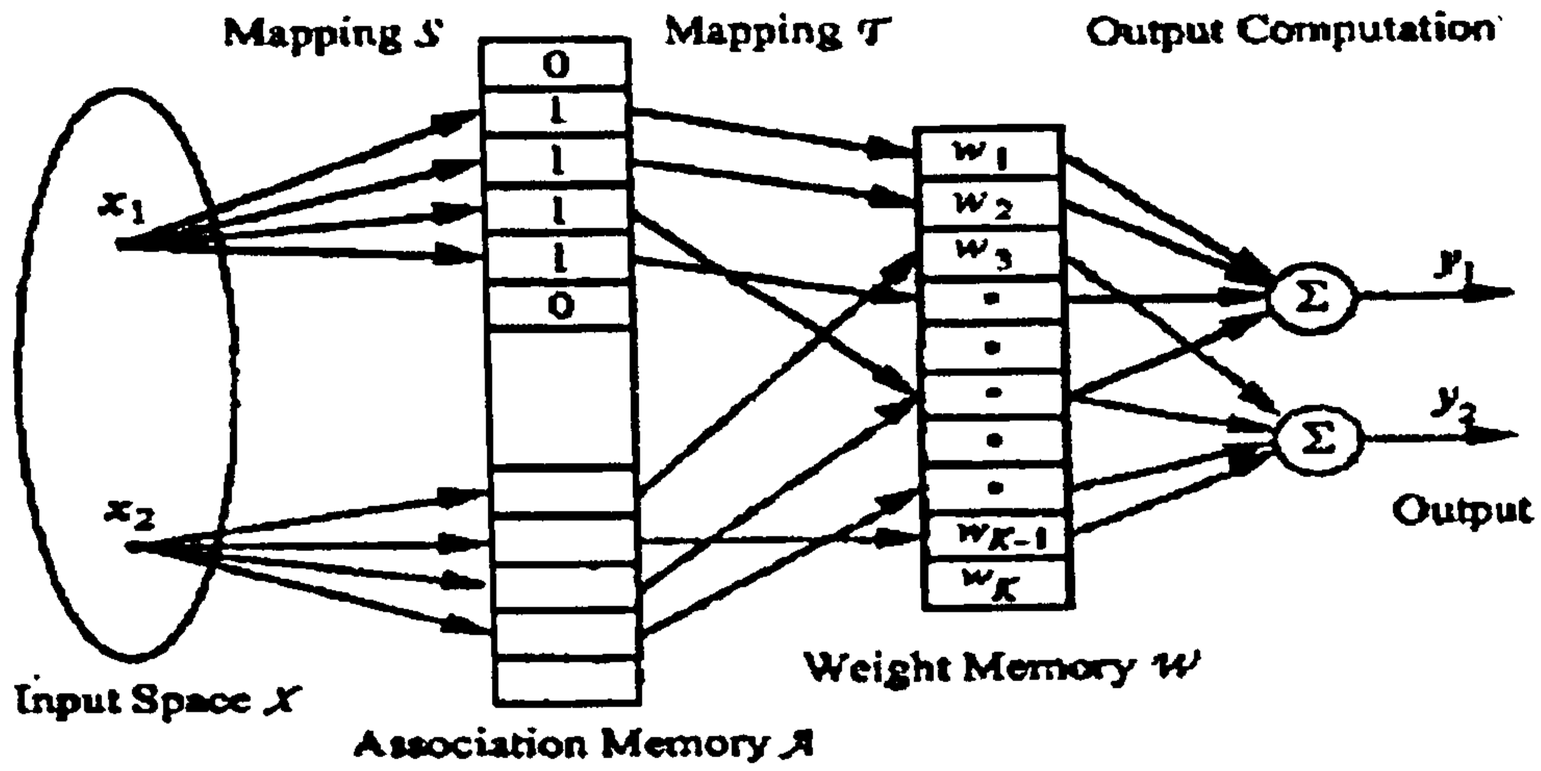

Figure 2.3 CMAC network structure (Shiraishi et al., 1995).

2.1.3 Fuzzy Logic Method

A fuzzy model is a set of fuzzy rules that describe the relationship between a set of inputs and a set of outputs in qualitative terms. Fuzzy logic resembles human decision making with its ability to work from approximate data and find precise solutions (Earl. C.,1994).

The main advantages of fuzzy schemes are (Klir et al., 1997).

- Fuzzy models can take into account the highly uncertain, nonlinear behaviour of HVAC equipment.
- Fuzzy FDD schemes are easier to commission because fuzzy rules are generic, to some extent.
- Available expert knowledge about the symptoms of faults is easily combined with knowledge learnt from measured data.
- Software implementation of fuzzy logic is computationally undemanding.

The main disadvantages of fuzzy schemes are:

- Less precise results are generated in comparison with other approaches.
- Rule-based descriptions are often less concise than quantitative descriptions.

ANFIS method

ANFIS stands for Adaptive Neuro-Fuzzy Inference System. It is a hybrid neuro-fuzzy technique that brings learning capabilities of neural networks to fuzzy inference systems. (Roger and Jang, 1993; Roger and Sun, 1995).

Advantages (Roger and Jang, 1993; Roger and Sun, 1995):

- The advantages over standard control theories, or the mathematical modelling method, are that any plant or problem can be modelled or described using the formal means of description equations. On the other hand fuzzy theory allows us to use human verbal description and this helps to overcome most of the uncertainties and instabilities the system could have.
- It is very difficult to create an appropriate rule base using the aid of an expert. The Neuro-Fuzzy Controller system offers the possibility to create this rule base automatically through a learning phase, evaluating the error response of the system.
- ANFIS is one of the best trade-off between neural and fuzzy systems, providing:

– smoothness, due to the fuzzy control interpolation

– adaptability, due to the neural network BP

Disadvantages:

- It has a single output. All output membership functions must be the same type and either be linear or constant.
- There is no rule sharing. Different rules cannot share the same output membership function; namely, the number of output membership functions must be equal to the number of rules.

The ANFIS model has been applied to the measured data in real office building in the Netherlands. The model output responded normally and during the faulty period, a big jump appeared. Finally, the model is shown to be a good candidate for energy diagnosis (Yu and Van Paassen, 2003).

2.2 Other Methods

The following methods have been reviewed for the project but have been considered not appropriate for this study.

2.2.1 White Box-Physical Based Methods

Physics-based models follow from fundamental physical laws such as conservation of mass and energy and Newton's laws of motion. The biggest advantages of physics-based models are that they provide insight into the physical process in a manner that is more precise (because we start from universal conservation law), and the parameters in such models are measurable, often using available techniques Rosenberg and Karnopp (1983).

The advantages and disadvantages of physical based models are listed below (Katipamula and Brambley, 2005).

The advantages of physical based models are:

- They are based on physical or engineering principles.
- Detailed models based on first principles can model both normal and "faulty" operation. Therefore, "faulty" operation can be easily distinguished from normal operation.
- The transient in a dynamic system can only be modelled with detailed physical models.

The disadvantages of physical based models are:

- They can be complex and computationally intensive and the effort required to develop a model is significant.
- They generally require many inputs to describe the system, some for which values may not be readily available. In addition, extensive user input creates opportunities for poor judgment or input errors that can have significant impacts on results.

Finally, in this project the physical based methods are not been used because of no possibility to extract the elements that are required for building physical based models.

2.2.2 Grey Box Method

It is possible that the physical laws can be applied to arrive at a model, but that not all parameters in this model are known. This case, which is a combination of white box and black box modelling, is called grey box modelling. All combinations of black box modelling and some prior knowledge are called grey box modelling. Fig. 2.4 illustrates the data requirements for the development, validation and application of WB, BB and GB models.

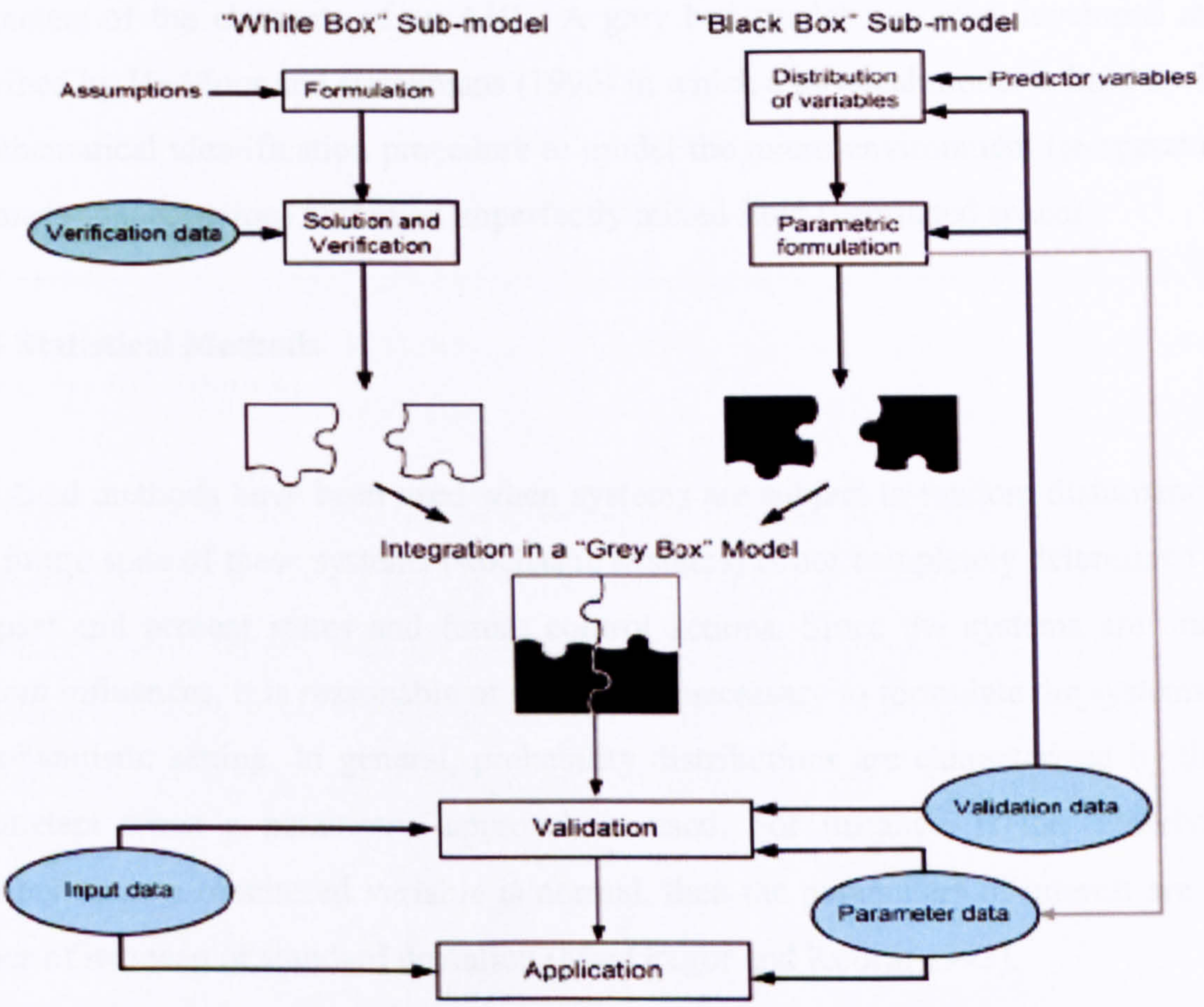

Figure 2.4 Flow diagrams illustrating the development processes of "grey box" models (Flores et al., 2006).

There are numerous applications of the Grey box method, some of which are presented below. A grey box model based method was used by Weyer et al. (2000) for fault detection of a heat exchanger. The model is based on a first principle model of the heat exchanger and on a grey box model of the fault, i.e. deterioration of the heat transfer surface due to aging.

Nielsen and Madsen (2006) present a model that links heat consumption to climate and calendar information. Theoretical relations known from the theory of heat transfer were used to select an initial model structure, and data on heat consumption and climate (temperature, wind speed and global radiation) were applied in combination with statistical methods to establish an actual mathematical grey box model of heat consumption. Dèquè et al. (2000) used grey box models to describe the thermal phenomena in building envelopes together with physical models, involving a large number of equations and parameters which must be entered to describe the building. Ghiaus et al. (2006) used the grey box approach for modelling and identifying the parameters of the elements of an AHU. A grey box model was also developed and described by De Moor and Berckmans (1996) in which a physical model is linked with a mathematical identification procedure to model the micro-environment (temperature and mass concentration) within an imperfectly mixed fluid (ventilated space).

2.2.3 Statistical Methods

Statistical methods have been used when systems are subject to random disturbances. The future state of these systems (stochastic systems) is not completely determined by the past and present states and future control actions. Since the systems are under random influences, it is reasonable or sometimes necessary to formulate the systems in a probabilistic setting. In general, probability distributions are characterized by their parameters when a parametric approach is used. For instance, if the underlying distribution of a monitored variable is normal, then the parameters of interest are the values of its mean or standard deviation (MacGregor and Kourti, 1995).

The main statistical techniques for modelling are:

- Principal component analysis (PCA)
- Least square method (LS)
- Maximum likehood method (ML)

In this project LS and ML methods are used inside black box linear mathematical models for calculation of their parameters (see chapter 3). Finally, the maximum likelihood method is presented in chapter 3, section 3.7.3.

The maximum likelihood method was used by Madsen and Holst (1995) to estimate the parameters in a continuous time series model for the heat dynamics of a building, where the data from an experimental laboratory were recorded for a period of five days with a sampling interval of 10 minutes.

Principal Component Analysis

Principal component analysis is a statistical technique that linearly transforms an original set of variables into a substantially smaller set of uncorrelated variables that represents most of the information in the original set of variables. Its objective is to reduce the dimensionality of the original data set.

This reduction is achieved by a linear transformation to a new set of variables, the principal component scores, which are uncorrelated, and ordered such that the first few retain most of the variation present in the original variables. The technique has been applied in many areas including chemical and industrial processes (Dunteman, 1989).

There are numerous applications of the PCA method, some of which are presented below. Wang and Cui (2005) present a PCA-based strategy, which uses Q-statistics as indexes of fault detection, and use the Q-contribution to isolate faults in chillers. Measured data under normal operating conditions have been monitored to model HVAC systems using PCA method (Hau et al., 2005). The PCA model has been adopted for on-line automatic FDD and to reconstruct an assumed faulty sensor in building central chilling systems. The square prediction error (SPE) based on the model and the sensor validity index (SVI) based on the construction are employed, respectively, to detect the sensor fault and identify the faulty sensor (Wang and Chen, 2004). Qin and Wang (2005), employed the PCA method to model and detect VAV terminal flow sensor biases and to reconstruct the faulty sensors.

Least Squares Method

Least squares (LS) method is known as a regression method, since the latent components obtained may be used instead of the original variables in regression to overcome the dimensionality problem (the data contain typically more variables than observations). As a supervised approach, it uses the response variable of interest in the dimension reduction step, which often makes it more efficient in prediction problems than the unsupervised PCA approach (Nguyen and Rocke, 2002).
The LS method is characterized by the following advantages (Boulesteix and Strimmer, 2005):

- High computational efficiency.
- Great flexibility and versatility in terms of the addressed concrete problems.
- The existence of a large variety of diverse algorithmic variants.

The first two points render the LS method very attractive for the analysis of microarray data. There are numerous applications of the LS method, some of which are presented below. Applications of LS method to regression problems were first proposed in the early 1980s and focused on the analysis of high-dimensional chemometric data. LS regression was studied from the point of view of statisticians, for example, Stone and Brooks (1990) and Frank and Friedman (1993). Namburu et al. (2005) employed a LS based technique to model a centrifugal chiller (HVAC system) for predicting system response under new operating conditions.

2.3 Conclusions

In this project the models are created using the black-box methods. This is because of the lack of available specific information related to the structure of the buildings such as windows, doors and building dimensions and the complexity of such details for a real case. In this project have been used linear parametric mathematical models and non-linear models (artificial neural networks).

CHAPTER 3 Modelling with Linear Parametric Mathematical Models

System identification deals with the problem of building mathematical models of dynamic systems based on observed data from the system. This chapter presents an overview of available systems identification methods, their properties, and how to use them. To obtain good prediction of real measurements, there are procedures for model development and validation, which are also presented in this chapter. In addition, a graphical user interface is presented, which can help us through the identification process and to apply advanced estimation techniques on multiple data sets and models. Finally, the chapter discusses a prediction error estimation method for model development.

3.1 Models

When we interact with a system, we need some concept of how its variables relate to each other. In broader terms, such an assumed relationship among observed signals is said to be a model of the system (Ljung, 1987). Models are very useful in forecasting or predicting the behaviour of the system. Therefore, we will find the relationship between different variables to model the thermal response of an office building.

3.2 Different Types of Mathematical Models

The mathematical models developed for different systems can have different characteristics depending on the properties of the system and the tools used.

Models can be classified as static and dynamic. If there is a direct, instantaneous link between the systems variables, then models that represent such systems are termed static models. If the systems variables are changed as a result of the earlier applied signals, then models that represent such systems are called dynamic models.

A mathematical model that describes the relationship between time-continuous signals is called a time-continuous model. A model that directly expresses the relationship between the values of signals at the sampling instants is called a discrete time model.

Differential equations are often used to describe time-continuous relationships whereas difference equations are used to describe discrete time relationships. Further classification can be made between parametric and non-parametric models. Parametric models depend on a finite number of real parameters. Any of the above models can be either single input single output (SISO), or multi-input single output, (MISO).

3.3 System Identification Approach

There are two modelling approach. The first is to analytically develop models based on physical principle, and the second use observations from the system operation in order to fit the models properties to those of the system (Ljung and Glad, 1994). Therefore, the system identification is the process by which mathematical representation of dynamic systems is obtained from data collected from the actual system in operation (Underwood, 1999). According to Kanjilal (1995), system identification is a prerequisite to adaptive prediction and control. It concerns the generation (for example, through specific experimentation) and collection of information, revealing the characteristic behaviour of the process, and development of a mathematical representation of it.

3.4 Modelling with System Identification Toolbox

3.4.1 Basic Entities

According to Ljung (1987) construction of a model using the system identification technique involves three basic entities:

- the data,
- a set of candidate models, and a rule by which models can be assessed using the data.

The data record

The input-output data are recorded during the experiment, in which the user may determine which signals to measure, when to measure them and also choose the input signals.

The set of models and a rule by which candidate models can be assessed

A set of candidate models is obtained by specifying within which collection of models we are going to look for a suitable one. In this case, prior knowledge and engineering intuition and insight have to be combined with formal properties of models. Sometimes the model set is obtained after careful physical modelling. Then, the model with some unknown physical parameters is constructed from basic physical laws and other well-established relationships. In other cases, standard linear models may be employed, without reference to the physical background. Finally, the assessment of model quality is typically based on the performance of models when they attempt to reproduce the measured data.

3.4.2 System Identification Procedure

System Identification involves three main stages:

- Identification of a suitable model structure,
- estimation of values of the model parameters, and
- verifying the resulting model using, ideally, data that were not used in the model estimation.

Identification of the Model Structure

The first step in the modelling procedure is to select a model structure (which will be described in section 3.5). Information from both physics and measurements are used to identify a suitable model parameterisation. The most important variables can be recognized, and insight of the most important dynamics can be achieved by examination of measurements from the system.

To model the impact from assumingly the most important variables, well-known thermodynamic relationships are used and formulated in terms of a system of ordinary differential equations.

Parameter Estimation

After determining the type of model structure, the parameters need to be estimated. According to Kanjilal (1995), these concerns determinations of the numerical values of the parameters of the process model which best describe the dynamic of the process. Eykhoff (1974) defines, parameter estimation as the experimental determination of parameter's values that govern dynamics and/or non-linear behaviour, assuming that the structure of the process model is known.

Model Validation

After selecting a particular model the model validation stage ensures whether it is "good enough", that is whether it is valid for its purpose.

Various procedures are involved to assess how the model relates to observed data, prior knowledge, and its intended use. Deficient model behaviour in these respects leads to rejection of the model, while good performance results in a certain confidence in the model. A model can never be accepted as a final and true description of the system. Rather, it can best be regarded as a good enough description of certain aspects that are of particular interest to us.

The schematic flowchart shown in Fig. 3.1 summarises the system identification procedure. All stages of schematic flowchart procedure were adopted in the present investigation for the linear models and adapted for use in the non-linear models.

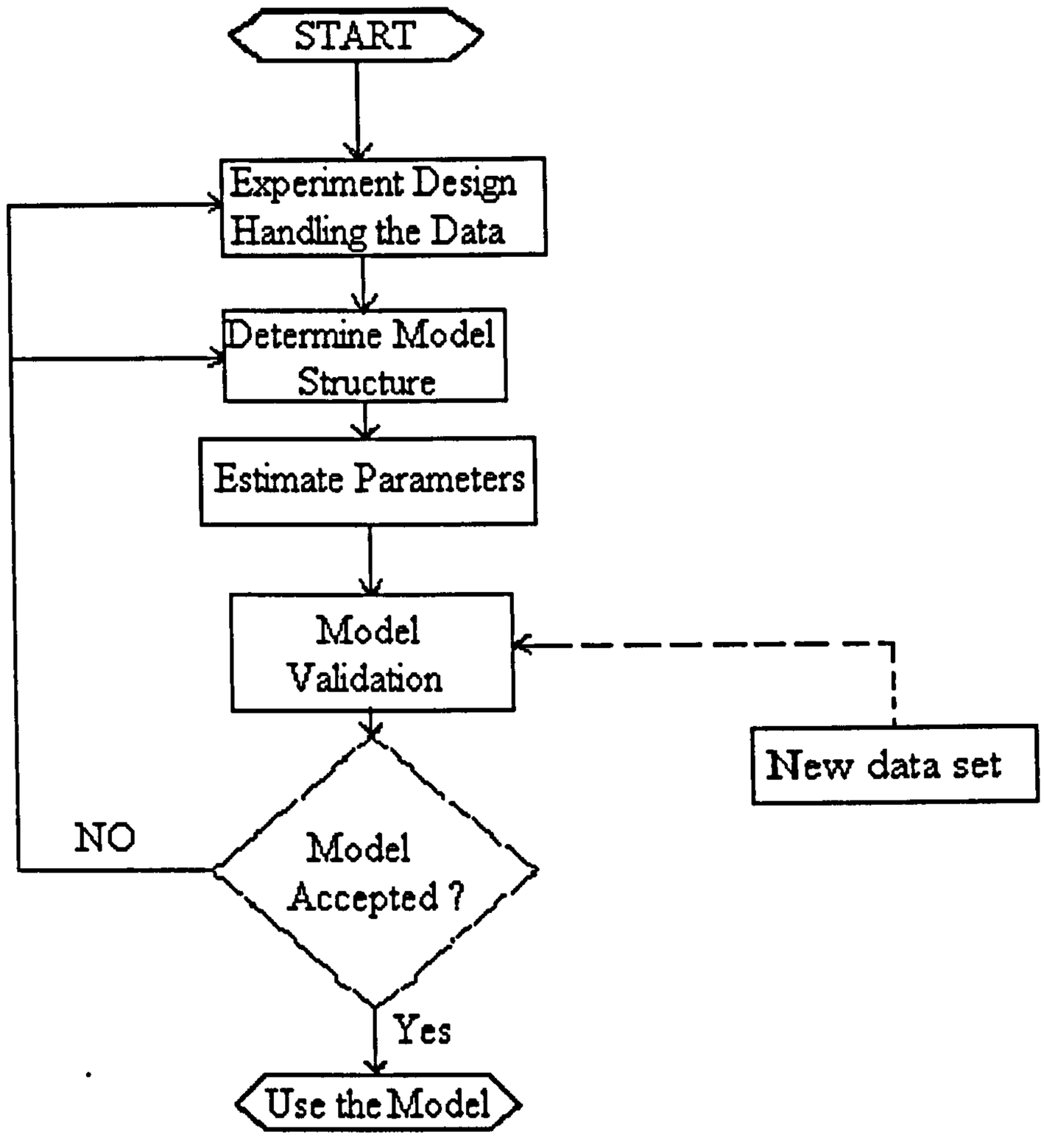

Figure 3.1 System identification procedures (Ljung, 1987)

There are different tools with which to evaluate model qualities. The techniques that have been used to evaluate model qualities using the System Identification Toolbox (Ljung, 1987), are outlined below:

Checking pole-zero cancellations

The poles relate to the "output-side" and the zeros relate to the "input-side" of the equation. The number of poles (zeros) is equal to the number of sampling intervals between the most and least delayed output (input). Checking cancellations gives a good indication of which orders to choose from model structures like ARMAX, OE, and BJ. If the confidence regions of a zero and a pole overlap, we have to try lower model orders.

Residual analysis

The criteria are that the residuals (prediction error 'e') associated with the data and a given model, are ideally white and independent of the input for the model to correctly describe the system. When applied the function 'Model Residuals' in the System Identification Toolbox is applied if the correlation functions go significantly outside these confidence intervals, the corresponding model is not accepted as a good description of the system.

Consistency of model input-output behaviour

The properties of the system that have been picked up by the models can be studied by Bode plots (frequency response), pole-zero plots, and model simulations (step response). Comparisons between spectral analysis estimates (see Ljung, 1987, Chapter 6) and Bode plots derived from parametric models are useful because they give a good feel for whether the essential features of the dynamics have been captured. Finally, if several models of different characters give similar Bode plots in the frequency range of interest, we can be fairly confident that these must reflect features of the true, unknown system, and we can choose the simplest model among these.

Comparing models with different structures: Cross - validation

A very good way of comparing two different models obtained in two different model structures is to evaluate their performance when applied to a data set to which neither of them was adjusted. There are several approaches for this. Probably the best known technique is Akaike's Final Prediction Error (FPE) criterion. It simulates the cross-*validation* situation, where the model is tested on another data set (see Ljung, 1987, chapter 16).

The FPE is formed as

$$FPE = \frac{1+\frac{d}{N}}{1-\frac{d}{N}}V$$

Where d is the total number of estimated parameters and N is the length of the data record. V is the loss function for the structure in question (see section 3.7).

According to Akaike's theory, in a collection of different models, choose the one with the smallest FPE. The FPE values are displayed with the model parameters, by just typing the model name.

Model fits and errors

Another way in obtaining insight into the quality of a model is to simulate it with input from a fresh data set, and compare the simulated output with the measured one. This gives a good feel for which properties of the system have been picked up by the model, and which have not. This test is obtained by checking the Model View Model Output (signal plot and error plot). Then the data set currently in the validation box will be used for the comparison. The fit is computed as the percentage of the output variation that is reproduced by the model, while the errors is ploted as the measured minus simulated model output (Ljung, 1999).

$$Model \quad Fit = 100 * (1 - norm(y_h - y) / norm(y - mean(y)))$$

Where,

- y_h the output that results when the model m is simulated with the input u
- y corresponding measured output
- mean(y) correspond to the mean value of the measured output
- norm($y_h - y$) is the Euclidean length of a vector ($y_h - y$)

Transient Response

Looking at the step response insight of the model provides a good insight into a model's dynamics. Furthermore, it is good practice to compare the transient response of a parametric model with the one that was estimated using correlation analysis. If there is good agreement between the two, we can be quite confident that some essentially correct features have been picked up.

3.5 Description of the Matlab System Identification Toolbox

The System Identification Toolbox (SIT) creates mathematical models of dynamic systems from measured input-output data. With it we can build and evaluate linear models of dynamic systems from measured input-output data. The toolbox supports virtually all polynomial (transfer function) and state-space model representations and model identification by non-parametric correlation and spectral analysis.

Toolbox functions can identify continuous or discrete-time models with an arbitrary number of input and output channels.

We can import and pre-process measured data, generate parametric and non-parametric models, and validate estimated models against measured data. We can interface with the toolbox via a graphical user interface or the matlab command line and programming language.

Fig. 3.2 shows the main graphical user interface (GUI), which can help us through the identification process and to apply advanced estimation techniques on multiple data sets and models. We can use this GUI to step through the identification process and apply advanced estimation techniques to multiple data sets and models (The MathWorks, 2003).

The key features of the SIT are:

- Loading and saving test data and identification sessions (import data)
- Parametric model identification using time domain data
- Specialized tools for identification of first, second and third order dynamic models (managing data sets and identified models graphically).
- Advice functions for evaluating test data and identified models
- Time domain data pre-processing tools, including offset removal, detrending (remove means), reconstructing missing data (preprocessing).
- Comparing multiple estimated models against validation data
- Tools for estimating time delays and frequency response

The key features and main tools/methods will now be discussed in more detail (The MathWorks, 2003).

Preprocessing measured data and choice of sampling interval

Measured data often have offsets, outliers, periods of missing values and other anomalies. These anomalies may lead to an improperly identified system. We can preprocess the measured data to remove these sources of error by:

- Detrending to remove data drift and offset
- Resampling to increase estimation speed and accuracy.

In the experiment, data sampling intervals had to be selected carefully because some information about the physical parameters can be partially hidden if longer sampling intervals are selected. The choice of sampling interval was coupled to the time constants of the system. It was thus valuable to first obtain the step response of the system. In this project the choice of sampling interval was 5 minutes, so that it corresponded to 5-8 sampling points over the rise time of the system's step response (Ljung and Glad, 1994).

Selecting data sets for identification and validation

The toolbox allows us to select two data sets from the measured data, one for identifying the model and one for validating it. We can use frequency and time domain data interchangeably to identify and validate models.

Estimating the models

We can try different methods and model structures to estimate the linear dynamics of the system under investigation. The toolbox allows us to estimate models using several predefined structures, providing three methods for estimating models:

- Parametric estimation
- Process model estimation

The method of parametric estimation will now be discussed. Parametric estimation allows us to select a model structure from predefined polynomial (transfer function) and state space forms. These are techniques to estimate parameters in given model structures. Basically, it is a matter of finding (by a numerical search) those numerical values of the parameters that give the best agreement between the model's (simulated or predicted) output and the measured one. After selecting the structure, we can edit the model order and choose a focus for the estimation, such as model stability or dynamic simulation.

Validating Models

The toolbox functions allows us to compare the estimated model output to an output data set to ensure that the estimated model output accurately represents the system dynamics.

The toolbox contains an advice function that suggests additional comparison tests and evaluates the model order, indicating when the order might be higher than needed. The toolbox provides five analysis tools to determine the fitness of the identified model:

- Model output: indicates how well the model dynamics were captured by comparing the model output against the validation set.
- Residual analysis: compares the outputs of the estimated models and the validation data.
- Frequency response: displays the model's frequency response to show damping levels and resonance frequencies
- Transient response: indicates the model's behaviour when excited by a step or impulse input
- Zeros and poles: displays the poles and zeros of estimated models.

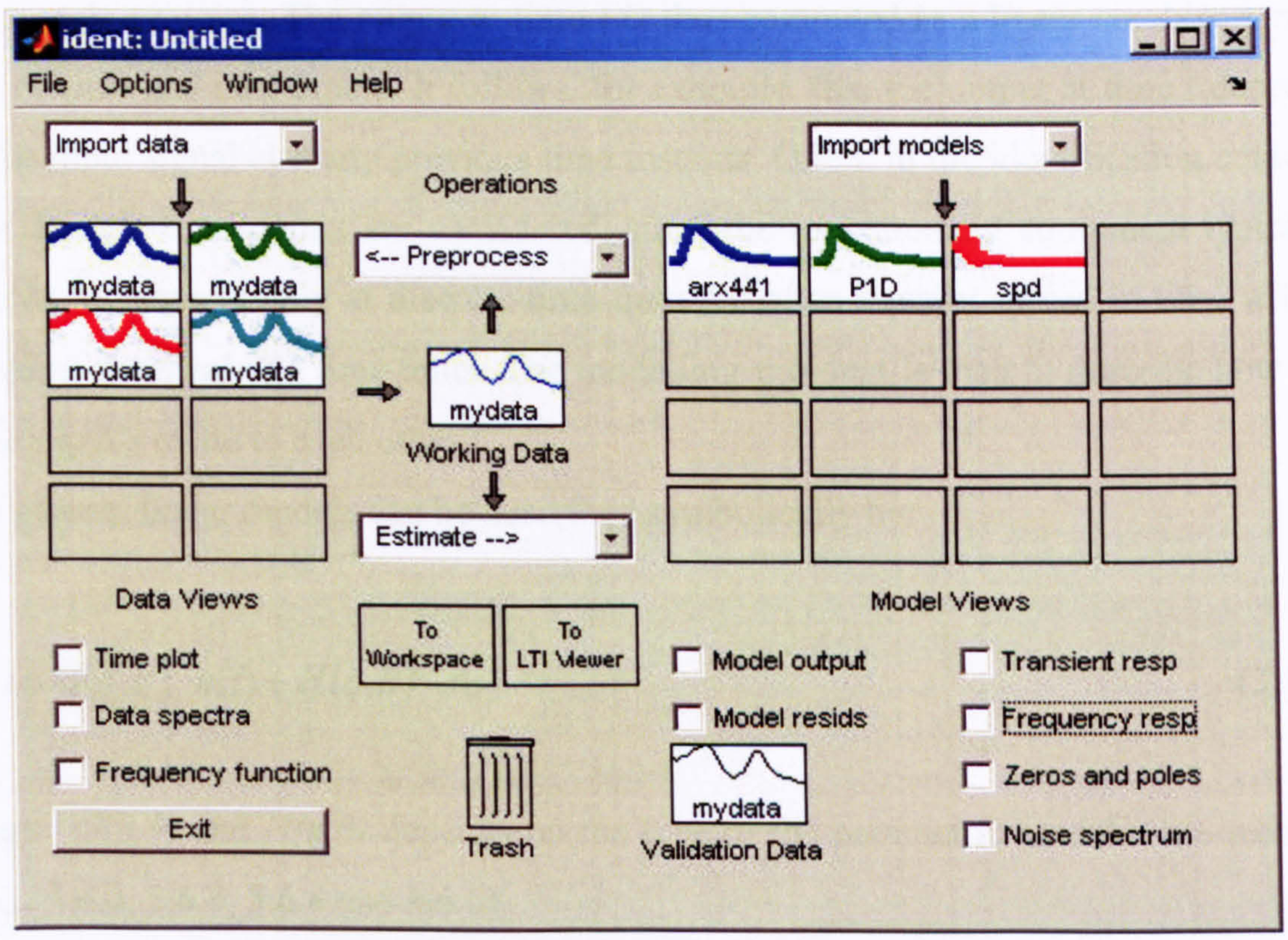

Figure 3.2 Graphical user interfaces (The MathWorks, 2003)

3.6 Model Structures

Selecting an appropriate model structure is the key step in the system identification procedure. Several model structures exist for the fitting of models to more detailed experimental data including the presence of disturbance or noise inputs.

In many cases, the nature of any known disturbances will determine the best model structure and it might often be desirable to test the results from a number of different model structures in order to find the best one. Verification will, therefore, determine whether the results obtained from a given model structure are adequate, or whether an alternative model structure should be investigated. It will also enable a choice to be made as to the best combination of parameters in a given model structure.

A brief review of the relevant parts of model structures is given below. The basic relationship in the autoregressive mathematical models is the **linear difference equation**. Models describe relationships between measured signals. It is convenient to distinguish between **input** *u(t)* signals and **output** *y(t)* signals. The outputs are then partly determined by the inputs. In most cases, the outputs are also affected by more signals than the measured inputs. Such "unmeasured inputs" are called **disturbance** *e(t)* signals or noise. The output at time t is thus computed as a linear combination of past outputs and past inputs. It follows, for example, that the output at time t depends on the input signal at many previous time instants. Often, in the identification context, only discrete-time points are considered, since the measurement equipment typically records the signals only at discrete-time instants, often equally spread in time with a sampling **interval** of t time units. The modelling problem is then to describe how the three signals relate to each other.

The general linear models can be described symbolically by:

$$y(t) = G(q,\theta)\ u(t) + H(q,\theta)\ e(t) \tag{3.1}$$

Where, $G(q,\theta)$ and $H(q,\theta)$ depends on the type of the parametric models (see sections 3.6.1, 3.6.2, 3.6.3, 3.6.4 and 3.6.5).

The (3.1) says that the measured output *y(t)* is a sum of one contribution that comes from the measured input *u(t)* and one contribution that comes from noise $H(q,\theta)e(t)$. The symbol G denotes the dynamic properties of the system, that is, how the output is formed from the input. For linear systems it is called the **transfer function** from input to output.

The symbol $H(q,\theta)$ refers to the noise properties, and is called the disturbance model. It describes how the disturbances in the output are formed from some standardized noise source $e(t)$ (Ljung and Glad, 1994).

There are several types of autoregressive mathematical models. Some of them are used in this project. The structures of these models are presented successively (Ljung, 1987).

3.6.1 The Autoregressive (AR) Structure

The simplest model structure that relates a time series output $y(t)$, to a noise or disturbance term $e(t)$ is, as follows:

$$y(t)+a_1y(t-1)+.....+a_ny(t-\mathrm{n})=e(t) \tag{3.2}$$

Where $y(t)$ refers to the measurements of the output at time t (sampling time). $y(t-n)$, $y(t-n+1)$, ... $y(t-1)$ are measurements of the output at successive time instants in the past, for example quarter hourly temperature readings. The above model can be expressed as:

$$y(t)=\frac{e(t)}{A(q)} \tag{3.3}$$

where,
$$A(q)=1+\mathrm{a}_1q^{-1}+\mathrm{a}_2q^{-2}+.....+\mathrm{a}_{\mathrm{na}}q^{-\mathrm{na}} \tag{3.4}$$

This forms the autoregressive (AR) model structure and A is a polynomial in q with parameters a_1, a_2.... a_{na}. The shift operator, q is defined as:

$$q^{-\mathrm{p}}y(t)=y(t-\mathrm{p}); \qquad \mathrm{p}=1,2,....\mathrm{na} \tag{3.5}$$

The adjustable parameters to be determined are:

$$\vartheta=[a_1,a_2.....a_{na}]^T \tag{3.6}$$

3.6.2 Autoregressive with Exogenous Input (ARX) Structure

If we consider an input signal to the system as $u(t)$, together with other disturbances $e(t)$, then the input output relationship can be defined as:

$$\begin{aligned}&y(t)+a_1y(t-1)+.....+a_{na}y(t-na)=b_0u(t)+b_1u(t-nk)+....\\&+b_{nb}u(t-nk-nb)+e(t)\end{aligned} \tag{3.7}$$

Which relates the current output *y(t)* to a finite number of past outputs *y(t-k)*, inputs *u(t-k)* and disturbance signal *e(t)*.

The structure is thus entirely defined by three integers *na*, *nb, nk*, where *na* is equal to the number of poles and *nb-1* is the number of zeros, while nk is the pure time delay (the dead time) in the system. For a system under sampled-data control, typically *nk* is equal to 1 if there is no dead-time. For multi-input systems, *nb* and *nk* are row vectors, where the i-th element gives the order/delay associated with the i-th input.

A multivariable ARX model with *nu* inputs and *ny* outputs can be represented in general form as follows:

$$y(t) = \frac{B(q)}{A(q)}u(t-nk) + \frac{1}{A(q)}e(t) \tag{3.8}$$

where, $$A(q) = I_{ny} + A_1 q^{-1} + ... + A_{na} q^{-na} \tag{3.9}$$

as well as the matrix

$$A(q) = \begin{pmatrix} a_{11}(q) & a_{12}(q) & ..... & a_{1ny}(q) \\ a_{21}(q) & a_{22}(q) & ..... & a_{2ny}(q) \\ ..... & ..... & ..... & ..... \\ a_{ny1}(q) & a_{ny2}(q) & ..... & a_{nyny}(q) \end{pmatrix} \tag{3.10}$$

where the entries a_{kj} are polynomials in the delay operator q^{-1}:

$$a_{kj}(q) = \delta_{kj} + a_{kj}^1 q^{-1} + ... + a_{kj}^{na_{kj}} q^{-na_{kj}} \tag{3.11}$$

This polynomial describes how old values of output number *j* affect output number *k*. Here δ_{kj} is the Kronecker-delta; it equals 1 when $k = j$, otherwise, it is 0. Similarly, B(q) is an *ny*-by-*nu* matrix

$$B(q) = B_0 + B_1 q^{-1} + ... + B_{nb} q^{-nb-1} \tag{3.12}$$

or

$$B(q) = \begin{pmatrix} b_{11}(q) & b_{12}(q) & ..... & b_{1nu}(q) \\ b_{21}(q) & b_{22}(q) & ..... & b_{2nu}(q) \\ ..... & ..... & ..... & ..... \\ b_{ny1}(q) & b_{ny2}(q) & ..... & b_{nynu}(q) \end{pmatrix}$$

with

$$b_{kj}(q) = b_{kj}^1 q^{-nk_{kj}} + ... + b_{kj}^{nb_{kj}} q^{-nk_{kj}-nb_{kj}-1} \tag{3.13a}$$

The delay from input number *j* to output number *k* is nk_{kj}.

$G(q,\theta)$ and $H(q,\theta)$ are given in (3.13b)

$$G(q,\theta)=\frac{B(q)}{A(q)},\ H(q,\theta)=\frac{1}{A(q)} \tag{3.13b}$$

and the adjustable parameters to be determined are:

$$\theta=[a_1,a_2.....a_{na}b_1,b_2.....b_{nb}]^T \tag{3.13c}$$

3.6.3 Autoregressive Moving Average with Exogenous Input (ARMAX) Structure

A further refinement for situations where noise or disturbance can be measured is to introduce a time-series disturbance parameter, which results in the *autoregressive moving average with exogenous input structure:*

$$y(t)=\frac{B(q)}{A(q)}u(t-nk)+\frac{C(q)}{A(q)}e(t) \tag{3.14}$$

Where,

$$A(q)=1+a_1q^{-1}+.....a_{na}q^{-na}$$

$$B(q)=b_1+b_2q^{-1}+....b_{nb}q^{-nb-1} \tag{3.15}$$

$$C(q)=1+c_1q^{-1}+c_2q^{-2}+.....+c_{nc}q^{-nc}$$

$$G(q,\theta)=\frac{B(q)}{A(q)},\qquad H(q,\theta)=\frac{C(q)}{A(q)}$$

and the adjustable parameters to be determined are:

$$\theta=[a_1,a_2.....a_{na}b_1,b_2.....b_{nb}c_1c_2.....c_{nc}]^T \tag{3.16}$$

The parameters *na*, *nb* and *nc* are the orders of the ARMAX model, and *nk* is the delay. For multi-input systems, *nb* and *nk* are row vectors, such that *k-th* corresponds to the order and delay associated with the *k-th* input. The term *A(q)y(t)* represents an auto regression and *C(q)e(t)* a moving average of white noise, while *B(q)u(t)* represents an extra input (an exogenous variable).

3.6.4 Output Error (OE) Structure

In the structure, the disturbance is treated as white measurements of noise and *e(t)* is regarded as an error with respect to the undisturbed output. The model structure is presented as:

$$y(t)=\frac{B(q)}{F(q)}u(t-nk)+e(t) \tag{3.17}$$

Where, $$B(q) = b_1 + b_2 q^{-1} + ...b_{nb} q^{-nb-1}$$

$$F(q) = 1 + f_1 q^{-1} + f_2 q^{-2} + ... + f_{nf} q^{-nf}$$

$$G(q,\theta) = \frac{B(q)}{F(q)} \quad , \quad H(q,\theta) = 1$$

The parameters *nb* and *nf* are the orders of the output-error model and *nk* is the delay.

The parameter vector θ of the output-error is estimated using a prediction error method.

$$\theta = [b_1, b_2 .....b_{nb} f_1, f_2 ..... f_{nf}]^T \tag{3.18}$$

3.6.5 Box–Jenkins (BJ) Structure

Further generalisation of the OE model structure is the BJ structure that gives:

$$y(t) = \frac{B(q)}{F(q)} u(t - nk) + \frac{C(q)}{D(q)} e(t)$$

Where,

$$B(q) = b_1 + b_2 q^{-1} + ... + b_{nb} q^{-nb-1}$$
$$C(q) = 1 + c_1 q^{-1} + ... + c_{nc} q^{-nc}$$
$$D(q) = 1 + d_1 q^{-1} + ... + d_{nd} q^{-nd}$$
$$F(q) = 1 + f_1 q^{-1} + ... + f_{nf} q^{-nf}$$

$$G(q,\theta) = \frac{B(q)}{F(q)}, \qquad H(q,\theta) = \frac{C(q)}{D(q)}$$

Where *nb*, *nc*, *nd* and *nf* are the orders of the Box-Jenkins model, and *nk* is the delay. The parameter vector θ of the Box-Jenkins model is estimated using a prediction error method.

$$\theta = [b_1 b_2 ....b_{nb} c_1 c_2 .....c_{nc} d_1 d_2 .....d_{nd} f_1 f_2 ....f_{nf}]^T \tag{3.19}$$

Finally, in chapters 4, 5, 6, 7 and 8 the orders and delays in ARMAX, OE and BJ models are presented with the following abbreviations:

- ARMAX models
  - amx [*na nb nc nk*], where the parameters *na*, *nb*, *nc* and *nk* are the orders and the delay (see section 3.6.3). In addition, *na, nb* and *nk* contain elements equal to the number of 'Common poles', 'Zeros +1' and 'Delay' respectively (The MathWorks, 2003; Appendixes 1B, 2B and 3B; section 3.4.2, pg. 28).
- OE models
  - oe [*nb nf nk*], where the parameters *nb*, *nf* and *nk* are the orders and the delay (see section 3.6.4). In addition, *nb, nf* and *nk* contain elements equal to the number of 'Poles', 'Zeros +1' and 'Delay' respectively (The MathWorks, 2003; Appendixes 1B, 2B and 3B; section 3.4.2, pg. 28).
- BJ models
  - bj [*nb nc nd nf nk*], where the parameters *nb*, *nc*, *nd*, *nf* and *nk* are the orders and the delay (see section 3.6.5). In addition, *nb, nf* and *nk* contain elements equal to the number of 'Poles', 'Zeros +1' and 'Delay' respectively (The MathWorks, 2003; Appendixes 1B, 2B and 3B; section 3.4.2, pg. 28).

3.7 Parameter Estimation Methods

Ljung, (1987) have analysed the problem of parameter estimation by considering a collected batch of data Z^N (3.21) and also a set of candidate models $M^*(\theta)$ (3.20) parameterized, then the search for the best model within the set becomes a problem of determining or estimating parameter vector θ (3.19).

$$M^* = \{M(\vartheta) \setminus \vartheta \in D_M\} \tag{3.20}$$

Where,

- M is a certain model structure with particular models $M(\theta)$ parametrized using the parameter vector $\theta \in D_M \subset R^d$

$$Z^N = [y(1), u(1), y(2), u(2), \ldots\ldots, y(n), u(n)]) \tag{3.21}$$

The most important aspect of the model is its prediction which judges its performance in this respect.

Thus let the prediction error ε given for a certain model $M(\theta)$ be presented by

$$\varepsilon(t,\vartheta) = y(t) - \hat{y}(t \setminus \theta) \tag{3.22}$$

where,

- $y(t)$ is the system description (see (3.1)), and
- $\hat{y}(t \setminus \theta)$ predicted output at time t using a model $M(\theta)$ (3.23).

$$\hat{y}(t \setminus \theta) = [1 - H^{-1}(q,\theta)\ ]\ \ y(t) + H^{-1}(q,\theta)G(q,\theta)u(t) \tag{3.23}$$

When the data set Z^N is known, these errors can be computed for $t = 1, 2,..., N$.

A "good" model, we say, is one that is good at predicting, that is, one that produces small prediction errors when applied to the observed data. A guiding principle for parameter estimation thus is based on Z^t we can compute the prediction error $\varepsilon(t,\theta)$ using (3.22). At time $t = N$, select θ_N so that the prediction errors $\varepsilon(t, \theta_N)$, $t = 1, 2,..., N$, become as small as possible.

There are two general procedures for estimating the parameter vector θ, and both deal with the sequence of prediction errors $\{\varepsilon(t,\theta)\}$ (explained successively) computed from the respective models using the observed data, and both could be said to aim at making this sequence "small". The first method is the *prediction-error identification approach* (PEM), which contains several procedures, such as the least-squares (LS) method and the maximum-likelihood (ML) method, and second is *correlation approach*, which contains the instrumental-variables (IV) technique. Correlation approach is not presented successively, because throughout analysis of the data only PEM has been used as parameter estimation method.

3.7.1 Prediction Error Identification Methods

Least square method (LS) and maximum likelihood (ML) methods are used for parameter estimation in PEM (successively presented). The prediction-error sequence in (3.22) is a vector in R^N and this leaves a substantial amount of choices. To minimize this amount of choices it has been presented the prediction-error approach in which a certain function $V_N(\theta, Z^N)$ given by (3.24) is minimized with respect to θ.

Then the estimate $\hat{\theta}_N$ is then defined by (3.25) (see Ljung, 1987, chapter 7):

$$V_N = (\theta, Z^N) = \frac{1}{N}\sum_{t=1}^{N} l(\varepsilon_f(t,\theta)) \tag{3.24}$$

$$\hat{\theta}_N = \hat{\theta}_N(Z^N) = \arg_{\theta \in D_M} \min V_N(\theta, Z^N) \tag{3.25}$$

Where,

- $l(\cdot)$ is a scalar-valued (typically positive) function (see Ljung. 1987, chapter 7)
- $V_N(\theta, Z^N)$ is, for given Z^N, a well defined scalar-valued function of the model parameter θ.
- $\varepsilon_f(t,\theta) = L(q)\varepsilon(t,\theta)$ (where $L(q) = 1$, since the option of prefiltering $L(q)$ is taken care of by the freedom in selecting $H(q,\theta)$ (see Ljung, 1987, chapter 7). In the next sections are presented the two methods for the determination of $V_N(\theta, Z^N)$.

Furthermore, an important aspect of this method is its properties (Ljung, 1987):

- Convergence
- consistency and
- Asymptotic distribution of parameter estimates.

Convergence

The convergence of $\hat{\theta}_N$ has been analysed in the way that for $N \to \infty$ the desired properties of $\hat{\theta}_N$ would be that it converge to θ_o (true value). It can be noted that if $v_o(t)$ is small compared to $\varphi(t)$ then the error term $[R(N)]^{-1}\frac{1}{N}\sum_{1}^{N}\varphi(t)v_o(t)$ (see 3.30b) will be small, and thus $\hat{\theta}_N$ will be close to θ_o.

As results of this analysis:

- $R(N) = \frac{1}{N}\sum_{t=1}^{N}\varphi(t)\varphi^T(t) \to R^*$ and
- $\frac{1}{N}\sum_{1}^{N}\varphi(t)v_o(t) \to h^*$

Consequently for $N \to \infty$, $\hat{\theta}_N \to \theta_o + (R^*)^{1} h^*$

Consistency

For PEM method to be consistent, that is, for $\hat{\theta}_N$ to converge to θ_o, it is requires:

- Matrix $R(N) \to R^* as\ N \to \infty$ and R^* is non-singular matrix. This will typically be the case, for example, if $\{u(t)\}$and $\{v_o(t)\}$ are independent and the m x m matrix, whose i, j entry is $R_u(i-j)$, is non-singular. In this case the input is said to be persistently exciting of order n_b.
- $h^* = 0$. This will be the case if either

a) $\{v_o(t)\}$ is a sequence of independent random variables with zero mean values (white noise). Then $v_o(t)$ does not depend on what was happened up to time t-1, and hence $E\varphi(t)v_o(t) = 0$. The input sequence $u(t)$ is independent of the zero-mean noise sequence $v_o(t)$ (white noise) and the (see 3.30b for $R(N)$) or

b) The input sequence $\{u(t)\}$ is independent of the zero mean noise sequence $\{v_o(t)\}$ and $n_a = 0$ in (3.27). Then $\varphi(t)$ contain only u terms and hence $E\varphi(t)v_o(t) = 0$.

Asymptotic distribution of parameter estimates

In addition to the convergences properties of$\hat{\theta}_N$, Ljung, (1987) have presented the asymptotic distribution of $\hat{\theta}_N$ (how fast the estimate $\hat{\theta}_N$ approaches the limit) by the covariance matrix $Cov\hat{\theta}_N$ and the assumptions:

- That the model structure is capable of giving a correct description of the system and
- the models that contains a disturbance model (H is estimated), will produce white residuals.

$$Cov\hat{\theta}_N \sim \frac{\lambda_o}{N}[\bar{E}\psi(t,\theta_o)\psi^T(t,\theta_o)]^{-1} \quad .$$

Where,

- λ_o is the variance of $\varepsilon(t,\theta_o) = e_o(t)$ independent random variables with zero mean and
- $\psi(t,\theta_o) = -\frac{d}{d\theta}\theta(t,\theta)|_{\theta=\theta_o} = \frac{d}{d\theta}\hat{y}(t\setminus\theta)|_{\theta=\theta_o}$ is the gradient of $\hat{y}$

3.7.2 Least Squares Method

The least-squares method is a special case of the prediction-error identification method. For linear regression model structures the predictor $\hat{y}(t/\theta)$ given by the equation (3.23) can also be presented as in (3.26).

$$\hat{y}(t/\theta) = \varphi^T(t)\theta \tag{3.26}$$

Where $\varphi(t)$ contains old values of observed inputs and outputs (3.27),

$$\varphi(t) = [-y(t-1) - y(t-2).....- y(t-n_a)u(t-1).....u(t-n_b)]^T \tag{3.27}$$

With (3.26) the prediction error becomes

$$\varepsilon(t,\theta) = y(t) - \varphi^T(t)\theta \tag{3.28}$$

The criterion function resulting from $\varepsilon_f(t,\theta) = L(q)\varepsilon(t,\theta)$ and (3.24), with $L(q) = 1$ and $l(\varepsilon) = \frac{1}{2}\varepsilon^2$ (see Ljung, 1987, chapter 7), is

$$V_N(\theta, Z^N) = \frac{1}{N}\sum_{t=1}^{N}\frac{1}{2}[y(t) - \varphi^T(t)\theta]^2 \tag{3.29}$$

This is the least-squares criterion for the linear regression (3.28). The unique feature of this criterion, developed from the linear parameterization and the quadratic criterion is that it is a quadratic function in θ. Therefore, it can be minimized analytically, which gives, provided the indicated inverse exists, the least-squares estimate (3.30a) (chapter 7, Ljung, 1987).

$$\hat{\theta}_N^{LS} = \arg\min V_N(\theta, Z^N) = [\frac{1}{N}\sum_{t=1}^{N}\varphi(t)\varphi^T(t)]^{-1}\frac{1}{N}\sum_{1}^{N}\varphi(t)y(t) \tag{3.30a}$$

or in the other way the formula (3.30a) can be presented as (3.30b) if we suppose that the observed data have been generated by $y(t) = \varphi^T(t)\theta_o + v_o(t)$. Where θ_o is the true value of θ and $v_o(t)$ includes the disturbances.

$$\hat{\theta}_N^{LS} = \theta_o + [R(N)]^{-1}\frac{1}{N}\sum_{1}^{N}\varphi(t)v_o(t) \tag{3.30b}$$

Where $R(N)$ is the $d \times d$ matrix given as

$$R(N) = \frac{1}{N}\sum_{t=1}^{N}\varphi(t)\varphi^T(t)$$

3.7.3 Maximum Likelihood Method for Parameter Estimation

Ljung and Glad (1994) have presented maximum likelihood method as that of system identification and parameter estimation, deals with the problem of extracting information from observations that themselves could be unreliable. The observations are then described as realizations of stochastic variables. It has been supposed that the observations are presented by the random variable $y^N = (y(1), y(2), ..., y(N))$ that takes values in R^N. The maximum likelihood method defines θ as:

$$\hat{\theta}_{ML}(y^N) = \arg\min \frac{1}{N} \sum_{t=1}^{N} l(\varepsilon(t,\theta),\theta,t) \tag{3.31}$$

Where,

$$l(\varepsilon,t,\theta) = -\log f_e(\varepsilon,t;\theta) \tag{3.32}$$

The formula (3.31) is valid under the following assumptions (Ljung and Glad (1994) :

- The errors are independent and have the probability density function (PDF) $f_e(x,t;\theta)$ (this means that f_e does not depend on $Z^t = (y(1),u(1)....y(t),u(t))$
- θ is considered to be a random vector with a certain prior distribution (Bayesian maximum a posteriori approach)
- The probabilities density functions between the true system and from the observations Z^t are minimized (Akaike's information criteria AIC).

Generally, the probability density function (PDF) of y^N is given in (3.32), (Ljung. 1987)

$$P(y^N \in A) = \int_{x^N \in A} f_y(\theta; x^N) dx^N \tag{3.33}$$

$$f(\theta; x_1, x_2, ..., x_N) = f_y(\theta; x^N)$$

CHAPTER 4 Data Analysis and Model Development for the Visa Building

In this chapter the system identification toolbox and, in particular, the autoregressive mathematical models discussed in chapter 3 are applied to the Visa building to build the thermal behaviour of a room positioned on the seventh floor. The model structures ARX, OE, ARMAX and BJ are the general choices. Chapter starts with a brief description of the Visa building and the room examined for model estimation and validation, followed by a detailed analysis of the inputs and the most appropriate models for building the thermal modelling of the room throughout the year.

After careful analysis of all the variables affecting the room temperature, several inputs and outputs were collected through the BMS for the entire year. Then, the SIT with autoregressive mathematical models, presented in chapter 3, was applied to the data collected for the year and the models chosen were those that best fit the real data.

The room's thermal behaviour in zone 1 and 2 was taken for model development and validation (Figs. 4.2 and 4.3). This room is a large open plan office and there are no significant differences in temperature between the two zones. The linear parametric mathematical models (apart from ARX models) cannot perform data analysis with two outputs, and for this reason analysis of these zones was performed separately. Because of the similarities of results obtained between the two zones, in this chapter only the results related to zone 2 are presented. Differently from linear parametric mathematical models, neural networks do not have any restriction when analysing data with more than one output. As a result, Chapter 7 presents data analysis and model development for the entire room.

Finally, the following sections explore the inputs and the models in terms of best fit with the real measurements of room temperature for the year 2005. However, because BMS behaviour differs between weekdays and weekends to begin the modelling process, the weekdays model was first developed.

4.1 Visa Building Description

The Visa Building (see Fig. 4.1) is located in Sheldon Square, London, close to Paddington Central Station. The BMS installed for monitoring and operation of the plant/building services is Invensys. The data were analysed by dividing them into weekdays (Monday Time 01:20 to Friday Time 19:00) and weekends (the latter is not presented because the HVAC plants are switched off on Saturday and Sunday).

To identify the parameters of the model describing the thermal response of a real building a time series of the relevant data was collected. The data collected had a sampling interval of 5 minutes and the collection consisted of:

- Room temperature zone 1 and 2, second floor (Output) in degrees Celsius (degC)
- Outside temperature in degrees Celsius (degC)
- Supply air flow rate AHU2 (air that is coming from the air handling unit 2 supplying zone 2, positioned on the roof of the building and flowing through the FCUs positioned in zone 2) in m^3/sec
- Supply air temperature AHU2 (air temperature that is coming from the air handling unit 2 supplying zone 2, positioned on the roof of the building and flowing through the FCUs positioned in zone 2) in degrees Celsius (degC)
- Chilled water temperature (chilled water that flows inside the fan coil units and comes from the chillers positioned on the roof) in degrees Celsius (degC).
- Hot water temperature (hot water that flows inside the fan coil units and comes from the boilers positioned on the roof) in degrees Celsius (degC).

The fan coil units (FCUs) are distributed throughout the room in zones 1 and 2 (see Fig 4.2) on the seventh floor (the fan coil units are numbered consecutively and there are 60 in total), while Fig. 4.3 shows a picture of a fan coil unit. The FCUs are composed of the following parts:

- Supply air: air with a determined temperature that is supplied to the room (air that is coming from the air handling unit 1 or 2 and flowing through the FCU).
- Heating coils: the hot water that comes from the boiler plants, situated on the roof of the building, circulates through the coils and heats up the air.
- Cooling coils: the chilled water that comes from the chiller plants, situated on the roof of the building, circulates through the coils and cools down the air.

- The fan that supplies air to the room
- The damper: Depending on its position the amount of air transferred can be controlled by the position of the damper, thereby enabling temperature to be increased or decreased as desired.

Figure 4.1 Visa building

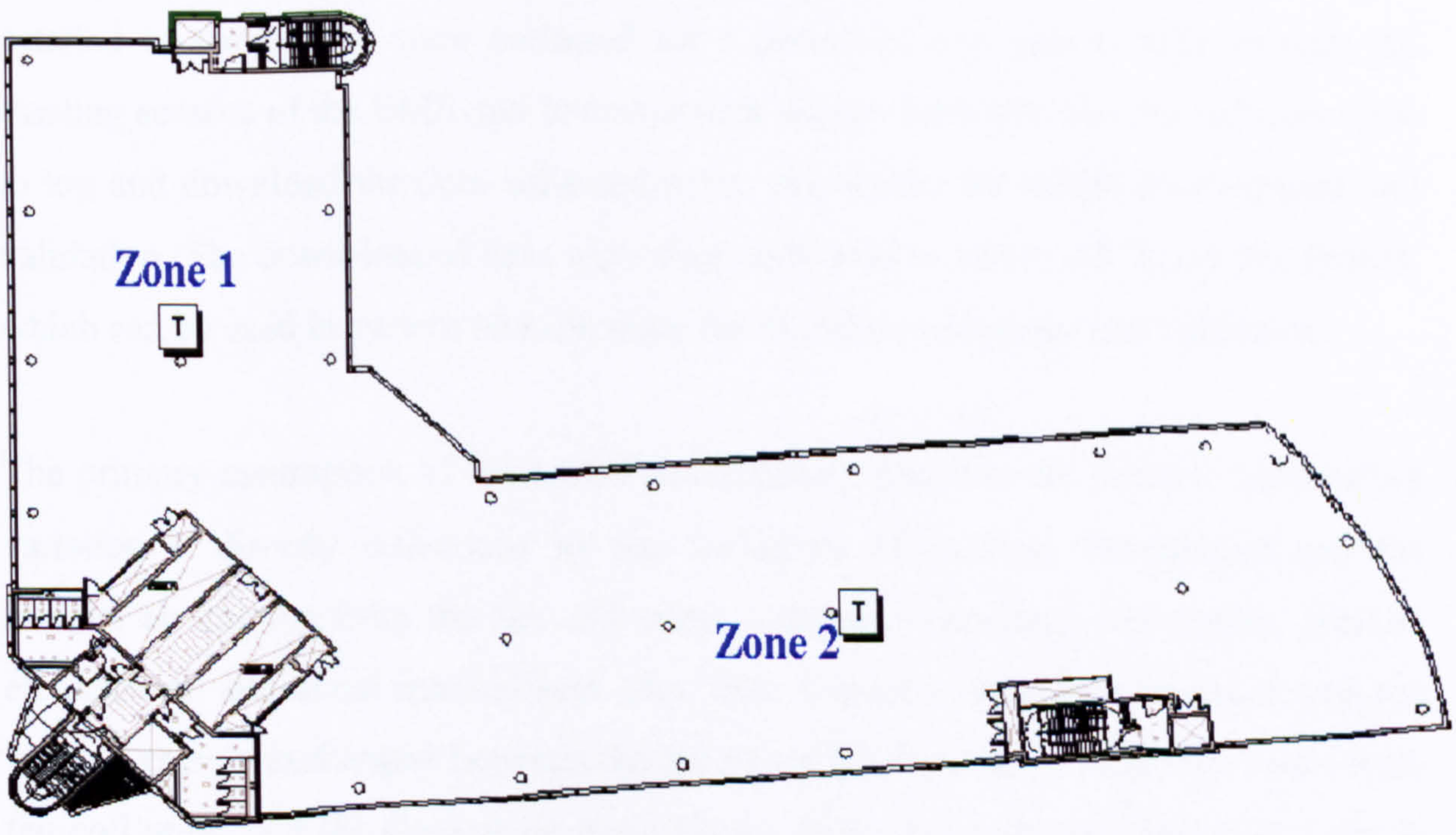

Figure 4.2 Layout of zone 1 and 2, seventh floor

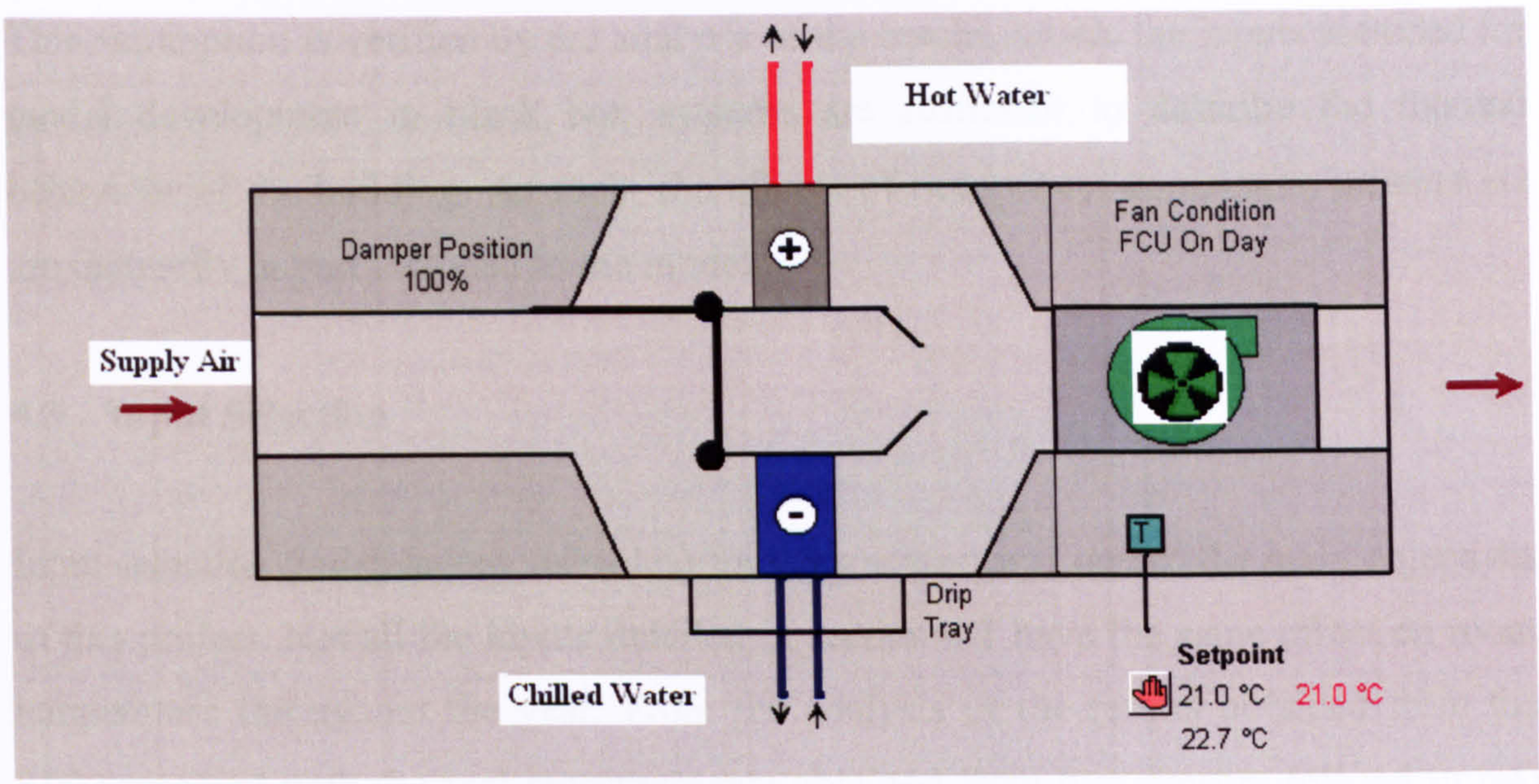

Figure 4.3 Picture of a fan coil unit

4.2 Data Collection Description

The data from the Visa building were collected for one year, and the choice of sampling interval was coupled to the time constants of the system. It was thus valuable to first obtain the step response of the system. In the Visa building the choice of sampling interval was 5 minutes, so that it corresponded to 5-8 sampling points over the rise time of the system's step response (Ljung and Glad, 1994). The data collected were stored in the BMS and downloaded every two weeks. The inputs and outputs detailed in section 4.1 were collected for a period of one year (2005) through the existing sensors of the BMS and Invensys data logger. Invensys was the software used to log and download the data collected every two weeks for model development and validation. The down-loaded data were then converted to Microsoft Excel file format, which can be used in system identification for model development and validation.

The primary assumption of the model development was that the internal temperature variation is directly influenced by the variations of external temperature and the internal air coming from the fan coil units. Although occupancy, computers, printers etc cause an additional internal heat gain, their impact is strongly correlated with the internal energy exchanged between the incoming air, that flows inside the room from fan coil units, and the circulating water (flows inside fan coil units and AHU) that is heated up and cooled down from the boiler and chiller plants respectively.

This assumption is verified by the analysis of the results, where the inputs included for model development in black box systems are sufficient to describe the thermal behaviour of the building. As such, the effects of occupancy, computers, printers etc are indirectly in part included in the model.

4.3 Input Selection

Input selection (independent variables) for each season was one of the main objectives of this project. Not all the inputs detailed in section 4.1 have the same effect on room temperature throughout the year. From the analysis of the results obtained from the SIT compared with the real measurements obtained from two sensors (placed in two zones which define the temperature for zones 1 and 2, see fig. 4.2), it was sufficient to include five inputs for model development for the entire year (zone 1 or 2).

In the Visa building, the models were developed for different seasons and each season was subdivided into three parts; beginning, middle and end of the season. Some inputs gave good models for a limited period of time (several weeks). Consequently, as reported below, the process of input selection and period of validity in obtaining models that give good thermal prediction (within the same period) were the key points in season subdivision. Although the same inputs can be used throughout the season this is not the case with the models because some of them are not valid throughout the season. This is other reason for dividing the season into beginning, middle and end (see section 4.4.4). In addition, obtaining a good model depends on the inputs used in the SIT for model development. If we include more inputs than required for developing models then the model performance does not improve or can even get worse. Generally, the procedure for input selections for each season was as follows:

- It began by including all the inputs in the process of model development
- The next stage was model development with the SIT.
- The process of input selection started by removing the first input and analysing if there was any improvement in the model's performance and how long (in weeks) it took. The procedure was based on sections 3.4, 3.5 and 3.6 (chapter 3), related to model estimation and validation.
- Finally, the process of removing the inputs stopped when the model's performance deteriorated by removing further inputs.

In this chapter, the models developed with the selected inputs have the following properties:

- The models can predict the thermal behaviour of the room for several weeks (four to nine weeks)
- Within the period of input validation, the change in models' performance is very small from one week to another (model validation procedure).

In the following sections the inputs selected for each season will be examined with the models that give the best thermal behaviour of the room.

4.4 Weekdays' Model Development and Validation

Model estimation and validation were carried out using the data for one week of working days (Monday Time 01:20 to Friday Time 19:00) called weekdays. The first part of the data was used for model estimation and the remainder for model validation. Finally, for each season, due to the similarities of the results, not all the graphs relating to weekdays are presented.

Different models were found to be most appropriate for different periods of the year. Thus, different models will be used for winter, spring, summer and autumn. In the following sections the best models in terms of best fits for each of these seasons are presented.

Finally, in relation to this building, the data were logged every 5 minutes, and model estimation and validation were analysed for four cases:

a) 213 Sampled-data model estimation (18 hours in day 1 – Time 01:20-19:00) and 213 sampled-data model validation (18 hours in day 2 – Time 01:20-19:00)

b) 900 Sampled-data model estimation (75 hours) and 465 sampled-data model validation (39 hours)

c) 800 Sampled-data model estimation (67 hours) and 565 sampled-data model validation (47 hours)

d) 1365 sampled-data model estimation (113.5 hours, weekdays) and 1365 sampled-data model validation in following weekdays (see Appendix 1A).

4.4.1 Model Development and Validation for the Spring Season

Different weeks of spring were examined for model estimation and validation. The results are divided into the middle and end of the spring season. The data related to the weeks 21-25 March 2005, 04-08 April 2005 and 11-15 April 2005 were lost due to sensor faults.

Middle and end of the spring season

The weeks between 18 April and 10 June 2005 were investigated and the results are given in Table 4.1. In addition, the week 25-29 April 2005 is shown in Figs. 4.4 and 4.6, and the errors between model output and measurements are presented in Figs. 4.5 and 4.7. Five inputs (outside temperature, hot water temperature, chilled water temperature, supply air temperature AHU2 and supply air flow rate AHU2) affects the results for the determination of the best model.

Throughout the spring season, the BJ models (bj [1 1 1 1 4] and bj [1 1 1 1 5]) give good results (see FPE and model fits in Table 4.1) for the prediction of room temperature. In conclusion, the FPE is of order 10^{-3} and the maximum model error is 0.6 degrees Celsius.

1-213 Data Estimation	1-900 Data Estimation	1-800 Data Estimation
289-501 Data Validation	901-1365 Data Validation	801-1365 Data Validation
Middle and end of spring	**Middle and end of spring**	**Middle and end of spring**
Five Inputs	**Five Inputs**	**Five Inputs**
Chilled water temp	Chilled water temp	Chilled water temp
Hot water temp	Hot water temp	Hot water temp
Supply air flow rate AHU2	Supply air flow rate AHU2	Supply air flow rate AHU2
Outside temp	Outside temp	Outside temp
Supply air temp AHU2	Supply air temp AHU2	Supply air temp AHU2
FPE ≈ 0.001	FPE ≈ 0.0015	FPE ≈ 0.0012
bj [1 1 1 1 4]: 50-60	bj [1 1 1 1 4]: 47-57	bj [1 1 1 1 4]: 55-60
bj [1 1 1 1 5]: 50-60	bj [1 1 1 1 5]: 52-58	bj [1 1 1 1 5]: 55-60

Table 4.1 Spring weekdays

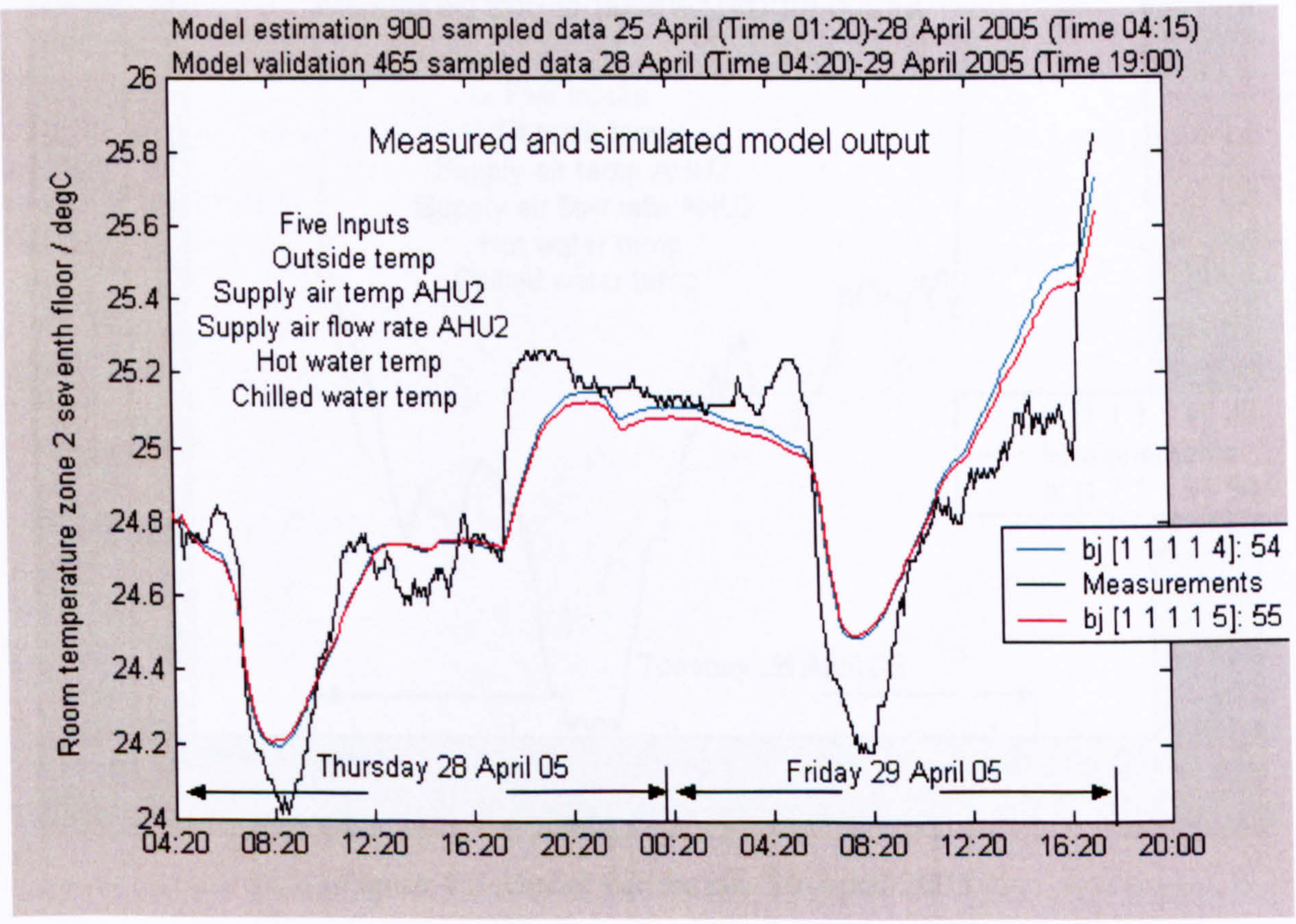

Figure 4.4 Model validation, weekdays 28-29 April 2005

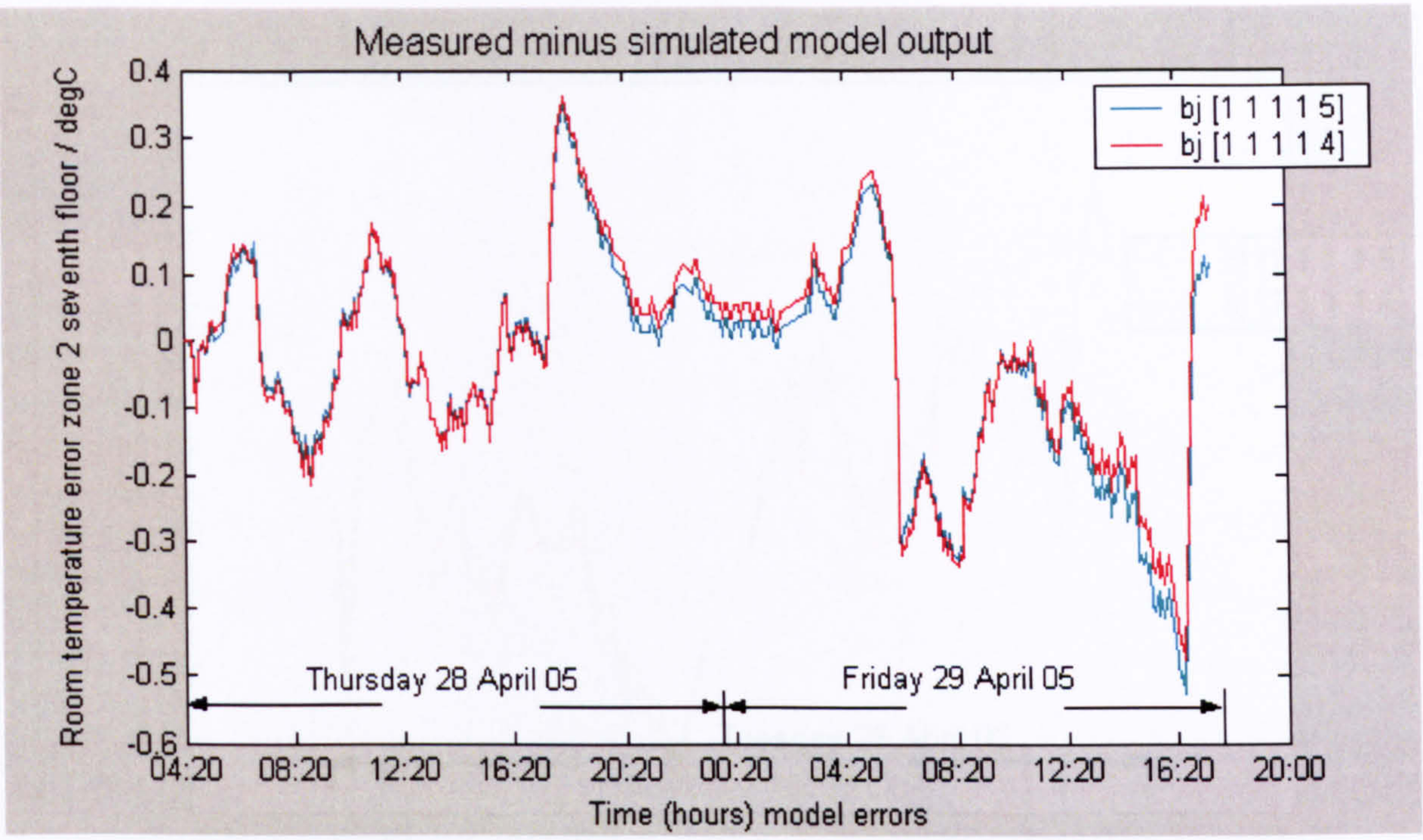

Figure 4.5 Model errors, weekdays 28-29 April 2005

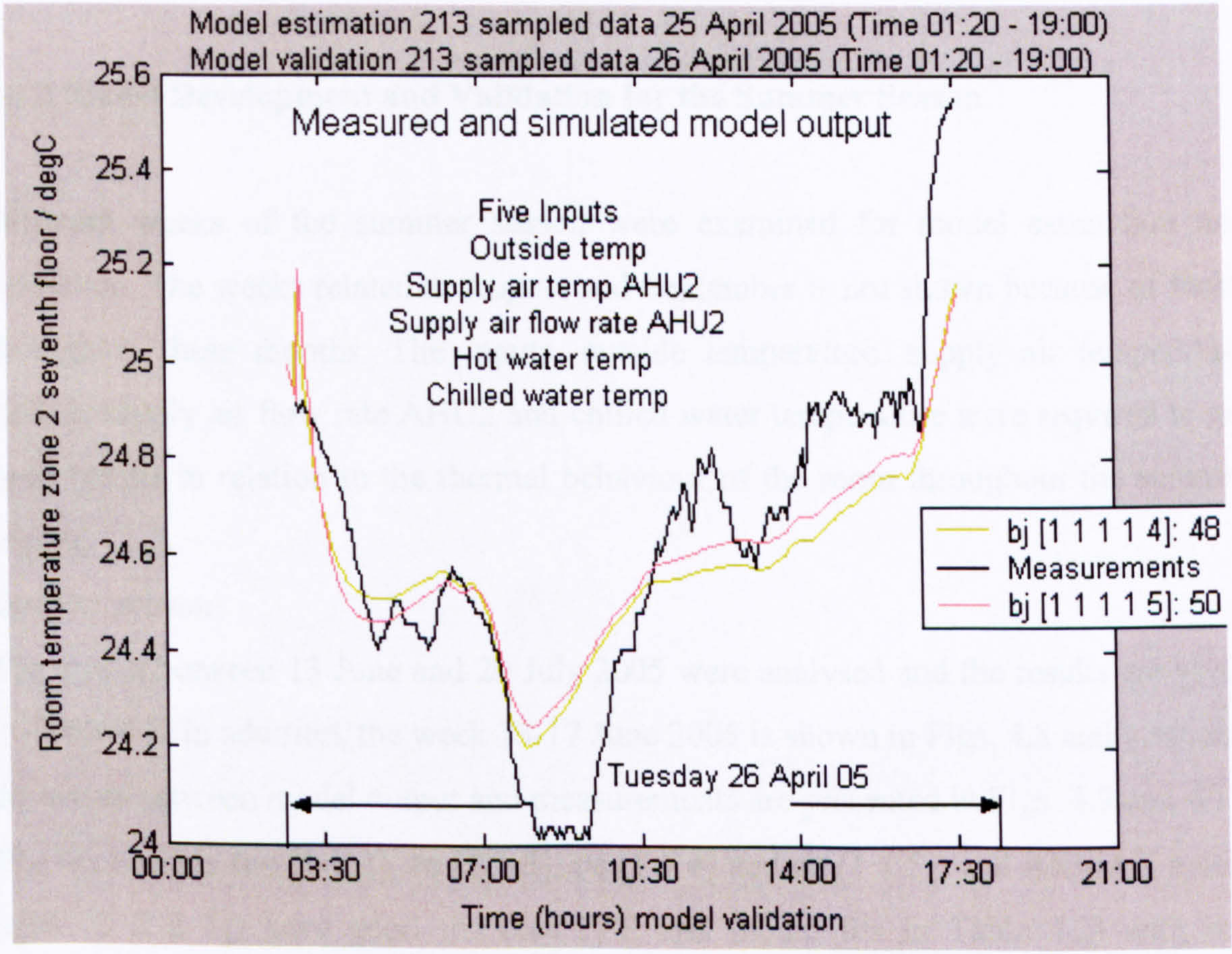

Figure 4.6 Model validation, 26 April 2005

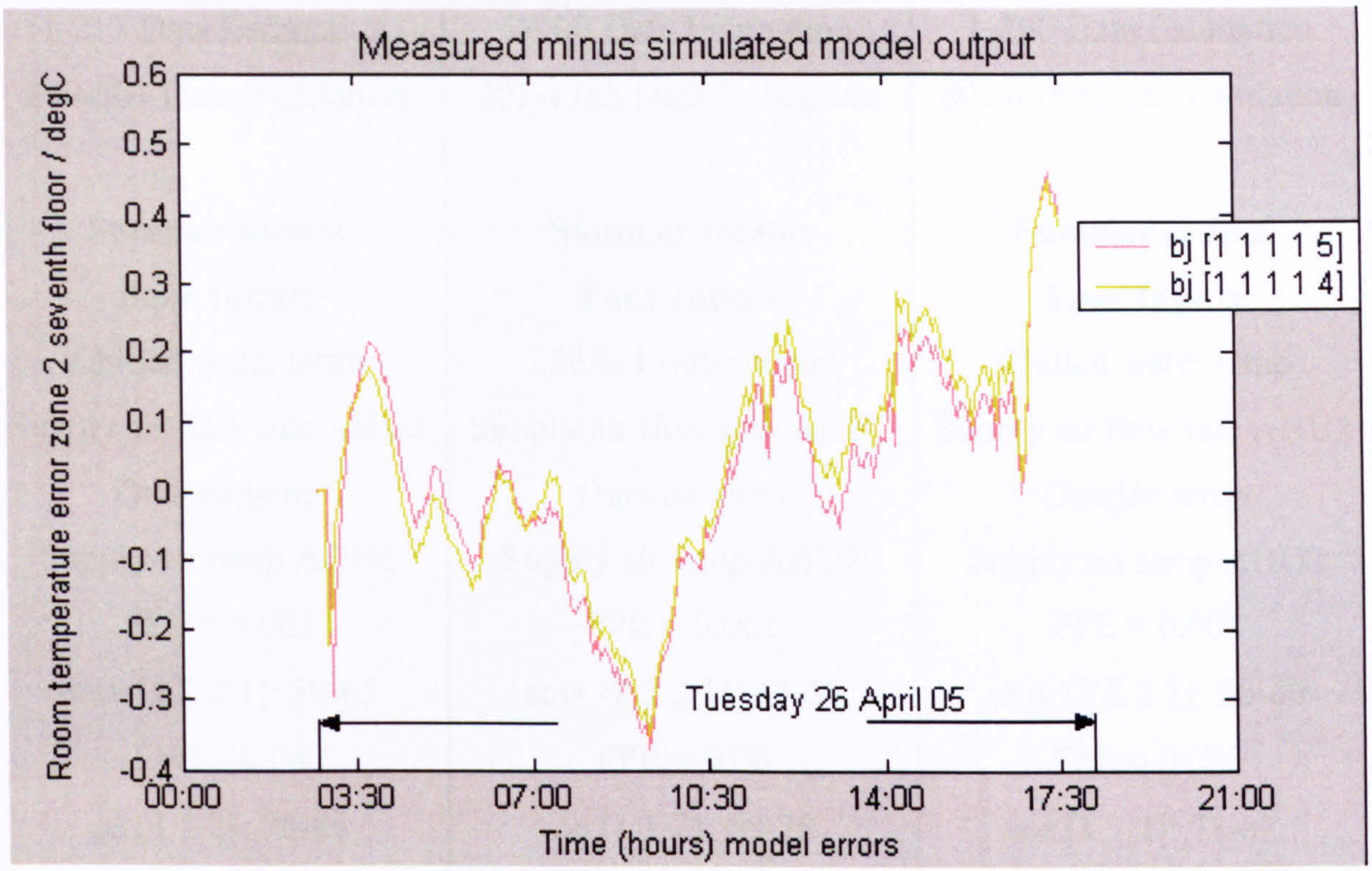

Figure 4.7 Model errors, 26 April 2005

4.4.2 Model Development and Validation for the Summer Season

Different weeks of the summer season were examined for model estimation and validation. The weeks related to August and September is not shown because of faults throughout these months. The inputs, outside temperature, supply air temperature AHU2, supply air flow rate AHU2 and chilled water temperature were required to get good results in relation to the thermal behaviour of the room throughout the summer season.

Summer season

The weeks between 13 June and 29 July 2005 were analysed and the results are given in Table 4.2. In addition, the week 13-17 June 2005 is shown in Figs. 4.8 and 4.10, and the errors between model output and measurements are presented in Figs. 4.9 and 4.11. The OE models (oe [1 1 2], oe [1 1 3], oe [1 1 4] and oe [1 1 5]) and ARMAX model (amx [2 2 2 1]) have good fits (see FPE and model fits in Table 4.2) with real measurements. Finally, the FPE is between 10^{-2} and 10^{-3} and the maximum model error is 0.8 degrees Celsius.

1-213 Data Estimation 289-501 Data Validation	1-900 Data Estimation 901-1365 Data Validation	1-800 Data Estimation 801-1365 Data Validation
Summer season	**Summer season**	**Summer season**
Four Inputs	**Four Inputs**	**Four Inputs**
Chilled water temp	Chilled water temp	Chilled water temp
Supply air flow rate AHU2	Supply air flow rate AHU2	Supply air flow rate AHU2
Outside temp	Outside temp	Outside temp
Supply air temp AHU2	Supply air temp AHU2	Supply air temp AHU2
FPE ≈ 0.002	FPE ≈ 0.001	FPE ≈ 0.001
amx [2 2 2 1]: 50-65	amx [2 2 2 1]: 45-50	amx [2 2 2 1]: 50-60
FPE ≈ 0.04	FPE ≈ 0.06	FPE ≈ 0.065
oe [1 1 2]: 75-85	oe [1 1 2]: 65-78	oe [1 1 2]: 73-83
oe [1 1 3]: 70-80	oe [1 1 3]: 65-77	oe [1 1 3]: 74-85
oe [1 1 4]: 70-80	oe [1 1 4]: 65-72	oe [1 1 4]: 70-80
oe [1 1 5]: 65-77	oe [1 1 5]: 60-70	oe [1 1 5]: 70-80

Table 4.2 Summer weekdays

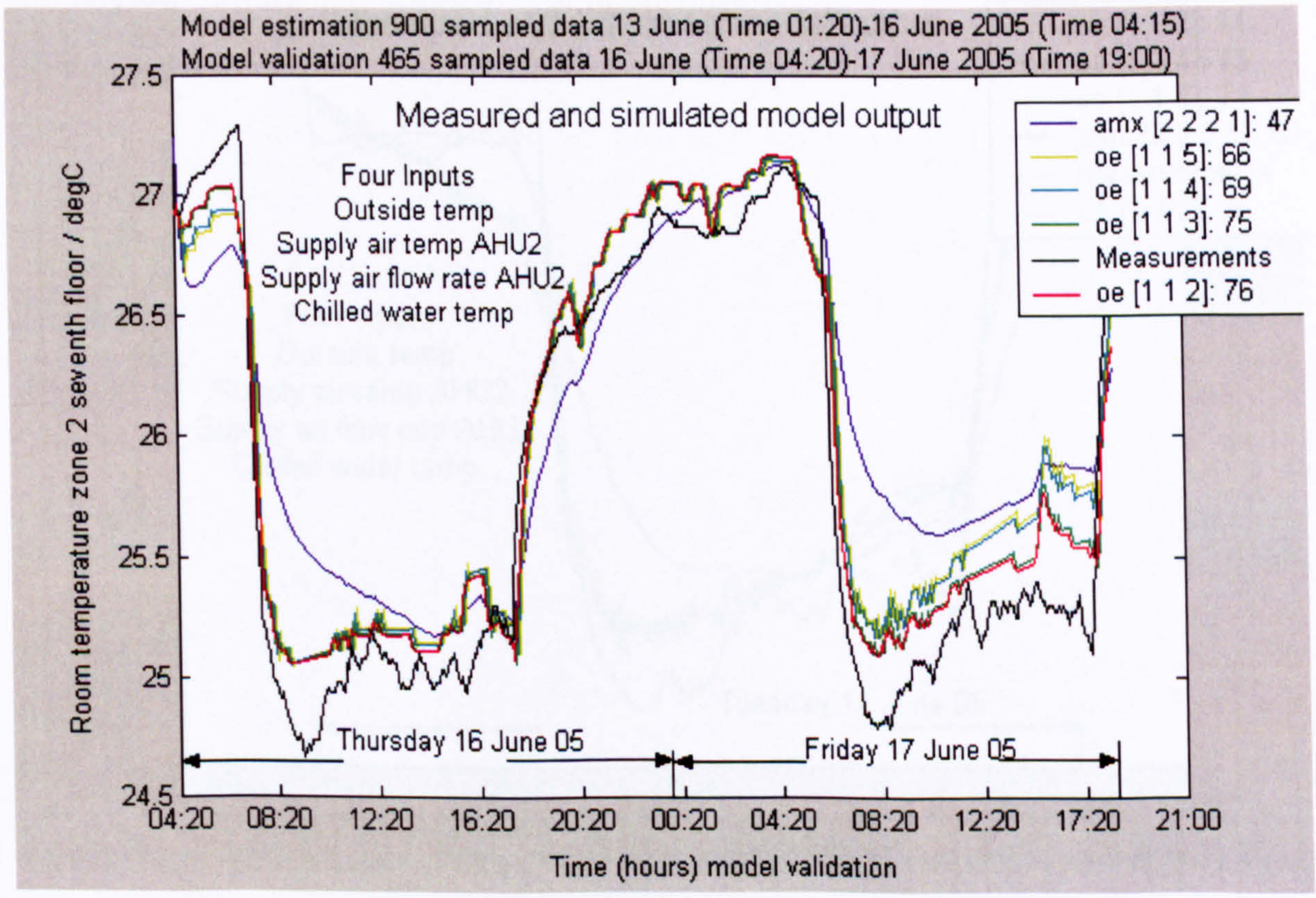

Figure 4.8 Model validation, weekdays 16-17 June 2005

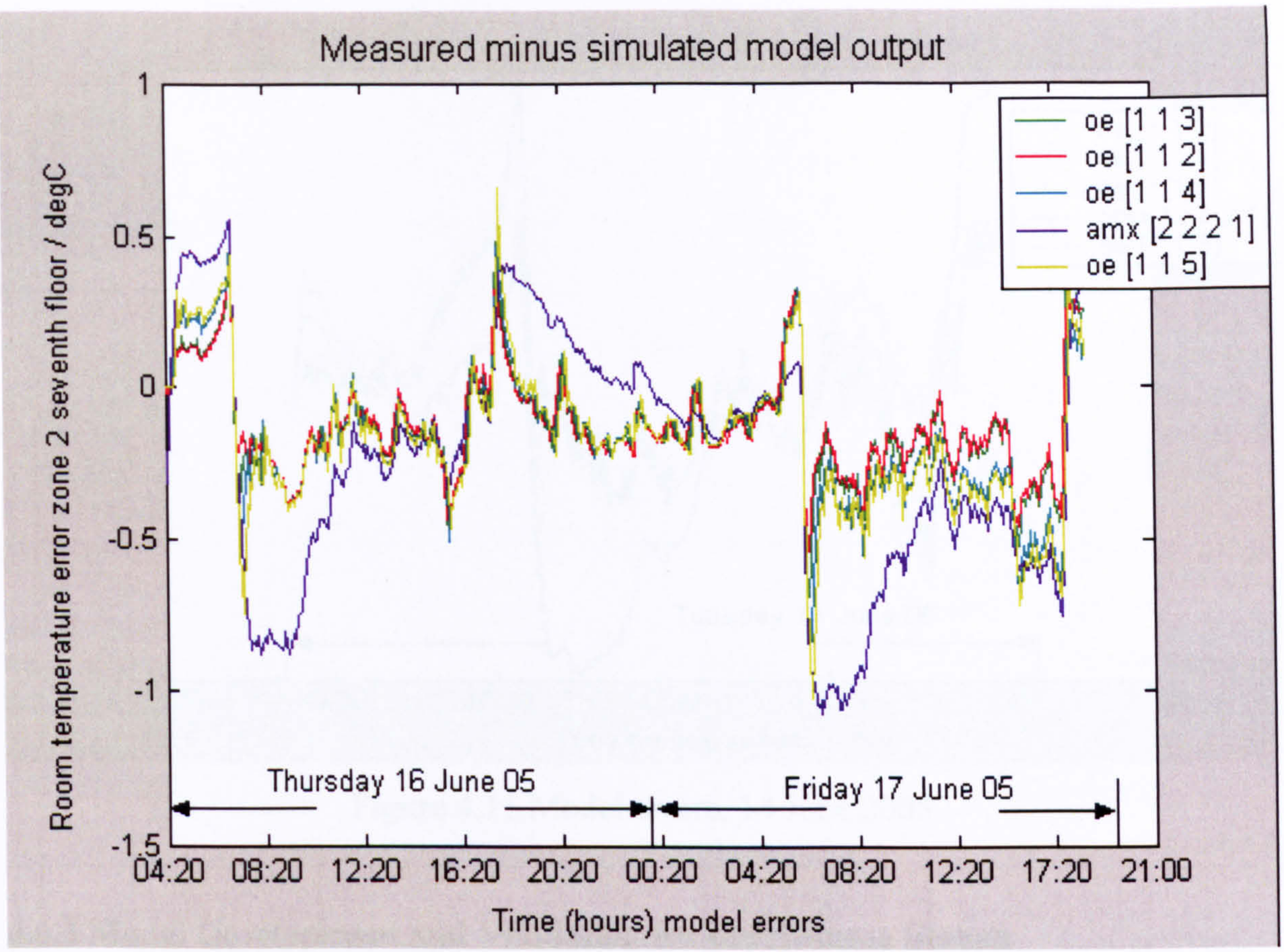

Figure 4.9 Model errors, weekdays 16-17 June 2005

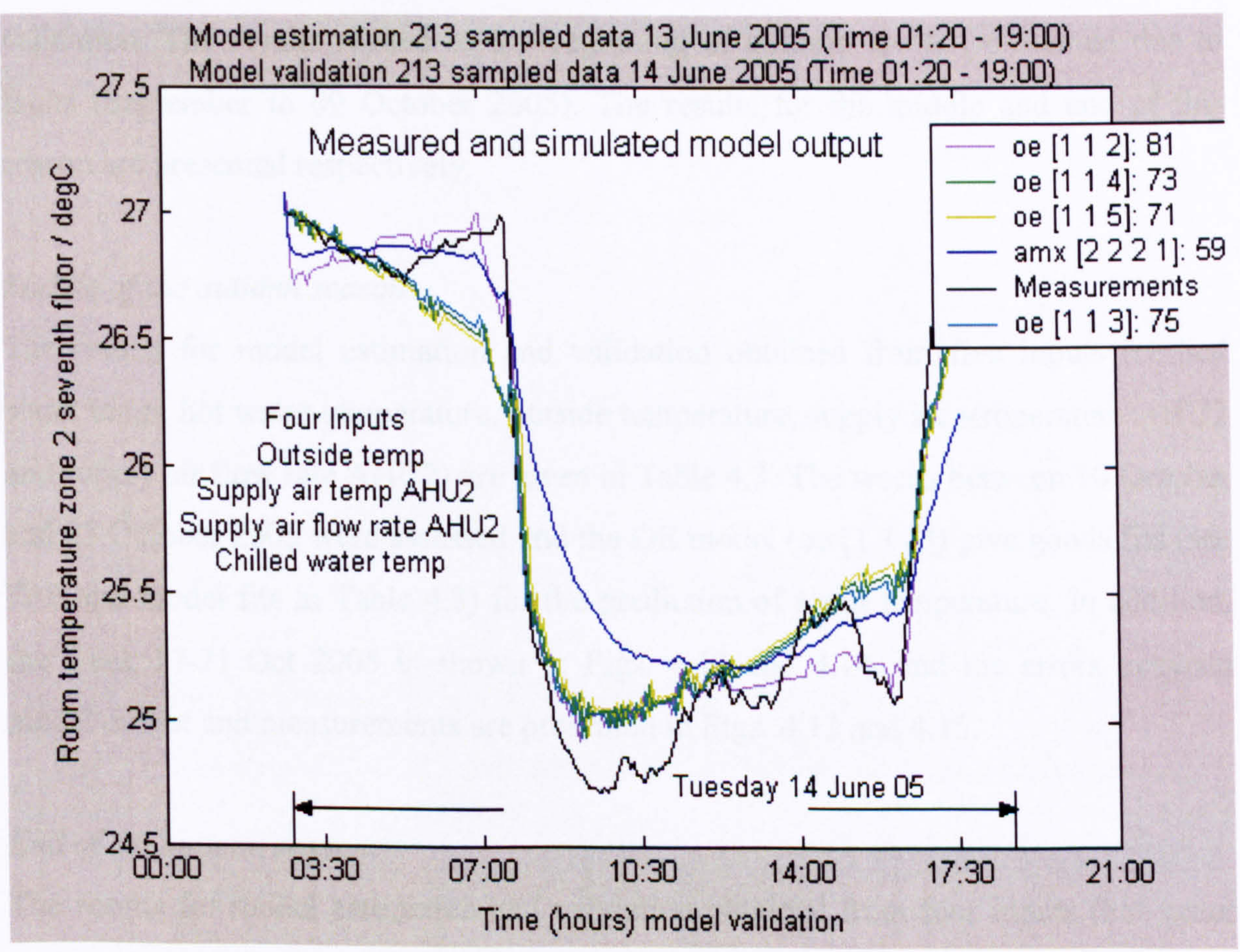

Figure 4.10 Model validation, 14 June 2005

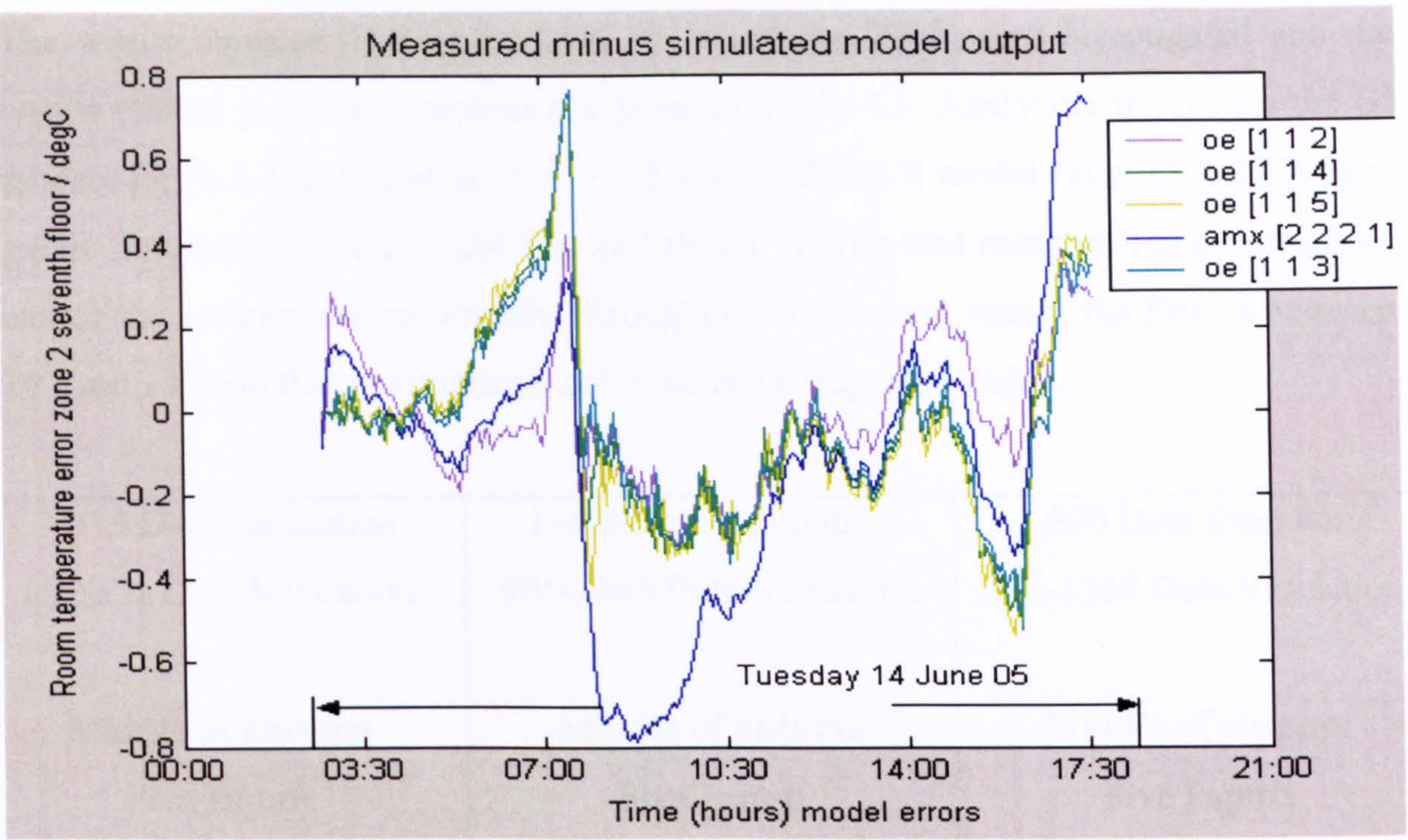

Figure 4.11 Model errors, 14 June 2005

4.4.3 Model Development and Validation for the Autumn Season

Different weeks of the autumn season have been examined for model estimation and validation. The results related to the beginning of autumn are not presented due to faults (September to 09 October 2005). The results for the middle and end of this season are presented respectively.

Middle of the autumn season

The results for model estimation and validation obtained from five inputs (chilled water temp, hot water temperature, outside temperature, supply air temperature AHU2 and supply air flow rate AHU2) are given in Table 4.3. The weeks between 10 October and 28 October 2005 were assessed and the OE model (oe [1 1 2]) give goods fits (see FPE and model fits in Table 4.3) for the prediction of room temperature. In addition, the week 17-21 Oct 2005 is shown in Figs. 4.12 and 4.14, and the errors between model output and measurements are presented in Figs. 4.13 and 4.15.

End of the autumn season

The results for model estimation and validation obtained from four inputs (hot water temp, outside temperature, supply air flow rate AHU2 and supply air temperature AHU2) are presented.

The weeks between 31 October and 09 December 2005 were investigated and the results related to the best models are given in Table 4.3. Analysing the results the BJ models (bj [1 1 1 1 2] and bj [1 1 1 1 3]) and ARMAX model (amx [2 2 2 1]) have goods fits (see FPE and model fits in Table 4.3) with real measurements throughout end of the autumn season. Finally, throughout the autumn season the FPE is between 10^{-2} and 10^{-3} and the maximum model error is 0.6 degrees Celsius.

1-213 Data Estimation 289-501 Data Validation	1-900 Data Estimation 901-1365 Data Validation	1-800 Data Estimation 801-1365 Data Validation
Middle of autumn	**Middle of autumn**	**Middle of autumn**
Five Inputs	**Five Inputs**	**Five Inputs**
Outside temp	Outside temp	Outside temp
Supply air flow rate AHU2	Supply air flow rate AHU2	Supply air flow rate AHU2
Supply air temp AHU2	Supply air temp AHU2	Supply air temp AHU2
Hot water temp	Hot water temp	Hot water temp
Chilled water temp	Chilled water temp	Chilled water temp
FPE ≈ 0.05	FPE ≈ 0.04	FPE ≈ 0.05
oe [1 1 2]: 50-65	oe [1 1 2]: 55-60	oe [1 1 2]: 55-60
End of autumn	**End of autumn**	**End of autumn**
Four Inputs	**Four Inputs**	**Four Inputs**
Outside temp	Outside temp	Outside temp
Supply air flow rate AHU2	Supply air flow rate AHU2	Supply air flow rate AHU2
Supply air temp AHU2	Supply air temp AHU2	Supply air temp AHU2
Hot water temp	Hot water temp	Hot water temp
FPE ≈ 0.001	FPE ≈ 0.001	FPE 0.001
bj [1 1 1 1 2]: 65-75	bj [1 1 1 1 2]: 65-75	bj [1 1 1 1 2]: 60-70
bj [1 1 1 1 3]: 60-75	bj [1 1 1 1 3]: 70-80	bj [1 1 1 1 3]: 60-70
FPE ≈ 0.001	FPE ≈ 0.001	FPE ≈ 0.001
amx [2 2 2 1]: 45-50	amx [2 2 2 1]: 40-50	amx [2 2 2 1]: 30-40

Table 4.3 Autumn weekdays

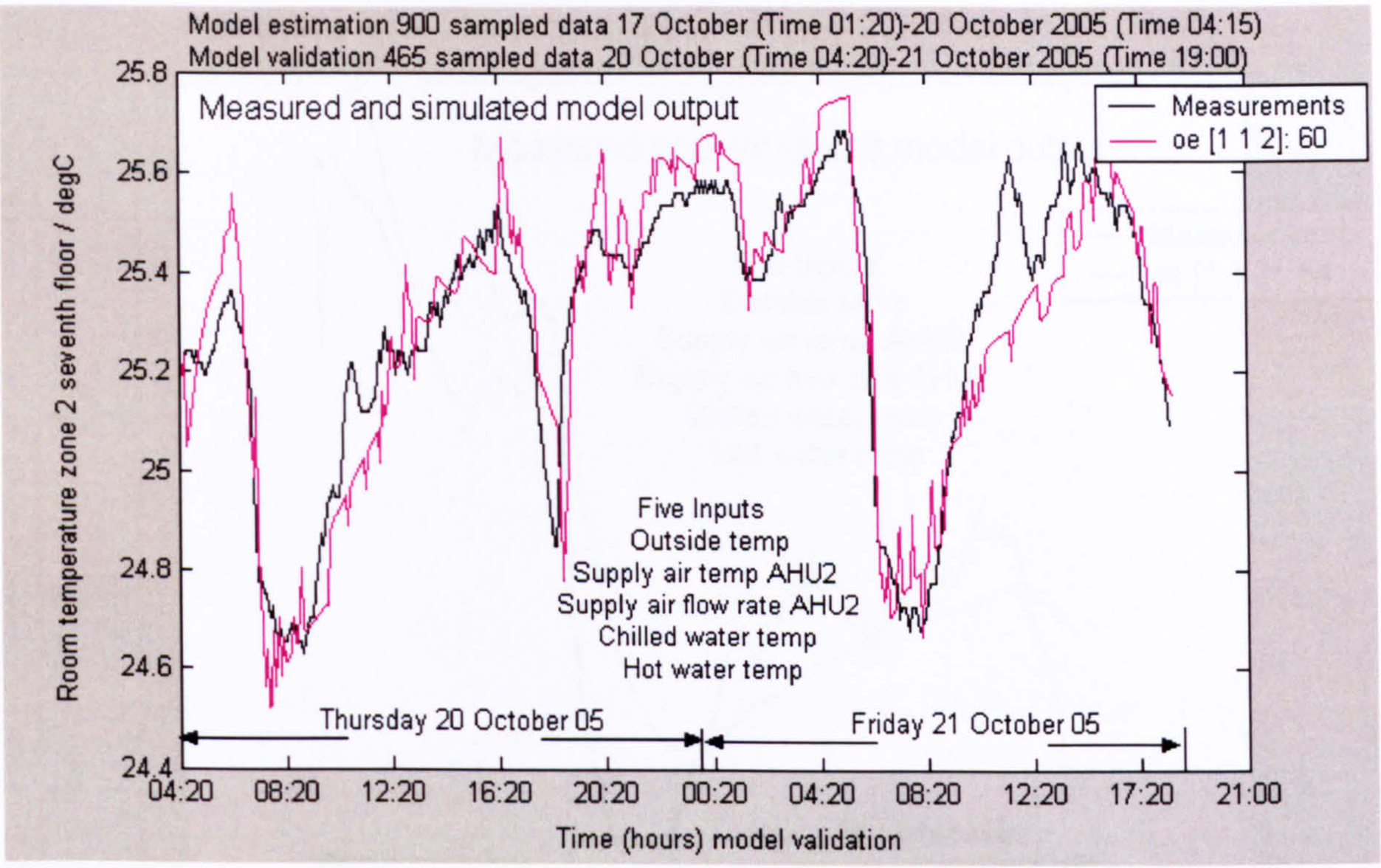

Figure 4.12 Model validation, weekdays 20-21 October 2005

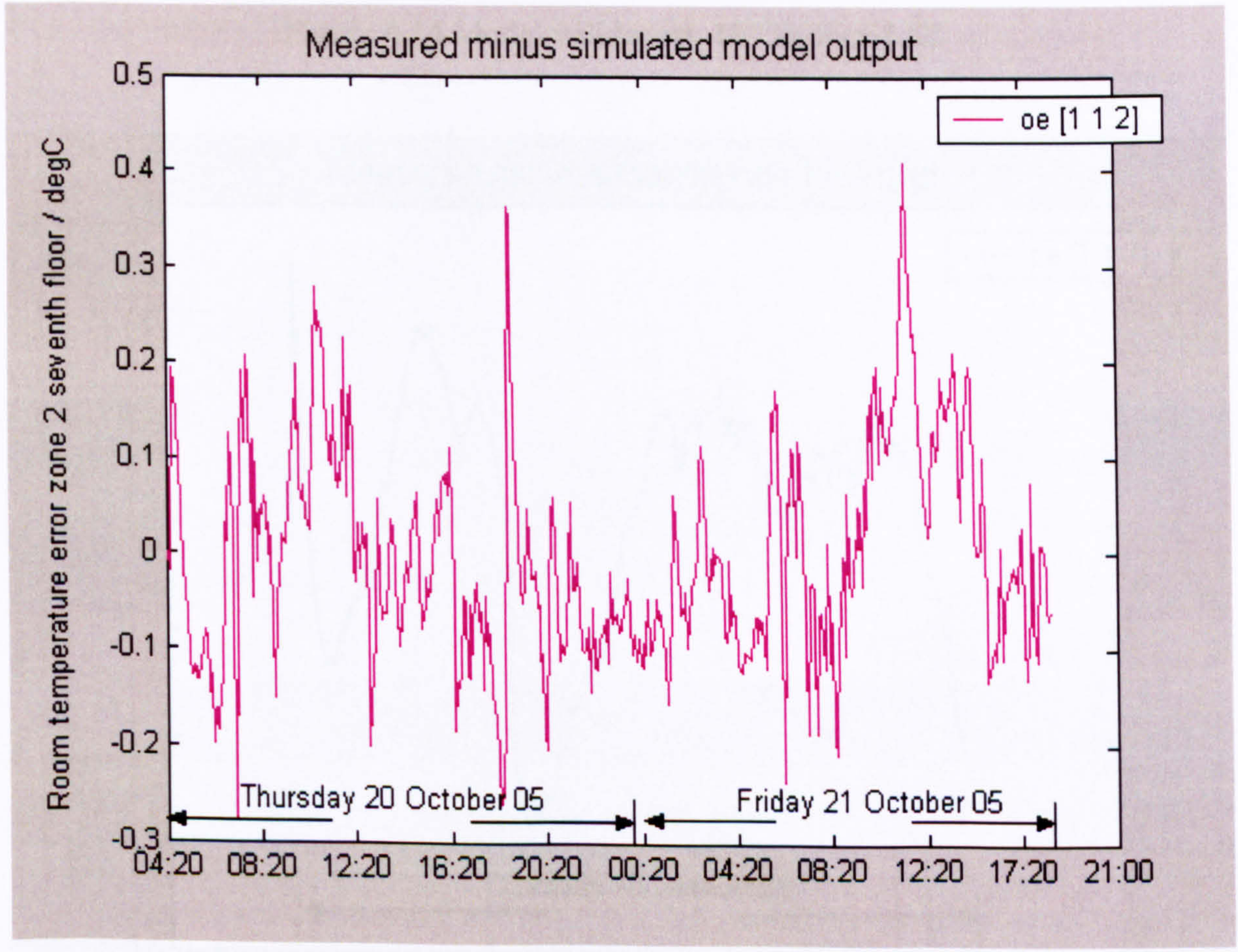

Figure 4.13 Model errors, weekdays 20-21 October 2005

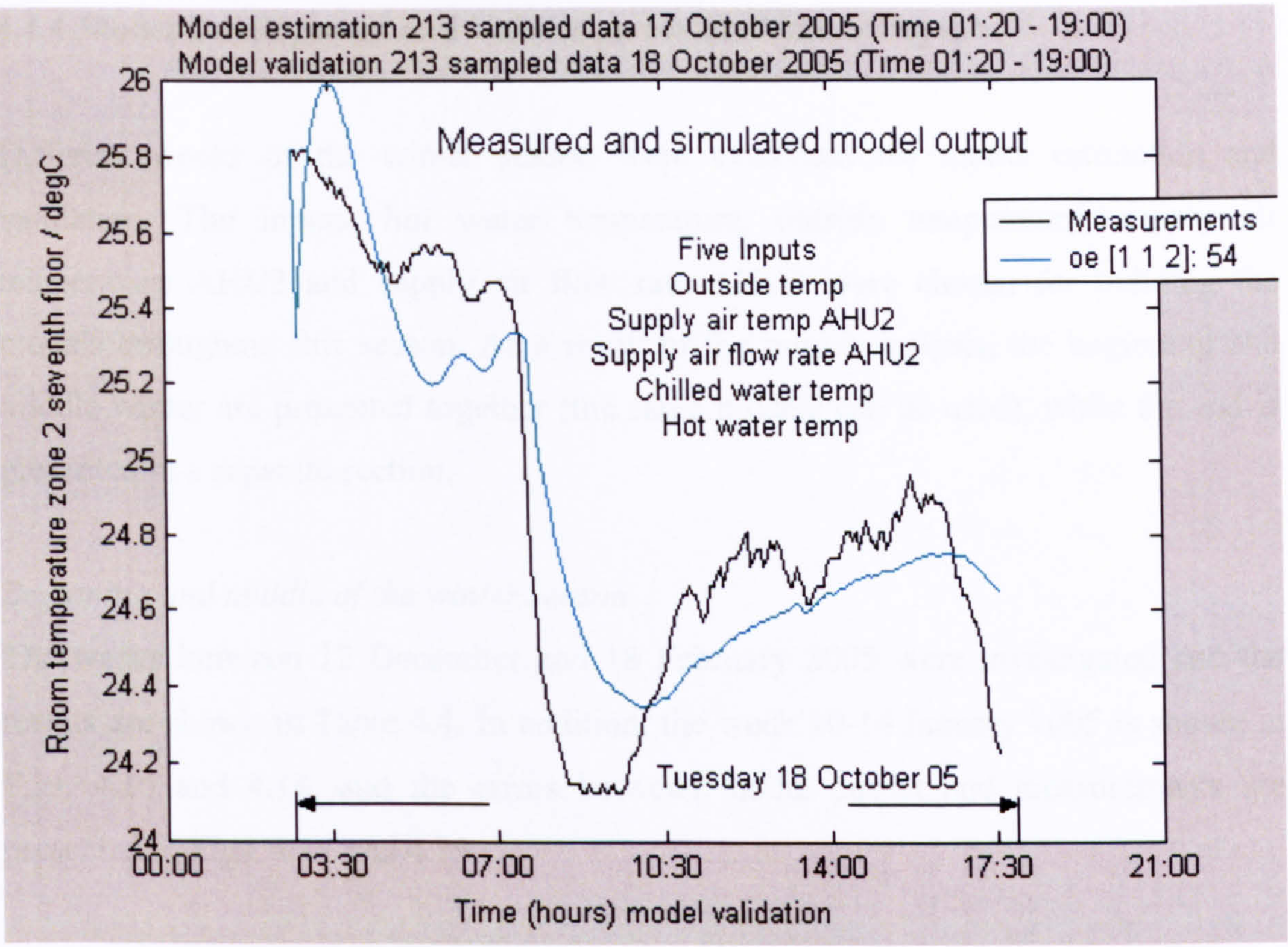

Figure 4.14 Model validation, 18 October 2005

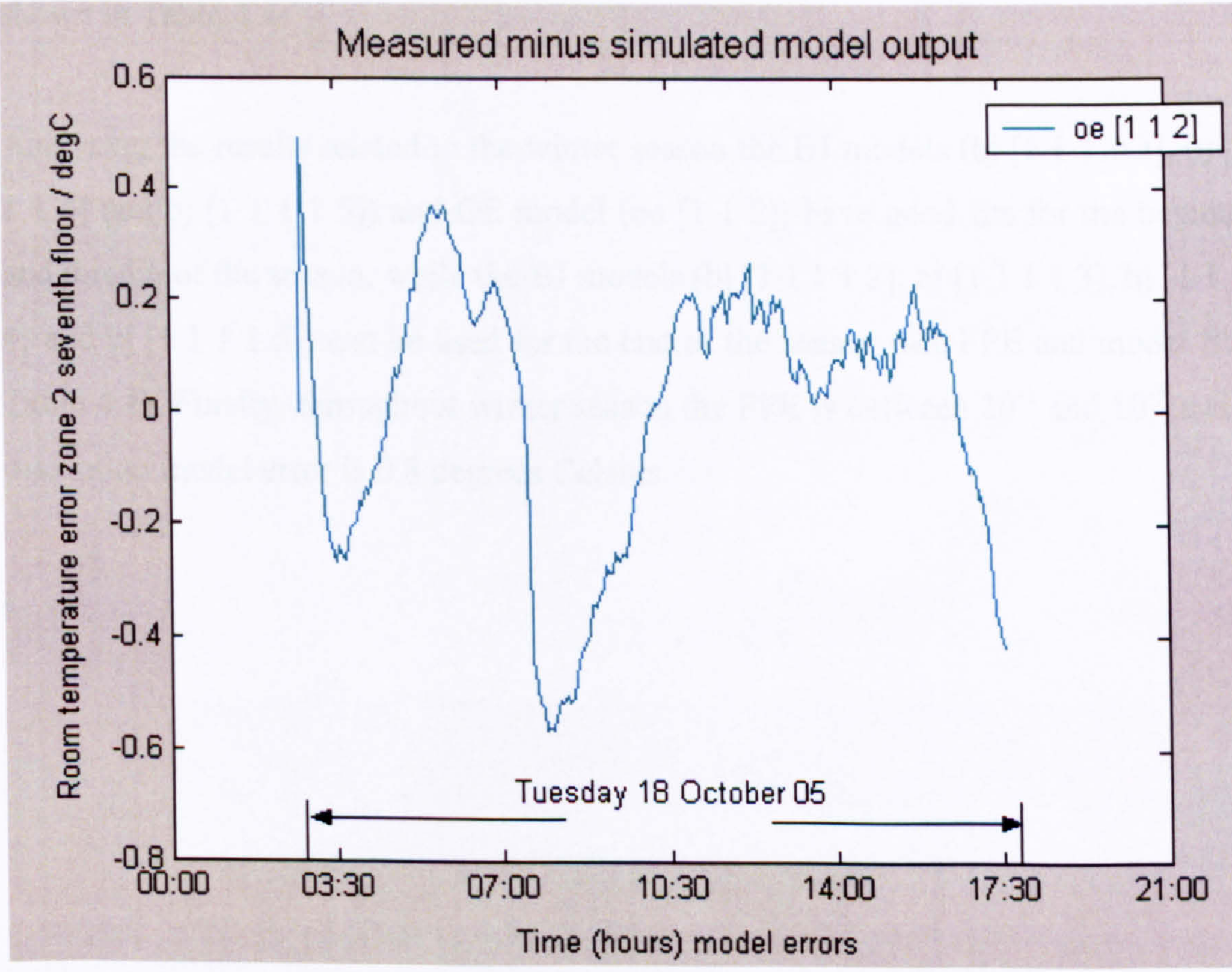

Figure 4.15 Model errors, 18 October 2005

4.4.4 Model Development and Validation for the Winter Season

Different weeks of the winter season were examined for model estimation and validation. The inputs, hot water temperature, outside temperature, supply air temperature AHU2 and supply air flow rate AHU2 were chosen for building the models throughout this season. As a result of the model analysis, the beginning and middle winter are presented together (the same models can be used), while the end is presented in a separate section.

Beginning and middle of the winter season

The weeks between 12 December and 18 February 2005 were investigated and the results are shown in Table 4.4. In addition, the week 10-14 January 2005 is shown in Figs. 4.16 and 4.18, and the errors between model output and measurements are presented in Figs. 4.17 and 4.19.

End of the winter season

The weeks between 21 February and 18 March 2005 were assessed and the results are shown in Table 4.4.

Analysing the results related to the winter season the BJ models (bj [1 1 1 1 3], bj [1 1 1 1 4] and bj [1 1 1 1 5]) and OE model (oe [1 1 2]) have good fits for the beginning and middle of the season, while the BJ models (bj [1 1 1 1 2], bj [1 1 1 1 3], bj [1 1 1 1 4] and bj [1 1 1 1 5]) can be used for the end of the season (see FPE and model fits in Table 4.4). Finally, throughout winter season the FPE is between 10^{-1} and 10^{-3} and the maximum model error is 0.8 degrees Celsius.

1-213 Data Estimation 289-501 Data Validation	1-900 Data Estimation 901-1365 Data Validation	1-800 Data Estimation 801-1365 Data Validation
Four Inputs	**Four Inputs**	**Four Inputs**
Outside temp	Outside temp	Outside temp
Supply air flow rate AHU2	Supply air flow rate AHU2	Supply air flow rate AHU2
Supply air temp AHU2	Supply air temp AHU2	Supply air temp AHU2
Hot water temp	Hot water temp	Hot water temp
Beginning and middle of winter	**Beginning and middle of winter**	**Beginning and middle of winter**
FPE ≈ 0.001	FPE ≈ 0.0015	FPE ≈ 0.0012
bj11113: 80-85 FPE 0.001	bj [1 1 1 1 3]: 60-65	bj [1 1 1 1 3]: 50-60
bj11114: 80-88 FPE 0.001	bj11114: 40-50	bj11114: 55-65
bj11115: 75-80 FPE 0.001	bj11115: 55-65	bj11115: 55-65
FPE ≈ 0.17	FPE ≈ 0.2	FPE ≈ 0.2
oe [1 1 2]: 80-85	oe [1 1 2]: 65-75	oe [1 1 2]: 45-55
End of winter	**End of winter**	**End of winter**
FPE ≈ 0.001	FPE ≈ 0.0015	FPE ≈ 0.0012
bj [1 1 1 1 2]: 85-95	bj [1 1 1 1 2]: 75-88	bj [1 1 1 1 2]: 80-90
bj [1 1 1 1 3]: 85-95	bj [1 1 1 1 3]: 80-90	bj [1 1 1 1 3]: 80-90
bj [1 1 1 1 4]: 85-95	bj [1 1 1 1 4]: 70-83	bj [1 1 1 1 4]: 65-75
bj [1 1 1 1 5]: 80-90	bj [1 1 1 1 5]: 70-83	bj [1 1 1 1 5]: 65-75

Table 4.4 Winter weekdays

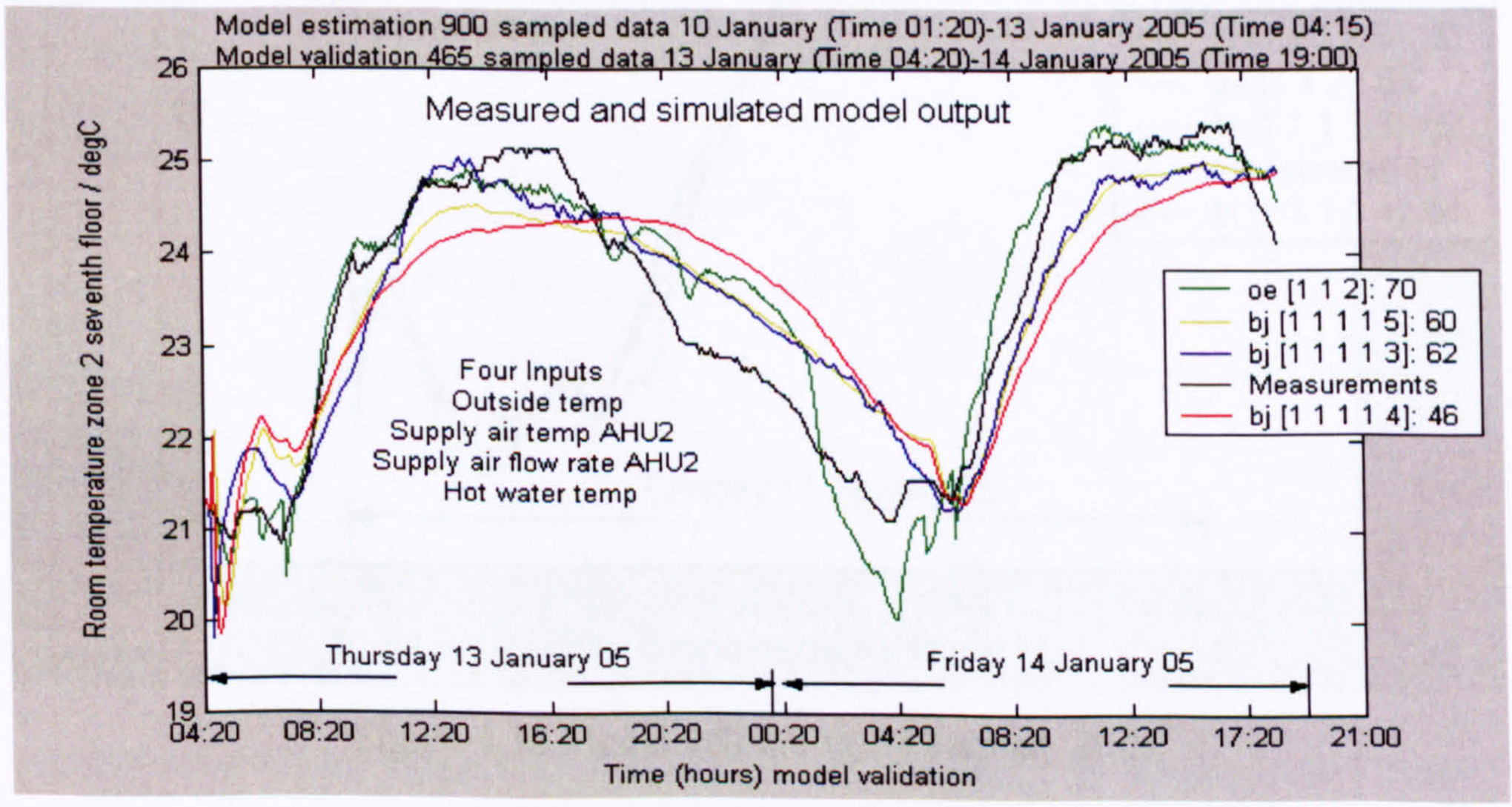

Figure 4.16 Model validation, weekdays 13-14 January 2005

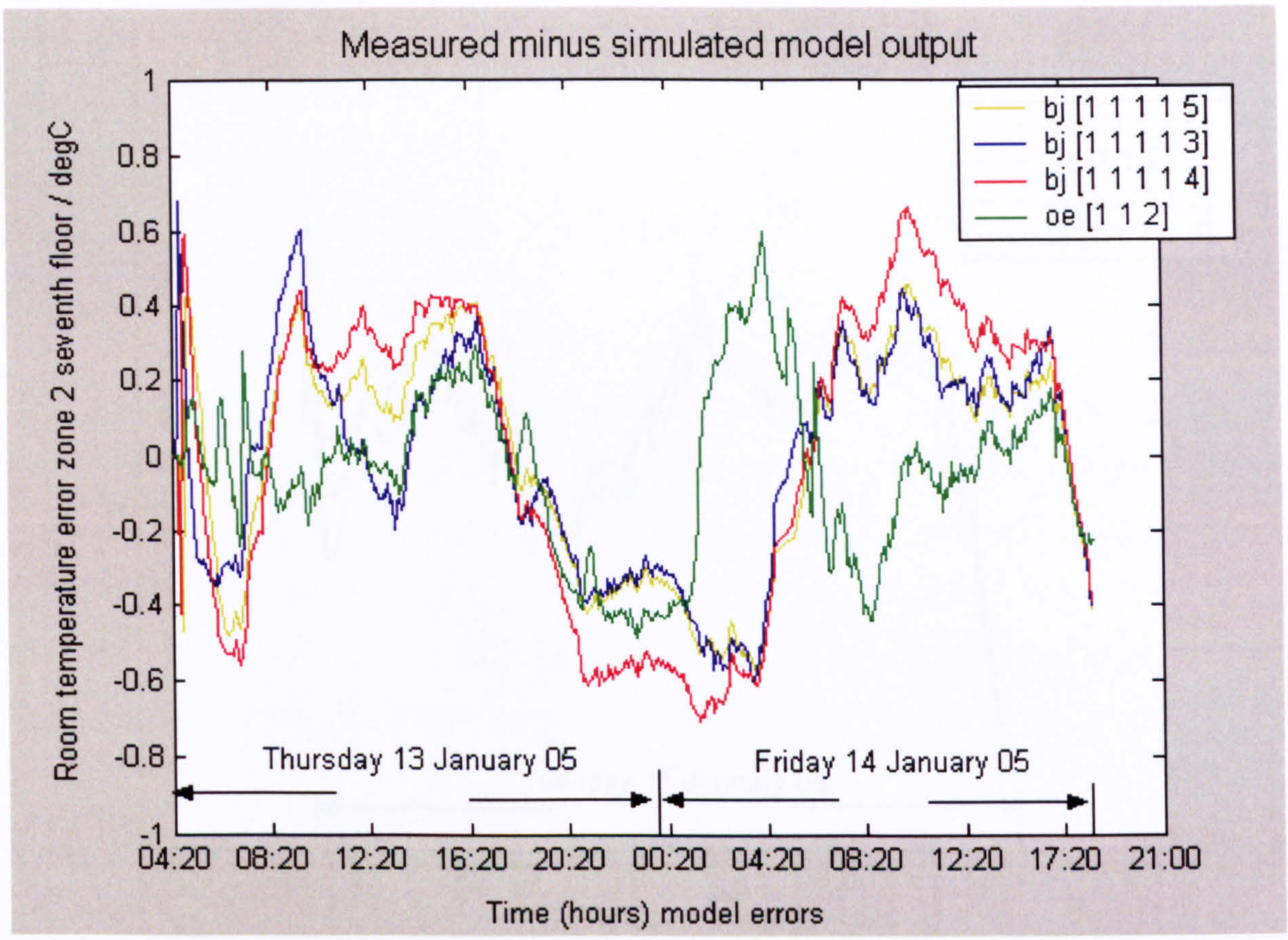

Figure 4.17 Model errors, 13-14 January 2005

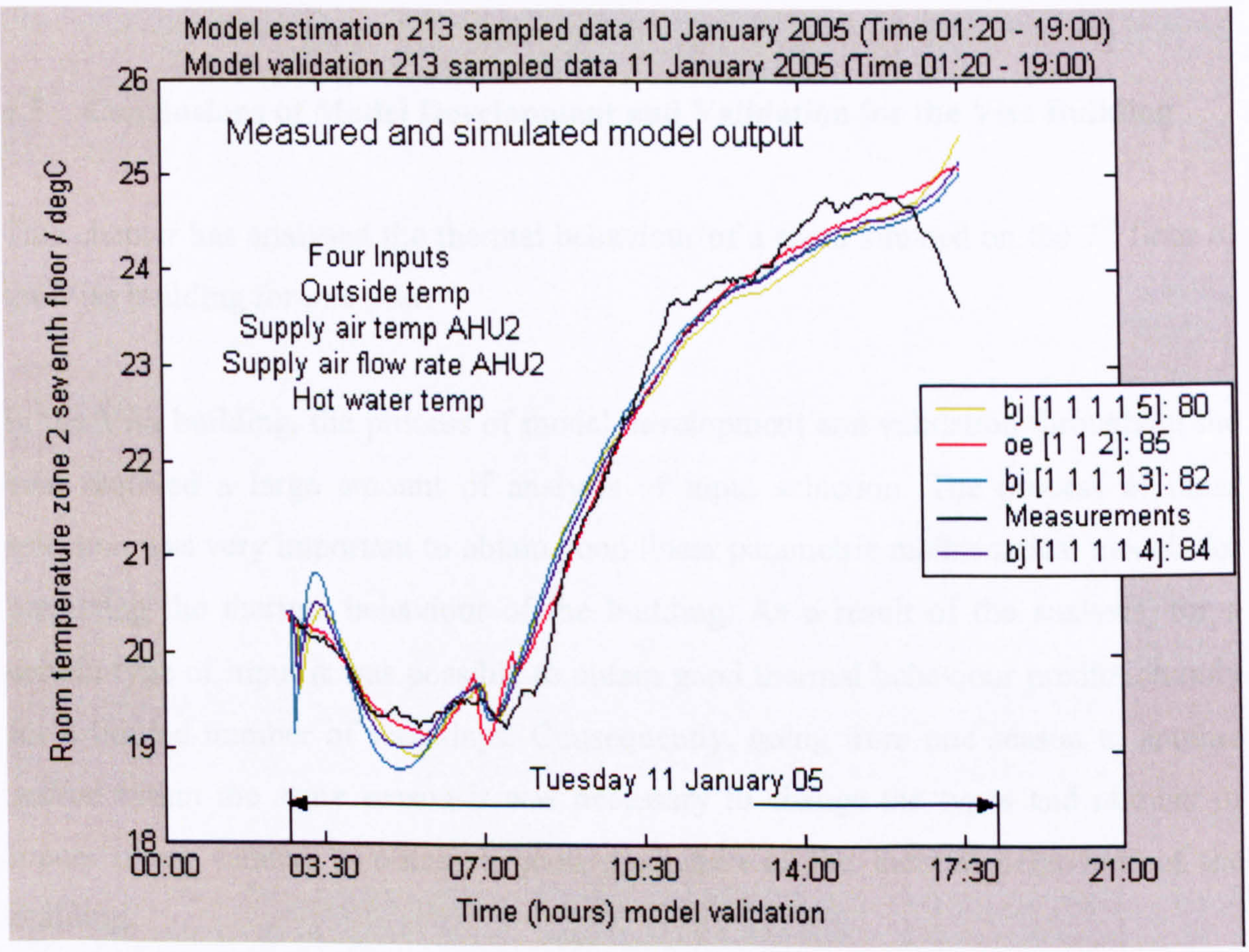

Figure 4.18 Model validation, 11 January 2005

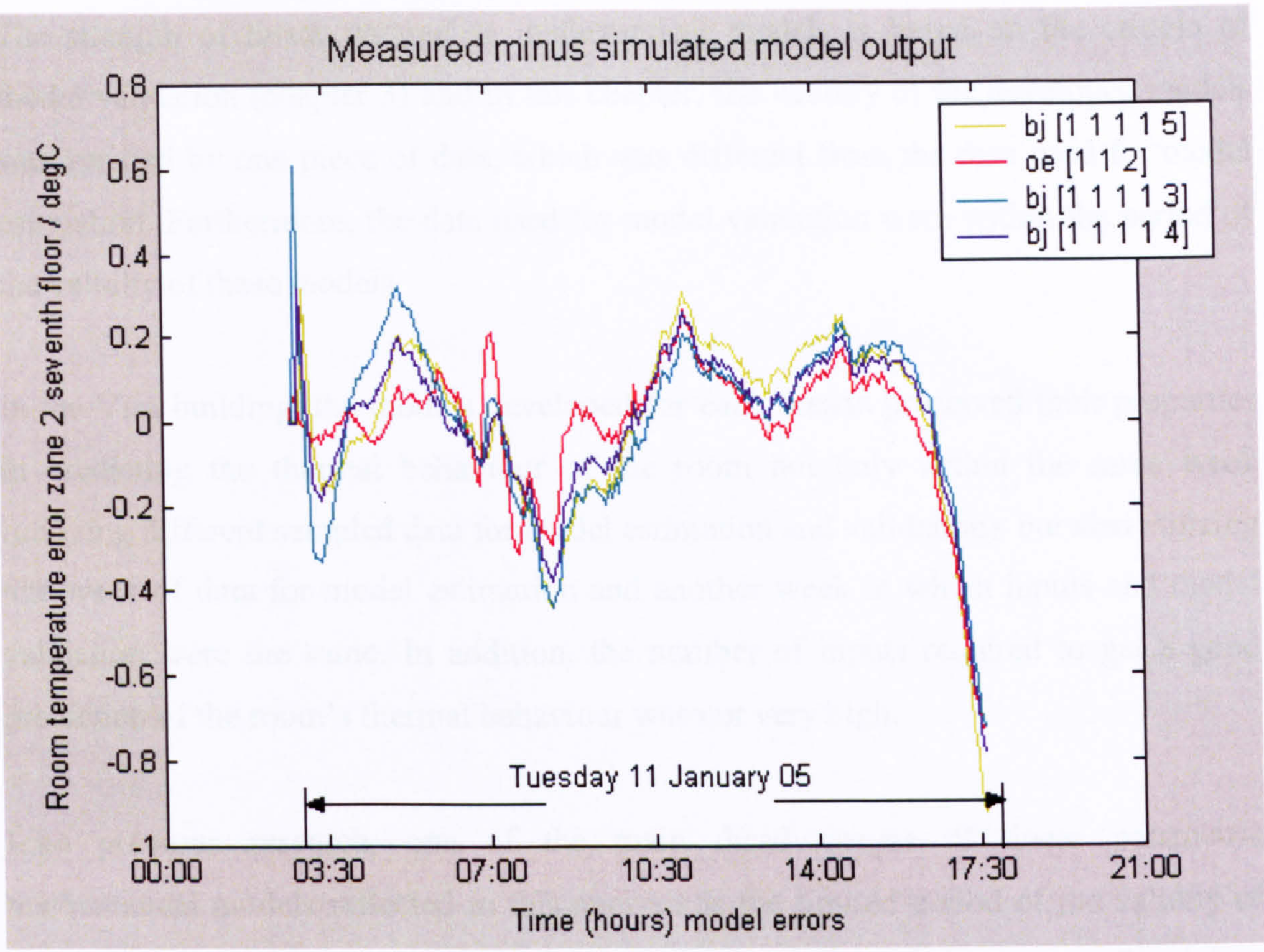

Figure 4.19 Model errors, 11 January 2005

4.5 Conclusions of Model Development and Validation for the Visa Building

This chapter has analysed the thermal behaviour of a room situated on the 7th floor of the Visa building for one year.

In the Visa building, the process of model development and validation throughout the year required a large amount of analysis of input selection. The process of input selection was very important to obtain good linear parametric mathematical models for predicting the thermal behaviour of the building. As a result of the analysis, for a certain type of input it was possible to obtain good thermal behaviour prediction only for a limited number of weekdays. Consequently, going from one season to another and/or within the same season it was necessary to change the types and number of inputs if we wanted to obtain a good prediction of the thermal behaviour of the building.

The strength of linear parametric mathematical models is based on the criteria of model validation (chapter 3) and in this chapter, the validity of the developed models was verified by one piece of data, which was different from the data used for model estimation. Furthermore, the data used for model validation were within the period of the validity of these models.

In the Visa building, the models developed for each season preserved their properties in predicting the thermal behaviour of the room not only within the same week (utilizing different sampled data for model estimation and validation), but also utilizing one week of data for model estimation and another week in which inputs and model validation were the same. In addition, the number of inputs required to get a good prediction of the room's thermal behaviour was not very high.

Like previous research, one of the main disadvantages of linear parametric mathematical models reflected in this analysis is the limited period of the validity of these models which is related to the period of validity of the inputs (Black-box models). Furthermore, these mathematical models are linear and this is another disadvantage, which can affect the period of validity of some of them. Although the same inputs can be used throughout the season this is not the case with the models because some of them are not valid throughout the season (see sections 4.4.1, 4.4.3 and 4.4.4).

Contrary to linear models, the period of validity of non-linear mathematical models is the same as that related to the inputs selected (see results related to neural networks, section 7.3). In the Visa building, some of the inputs of less importance, including the internal gain of the buildings (where in part they are included within the inputs selected), were not provided by the BMS and this is a disadvantage. Finally, the prediction of the room's thermal behaviour decreased slightly if we changed from using the same week to different weeks for model estimation and validation (see Appendix 1A). This is another limitation of using a linear parametric mathematical model with a large amount of data.

The results related to inputs selected and mathematical models appropriate for each season will now be summarized in turn.

For middle and end of the spring season five inputs, (outside temperature, supply air flow rate AHU2, supply air temperature AHU2, hot water temperature and chilled water temperature) can be used for the predictions of room temperature. The BJ models (bj [1 1 1 1 4] and bj [1 1 1 1 5]) give good fits for spring.

The OE models (oe [1 1 2], oe [1 1 3], oe [1 1 4] and oe [1 1 5]) and ARMAX model (amx [2 2 2 1]) have goods fits for the summer season where there are four inputs (outside temperature, supply air temperature AHU2, supply air flow rate AHU2 and chilled water temperature).

Throughout the middle of the autumn season the OE model (oe [1 1 2]) has a good fit when the inputs are outside temperature, supply air temperature AHU2, supply air flow rate AHU2, chilled water temperature and hot water temperature. The inputs outside temperature, supply air temperature AHU2, supply air flow rate AHU2 and hot water temperature were used for the end of the autumn season, where the BJ models (bj [1 1 1 1 2] and bj [1 1 1 1 3]) and ARMAX model (amx [2 2 2 1]) have good fits with real measurements.

For the winter season, the BJ models (bj [1 1 1 1 3], bj [1 1 1 1 4] and bj [1 1 1 1 5]) and OE model (oe [1 1 2]) have good fits for the beginning and middle of the season, while for the end of this season the BJ models (bj [1 1 1 1 2], bj [1 1 1 1 3], bj [1 1 1 1 4] and bj [1 1 1 1 5]) can be used. For the winter, four inputs (outside temperature, supply air flow rate AHU2, supply air temperature AHU2 and hot water temperature) can be used for the predictions of room temperature.

In addition to the previous analysis, one week was investigated for model estimation and another week was used for model validation. This analysis was done for the whole year (2005) and the results are given in Appendix 1A.

The contributions of the analysis presented in this chapter are:

- Previous researchers have applied parametric mathematical models in experimental rooms (many sensors are installed). On the contrary, in this chapter the analysis of the room's thermal behaviour was executed in a real office with no additional sensors. For example, the office examined on the second floor had only two sensors to measure the room temperature placed in the same position at each end of the room (see fig. 4.2)
- In this work, the thermal behaviour of the office was examined for a period of one year while, in the past, similar studies have analysed only a few weeks to a few months of collected data.
- In the past, thermal modelling of buildings was mainly concentrated on developing models for HVAC plants, with the purpose of fault detection and diagnostics. In contrast, this work presents an overall study of the thermal behaviour of the room in terms of inputs selected and the subsequent development of different models.
- Due to the short periods of data collection in previous researches, thermal models have been developed for the same inputs throughout their analysis. In this study, the inputs used for the development of models were different from one season to another.

Finally, the results obtained for appropriate models throughout the year have similar fits with those for the previous analysis (using the same week's data for model estimation and validation). This means that linear parametric mathematical models' structures are suitable for thermal behaviour prediction for not more than one week. In addition, in the Visa building throughout the year FPE varied between 10^{-1} and 10^{-3}, while model errors varied between 0.6 and 0.8 degrees Celsius. Appendix 1B details some of the mathematical models in terms of their parameters.

CHAPTER 5 Data Analysis and Model Development for Portman House

The process of model development in this chapter is similar to the Visa building analysis presented in the previous chapter. The model structures ARX, OE, ARMAX and BJ are the general choices for model development in Portman House. The data are analysed by dividing them into weekdays (Monday Time 01:20 to Friday Time 19:00) and weekends (the latter is not presented because the HVAC plants are switched off on Saturday and Sunday).

This chapter starts with a brief description of Portman House and the room examined for model development and validation. The following sections present a detailed analysis of the inputs and the most appropriate models for building the thermal modelling of the room for the four seasons.

After careful analysis of all the variables affecting room temperature, several inputs and outputs were collected through the BMS for the entire year. Then, the SIT with parametric models presented in chapter 3 was applied to the data collected for one year (13 June 2005 – 09 June 2006) and the models chosen were those that best fit the real data.

The room's thermal behaviour in zones 1 and 2 was taken for model development and validation in this building (Fig. 5.2). This room is a large open plan office and there are no significant differences in temperature between the two zones. As for the Visa building, in this chapter only the results related to zone 1 are presented (positioned on the left hand side of Fig. 5.2).

Finally, the following sections explore the inputs and the models in terms of best fit with the real measurements of room temperature throughout the four seasons.

5.1 Portman House Description

Portman House (see Fig. 5.1) is located in the centre of London in Oxford Street, close to Marble Arch tube station. Invensys is the BMS installed in the building for the monitoring and operation of plant/building services. It enables the user to monitor the plant/building services, and make changes to the way the building is controlled using colour graphics displays.

Zone 1, which is on the left-hand side of the second floor, was used for model estimation and validation (see Fig. 5.2).

To identify the parameters of the models describing the thermal response of a real building a time series of the relevant data was collected. The data were collected every 5 minutes and the collection consisted of:

- Room temperature zones 1 and 2, second floor (Output) in degrees Celsius (degC)
- Outside temperature in degrees Celsius (degC)
- Supply air flow rate AHU1 (air that is coming from the air handling unit 1, supplying zone 1, positioned on the roof of the building and flowing through the FCUs positioned in zone 1) in m^3/sec
- Supply air temperature AHU1 (air temperature that is coming from the air handling unit 1 supplying zone 1, positioned on the roof of the building and flowing through the FCUs positioned in zone 1) in degrees Celsius (degC)
- Chilled water temperature (chilled water that flows inside the fan coil units and comes from the chillers positioned on the roof) in degrees Celsius (degC).
- Hot water temperature (hot water that flows inside the fan coil units and comes from the boilers positioned on the roof) in degrees Celsius (degC).

Fan coil units (FCUs) are distributed throughout the room (zones 1 and 2) on the second floor (see Fig. 4.3, chapter 4).

Figure 5.1 Portman House Site Plan

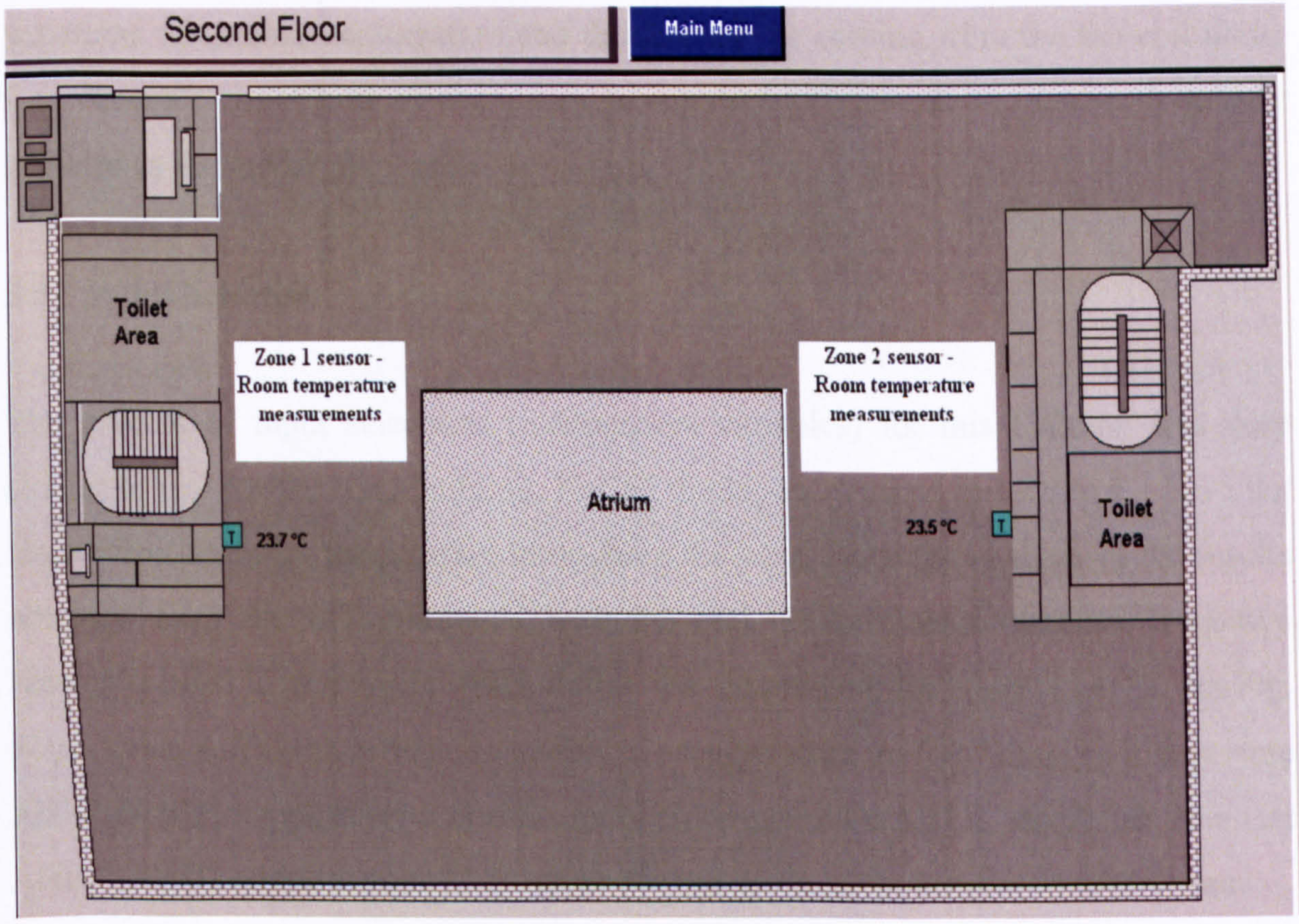

Figure 5.2 Portman House Building, second floor – Layout

5.2 Data Collection Description

In the experiment, data sampling intervals had to be selected carefully because some information about the physical parameters can be partially hidden if longer sampling intervals are selected. In Portman House the choice of sampling interval was 5 minutes, so that it corresponded to 5-8 sampling points over the rise time of the system's step response (Ljung and Glad, 1994).

Before analysis, all the data collected through the BMS and data logging machine were processed. The recorded data were downloaded every 15 days. The downloading format was then transferred to Microsoft Excel so that the data file could be used directly with slight adjustments. Finally, these data were transferred to Matlab and elaborated inside the SIT.

As for the Visa building, in Portman House the primary assumption of the model development was that the internal temperature variation is directly influenced by the variations of external temperature and the internal air coming from the fan coil units. Consequently, the effects of occupancy, computers, printers etc are indirectly in part included in the model.

5.3 Input Selection

The process of input selections (independent variables) for this building was very similar to that for the Visa building. Not all the inputs detailed in section 5.1 have the same effect on room temperature throughout the year. From the analysis of the results obtained from the SIT compared with the real measurements obtained from two sensors (placed in two zones which define the temperature for zones 1 and 2, see Fig. 5.2), it was sufficient to include supply air temperature AHU1, supply air flow rate AHU1 (AHU1 supplies zone 1) and supply air temperature AHU2, supply air flow rate AHU2 (AHU2 supplies zone 2) as inputs for model development for the entire year.

As for the Visa building, the models in this chapter were developed for different seasons and each season was subdivided into three parts: beginning, middle and end. Some inputs gave good models for a limited period of time (several weeks).

Consequently, as reported below, the process of input selection and the period of validity of models obtained that can give good thermal prediction (within the same period) were the key points in deciding season subdivision. In addition, obtaining a good model depends on the inputs used in the SIT for model development. If we include more inputs than required for developing models then the model's performance does not improve and it may get worse.

For Portman House, the procedure of input selection is not presented because it was similar to that presented for the Visa building (see section 4.3).

In conclusion, the following sections will examine the inputs selected for each season with the models that give the best thermal behaviour of the room.

5.4 Weekdays' Model Development and Validation

Model estimation and validation were carried out using one set of weekdays data (Monday Time 01:20 to Friday Time 19:00). The first part of the data was used for model estimation and the remaining part was used for model validation. Finally, as for Visa in Portman House building for each season, due to the similarities of the results, not all the graphs relating to weekdays are presented.

Model estimation and validation were analysed respectively for four cases:

a) 213 Sampled-data model estimation (18 hours in day 1 – Time 01:20-19:00) and 213 sampled-data model validation (18 hours in day 2 – Time 01:20-19:00)
b) 900 Sampled-data model estimation (75 hours) and 465 sampled-data model validation (39 hours)
c) 800 Sampled-data model estimation (67 hours) and 565 sampled-data model validation (47 hours)
d) 1365 sampled-data model estimation (113.5 hours, weekdays) and 1365 sampled-data model validation in following weekdays (see Appendix 2A).

Different models were found to be most appropriate for different periods of the year. Thus different models will be used for winter, spring, summer and autumn. In the following sections the best models in terms of best fit for each of these weather conditions are investigated.

5.4.1 Model Development and Validation for the Winter Season

Different weeks of the winter season were examined for model estimation and validation and the weeks presented represent the middle and end of the winter season. The beginning of the winter season is not presented due to faults in the recording system.

Winter and beginning of the spring season

This period means from the beginning of January up to middle of April. The weeks between 09 January and 14 April 2006 have been taken to represent this period and the models that give good fits are shown in Table 5.1. In addition, the week 09-13 January 2006 is shown in Figs. 5.3 and 5.5, and the errors between model output and measurements are presented in Figs. 5.4 and 5.6. As a result of the analysis during these weeks, the inputs that affect the results (room temperature zone 1) are: hot water temperature, outside temperature, supply air temperature AHU1 and supply air flow rate AHU1.

In conclusion, throughout winter season six inputs are required to obtain good results and the BJ models (bj [1 1 1 1 2], bj [1 1 1 1 3] and bj [1 1 1 1 4]) can predict the room temperature very well (see FPE and model fits in Table 5.1). Throughout the winter season the FPE is of the order 10^{-3} and the maximum model error is 0.6 degrees Celsius.

1-213 Data Estimation 289-501 Data Validation	1-900 Data Estimation 901-1365 Data Validation	1-800 Data Estimation 801-1365 Data Validation
Winter season	**Winter season**	**Winter season**
Four Inputs	**Four Inputs**	**Four Inputs**
Outside temp	Outside temp	Outside temp
Hot water temp	Hot water temp	Hot water temp
Supply air temp AHU1	Supply air temp AHU1	Supply air temp AHU1
Supply air flow rate AHU1	Supply air flow rate AHU1	Supply air flow rate AHU1
FPE ≈ 0.0035	FPE ≈ 0.004	FPE ≈ 0.004
bj [1 1 1 1 2]: 80-90	bj [1 1 1 1 2]: 40-50	bj [1 1 1 1 2]: 52-65
bj [1 1 1 1 3]: 80-90	bj [1 1 1 1 3]: 45-55	bj [1 1 1 1 3]: 45-55
bj [1 1 1 1 4]: 70-80	bj [1 1 1 1 4]: 50-60	bj [1 1 1 1 4]: 35-45

Table 5.1 Winter weekdays

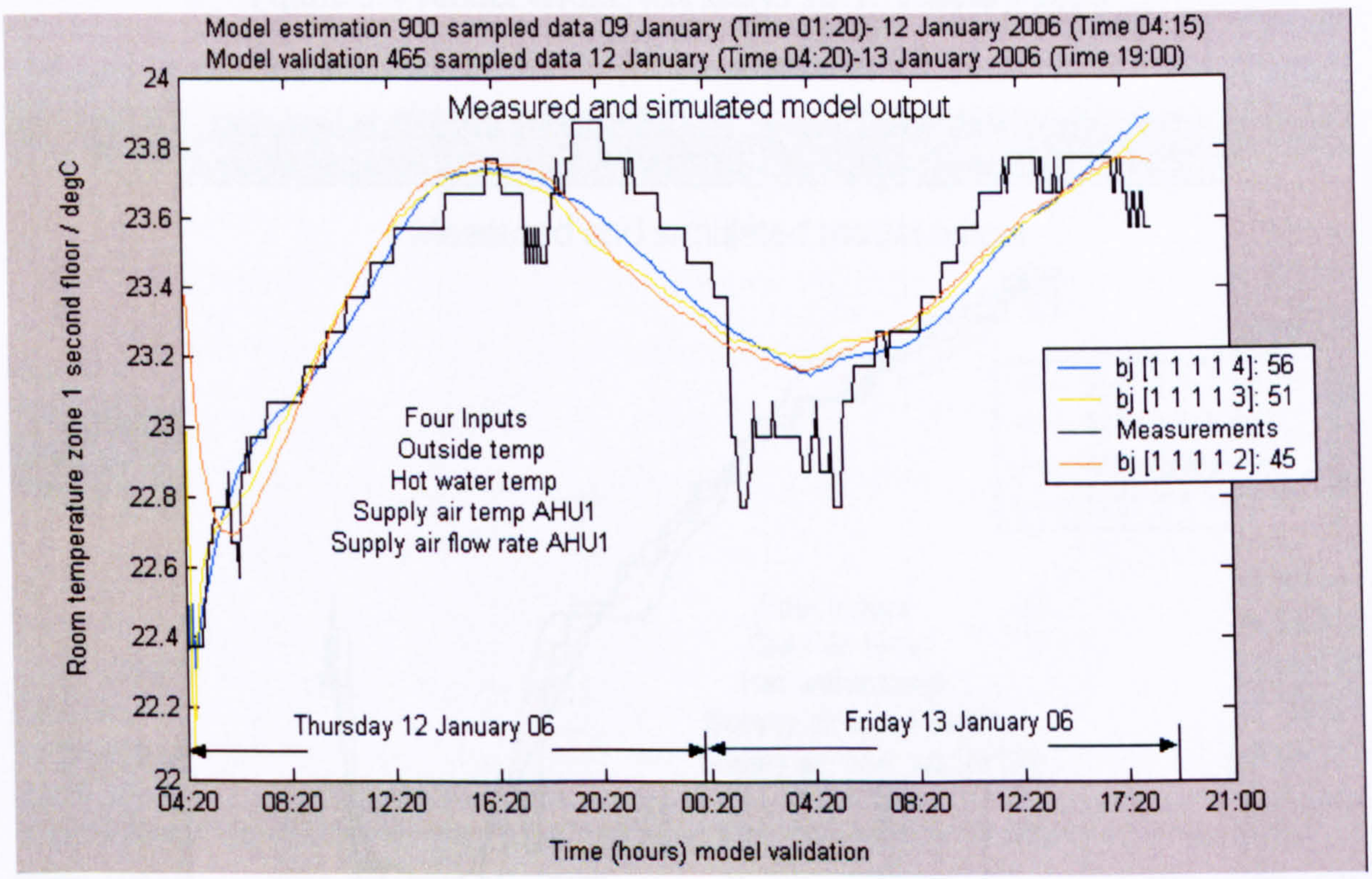

Figure 5.3 Model validation, weekdays 12-13 January 2006

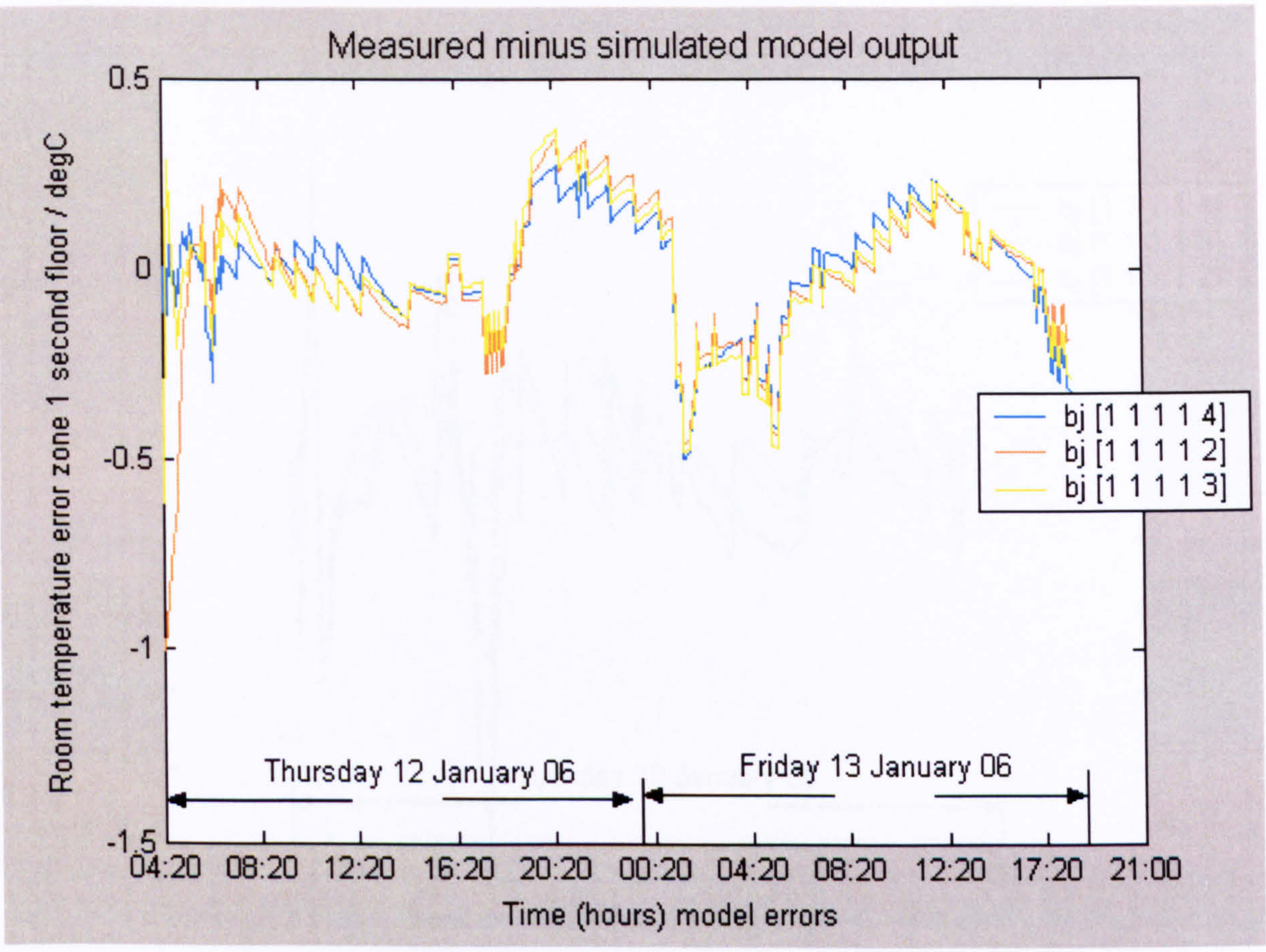

Figure 5.4 Model errors, weekdays 12-13 January 2006

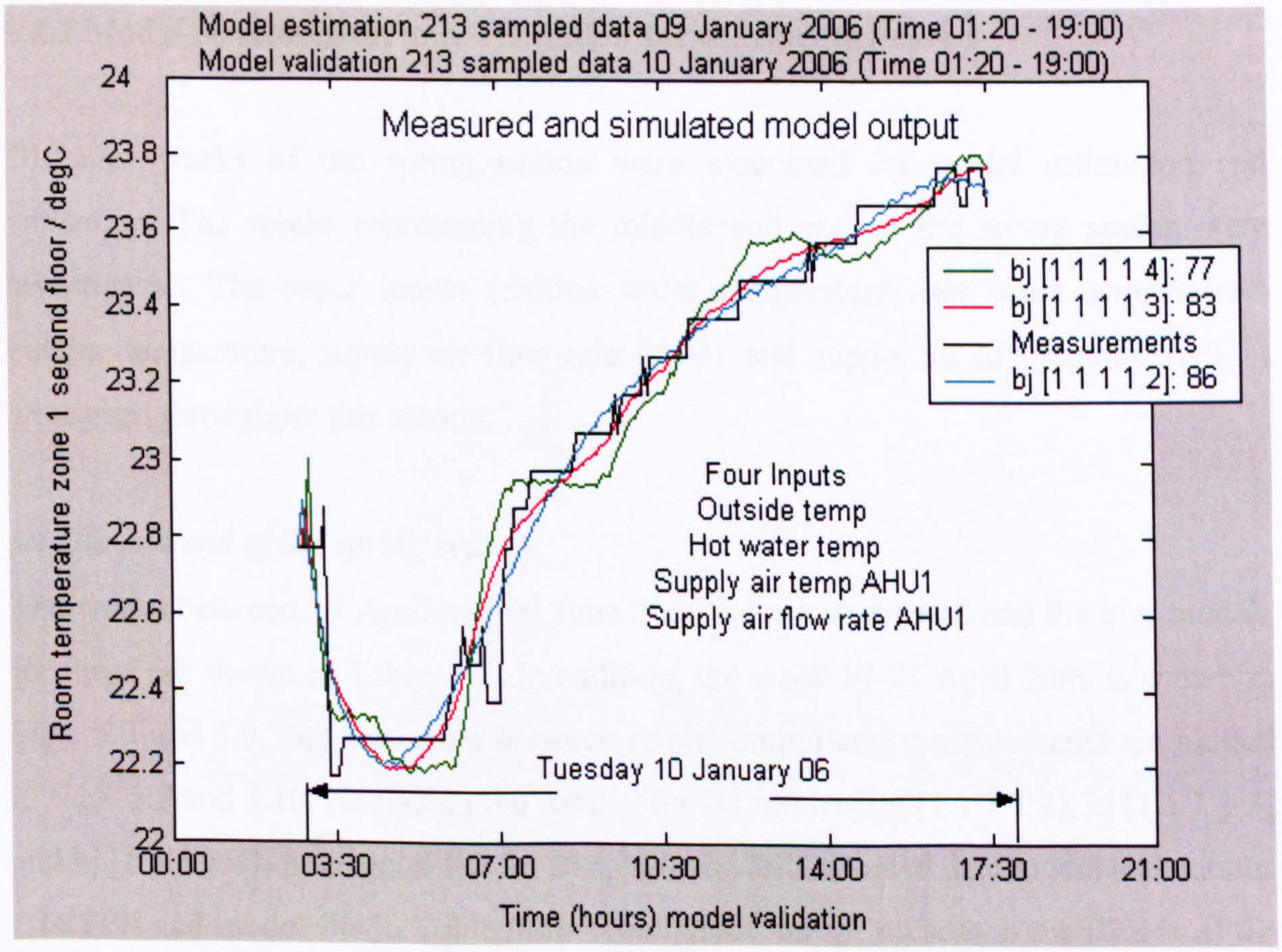

Figure 5.5 Model validation, 10 January 2006

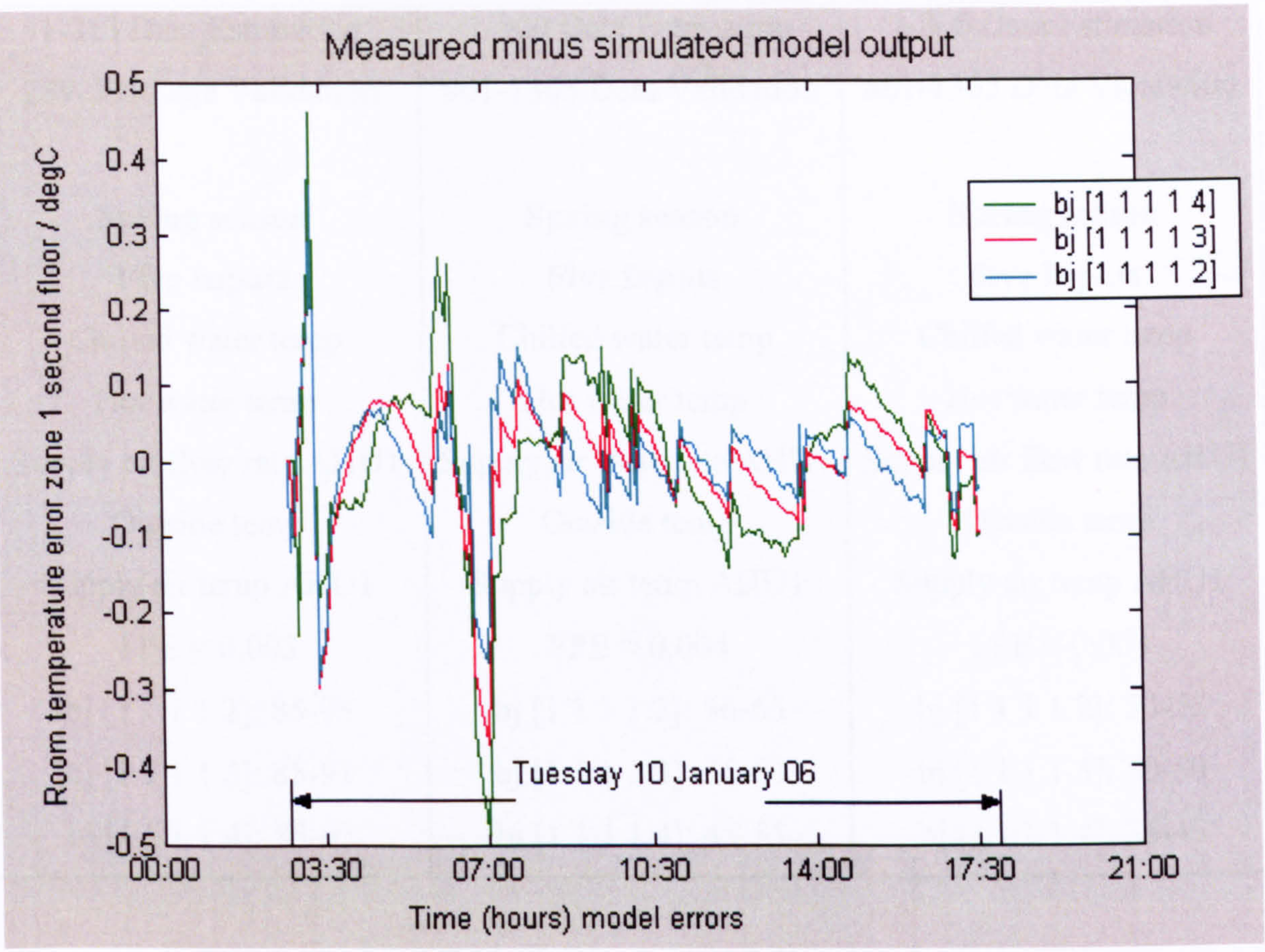

Figure 5.6 Model errors, 10 January 2006

5.4.2 Model Development and Validation for the Spring Season

Different weeks of the spring season were examined for model estimation and validation. The weeks representing the middle and end of the spring season were investigated. The same inputs (chilled water temperature, hot water temperature, outside temperature, supply air flow rate AHU1 and supply air temperature AHU1) were used throughout this season.

Middle and end of the spring season

The weeks between 17 April and 09 June 2006 were investigated and the best models for these are shown in Table. 5.2. In addition, the week 17-21 April 2006 is shown in Figs. 5.7 and 5.9, and the errors between model output and measurements are plotted in Figs. 5.8 and 5.10. Analysing the results, the BJ models (bj [1 1 1 1 2], bj [1 1 1 1 3] and bj [1 1 1 1 4]) have good fits for 213, 900 and 800 sampled data model estimations (see FPE and model fits in Table 5.2). Throughout the spring season the FPE is of the order 10^{-3} and the maximum model error is 0.6 degrees Celsius.

1-213 Data Estimation	1-900 Data Estimation	1-800 Data Estimation
289-501 Data Validation	901-1365 Data Validation	801-1365 Data Validation
Spring season	**Spring season**	**Spring season**
Five Inputs	**Five Inputs**	**Five Inputs**
Chilled water temp	Chilled water temp	Chilled water temp
Hot water temp	Hot water temp	Hot water temp
Supply air flow rate AHU1	Supply air flow rate AHU1	Supply air flow rate AHU1
Outside temp	Outside temp	Outside temp
Supply air temp AHU1	Supply air temp AHU1	Supply air temp AHU1
FPE ≈ 0.003	FPE ≈ 0.004	FPE ≈ 0.004
bj [1 1 1 1 2]: 85-95	bj [1 1 1 1 2]: 56-65	bj [1 1 1 1 2]: 50-55
bj [1 1 1 1 3]: 85-93	bj [1 1 1 1 3]: 55-63	bj [1 1 1 1 3]: 40-50
bj [1 1 1 1 4]: 85-95	bj [1 1 1 1 4]: 45-55	bj [1 1 1 1 4]: 35-45

Table 5.2 Spring weekdays

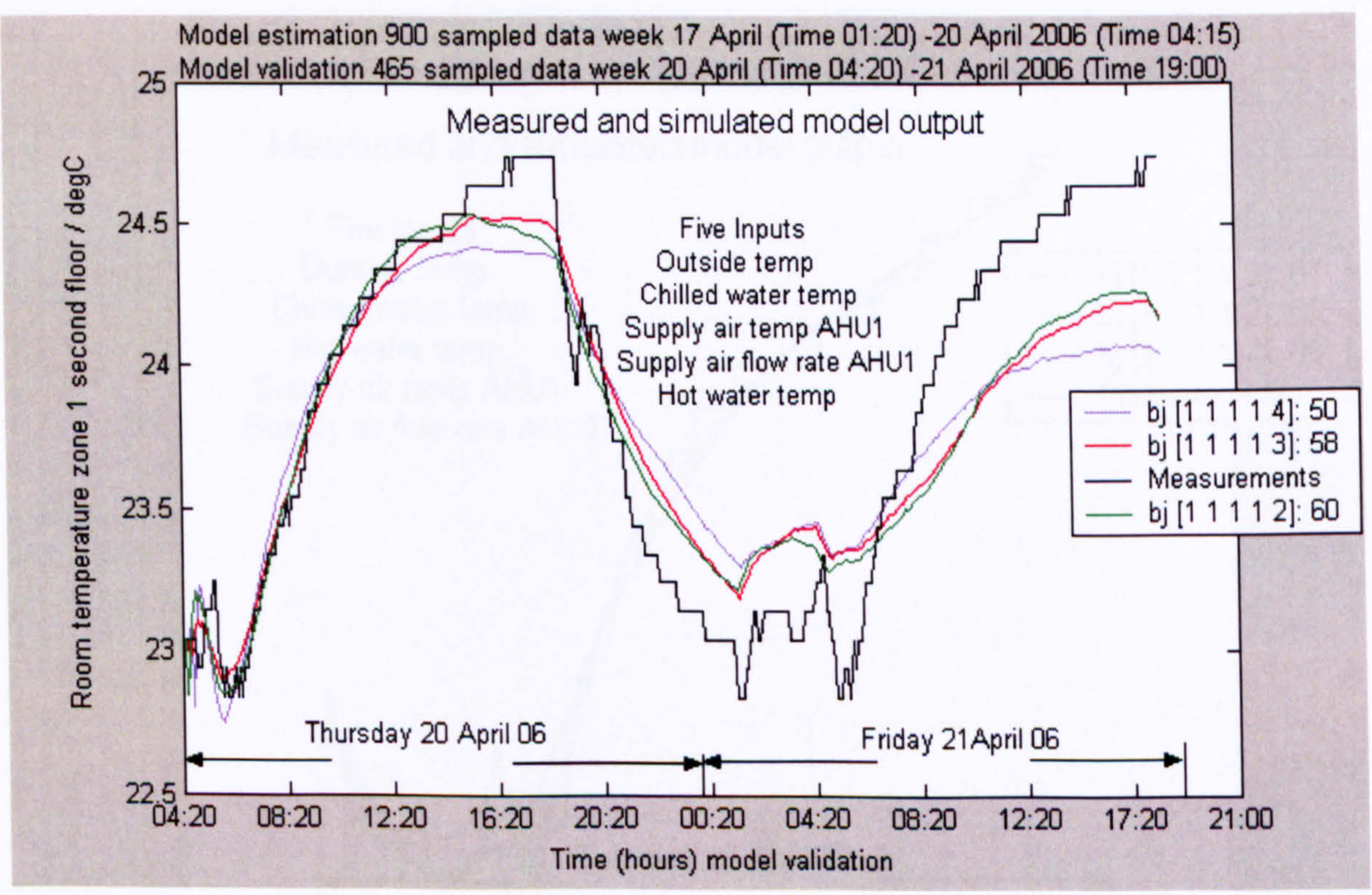

Figure 5.7 Model validation, weekdays 20-21 April 2006

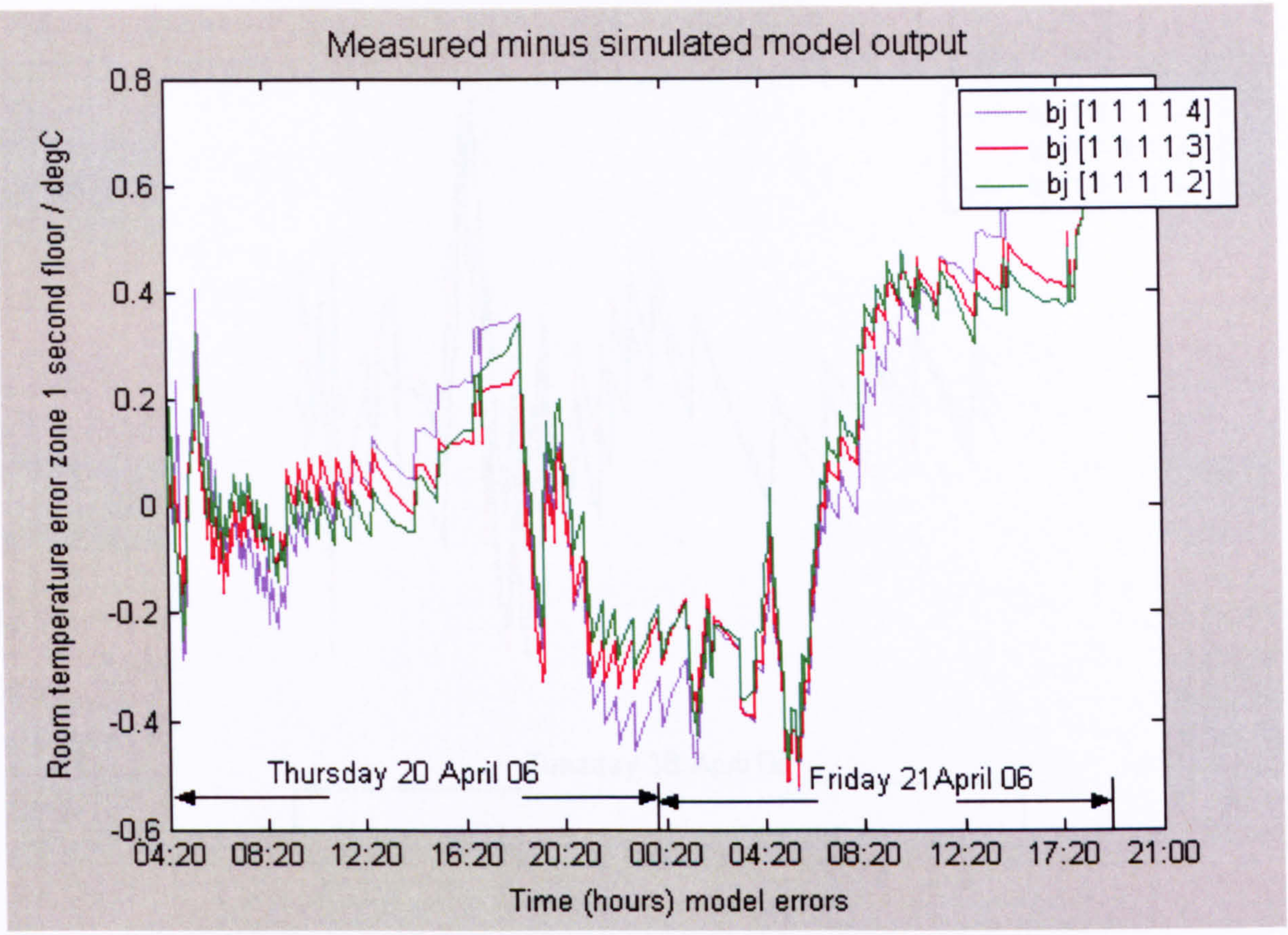

Figure 5.8 Model errors, weekdays 20-21 April 2006

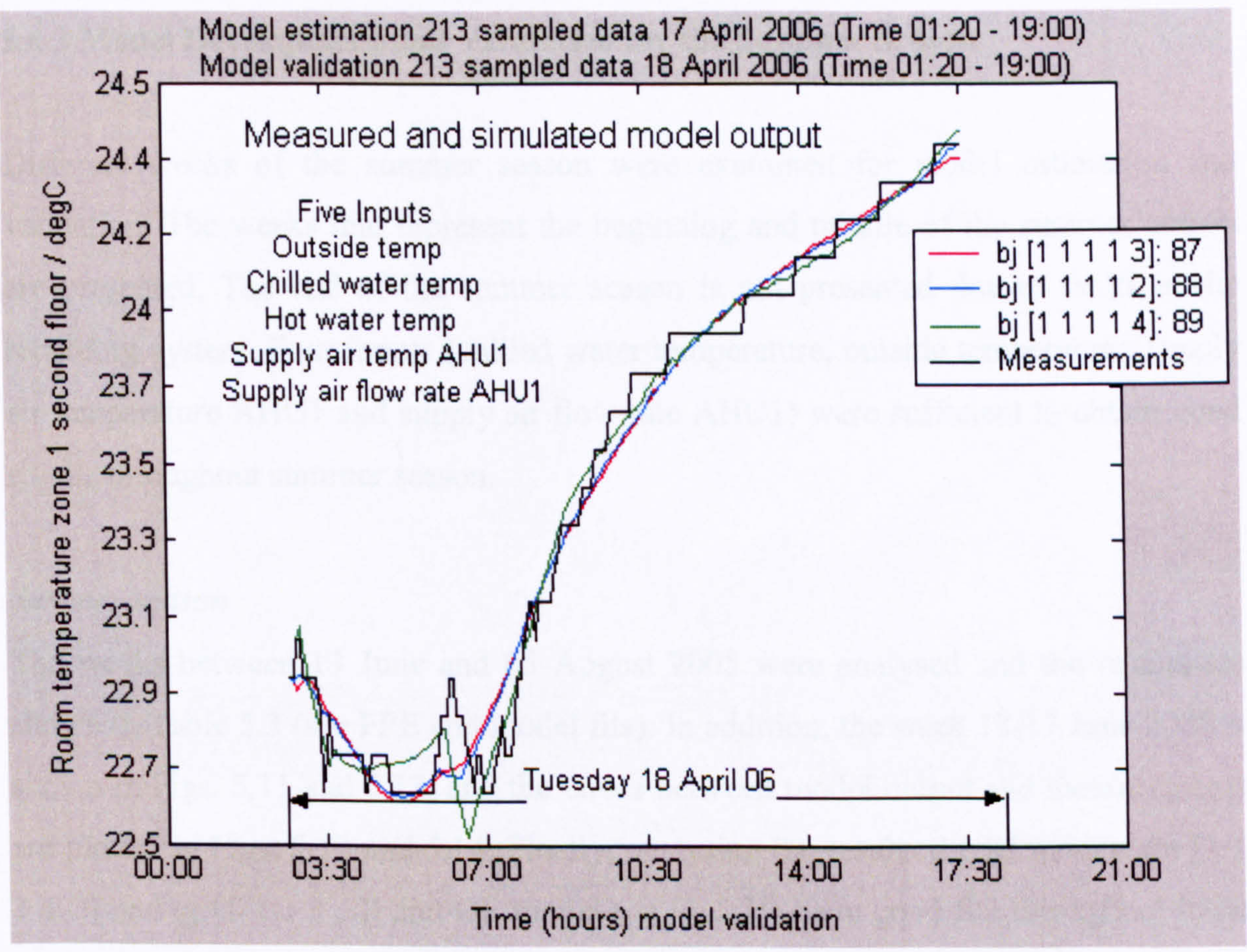

Figure 5.9 Model validation, 18 April 2006

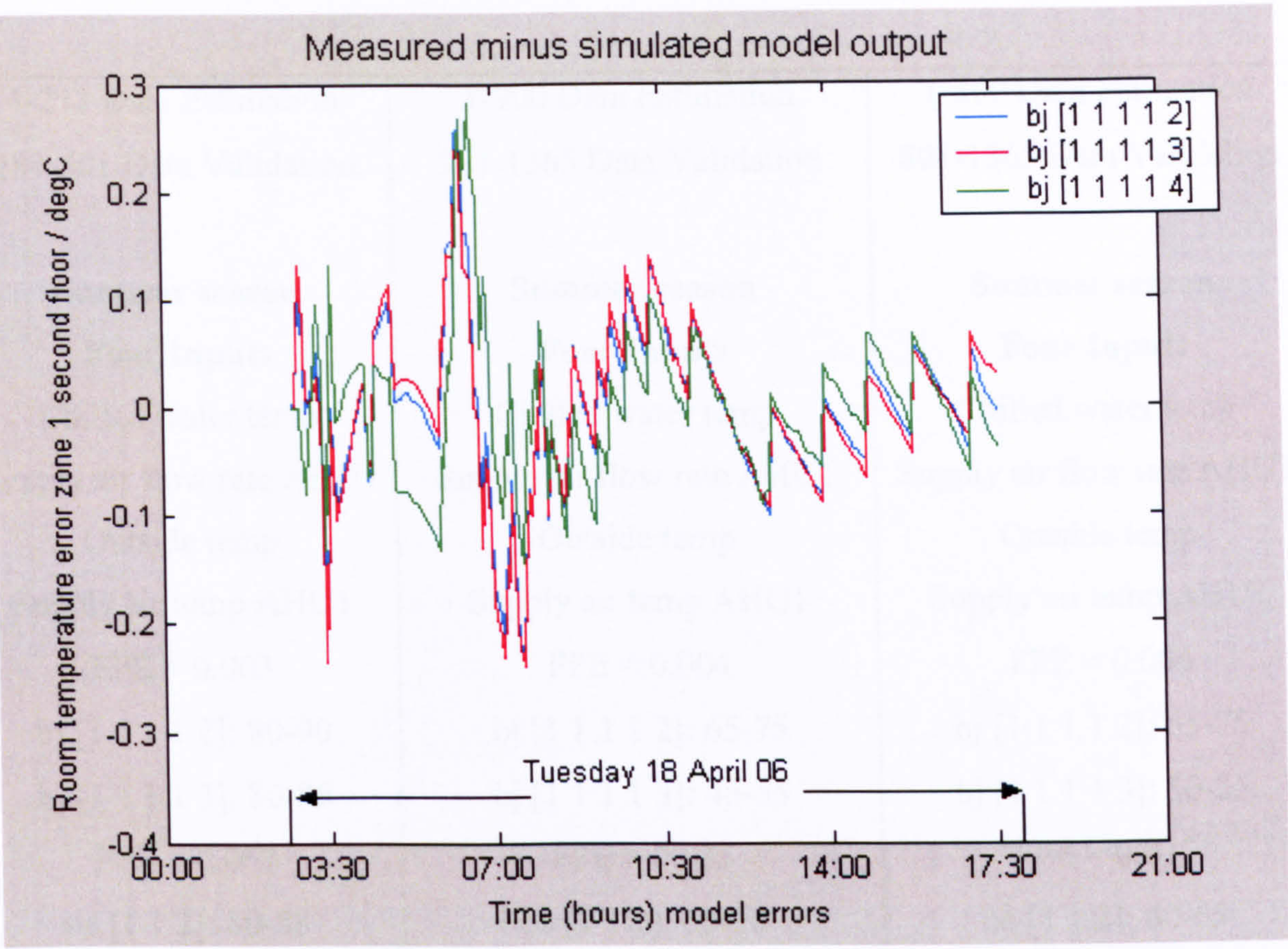

Figure 5.10 Model errors, 18 April 2006

5.4.3 Model Development and Validation for the Summer Season

Different weeks of the summer season were examined for model estimation and validation. The weeks that represent the beginning and middle of the summer season are presented. The end of the summer season is not presented due to faults in the recording system. Four inputs (chilled water temperature, outside temperature, supply air temperature AHU1 and supply air flow rate AHU1) were sufficient to obtain good results throughout summer season.

Summer season

The weeks between 13 June and 05 August 2005 were analysed and the results are shown in Table 5.3 (see FPE and model fits). In addition, the week 13-17 June 2005 is shown in Figs. 5.11 and 5.13, and the errors between model output and measurements are plotted in Figs. 5.12 and 5.14. Finally, analysing the results the BJ models (bj [1 1 1 1 2] and bj [1 1 1 1 3]) and OE model (oe [1 1 2]) have good fits throughout these weeks. Throughout the summer season the FPE is between the orders 10^{-2} and 10^{-3} and the maximumu model error is 0.7 degrees Celsius.

1-213 Data Estimation 289-501 Data Validation	1-900 Data Estimation 901-1365 Data Validation	1-800 Data Estimation 801-1365 Data Validation
Summer season	**Summer season**	**Summer season**
Four Inputs	**Four Inputs**	**Four Inputs**
Chilled water temp	Chilled water temp	Chilled water temp
Supply air flow rate AHU1	Supply air flow rate AHU1	Supply air flow rate AHU1
Outside temp	Outside temp	Outside temp
Supply air temp AHU1	Supply air temp AHU1	Supply air temp AHU1
FPE ≈ 0.003	FPE ≈ 0.004	FPE ≈ 0.004
bj [1 1 1 1 2]: 80-90	bj [1 1 1 1 2]: 65-75	bj [1 1 1 1 2]: 65-75
bj [1 1 1 1 3]: 80-85	bj [1 1 1 1 3]: 45-55	bj [1 1 1 1 3]: 30-35
FPE ≈ 0.007	FPE ≈ 0.035	FPE ≈ 0.035
oe [1 1 2]: 80-88	oe [1 1 2]: 65-75	oe [1 1 2]: 60-65

Table 5.3 Summer weekdays

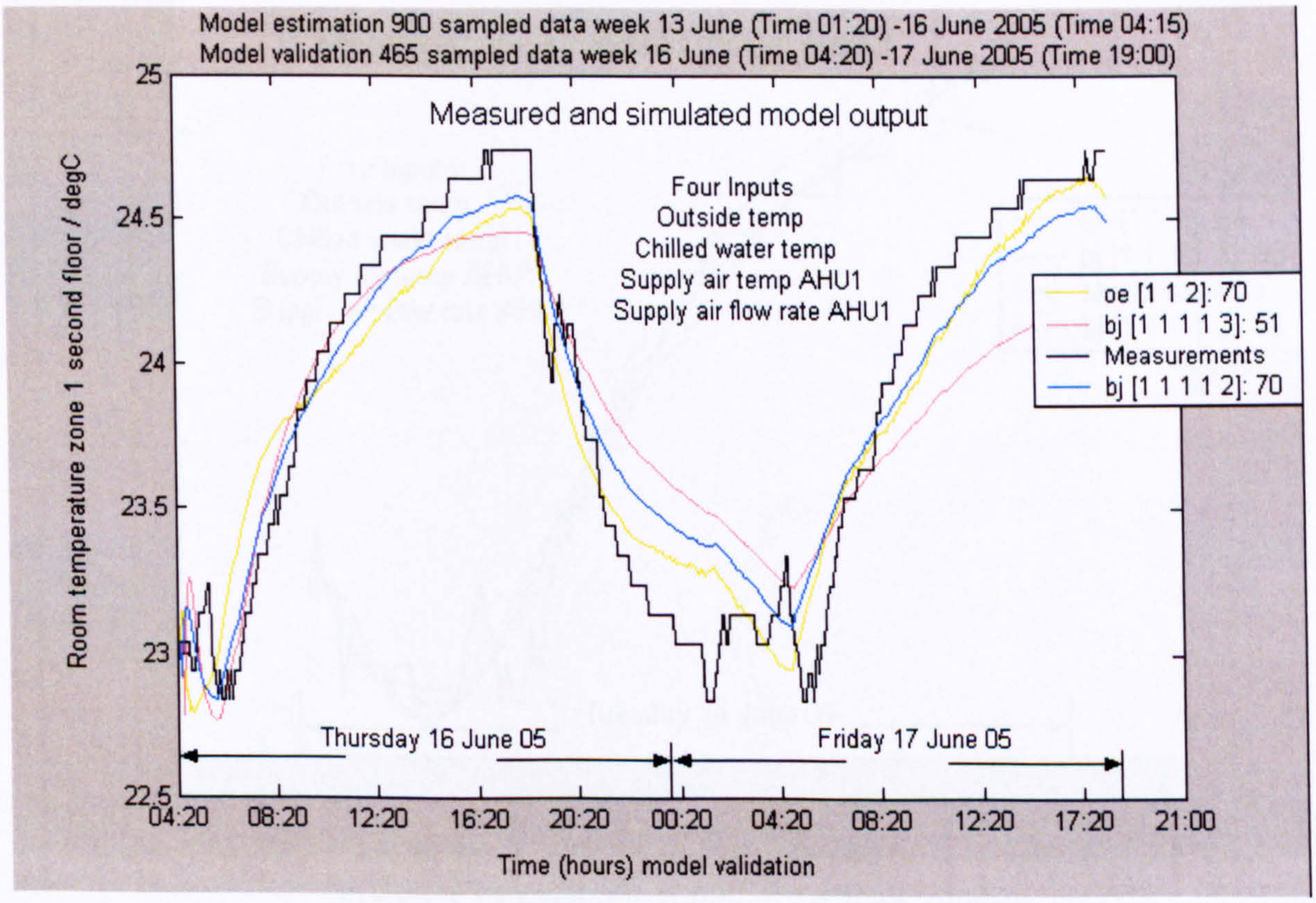

Figure 5.11 Model validation, weekdays 16-17 June 2005

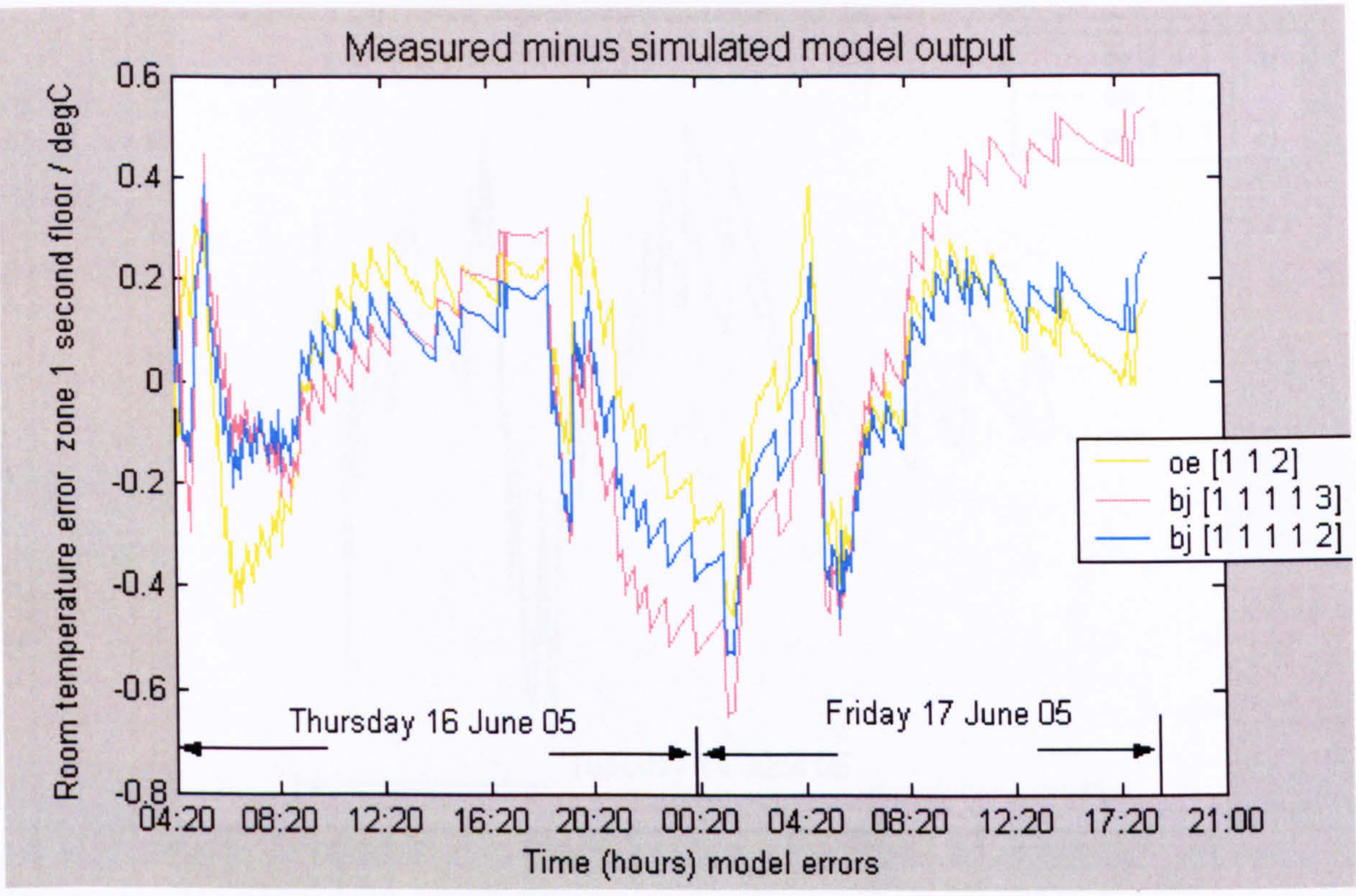

Figure 5.12 Model errors, weekdays 16-17 June 2005

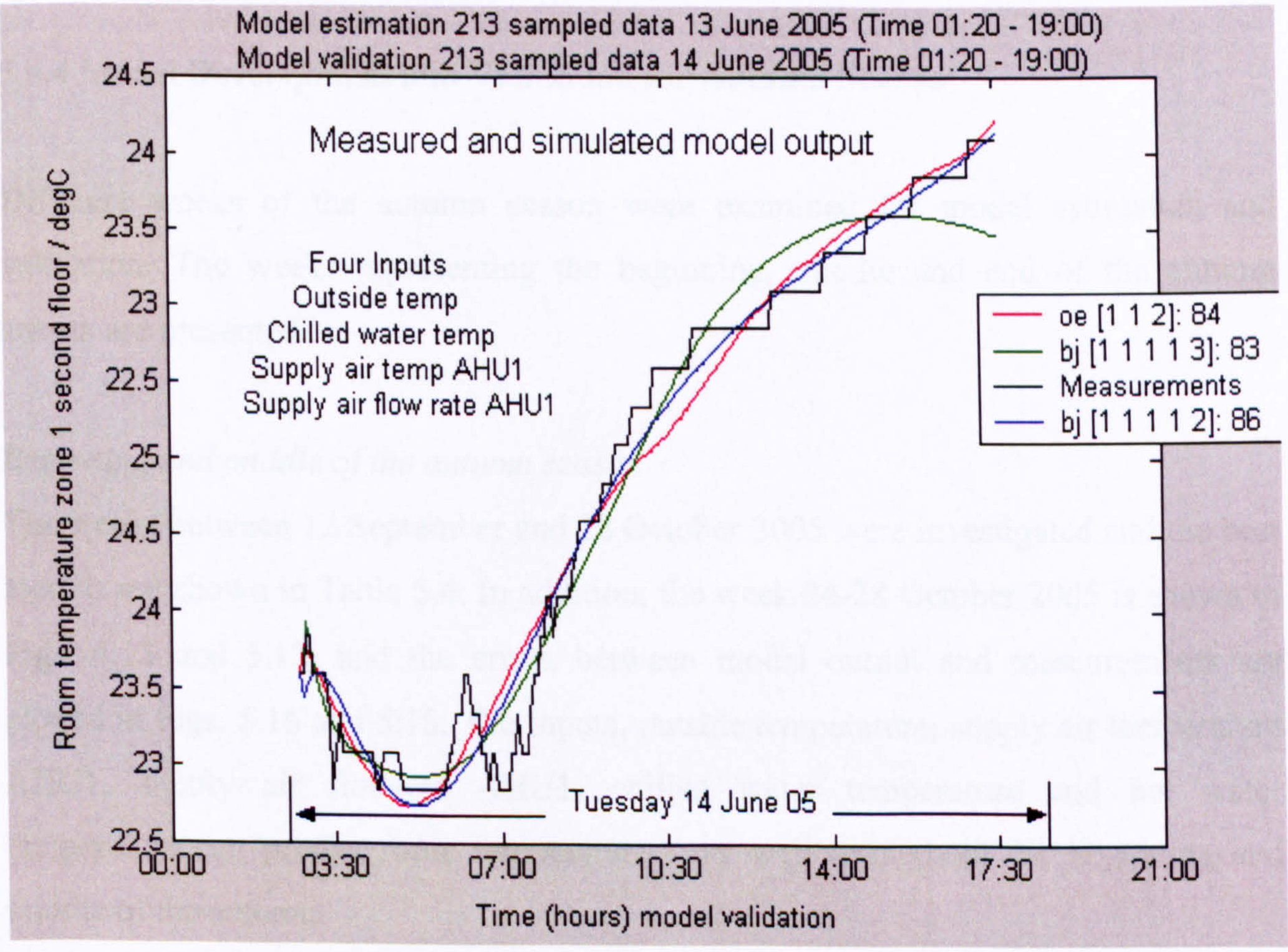

Figure 5.13 Model validation, 14 June 2005

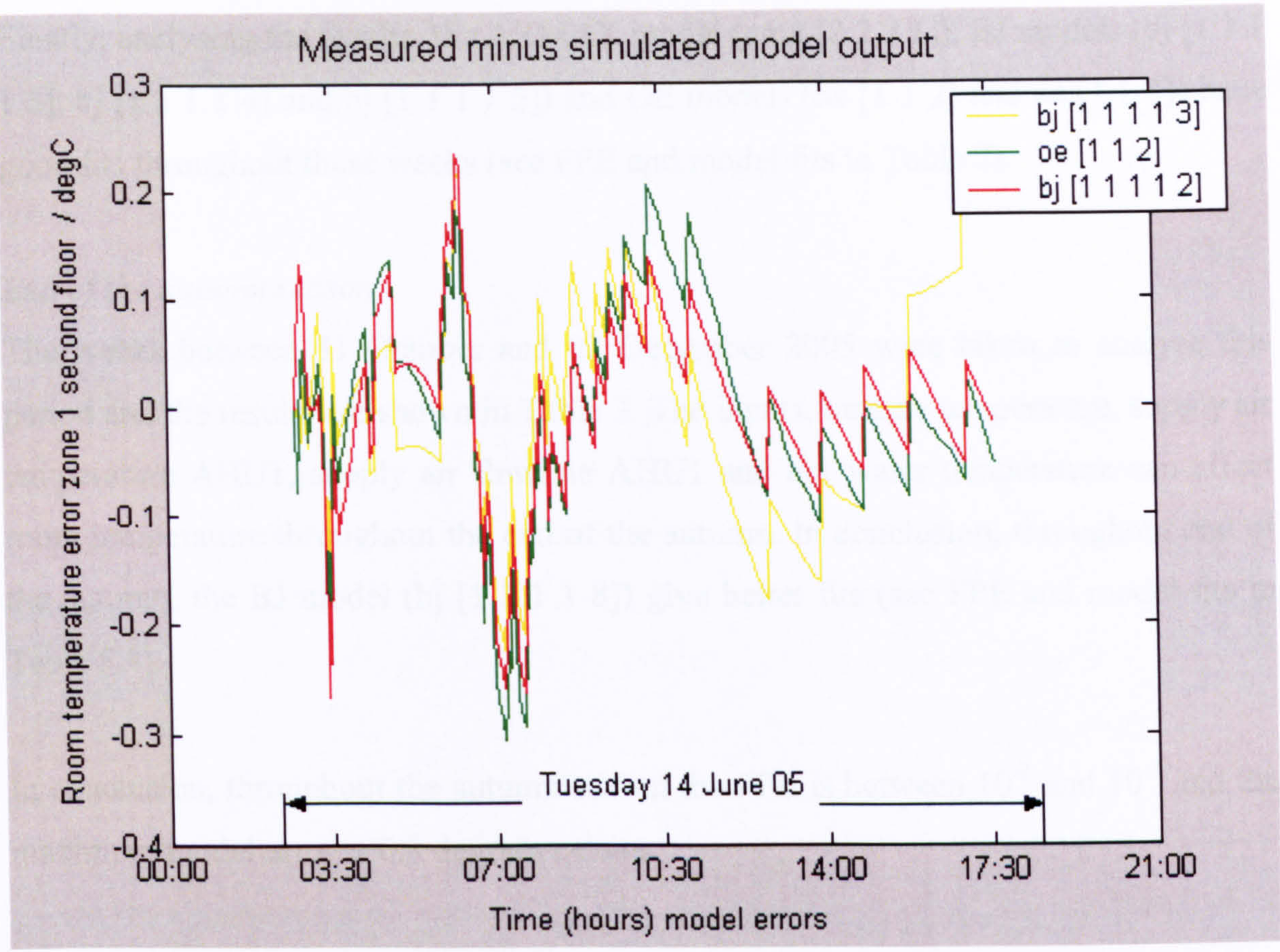

Figure 5.14 Model errors, 14 June 2005

5.4.4 Model Development and Validation for Autumn Season

Different weeks of the autumn season were examined for model estimation and validation. The weeks representing the beginning, middle and end of the autumn season are presented.

Beginning and middle of the autumn season

The weeks between 12 September and 28 October 2005 were investigated and the best models are shown in Table 5.4. In addition, the week 24-28 October 2005 is shown in Figs. 5.15 and 5.17, and the errors between model output and measurements are plotted in Figs. 5.16 and 5.18. The inputs, outside temperature, supply air temperature AHU1, supply air flowrate AHU1, chilled water temperature and hot water temperature can predict room temperature very well throughout the beginning and middle of the autumn.

Finally, analysing the results, the ARMAX model (amx [2 2 2 1]), BJ models (bj [1 1 1 1 3], bj [1 1 1 1 4] and bj [1 1 1 1 5]) and OE models (oe [1 1 2] and oe [1 1 3]) have good fits throughout these weeks (see FPE and model fits in Table 2).

End of the autumn season

The weeks between 31 October and 02 December 2005 were taken to analyse this period and the results are shown in Table 3. The inputs, outside temperature, supply air temperature AHU1, supply air flowrate AHU1 and hot water temperature can affect room temperature throughout the end of the autumn. In conclusion, throughout end of the autumn, the BJ model (bj [1 1 1 1 8]) give better fits (see FPE and model fits in Table 5.4).

In conclusion, throughout the autumn season the FPE is between 10^{-2} and 10^{-3} and the maximum model error is 0.8 degrees celsius.

1-213 Data Estimation 289-501 Data Validation	1-900 Data Estimation 901-1365 Data Validation	1-800 Data Estimation 801-1365 Data Validation
Beginning and middle of autumn	**Beginning and middle of autumn**	**Beginning and middle of autumn**
Five Inputs	**Five Inputs**	**Five Inputs**
Chilled water temp	Chilled water temp	Chilled water temp
Hot water temp	Hot water temp	Hot water temperature
Supply air flow rate AHU1	Supply air flow rate AHU1	Supply air flow rate AHU1
Outside temp	Outside temp	Outside temp
Supply air temp AHU1	Supply air temp AHU1	Supply air temp AHU1
FPE ≈ 0.003	FPE ≈ 0.005	FPE ≈ 0.005
bj [1 1 1 1 3]: 68-78	bj [1 1 1 1 3]: 65-70	bj [1 1 1 1 3]: 65-75
bj [1 1 1 1 4]: 68-78	bj [1 1 1 1 4]: 65-75	bj [1 1 1 1 4]: 70-75
bj [1 1 1 1 5]: 40-50	bj [1 1 1 1 5]: 65-75	bj [1 1 1 1 5]: 65-75
FPE ≈ 0.035	FPE ≈ 0.04	FPE ≈ 0.04
oe [1 1 2]: 55-60	oe [1 1 2]: 65-75	oe [1 1 2]: 70-75
oe [1 1 3]: 55-65	oe [1 1 3]: 65-75	oe [1 1 3]: 70-75
End of autumn	**End of autumn**	**End of autumn**
Four Inputs	**Four Inputs**	**Four Inputs**
Hot water temp	Hot water temp	Hot water temp
Supply air flowrate AHU1	Supply air flow rate AHU1	Supply air flow rate AHU1
Outside temp	Outside temp	Outside temp
Supply air temp AHU1	Supply air temp AHU1	Supply air temp AHU1
FPE ≈ 0.002	FPE ≈ 0.004	FPE ≈ 0.005
bj [1 1 1 1 8]: 45-55	bj [1 1 1 1 8]: 45-55	bj [1 1 1 1 8]: 15-20

Table 5.4 Autumn weekdays

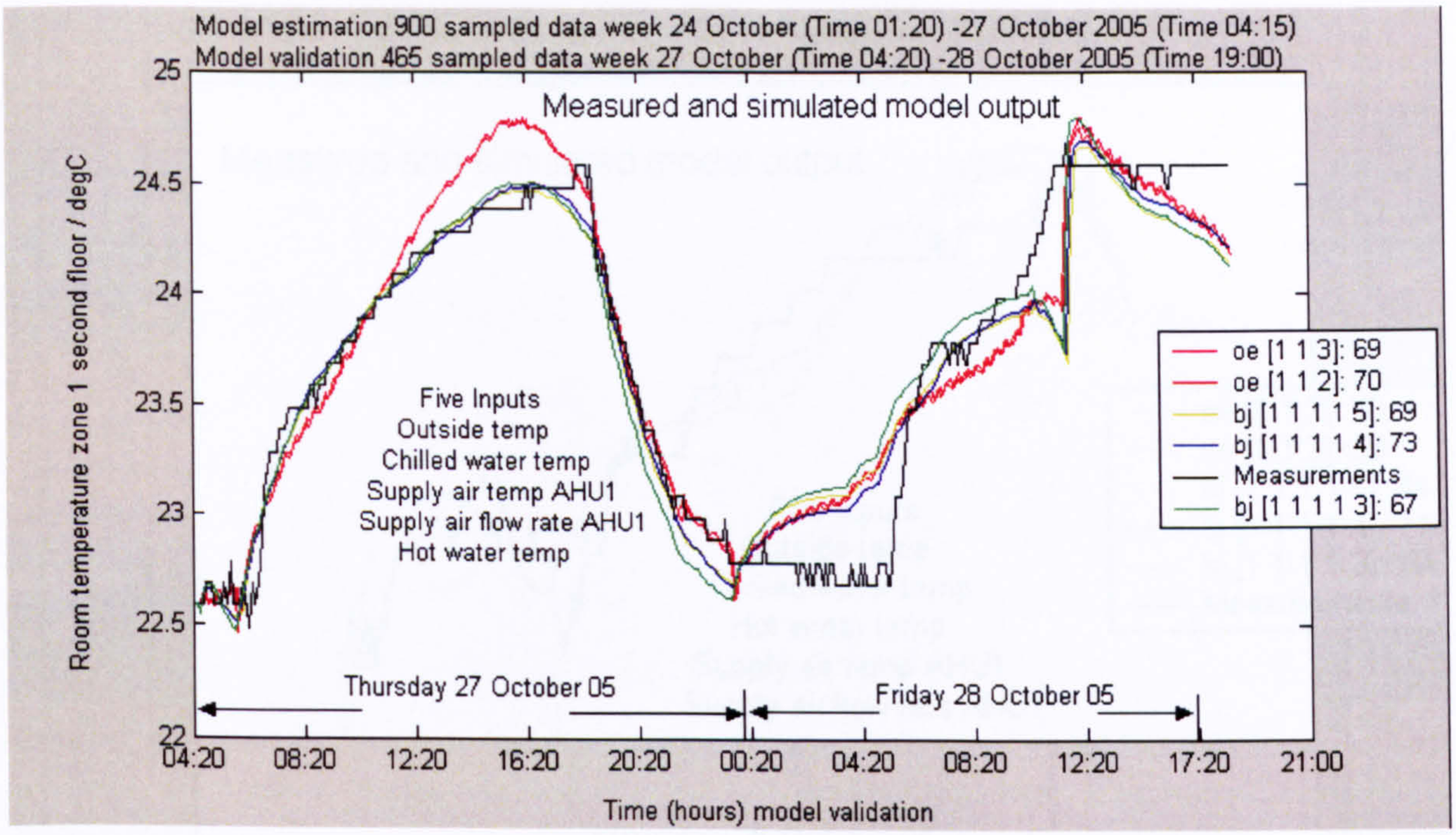

Figure 5.15 Model validation, weekdays 27-28 October 2005

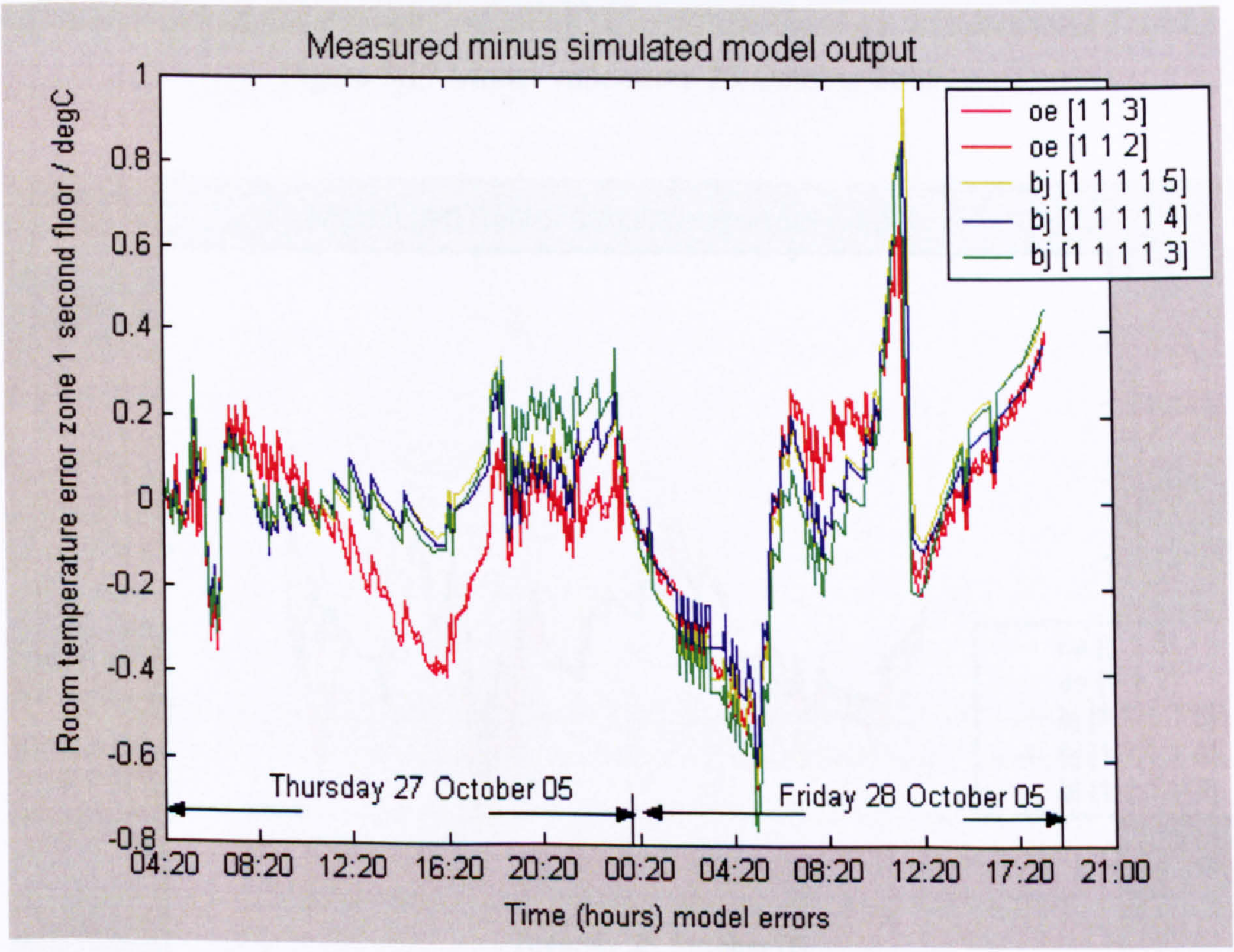

Figure 5.16 Model errors, weekdays 27-28 October 2005

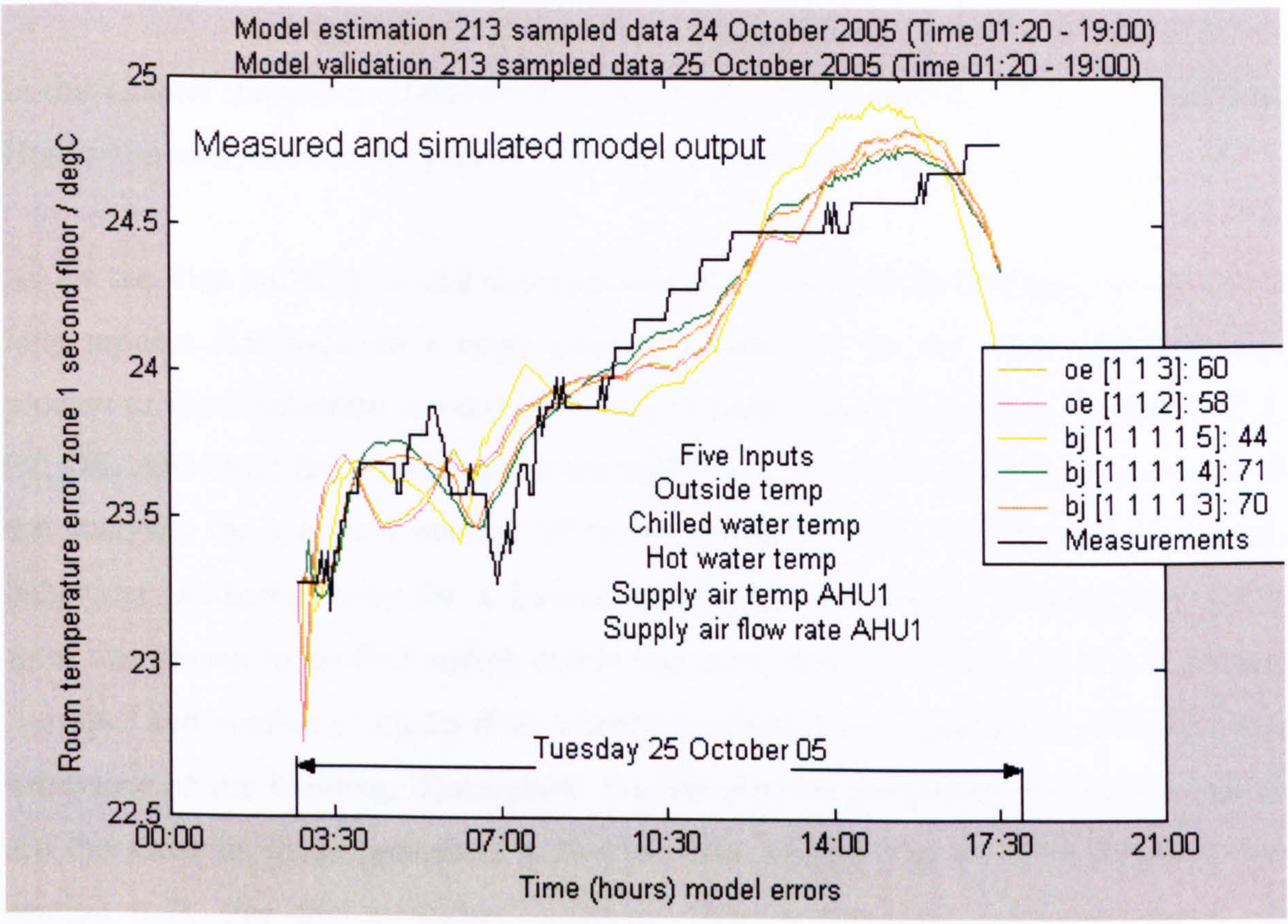

Figure 5.17 Model validation, 25 October 2005

Figure 5.18 Model errors, 25 October 2005

5.5 Conclusions of Model Development and Validation for Portman House

In this chapter the thermal behaviour of the room, situated on the 2nd floor in Portman House was analysed for one year (13 June 2005 – 09 June 2006).

As for the Visa building, model development and validation for Portman House was a long process that required a large amount of analysis for the input selection. The process of input selection is very important to obtain good parametric models (ARX, BJ, OE, ARMAX) for predicting the thermal behaviour of the building. As a result of the analysis, for a certain number of inputs it was possible to obtain good thermal behaviour prediction only for a limited number of weekdays. Consequently, going from one season to another and/or within the same season it was necessary to change the types and number of inputs if we wanted to obtain a good prediction of the thermal behaviour of the building. Throughout this chapter the procedures of input selection are the same as those presented in the previous chapter for the Visa building (see section 4.3). For the weekdays' analysis, like in the Visa building, supply air temperature AHU1, supply air flow rate AHU1 and outside temperature were the inputs affecting room temperature throughout the year, while the inputs related to hot and chilled water had different effects from one season to another.

In Portman House, the models were developed by utilizing different sampled data for model estimation and validation, and it is was demonstrated that they preserve their properties in predicting the thermal behaviour of the room not only within the same week (utilizing different sampled data for model estimation and validation), but also utilizing one week of data for model estimation and another week for model validation.

The results related to the inputs selected and mathematical models appropriate for each season will now be summarized in turn.

In the winter and beginning of the spring season, four inputs (outside temperature, hot water temperature, supply air temperature AHU1 and supply air flow rate AHU1) are required to obtain good results and the BJ models (bj [1 1 1 1 2], bj [1 1 1 1 3] and bj [1 1 1 1 4]) offer the best fits.

The same inputs (outside temperature, chilled water temperature, hot water temperature, chilled water temperature, supply air flow rate AHU1 and supply air temperature AHU1) are required for different periods of the year (as shown below) and the models that offer good fits are:

- Middle and end of Spring: BJ models (bj [1 1 1 1 2], bj [1 1 1 1 3] and bj [1 1 1 1 4])
- Beginning and middle of autumn: BJ models (bj [1 1 1 1 3], bj [1 1 1 1 4] and bj [1 1 1 1 5]) and OE models (oe [1 1 2] and oe [1 1 3]).

For the end of autumn the BJ model (bj [1 1 1 1 8]) predicts the thermal behaviour of the building very well for four inputs (hot water temperature, outside temperature, supply air flow rate AHU1 and supply air temperature AHU1).

The inputs (outside temperature, chilled water temperature, outside temperature, supply air flow rate AHU1 and supply air temperature AHU1) were selected for the summer season and for this period the BJ models (bj [1 1 1 1 2] and bj [1 1 1 1 3]) and OE model (oe [1 1 2]) have good fits.

In addition to the previous analysis one week was investigated for model estimation and another week was used for model validation. This analysis was done for one year (13 June 2005 – 09 June 2006) and the results are given in Appendix 2A. As in the Visa building, the prediction of the room's thermal behaviour in Portman House decreased slightly when we changed from using the same week to different weeks for model estimation and validation (see Appendix 2A). Consequently, to obtain good thermal prediction for the room the amount of data should not be more than one week for model estimation and validation.

As for the Visa building, one of the main disadvantages of linear parametric mathematical models reflected in this analysis is the limited period of the validity of these models, which is related to the period of validity of the inputs (Black - box models). Although the same inputs can be used throughout the season this is not the case with the models because some of them are not valid throughout the season (see sections 5.4.1, 5.4.2 and 5.4.4).

As for the Visa building, some of the inputs of less importance, including the internal gain of the building (where in part they were included within the main inputs), were not been provided by the BMS and this is a further disadvantage. The results obtained for appropriate models throughout the year have similar fits to those for the previous analysis (using the same week's data for model estimation and validation). This means that linear parametric mathematical models are suitable for thermal behaviour prediction for the maximum period of one week.

The contributions of the analysis in this chapter are the same as those in the previous chapter (see section 4.5). However, in addition, in Portman House the mathematical models required were different throughout the year, because it is a different type of building and consequently, BMS behaviour is different. Furthermore in Portman House over the course of the year FPE varied between 10^{-2} and 10^{-3}, while model errors varied between 0.6 and 0.8 degrees Celsius. Compared to the Visa building, overall, Portman House has higher values of FPE.

Finally, an overview of the weekday results obtained for the Visa building and Portman House is given in Tables 5.5, 5.6, 5.7 and 5.8, including a comparison of the results and inputs selected for each season. Appendix 2B details some of the mathematical models in terms of their parameters.

Spring Season	Visa building (Year 2005)	Portman House (13 June 2005 – 09 June 2006)
Beginning 15/03 15/04	Faults	1) Outside temperature 2) Hot water temperature 3) Supply air temperature AHU1 4) Supply air flow rate AHU1 BJ (bj [1 1 1 1 2], bj [1 1 1 1 3] and bj [1 1 1 1 4])
Middle 15/04 15/05	1) Chilled water temperature 2) Outside temperature 3) Hot water temperature 4) Supply air temperature AHU2 5) Supply air flow rate AHU2 BJ (bj [1 1 1 1 4] and bj [1 1 1 1 5])	1) Chilled water temperature 2) Outside temperature 3) Hot water temperature 4) Supply air temperature AHU1 5) Supply air flow rate AHU1 BJ (bj [1 1 1 1 2], bj [1 1 1 1 3] and bj [1 1 1 1 4])
End 15/05 15/06	1) Chilled water temperature 2) Outside temperature 3) Hot water temperature 4) Supply air temperature AHU2 5) Supply air flow rate AHU2 BJ (bj [1 1 1 1 4] and bj [1 1 1 1 5])	1) Chilled water temperature 2) Outside temperature 3) Hot water temperature 4) Supply air temperature AHU1 5) Supply air flow rate AHU1 BJ (bj [1 1 1 1 2], bj [1 1 1 1 3] and bj [1 1 1 1 4])

Table 5.5 Visa and Portman House buildings comparison spring season weekdays

Summer Season	Visa building (Year 2005)	Portman House (13 June 2005 – 09 June 2006)
Beginning 15/06 15/07	1) Chilled water temperature 2) Outside temperature 3) Supply air temperature AHU2 4) Supply air flow rate AHU2 OE (oe [1 1 2], oe [1 1 3], oe [1 1 4] and oe [1 1 5]) ARMAX (amx [2 2 2 1])	1) Chilled water temperature 2) Outside temperature 3) Supply air temperature AHU1 4) Supply air flow rate AHU1 BJ (bj [1 1 1 1 2] and bj [1 1 1 1 3]) OE (oe [1 1 2])
Middle 15/07 15/08	1) Chilled water temperature 2) Outside temperature 3) Supply air temperature AHU2 4) Supply air flow rate AHU2 OE (oe [1 1 2], oe [1 1 3], oe [1 1 4] and oe [1 1 5]) ARMAX (amx [2 2 2 1])	1) Chilled water temperature 2) Outside temperature 3) Supply air temperature AHU1 4) Supply air flow rate AHU1 BJ (bj [1 1 1 1 2] and bj [1 1 1 1 3]) OE (oe [1 1 2])
End 15/08 15/09	Faults	Faults

Table 5.6 Visa and Portman House buildings comparison summer season weekdays

Autumn Season	Visa building (Year 2005)	Portman House (13 June 2005 – 09 June 2006)
Beginning 15/09 15/10	Faults	1) Chilled water temperature 2) Outside temperature 3) Hot water temperature 4) Supply air temperature AHU1 5) Supply air flow rate AHU1 BJ (bj [1 1 1 1 3], bj [1 1 1 1 4] and bj [1 1 1 1 5]) OE (oe [1 1 2] and oe [1 1 3])
Middle 15/10 28/10	1) Chilled water temperature 2) Outside temperature 3) Hot water temperature 4) Supply air temperature AHU2 5) Supply air flow rate AHU2 OE (oe [1 1 2])	1) Chilled water temperature 2) Outside temperature 3) Hot water temperature 4) Supply air temperature AHU1 5) Supply air flow rate AHU1 BJ (bj [1 1 1 1 3], bj [1 1 1 1 4] and bj [1 1 1 1 5]) OE (oe [1 1 2] and oe [1 1 3])
End 31/10 15/12	1) Outside temperature 2) Hot water temperature 3) Supply air temperature AHU2 4) Supply air flow rate AHU2 BJ (bj [1 1 1 1 2] and bj [1 1 1 1 3]) ARMAX (amx [2 2 2 1])	1) Outside temperature 2) Hot water temperature 3) Supply air temperature AHU1 4) Supply air flow rate AHU1 BJ (bj [1 1 1 1 8])

Table 5.7 Visa and Portman House buildings comparison autumn season weekdays

Winter Season	Visa building (Year 2005)	Portman House (13 June 2005 – 09 June 2006)
Beginning 15/12 15/01	1) Outside temperature 2) Hot water temperature 3) Supply air temperature AHU2 4) Supply air flow rate AHU2 BJ (bj [1 1 1 1 3], bj [1 1 1 1 4] and bj [1 1 1 1 5]) and OE (oe [1 1 2])	Faults
Middle 15/01 15/02	1) Outside temperature 2) Hot water temperature 3) Supply air temperature AHU2 4) Supply air flow rate AHU2 BJ (bj [1 1 1 1 3], bj [1 1 1 1 4] and bj [1 1 1 1 5]) and OE (oe [1 1 2])	1) Outside temperature 2) Hot water temperature 3) Supply air temperature AHU1 4) Supply air flow rate AHU1 BJ (bj [1 1 1 1 2], bj [1 1 1 1 3] and bj [1 1 1 1 4])
End 15/02 15/03	1) Outside temperature 2) Hot water temperature 3) Supply air temperature AHU2 4) Supply air flow rate AHU2 BJ (bj [1 1 1 1 2], bj [1 1 1 1 3] bj [1 1 1 1 4] and bj [1 1 1 1 5])	1) Outside temperature 2) Hot water temperature 3) Supply air temperature AHU1 4) Supply air flow rate AHU1 BJ (bj [1 1 1 1 2], bj [1 1 1 1 3] and bj [1 1 1 1 4])

Table 5.8 Visa and Portman House buildings comparison winter season weekdays

CHAPTER 6 Data Analysis and Model Development for the Rockefeller Building

This chapter gives a brief description of the Rockefeller building and the room that is examined for model estimation and validation. The data collected are for one year (2006) and the models chosen are those that best fit the real data. Different models and inputs have been found to be most appropriate for winter, spring, summer and autumn. The following sections explore the models in terms of best fit for each of the seasons. The model structures ARX, OE, ARMAX and BJ are the general choices for model development in the Thomas Lewis Room (Rockefeller building).

6.1 Rockefeller Building Description

Rockefeller Building (see Fig. 6.1) is located in London and is part of University College London. Rockefeller is an old construction (1920) and its thermal behaviour is different to the Visa and Portman House Buildings. In addition, the room examined only has a heating system, provided by radiators, and this is another difference compared to the other two buildings. There is no air conditioning system in this room. The data collected were from the Thomas Lewis room (see Fig. 6.2 left hand side) located on the ground floor of the Rockefeller Building. Invensys is the building management system installed in the Rockefeller Building for the monitoring and operation of plant/building services.

Figure 6.1 Rockefeller building

6.2 Data Collection Description

The data from the Rockefeller building were collected for one year, with a sampling interval of 5 minutes. The data collected, were stored in the BMS and downloaded every two weeks. The inputs and output are presented in section 6.1 were collected for a period of one year (2006) through the existing sensors of the BMS and Invensys data logger. Invensys is software used to log and download the data collected every two weeks for model development and validation. The down-loaded data was then converted to Microsoft Excel file format, which were used in system identification for model development and validation.

The primary assumption of the model development was that the internal temperature variation is directly influenced by the variations of external temperature and the internal heating water that flows through the radiators. Thomas Lewis Room is a large office and approximately five persons work in it. The effects of additional internal heat gain caused by occupancy, computers and printers were assumed to be small. Consequently, their effect is small compared to the external temperature and hot water temperature circulating throughout the cold season.

6.3 Input Selection

Differently from the Visa and Portman House buildings, input (independent variables) and output selection for this building consisted only of outside temperature and hot water temperature across the radiators and room temperature (output). There was only one sensor for measuring the room temperature, and it was positioned in the centre.

As for the Visa and Portman house buildings, the models were developed for different seasons and each season was subdivided into three parts; beginning, middle and end. In this building, differently from Portman house and Visa buildings, this subdivision depended principally on the limited period that different linear parametric models could give good results related to room prediction temperature.

In this chapter, the models developed have the following properties:

- The models can predict the thermal behaviour of the room for several weeks four to nine weeks

- Within the period of models validation, the change in models' performance is very small from one week to another.

Finally, in the following sections the models that give the best thermal behaviour of the room for each season are examined.

Figure 6.2 Thomas Lewis room (Ground floor, Rockefeller building)

6.4 Weekdays Model Development and Validation

Listed below are the inputs and output, logged every five minutes, collected for the Thomas Lewis Room. This room only has a heating system and as a result only two inputs (outside temperature and hot water temperature) and one output (Thomas Lewis room temperature) can be used for model estimation. The data are analysed by dividing them into weekdays (Monday Time 01:20 to Friday Time 19:00) and weekends (the latter is not presented). Finally, for each season, due to the similarities of the results, not all the graphs relating to weekdays are presented.

Thomas Lewis Room

- Thomas Lewis Room temperature (output) in degrees Celsius (degC)
- Outside temperature (input) in degrees Celsius (degC)
- Hot water temperature (input) in degrees Celsius (degC)

Finally, model development and validation are analysed respectively for four cases:

a) 213 Sampled-data model estimation (18 hours in day 1 – Time 01:20-19:00) and 213 sampled-data model validation (18 hours in day 2 – Time 01:20-19:00)

b) 900 Sampled-data model estimation (75 hours) and 465 sampled-data model validation (39 hours)

c) 800 Sampled-data model estimation (67 hours) and 565 sampled-data model validation (47 hours)

d) 1365 sampled-data model estimation (113.5 hours, weekdays) and 1365 sampled-data model validation in following weekdays (see Appendix 3A).

In the following sections the model fits for each season are analysed.

6.4.1 Model Development and Validation for the Summer Season

Different weeks working days (Monday Time 01:20 to Friday Time 19:00) of the summer season were examined for model estimation and validation. During summer time the heater is off and the outside temperature is the input that affects room temperature. The results, for model estimation and validation, obtained for one input and one output (Thomas Lewis room temperature) are presented respectively for the beginning, middle and end of the summer season.

Beginning of the summer season

The weeks 12-16 June 2006, 19-23 June 2006 and 26-30 June 2006 were analysed. It can be noted that the bj [1 1 1 1 2] and bj [2 2 2 2 5] models are very flexible and can predict the room temperature respectively for 213, 900 and 800 sampled-data model estimations. Finally, the bj [1 1 1 1 2] and bj [2 2 2 2 5] models can be used for the three weeks for different ranges of sampled-data model estimations (see FPE and model fits in Table 6.1).

Middle of the summer season

The weeks between 10 July and 18 August 2006 were analysed. The results related to the week 10-14 July 2006 are shown in Figs. 6.3 and 6.5, and the errors between model output and measurements are presented in Figs. 6.4 and 6.6. Finally, none of the models gave good fits, so the best model to use even though it has a poor fit, is the amx [1 1 1 2] model (see FPE and model fits in Table 6.1).

End of the summer season

To analyse this season the weeks 21-25 August 2006, 28 August-01 September 2006 and 04-08 September 2006 were taken for model estimation. The results are shown in Table 6.1. Analysing the results, the ARMAX model (amx [2 2 2 1]) and BJ model (bj [2 2 2 2 1]) offers a good fits (see FPE and model fits in Table 6.1).

In conclusion, throughout the autumn season the FPE is between 10^{-2} and 10^{-3} and the maximum model error is 0.8 degrees Celsius.

1-213 Data Estimation 289-501 Data Validation	1-900 Data Estimation 901-1365 Data Validation	1-800 Data Estimation 801-1365 Data Validation
One Input	**One Input**	**One Input**
Outside temperature	Outside temperature	Outside temperature
Beginning of summer	**Beginning of summer**	**Beginning of summer**
FPE ≈ 0.001	FPE ≈ 0.005	FPE ≈ 0.005
bj [2 2 2 2 5]: 85-90	bj [2 2 2 2 5]: 70-80	bj [2 2 2 2 5]: 75-80
bj [1 1 1 1 2]: 65-70	bj [1 1 1 1 2]: 35-45	bj [1 1 1 1 2]: 60-65
Middle of summer	**Middle of summer**	**Middle of summer**
FPE ≈ 0.001	FPE ≈ 0.01	FPE ≈ 0.01
amx [1 1 1 2]: 70-80	amx [1 1 1 2]: 25-30	amx [1 1 1 2]: 25-35
End of summer	**End of summer**	**End of summer**
FPE ≈ 0.001	FPE ≈ 0.01	FPE ≈ 0.01
amx [2 2 2 1]: 50-60	amx [2 2 2 1]: 25-30	amx [2 2 2 1]: 40-50
bj [2 2 2 2 1]: 50-55	bj [2 2 2 2 1]: 15-20	bj [2 2 2 2 1]: 15-25

Table 6.1 Summer weekdays

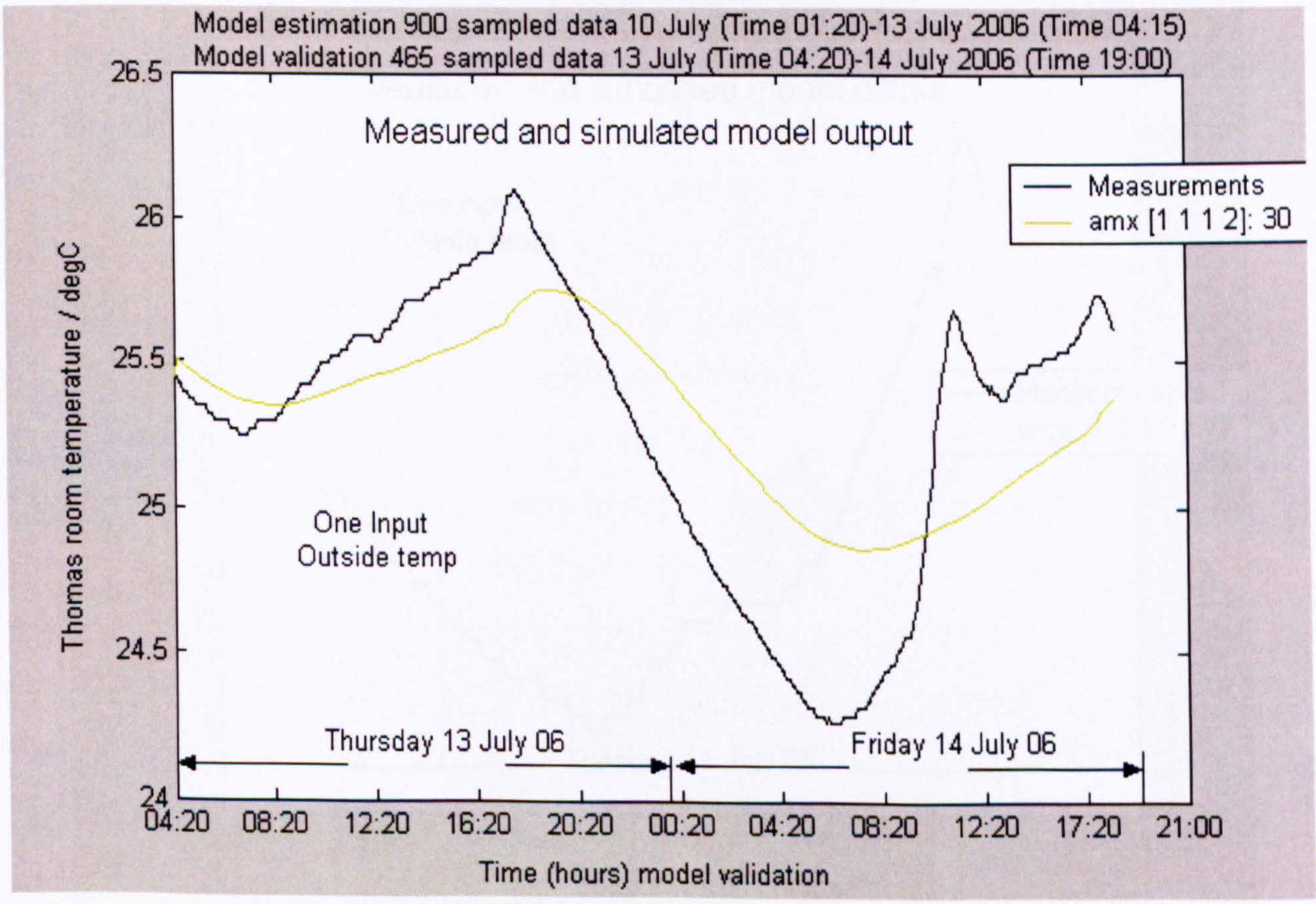

Figure 6.3 Model validation, weekdays 13 -14 July 2006

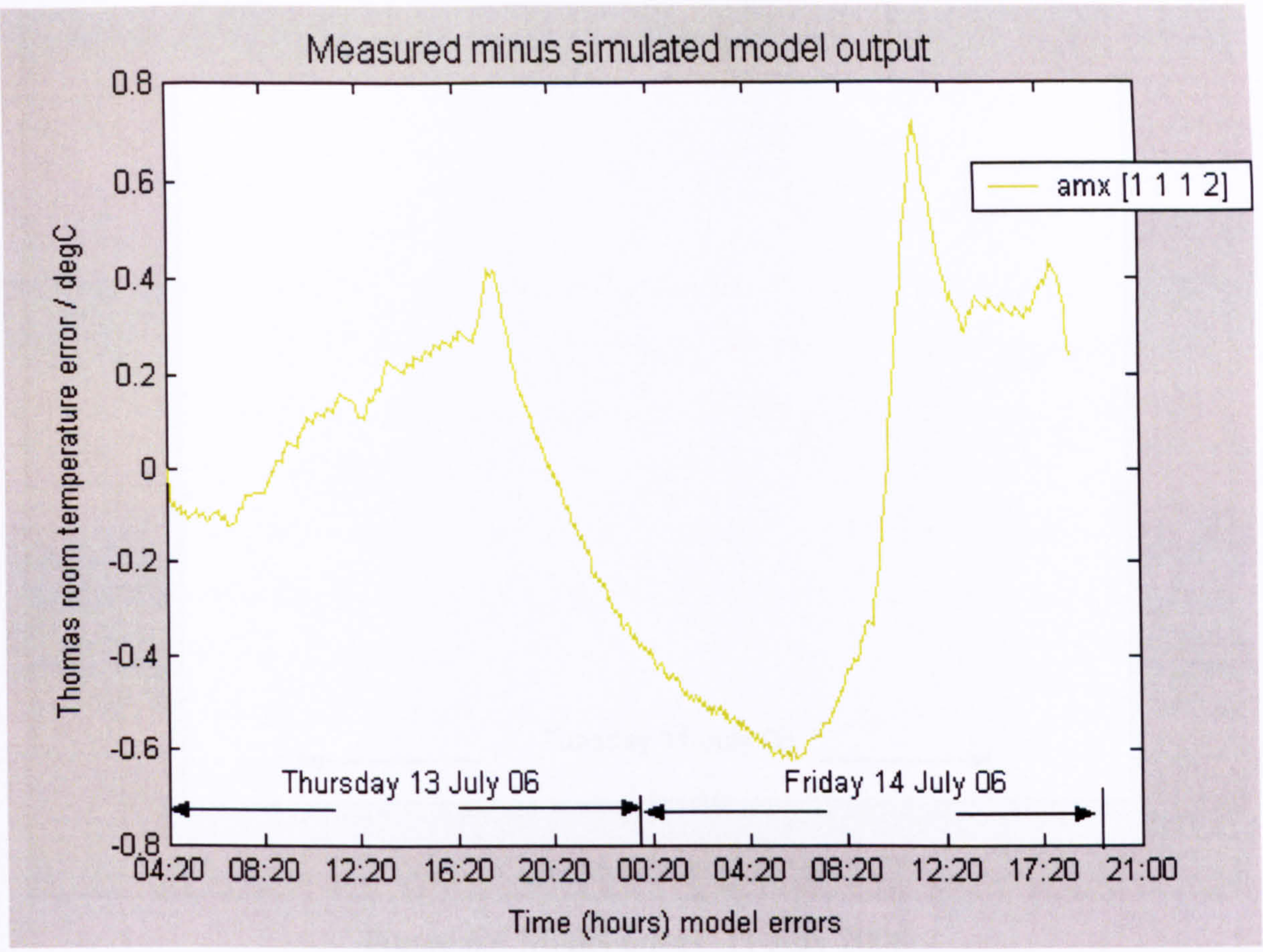

Figure 6.4 Model errors, weekdays 13 -14 July 2006

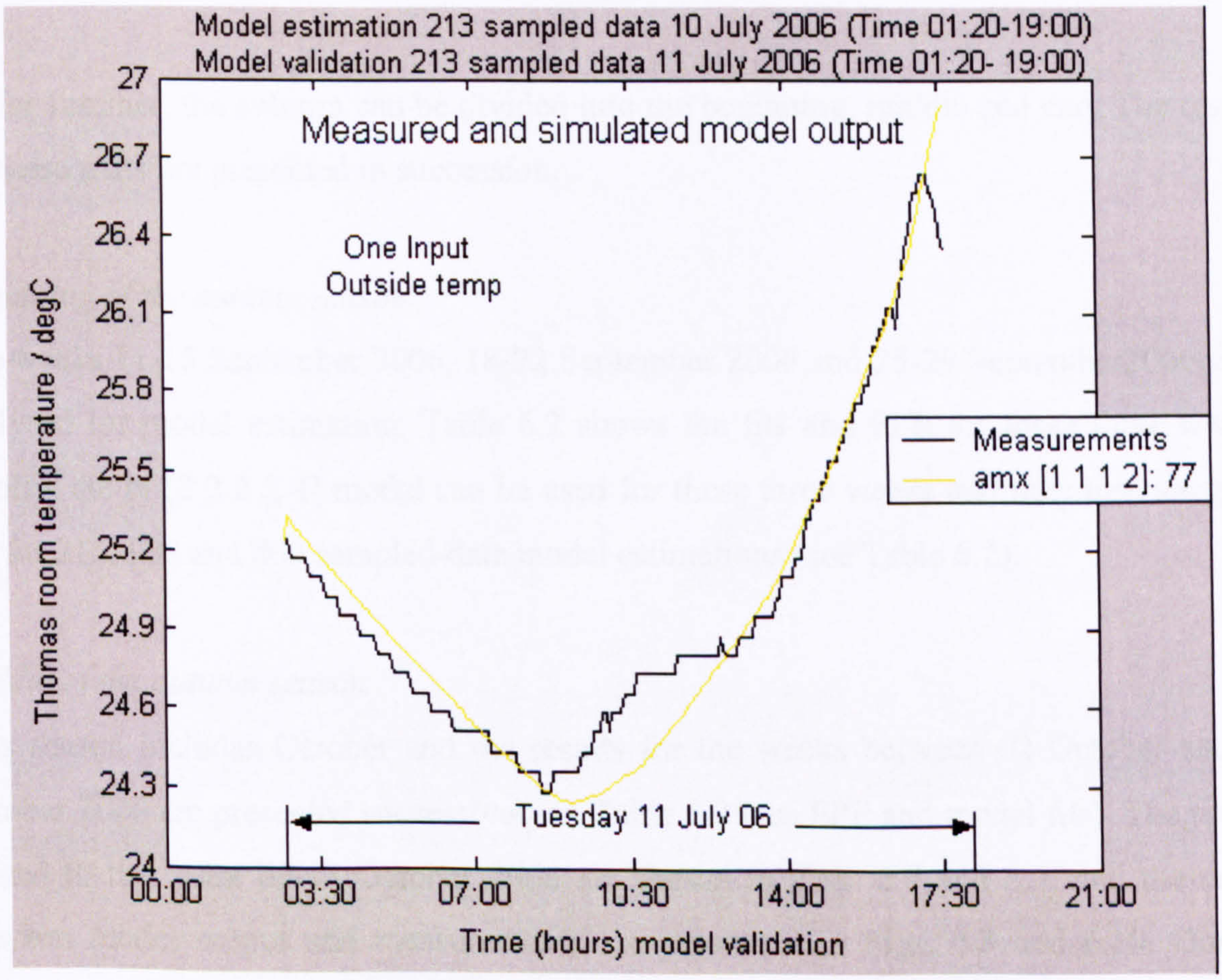

Figure 6.5 Model validation, 11 July 2006

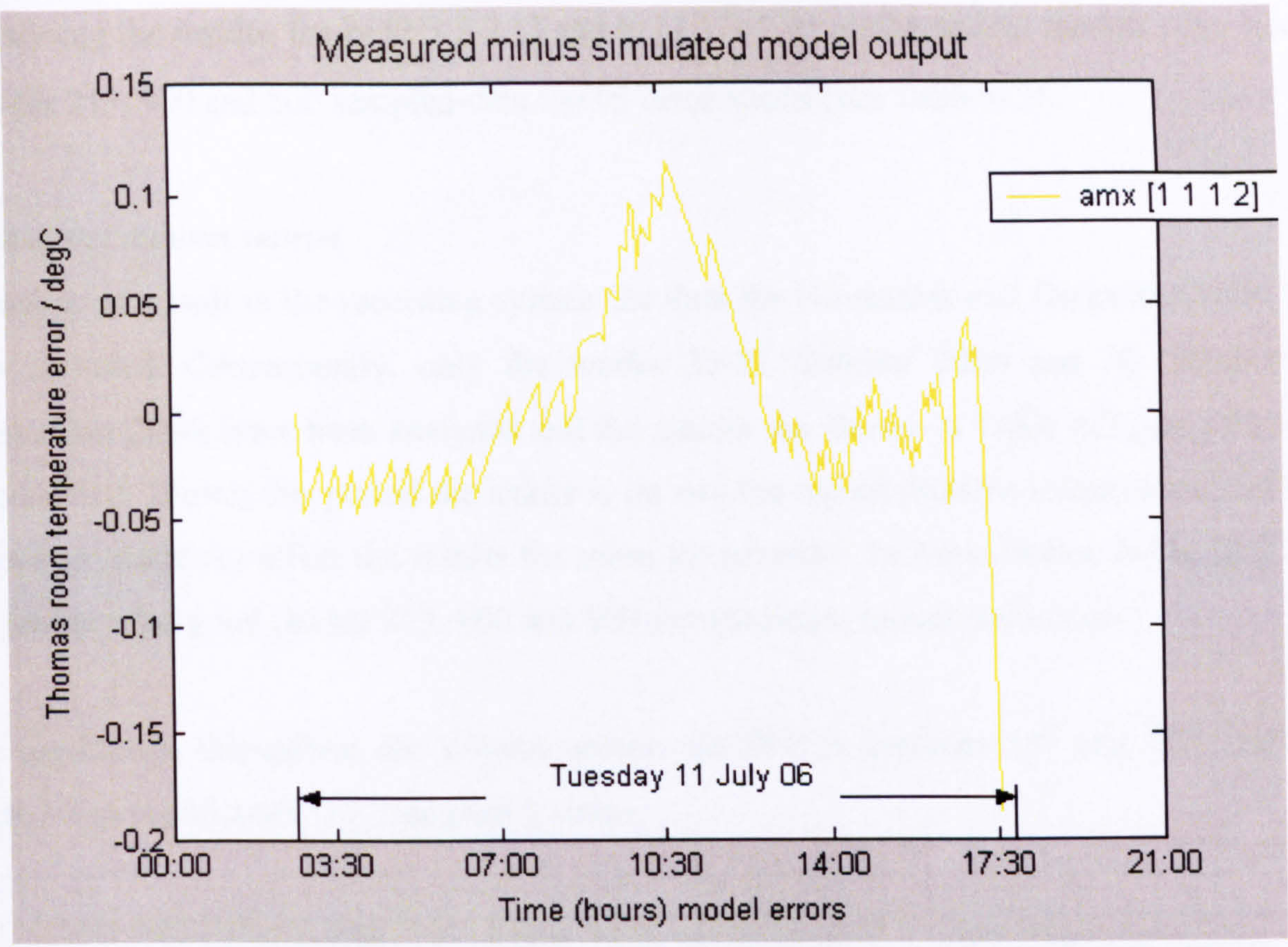

Figure 6.6 Model errors, 11 July 2006

6.4.2 Model Development and Validation for the Autumn Season

As for summer, the autumn can be divided into the beginning, middle and end. The results for these parts are presented in succession.

Beginning of the autumn season

The weeks 11-15 September 2006, 18-22 September 2006 and 25-29 September2006 were analysed for model estimation. Table 6.2 shows the fits and FPE for these three weeks. Finally, the bj [2 2 2 2 4] model can be used for these three weeks and they provide good fits for 213, 900 and 800 sampled-data model estimations (see Table 6.2).

Middle of the autumn season

This season includes October and the results for the weeks between 02 October and 20 October 2006 are presented successively in Table 6.2 (see FPE and model fits). The results related to the week 09-13 October 2006 are shown in Figs. 6.7 and 6.9, and the errors between model output and measurements are presented in Figs. 6.8 and 6.10. Outside temperature is the only input that affects room temperature.

Analysing the results, the bj [2 2 2 2 1] and bj [1 1 1 1 2] mathematical models offer good fits for 213, 900 and 800 sampled-data model estimations (see Table 6.2).

End of the autumn season

Because of a fault in the recording system the data for November and December 2006 are not included. Consequently, only the weeks 23-27 October 2006 and 30 October-03 November 2006, have been analysed and the results are shown in Table 6.2 (see FPE and model fits). During this period the heater is on and the inputs (outside temperature and hot water temperature) affect the results for room temperature. In these weeks, the bj [2 2 2 2 4] model offer good fits for 213, 900 and 800 sampled-data model estimation.

In conclusion, throughout the autumn season the FPE is between 10^{-2} and 10^{-3} and the maximum model error is 1.2 degrees Celsius.

1-213 Data Estimation 289-501 Data Validation	1-900 Data Estimation 901-1365 Data Validation	1-800 Data Estimation 801-1365 Data Validation
One Input	**One Input**	**One Input**
Outside temperature	Outside temperature	Outside temperature
Beginning of autumn	**Beginning of autumn**	**Beginning of autumn**
FPE ≈ 0.005	FPE ≈ 0.003	FPE ≈ 0.003
bj [2 2 2 2 4]: 40-45	bj [2 2 2 2 4]: 60-65	bj [2 2 2 2 4]: 40-50
Middle of autumn	**Middle of autumn**	**Middle of autumn**
FPE ≈ 0.001	FPE ≈ 0.01	FPE ≈ 0.015
bj [2 2 2 2 1]: 55-60	bj [2 2 2 2 1]: 15-20	bj [2 2 2 2 1]: 5-10
bj [1 1 1 1 2]: 50-55	bj [1 1 1 1 2]: 20-25	bj [1 1 1 1 2]: 15-20
End of autumn	**End of autumn**	**End of autumn**
Two Inputs	**Two Inputs**	**Two Inputs**
Outside temperature	Outside temperature	Outside temperature
Hot water temperature	Hot water temperature	Hot water temperature
FPE ≈ 0.001	FPE ≈ 0.002	FPE ≈ 0.002
bj [2 2 2 2 4]: 75-85	bj [2 2 2 2 4]: 70-80	bj [2 2 2 2 4]: 75-85

Table 6.2 Autumn weekdays

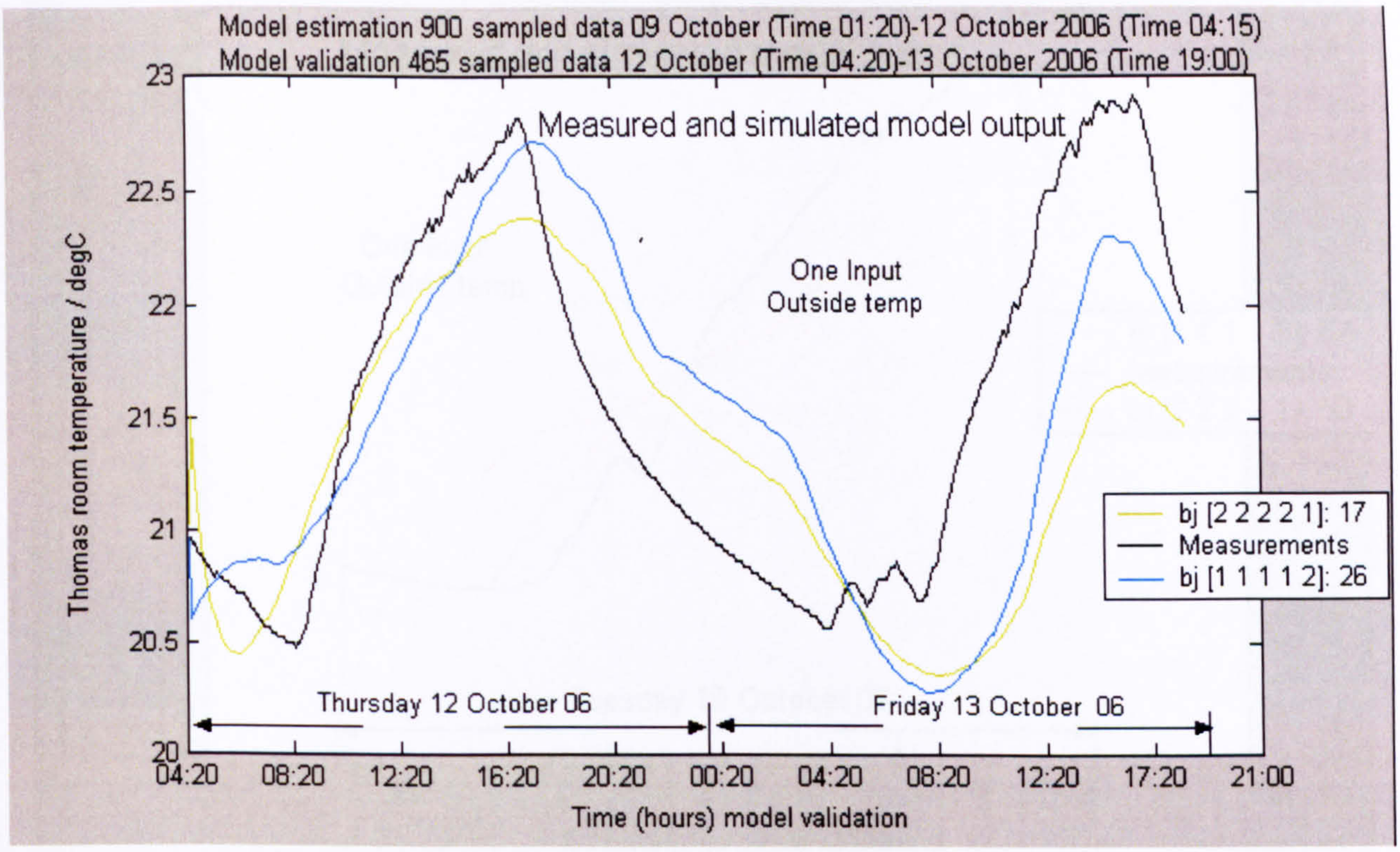

Figure 6.7 Model validation, weekdays 12-13 October 2006

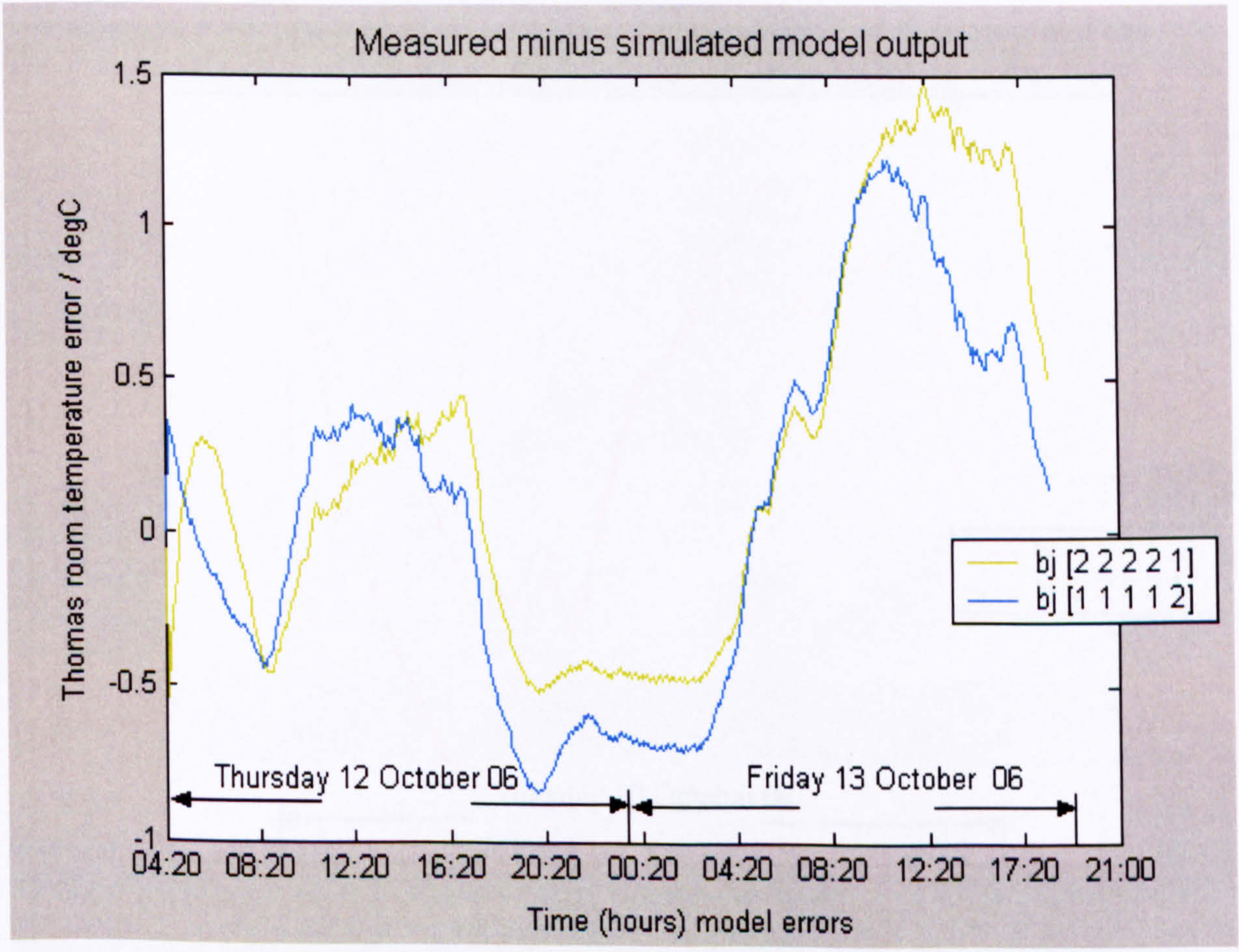

Figure 6.8 Model errors, weekdays 12-13 October 2006

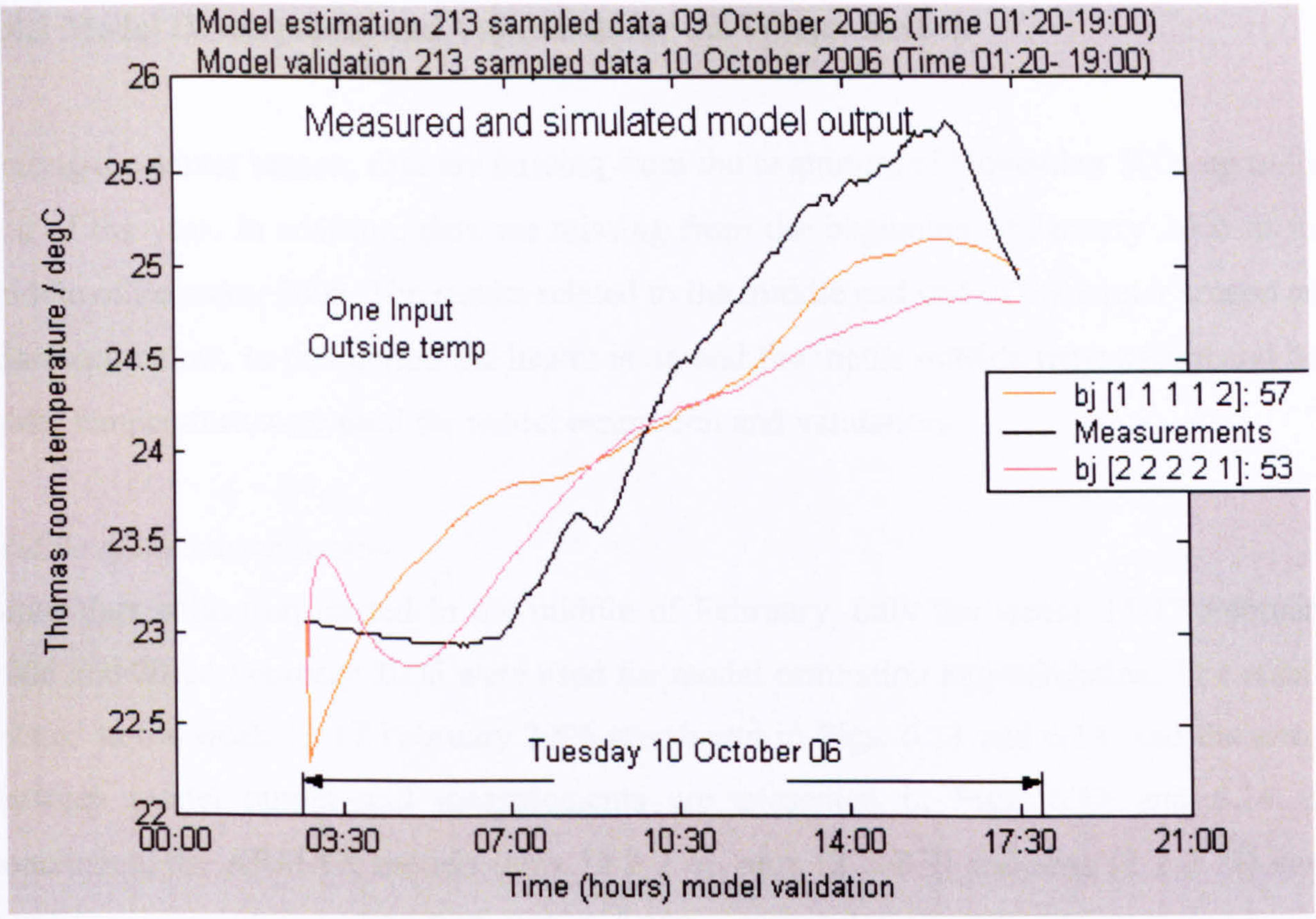

Figure 6.9 Model validation, 10 October 2006

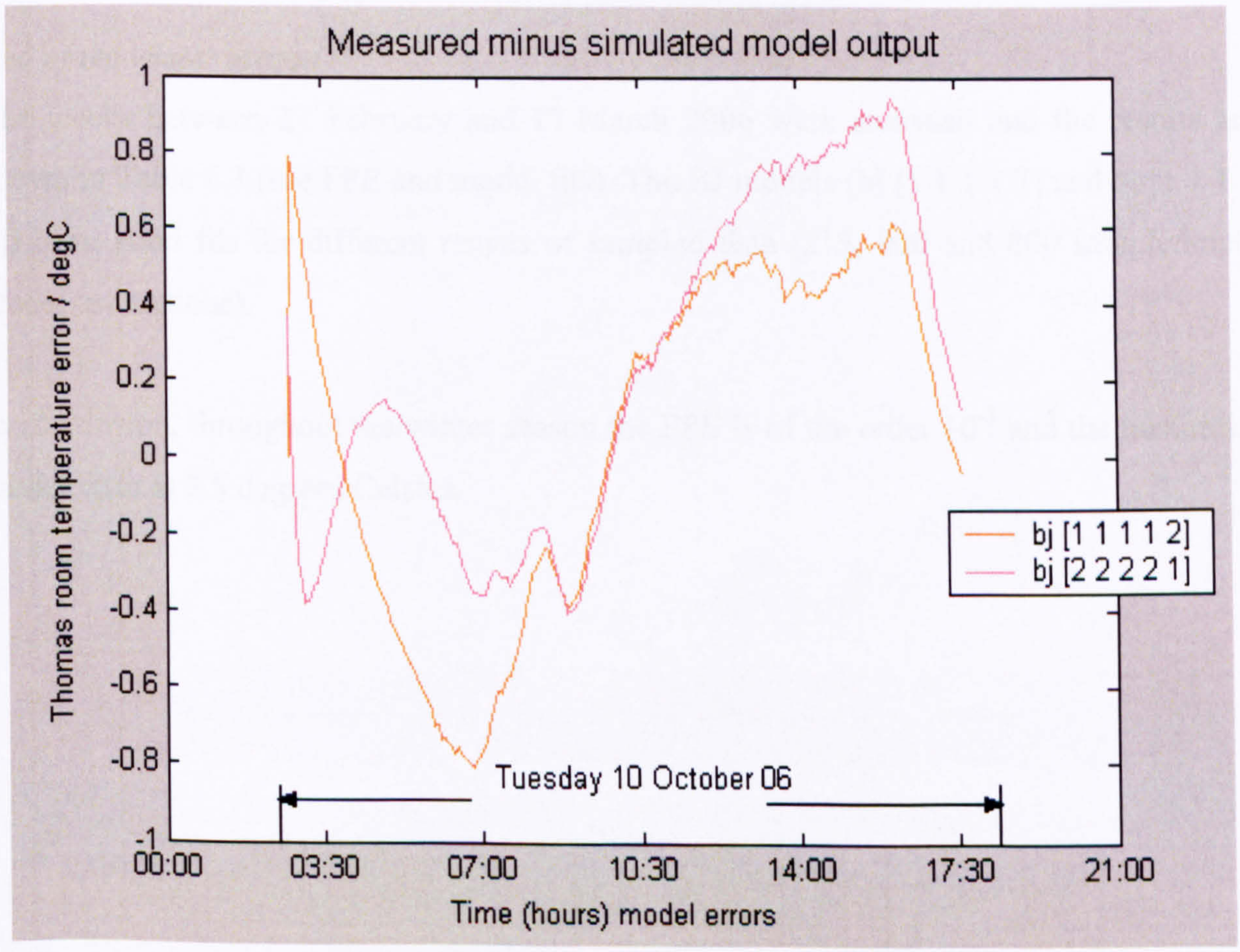

Figure 6.10 Model errors, 10 October 2006

6.4.3 Model Development and Validation for the Winter Season

During the winter season, data are missing from the beginning of November 2006 up to the end of the year. In addition, data are missing from the beginning of January 2006 to the middle of February 2006. The results related to the middle and end of the winter season are discussed below. In this period the heater is on and the inputs outside temperature and hot water temperature were used for model estimation and validation.

Middle of the winter season

Since data collection started in the middle of February, only the weeks 13-17 February 2006 and 20-24 February 2006 were used for model estimation and validation. The results related to the week 13-17 February 2006 are shown in Figs. 6.11 and 6.13, and the errors between model output and measurements are presented in Figs. 6.12 and 6.14. In conclusion, the ARMAX models (amx [2 2 2 6], amx [2 2 2 7] and amx [2 2 2 8]) have good fits and can be used for 213, 900 and 800 sampled-data model estimations with very good results.

End of the winter season

The weeks between 27 February and 17 March 2006 were analysed and the results are shown in Table 6.3 (see FPE and model fits). The BJ models (bj [1 1 1 1 7] and bj [1 1 1 1 8]) have good fits for different ranges of sampled data (213, 900 and 800 sampled-data model estimations).

In conclusion, throughout the winter season the FPE is of the order 10^{-3} and the maximum model error is 2.5 degrees Celsius.

1-213 Data Estimation 289-501 Data Validation	1-900 Data Estimation 901-1365 Data Validation	1-800 Data Estimation 801-1365 Data Validation
Two Inputs	**Two Inputs**	**Two Inputs**
Outside temperature	Outside temperature	Outside temperature
Hot water temperature	Hot water temperature	Hot water temperature
Middle of winter	**Middle of winter**	**Middle of winter**
FPE ≈ 0.002	FPE ≈ 0.001	FPE ≈ 0.001
amx [2 2 2 6]: 20-25	amx [2 2 2 6]: 45-50	amx [2 2 2 6]: 45-55
amx [2 2 2 7]: 15-25	amx [2 2 2 7]: 50-55	amx [2 2 2 7]: 60-65
amx [2 2 2 8]: 15-25	amx [2 2 2 8]: 50-55	amx [2 2 2 8]: 55-65
End of winter	**End of winter**	**End of winter**
FPE ≈ 0.002	FPE ≈ 0.001	FPE ≈ 0.001
bj [1 1 1 1 7]: 25-35	bj [1 1 1 1 7]: 45-50	bj [1 1 1 1 7]: 55-65
bj [1 1 1 1 8]: 20-25	bj [1 1 1 1 8]: 45-50	bj [1 1 1 1 8]: 55-65

Table 6.3 Winter weekdays

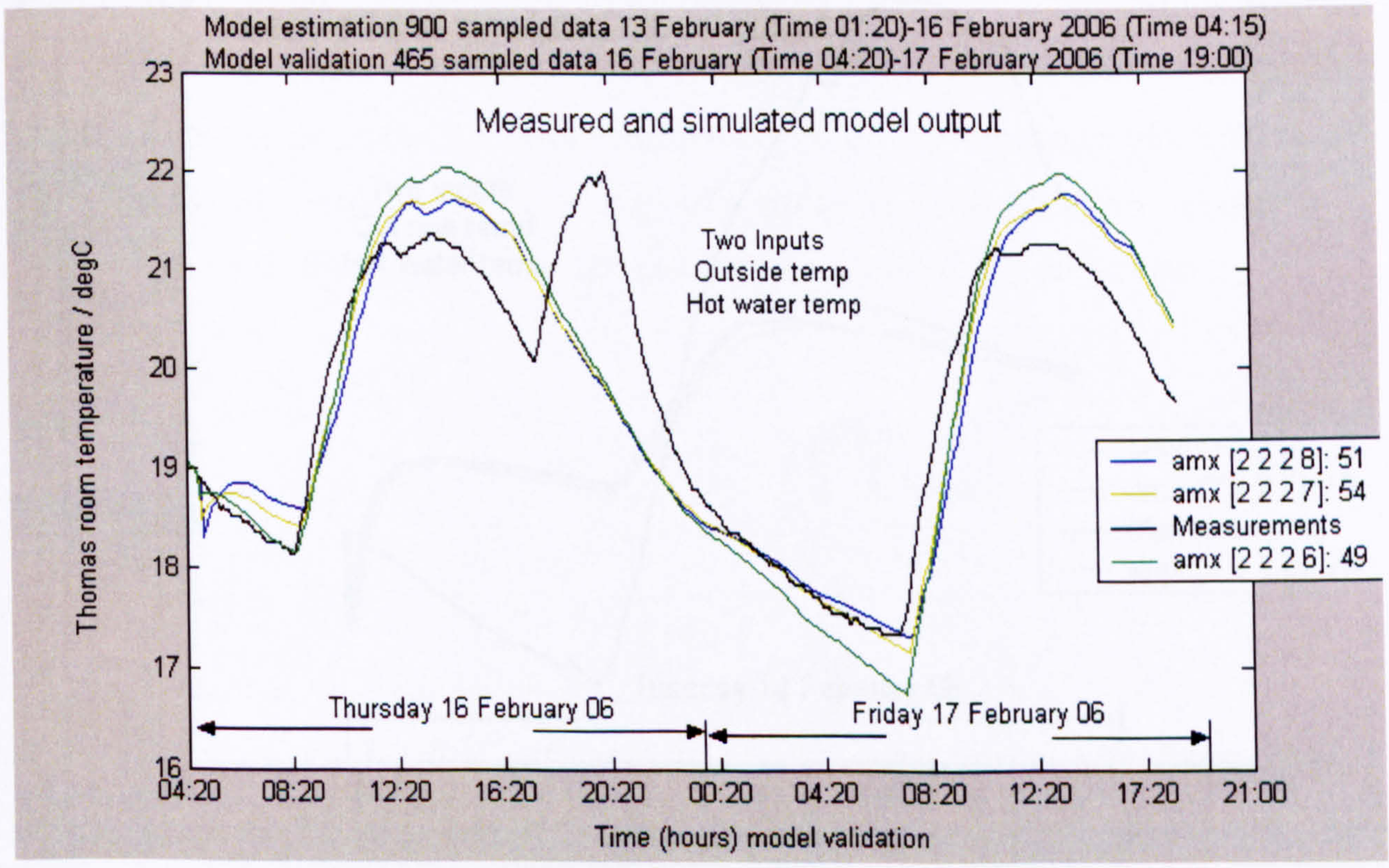

Figure 6.11 Model validation, weekdays 16-17 February 2006

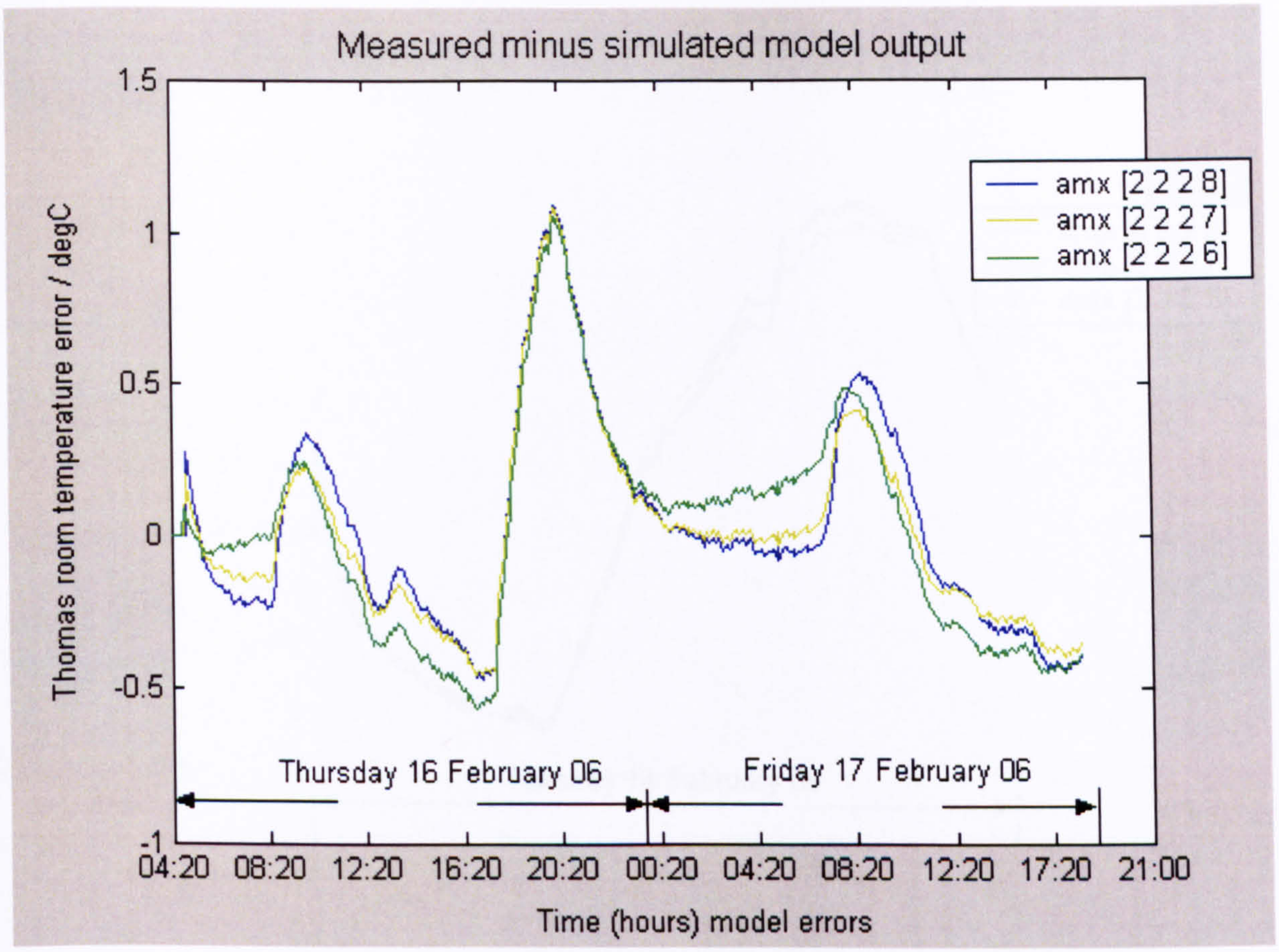

Figure 6.12 Model errors, weekdays 16-17 February 2006

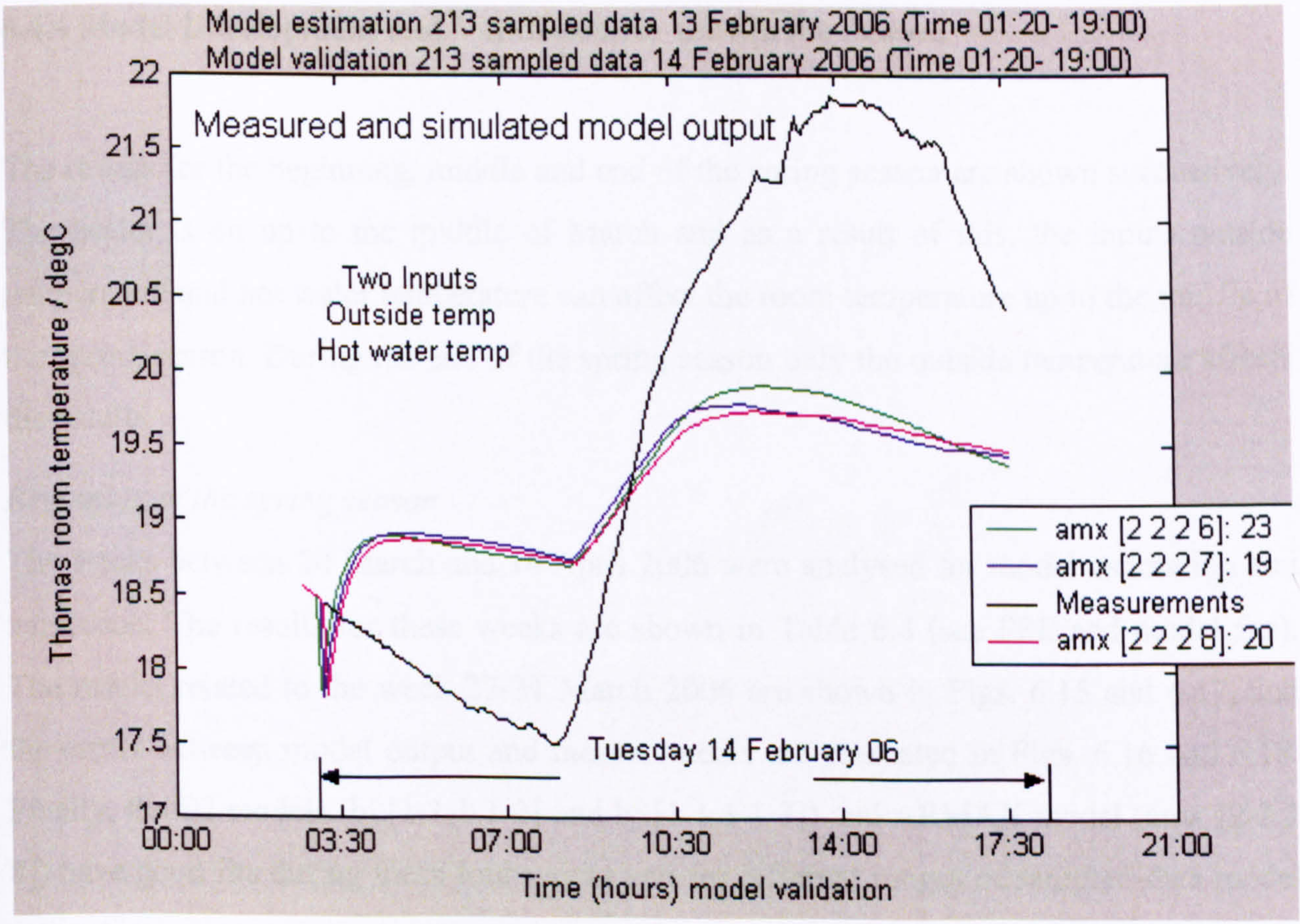

Figure 6.13 Model validation, 14 February 2006

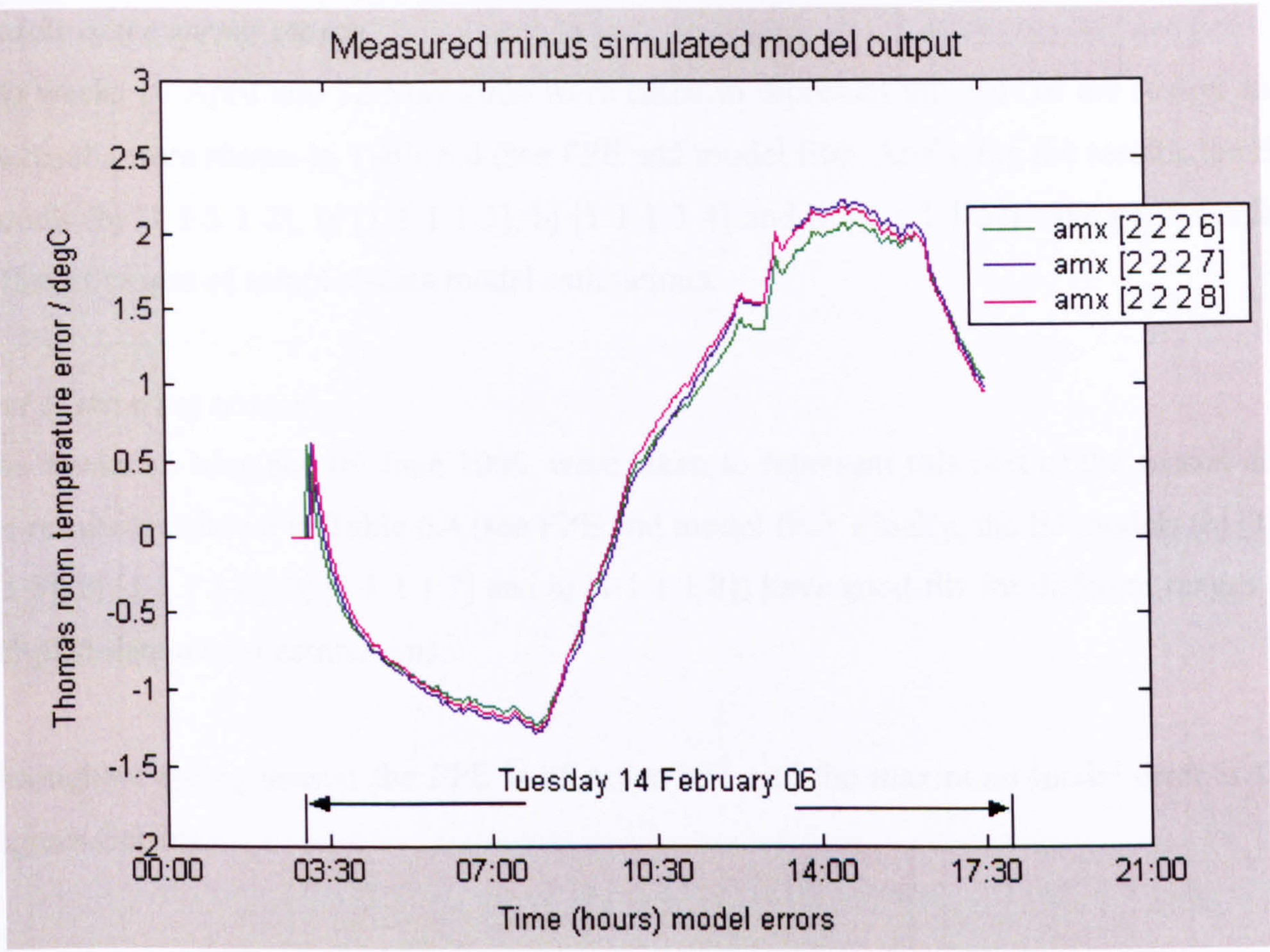

Figure 6.14 Model errors, 14 February 2006

6.4.4 Model Development and Validation for the Spring Season

The results for the beginning, middle and end of the spring season are shown successively. The heater is on up to the middle of March and as a result of this, the inputs outside temperature and hot water temperature can affect the room temperature up to the middle of the spring season. During the end of the spring season only the outside temperature affects the results.

Beginning of the spring season

The weeks between 20 March and 14 April 2006 were analysed for model estimation and validation. The results for these weeks are shown in Table 6.4 (see FPE and model fits). The results related to the week 27-31 March 2006 are shown in Figs. 6.15 and 6.17, and the errors between model output and measurements are presented in Figs. 6.16 and 6.18. Finally, the BJ models (bj [1 1 1 1 2] and bj [1 1 1 1 3]) and ARMAX model (amx [2 2 2 8]) have good fits during these four weeks and for different ranges of sampled-data model estimations.

Middle of the spring season

The weeks 17 April and 12 May 2006 were taken to represent this part of the season and the results were shown in Table 6.4 (see FPE and model fits). Analysing the results, the BJ models (bj [1 1 1 1 2], bj [1 1 1 1 3], bj [1 1 1 1 4] and bj [1 1 1 1 5]) have good fits for different ranges of sampled-data model estimations.

End of the sring season

The weeks 15 May and 09 June 2006, were taken to represent this part of the season and the results are shown in Table 6.4 (see FPE and model fits). Finally, the BJ models (bj [1 1 1 1 5], bj [1 1 1 1 6], bj [1 1 1 1 7] and bj [1 1 1 1 8]) have good fits for different ranges of sampled-data model estimations.

Throughout spring season the FPE is of order 10^{-3} and the maximum model error is 0.8 degrees Celsius.

1-213 Data Estimation 289-501 Data Validation	1-900 Data Estimation 901-1365 Data Validation	1-800 Data Estimation 801-1365 Data Validation
Two Inputs	**Two Inputs**	**Two Inputs**
Outside temperature	Outside temperature	Outside temperature
Hot water temperature	Hot water temperature	Hot water temperature
Beginning of spring	**Beginning of spring**	**Beginning of spring**
FPE ≈ 0.001	FPE ≈ 0.002	FPE ≈ 0.002
amx [2 2 2 8]: 50-55	amx [2 2 2 8]: 50-55	amx [2 2 2 8]: 55-60
bj [1 1 1 1 2]: 80-90	bj [1 1 1 1 2]: 60-65	bj [1 1 1 1 2]: 55-60
bj [1 1 1 1 3]: 85-95	bj [1 1 1 1 3]: 60-65	bj [1 1 1 1 3]: 55-65
Middle of spring	**Middle of spring**	**Middle of spring**
FPE ≈ 0.001	FPE ≈ 0.002	FPE ≈ 0.002
bj [1 1 1 1 2]: 55-65	bj [1 1 1 1 2]: 40-50	bj [1 1 1 1 2]: 40-45
bj [1 1 1 1 3]: 55-65	bj [1 1 1 1 3]: 40-50	bj [1 1 1 1 3]: 40-45
bj [1 1 1 1 4]: 50-60	bj [1 1 1 1 4]: 40-50	bj [1 1 1 1 4]: 40-45
bj [1 1 1 1 5]: 55-65	bj [1 1 1 1 5]: 45-50	bj [1 1 1 1 5]: 35-45
End of spring	**End of spring**	**End of spring**
One Input	**One Input**	**One Input**
Outside temperature	Outside temperature	Outside temperature
FPE ≈ 0.001	FPE ≈ 0.002	FPE ≈ 0.002
bj [1 1 1 1 5]: 50-60	bj [1 1 1 1 5]: 40-45	bj [1 1 1 1 5]: 50-55
bj [1 1 1 1 6]: 50-55	bj [1 1 1 1 6]: 45-50	bj [1 1 1 1 6]: 50-55
bj [1 1 1 1 7]: 55-60	bj [1 1 1 1 7]: 40-45	bj [1 1 1 1 7]: 50-55
bj [1 1 1 1 8]: 55-60	bj [1 1 1 1 8]: 40-45	bj [1 1 1 1 8]: 45-55

Table 6.4 Spring weekdays

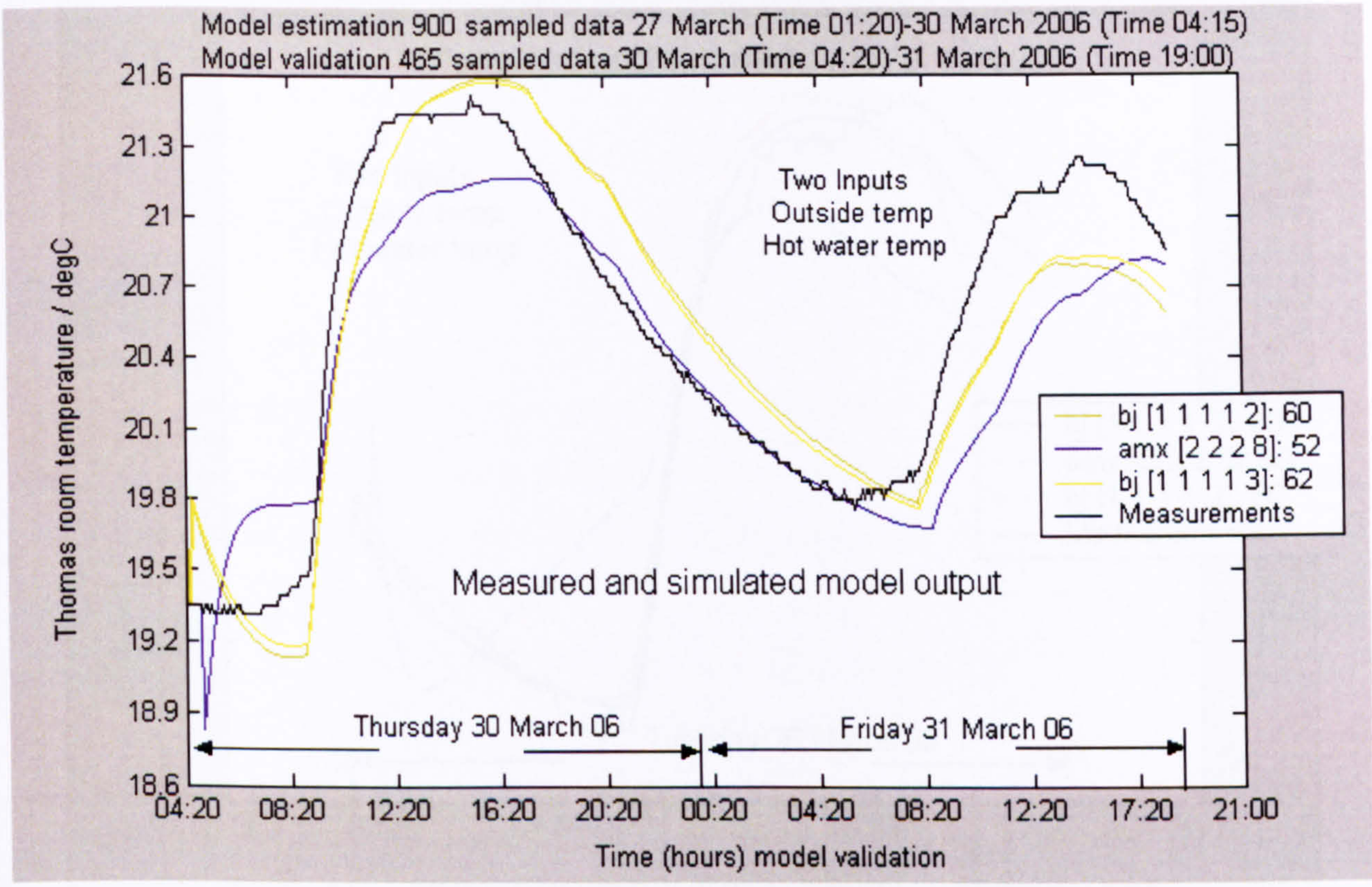

Figure 6.15 Model validation, weekdays 30-31 March 2006

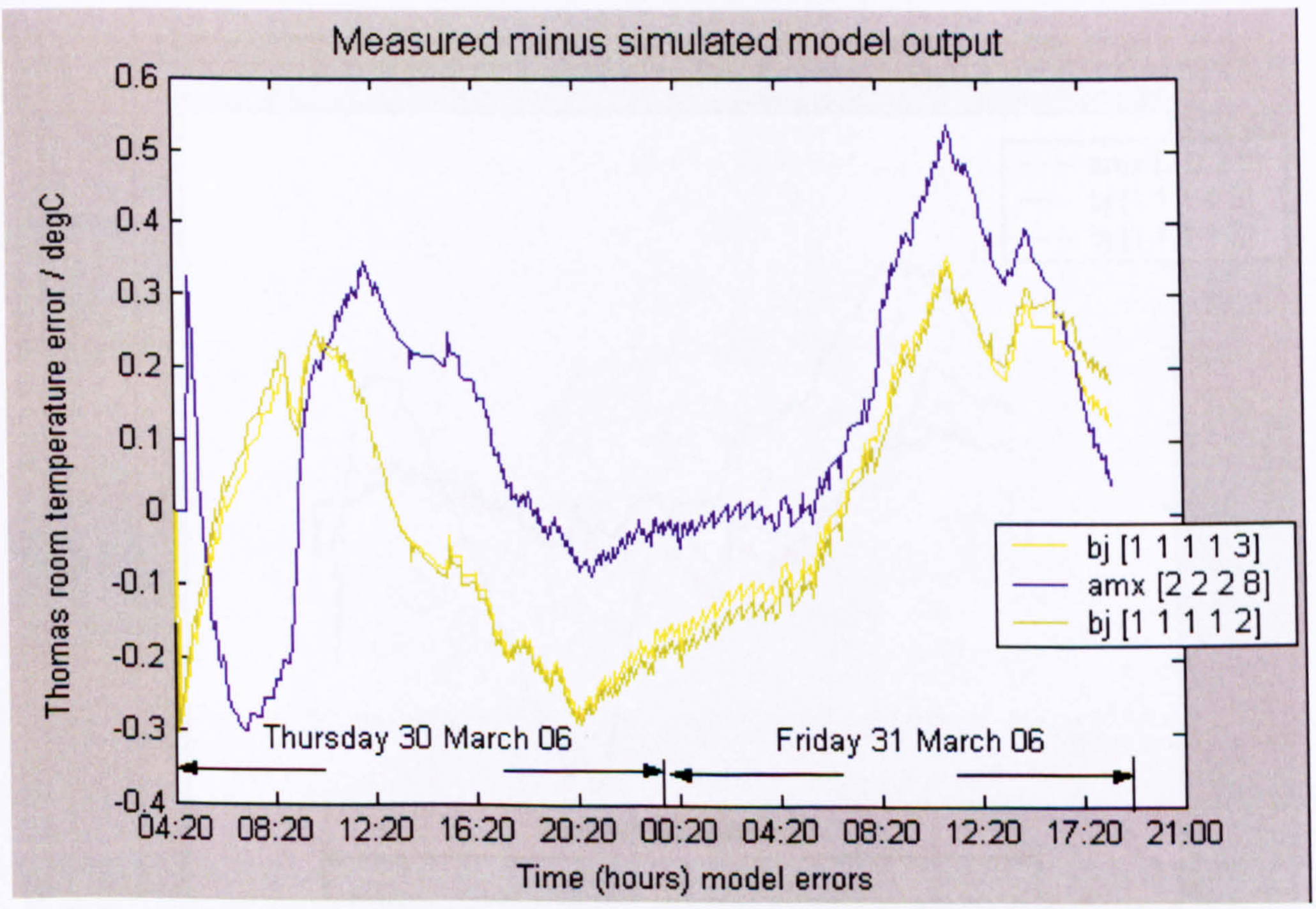

Figure 6.16 Model errors, weekdays 30-31 March 2006

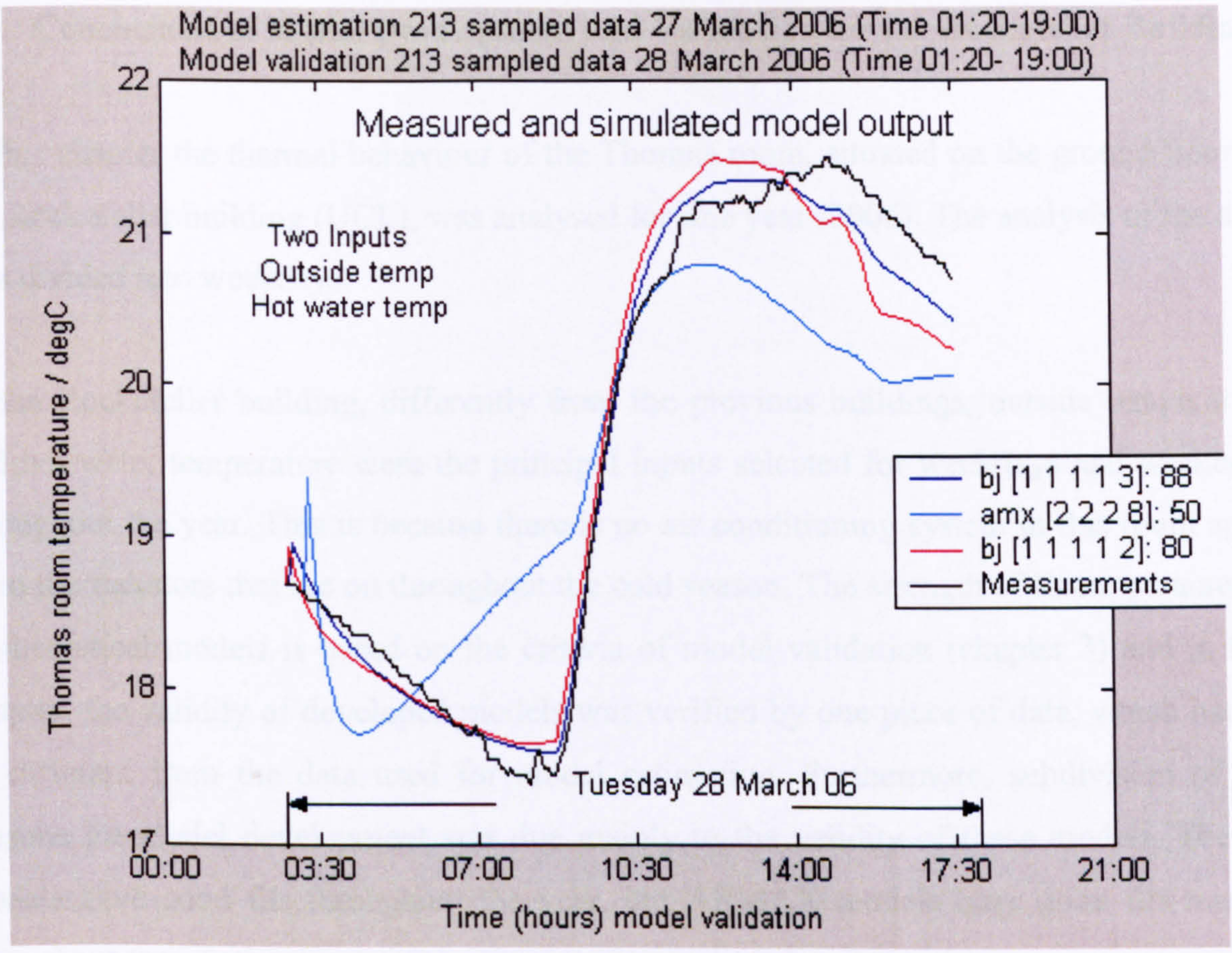

Figure 6.17 Model validation, 28 March 2006

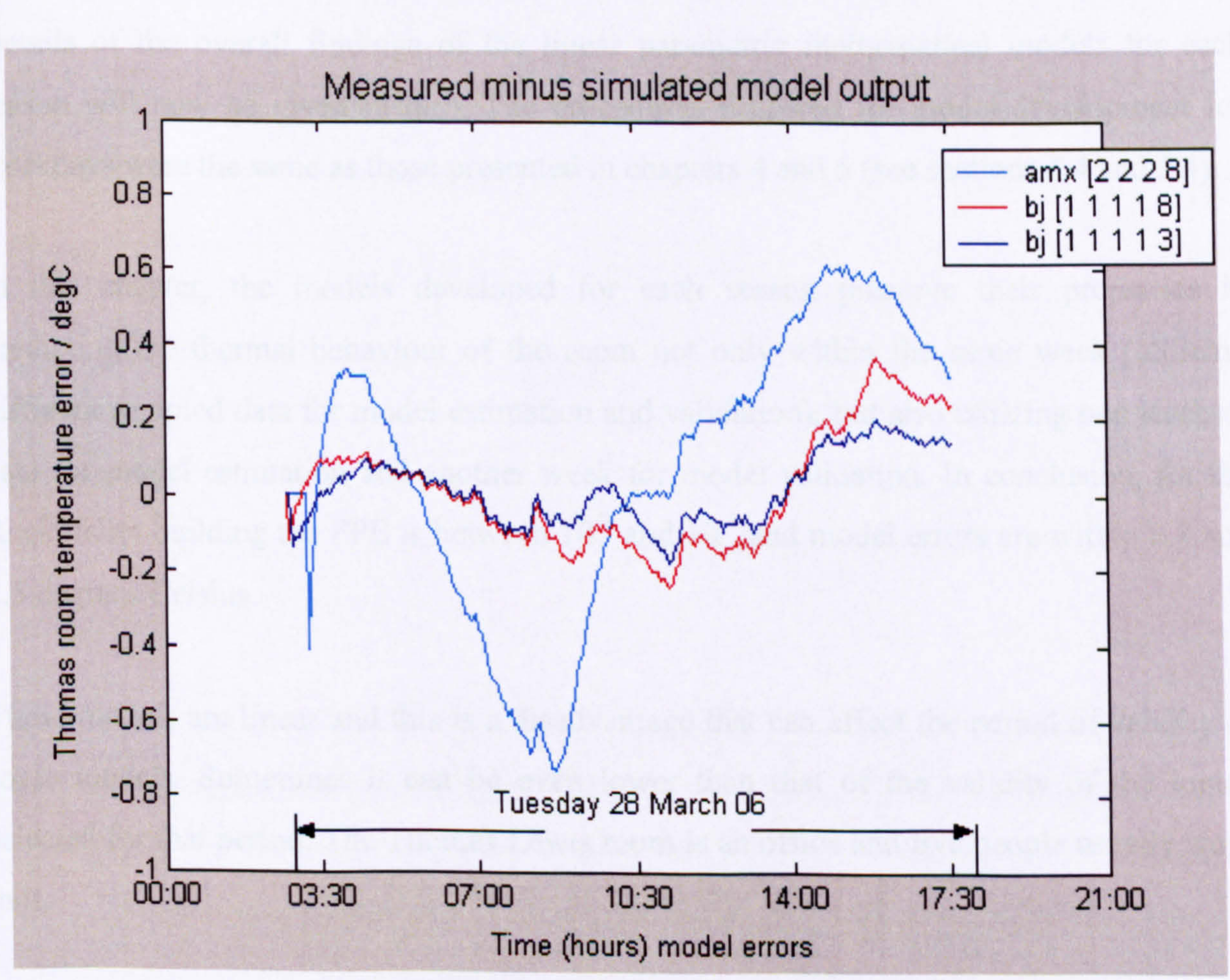

Figure 6.18 Model errors, 28 March 2006

6.5 Conclusions of Model Development and Validation for the Rockefeller Building

In this chapter the thermal behaviour of the Thomas room, situated on the ground floor of the Rockefeller building (UCL), was analysed for one year (2006). The analysis of the data was divided into weekdays.

In the Rockefeller building, differently from the previous buildings, outside temperature and hot water temperature were the principal inputs selected for weekdays and weekends throughout the year. This is because there is no air conditioning system in this room apart from the radiators that are on throughout the cold season. The strength of linear parametric mathematical models is based on the criteria of model validation (chapter 3) and in this chapter, the validity of developed models was verified by one piece of data, which had to be different from the data used for model estimation. Furthermore, subdivision of the seasons for model development was due mainly to the validity of these models. The BJ models have good fits throughout the year, but ARMAX models have good fits mainly throughout the winter season.

Details of the overall findings of the linear parametric mathematical models for each season will now be given in turn. The procedures followed for model development for weekdays were the same as those presented in chapters 4 and 5 (see sections 4.4 and 5.4).

In this chapter, the models developed for each season preserve their properties in predicting the thermal behaviour of the room not only within the same week (utilizing different sampled data for model estimation and validation), but also utilizing one week of data for model estimation and another week for model validation. In conclusion, for the Rockefeller building the FPE is between 10^{-2} and 10^{-3} and model errors are within 0.8 and 2.5 degrees Celsius.

These models are linear and this is a disadvantage that can affect the period of validity of some models. Sometimes it can be even lower than that of the validity of the inputs selected for that period. The Thomas Lewis room is an office and five people usually work in it.

Because of the room's large dimensions, the effects of additional internal heat gain caused by occupancy, computers and printers were assumed to be small throughout the weekdays compared to the external temperature and hot water temperature circulating throughout the cold season.

In addition to the first three contributions stated in relation to the Visa building (section 4.5) which are the same for the Rockefeller building, other contributions of the analysis developed for the Thomas Lewis room are:

- The Visa building and Portman House are new buildings, while the Rockefeller building is an old heavy concrete building. Consequently, its thermal behaviour is very different from the previous two buildings.
- The Thomas Lewis room only has a heating system while the Visa and Portman House buildings have an air conditioning system.
- In this building, the results obtained throughout the hot season for weekdays have lower fits compared to those obtained for Portman House and the Visa building.
- In the Rockefeller building the models' errors are bigger than those obtained in the other two buildings.

For the autumn season the fits related to weekdays are low except when we use 213 sampled data for model estimation (the bj [1 1 1 1 2] and bj [2 2 2 2 4] models fit are good from September to October).

The results obtained throughout the spring season are good and the BJ models (bj [1 1 1 1 2], bj [1 1 1 1 3], bj [1 1 1 1 4], bj [1 1 1 1 5], bj [1 1 1 1 6], bj [1 1 1 1 7] and bj [1 1 1 1 8]) have good fits for weekdays. In contrast to the previous seasons, for winter the ARMAX models (amx [2 2 2 6], amx [2 2 2 7] and amx [2 2 2 8]) and BJ models (bj [1 1 1 1 7] and bj [1 1 1 1 8]) have good fits.

The input, outside temperature, was selected for the summer season and for this period the BJ models (bj [2 2 2 2 1], bj [2 2 2 2 5] and bj [1 1 1 1 2]) and ARMAX models (amx [2 2 2 1] and amx [1 1 1 2]) have good fits. Finally, in the Rockefeller building due to the lack of data collected by the BMS, the fits were lower than those obtained in the Visa building and Portman House. However, the fits get worse if we want to predict more than seven days. Appendix 3B details some of the mathematical models in terms of their parameters.

Chapter 7 Model Development and Validation with Artificial Neural Networks

The previous chapters presented an analysis of the results related to linear models for the three buildings for one year. In this chapter, the model development and validation for the same rooms and year are analysed using neural networks.

The first part of this chapter reviews the theoretical framework for neural networks, focusing in the second part on three types of networks, feedforward backpropagation (FFBP), nonlinear autoregressive mathematical models with series-parallel arrangement (NARXSP) and parallel arrangement (NARX). The third part presents the results obtained in applying these three types of networks to the three buildings. The weeks for the beginning, middle and end of each season are the same as those reported throughout chapters 4, 5 and 6.

7.1 Neural Networks' Background

A neural is a network capable of information processing, in which a large number of relatively simple information processing units are connected together and in which these units communicate with each other by relatively simple signals. Therefore, the important components of neural networks are "neurons" and "connections".

A neuron is an information-processing unit that is fundamental to the operation of a neural network. The three basic elements of neuron models, as depicted in Fig. 7.1 are:

- A set of connecting links, each of which is characterized by a weight or strength of its own.
- An adder for slimming the input signals, weighted by the respective connecting links of the neuron; the operation described here constitutes a linear combiner.
- An activation function for limiting the amplitude of the output of a neuron. This limits the permissible amplitude range of the output signal to some finite value.

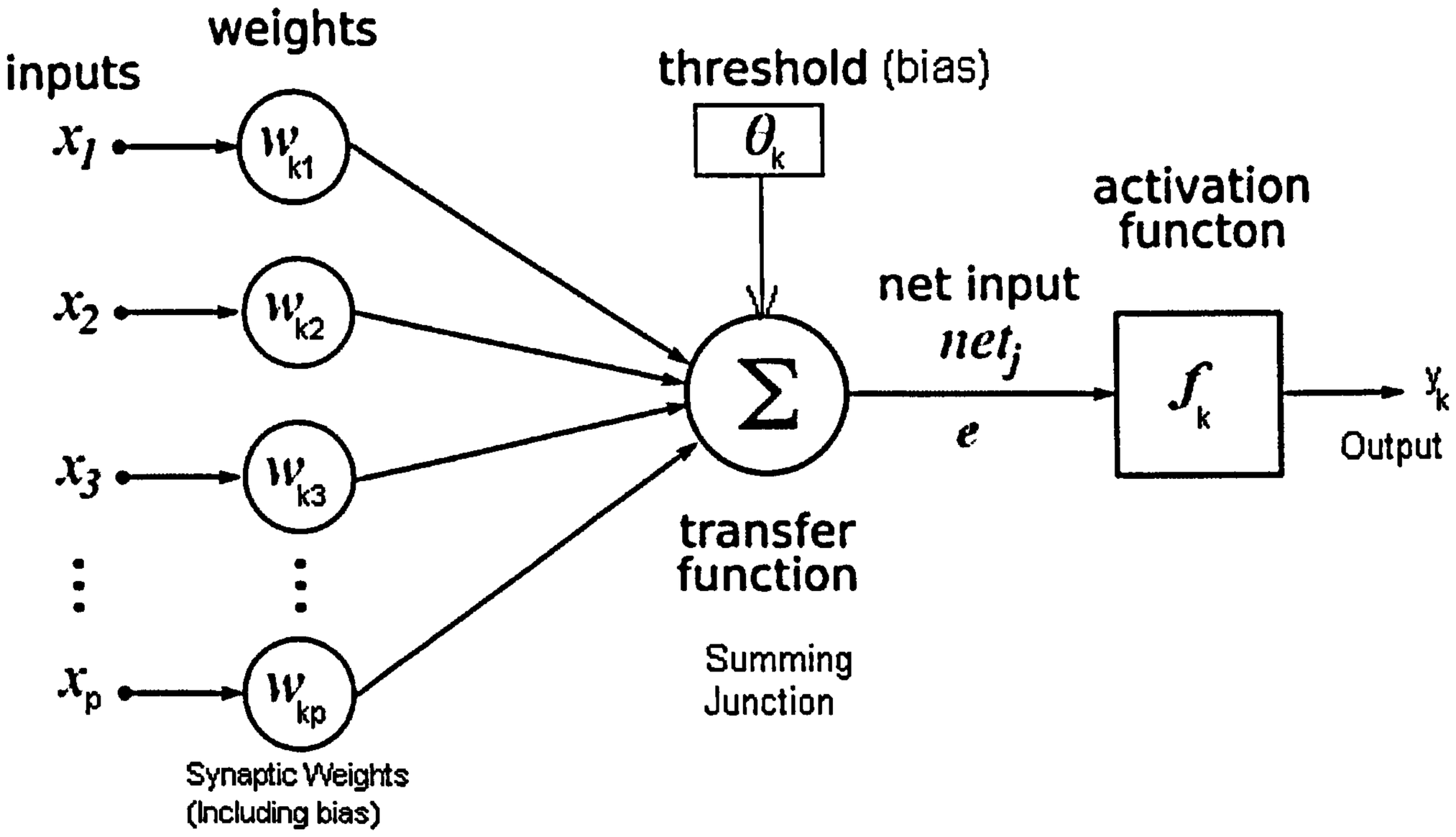

Figure 7.1 A neuron with a single R-element input vector (Laurene, 1994 and Patterson, 1996)

Nonlinear Neuron Model

The neuron in Fig. 7.1 can be described by the input u_k and output y_k.

$$e = \sum_{j=1}^{p} w_{kj} x_j - \theta_k \tag{7.1}$$

$$y_k = f_k \left(e \right); \tag{7.2}$$

where,

- x_j are input signals
- $w_{k1}, w_{k2}, \ldots\ldots, w_{kp}$ are synaptic weights of the neuron k
- e linear combiner input
- θ_k threshold or bias and
- f_k transfer function (presented successively).

The transfer function denoted by f_k defines the output of a neuron in terms of activity level at its input. We may identify three basic types of transfer functions, used throughout the project (Hassoun, 1995):

1-Linear function. For the piecewise-linear function, shown in Fig. 7.2 we have:

$$f_k(e) = purelin \quad (e) \tag{7.3}$$

Where, the amplification factor inside the linear region of operation is assumed to be unity. This transfer function is used on the second layer (corresponding to the output layer) in this project.

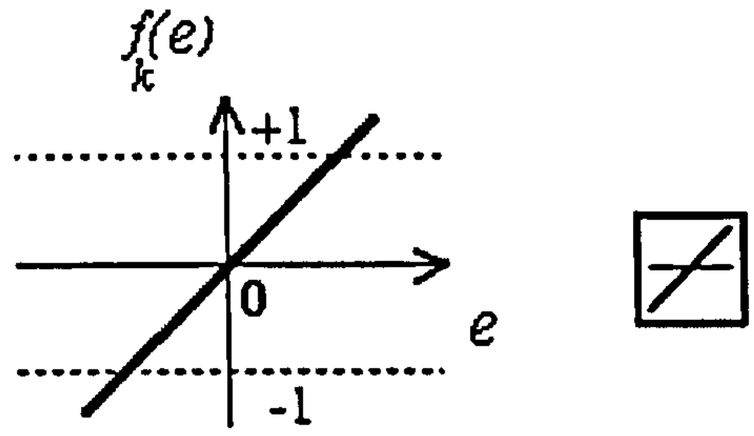

Figure 7.2 Linear transfer function

2-Continuous Log-Sigmoid Function. This is the most common form of transfer function used in the construction of artificial neural networks (see Fig. 7.3). It is defined as a strictly increasing function that exhibits smoothness and asymptotic properties (used in this project for the first layer). An example of this function is defined as:

$$f_k(e) = \frac{1}{1 - \exp(-a \cdot e)} \tag{7.4}$$

.

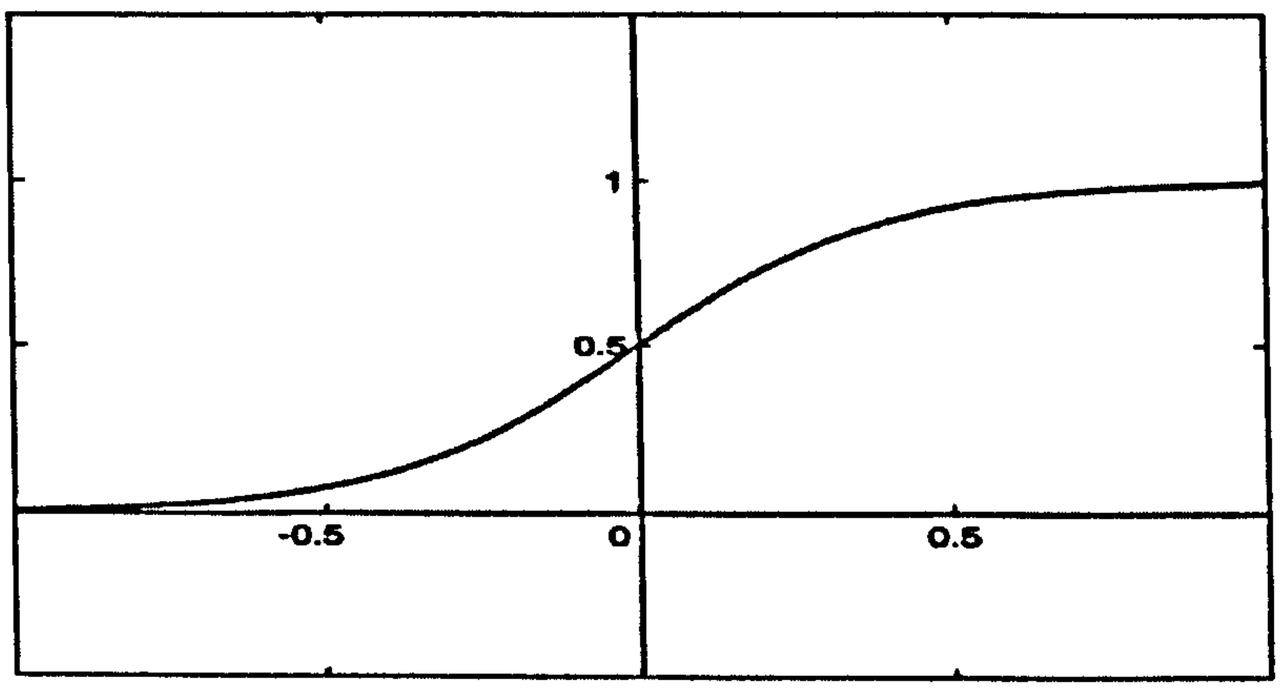

Figure 7.3 Log sigmoid transfer function

3- Hyperbolic tangent function. The transfer function tanh may be more accurate and is recommended for applications requiring the hyperbolic tangent (see 7.5):

$$f_k(e) = \tanh\left(\frac{e}{2}\right) = \frac{1-\exp(-e)}{1+\exp(-e)} \qquad (7.5)$$

Backpropagation (BP) is a learning algorithm (procedure) proposed for feedforward neural network and is the algorithm that has been used for data analysis in this project. Feedforward neural network, BP, NARXSP and NARX are presented in the following sections.

7.2 Feedforward Multilayer Neural Networks (FFNN)

Feedforward neural networks are the most popular and widely used models in many practical applications. A feedforward multilayer neural network (FFNN) consists of a number of layers of neurons, with the output from each neuron propagating to the input of each neuron of the next layer (Fig. 7.4). It has been proved that an FFNN with only one hidden layer of neurons and a specific type of activation function (e.g. sigmoidal function and hyperbolic tangent) can approximate well any functional relation arbitrarily, provided that enough hidden neurons are available (Hornik et al., 1989, Hornik, 1991). FFNNs are typically trained with BP algorithms. In an FFNN network all parameters are usually adapted simultaneously by an optimization procedure. Learning proceeds as follows: a pattern is presented at the inputs. This is transformed in its passage through the layers of the network until it reaches the output layer. The units in the output layer all belong to a different category. The outputs of the network as they are now are compared with the outputs as they ideally would have been if this pattern were correctly classified. In the latter case the unit with the correct category would have the largest output values while the other output units would be very small. On the basis of this comparison all the connections' weights are modified a little bit to guarantee that the next time this same pattern is presented at the inputs, the value of the output unit with the correct category is a little bit higher than it is now and that, at the same time, the output values of all the other incorrect outputs are a little bit lower than they are now. This training procedure is supervised since it minimizes an error function measuring the difference between the network output and the teacher signal that provides the correct output (Schwenker et al., 2001).

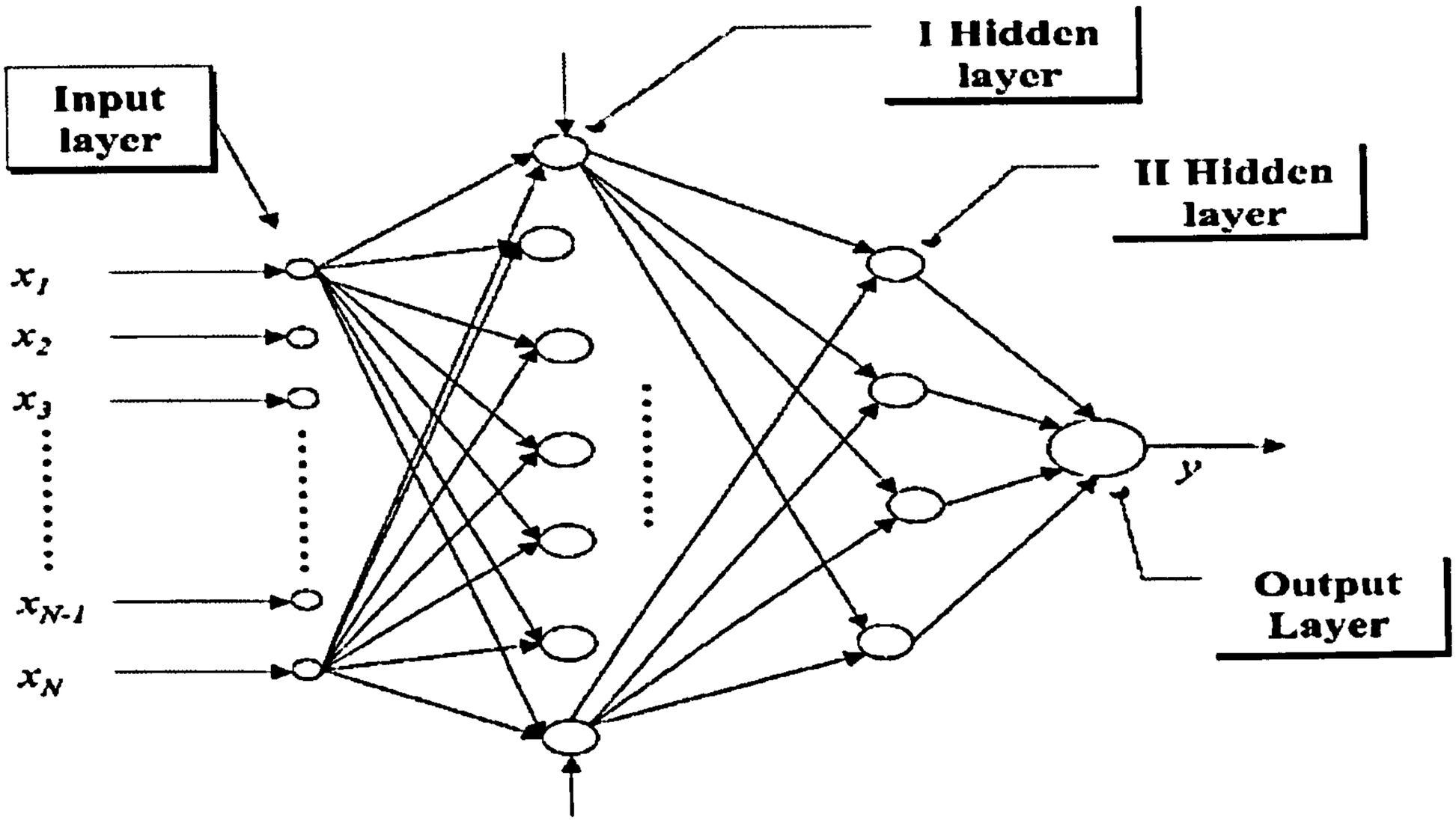

Figure 7.4 Feedforward multilayer neural network architecture (Schwenker et al., 2001)

The advantage of FFNNs is that any continuous function can be uniformly approximated to within an arbitrary accuracy (Bechtler et al., 2001).

Schwenker et al. (2001) found that RBF networks and FFNN networks with one hidden layer have the following similarities:

- Both are based on a universal approximation scheme, where the network complexity simply increases with the number of hidden FFNNs or RBF.
- In both cases, there is the statistical problem of choosing the right model complexity

They also identified the folowing differences:

- Supervised optimization, usually implemented as BP or one of its variants, is essentially the only resource for training an FFNN network.
- In FFNN networks there is no option for training the two network layers separately and there is no opportunity for network initialization as in RBF networks.
- FFNN units in the hidden layer can be viewed as soft decision hyperplanes defining certain composite features that are then used to separate the data as in a decision tree.

- The RBF units, on the other hand, can be viewed as smoothed typical data points.
- Given a new data point, the RBF network essentially makes a decision based on the similarity to known data points, whereas the FFNN network makes a decision based on other factors.
- It seems that decisions made by FFNN networks are more rule-based, whereas those made by RBF networks are more case-based.

There are numerous applications of FFNN neural networks, and some of them are presented below.

Kukolj et al. (2001) presented the results of research into the possibilities of applying a multilayer perceptron type of neural network for fault diagnosis, state estimation, and prediction in a gas pipeline transmission network. The FFNN neural network was trained using the error BP method. Experiments have shown that among the factors considered, the sampling period and the number of inputs might be the most effective in decreasing the error of the neural network based supervisory functions. Datta and Tassou (1997) used FFNN and RBF networks for prediction of the electrical load in supermarkets. They found that the simple FFNN network performed better than the RBF. Mahdi and Araabi (2004) studied the dynamics of a heat exchanger pilot plant, using an FFNN neural network while Parlos et al. (1994) developed a non-linear dynamic model for a heat exchanger using a recurrent FFNN neural network.

7.2.1 Backpropagation Batch Gradient Descent Algorithm

Backpropagation (BP) is a gradient descent algorithm in which the network weights are moved along the negative of the gradient of the performance function. The purpose of BP is to adjust the internal state (weights and biases) of the FFNN so that the FFNN produces the desired output for the specific input.

To teach the neural network we need a training data set. This consists of input signals (x_1 and x_2) assigned a corresponding target (desired output) z. As seen in Figs. 7.5, 7.6, 7.7, 7.8, 7.9 and 7.10 the network training is an iterative process.

In each iteration coefficients of weights of nodes are modified using new data from the training data set. Modification is calculated using algorithm described below (Rumelhart et al., 1986; Rojas, 1996):

First Step: Each teaching step starts by forcing both input signals from the training set. After this stage we can determine the output signal value for each neuron in each network layer. The figures below illustrate how a signal propagates through the network. The $w_{(xm)n}$ symbols represent weights of connections between network input x_m and neuron n in the input layer. y_n The symbols represent the output signal of neuron n.

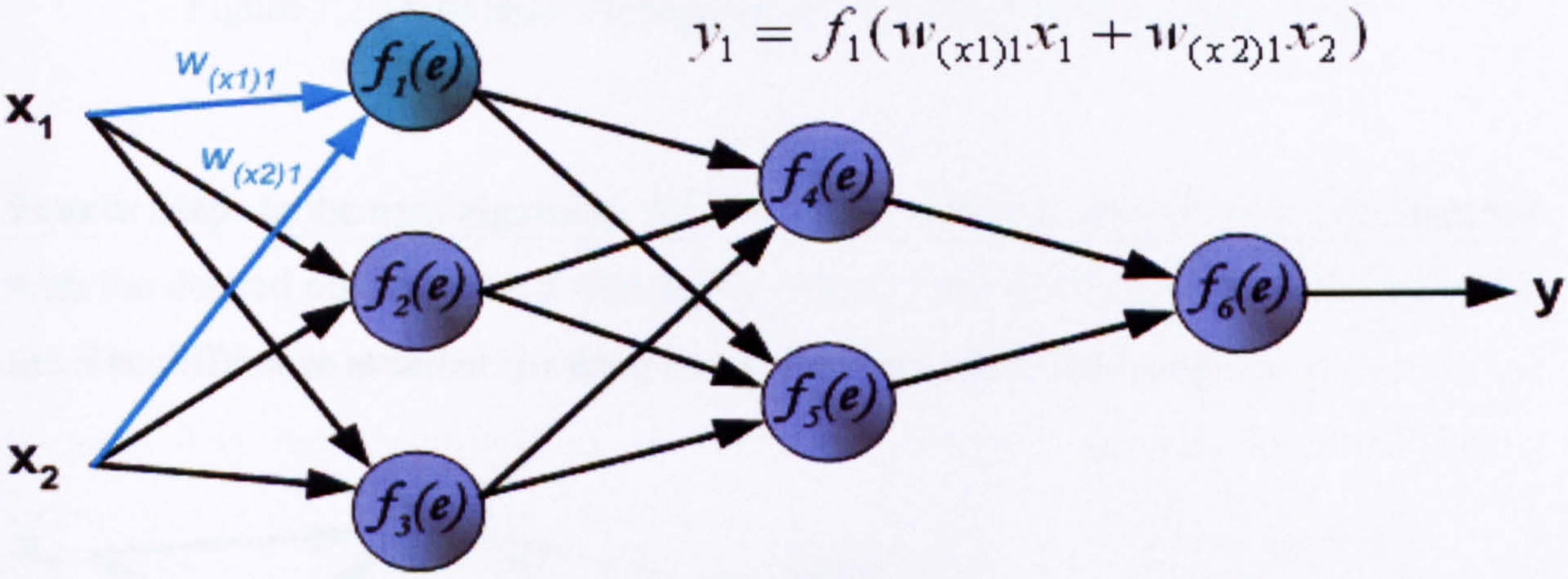

Figure 7.5 First step: Propagation of data from inputs to hidden layer

Second Step: Propagation of signals through the hidden layer. The w_{mn} symbols represent weights of connections between the output of neuron m and the input of neuron n in the next layer.

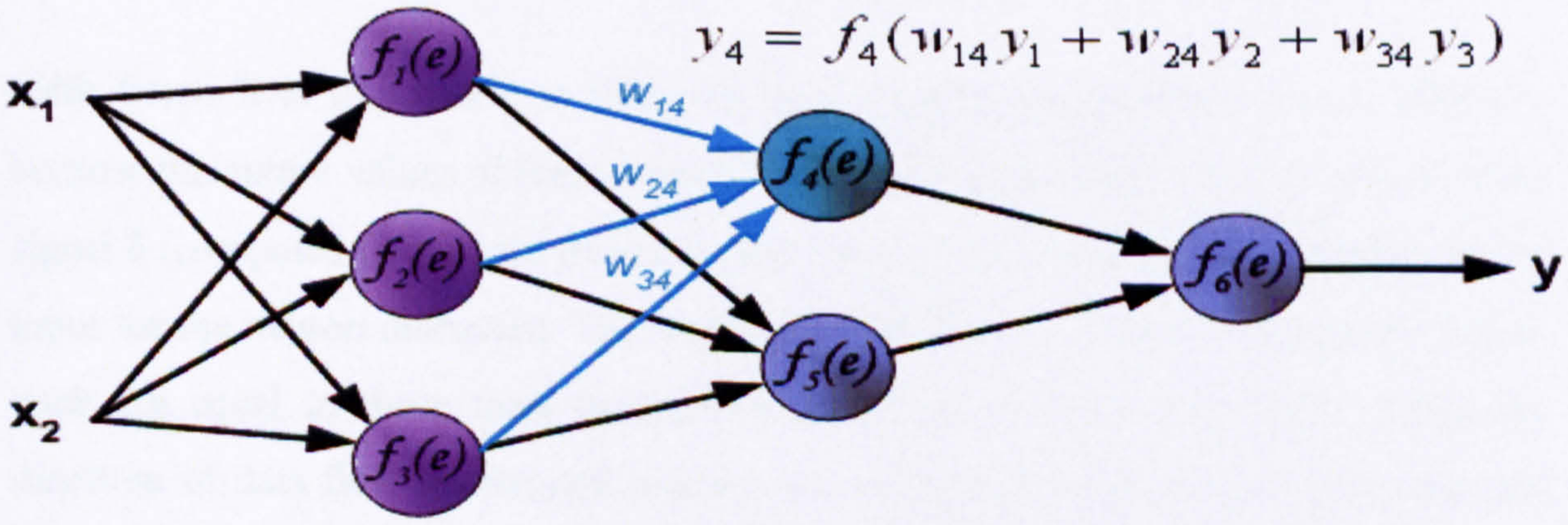

Figure 7.6 Second step: Propagation of data through the hidden layer

Third Step: Propagation of signals through the output layer.

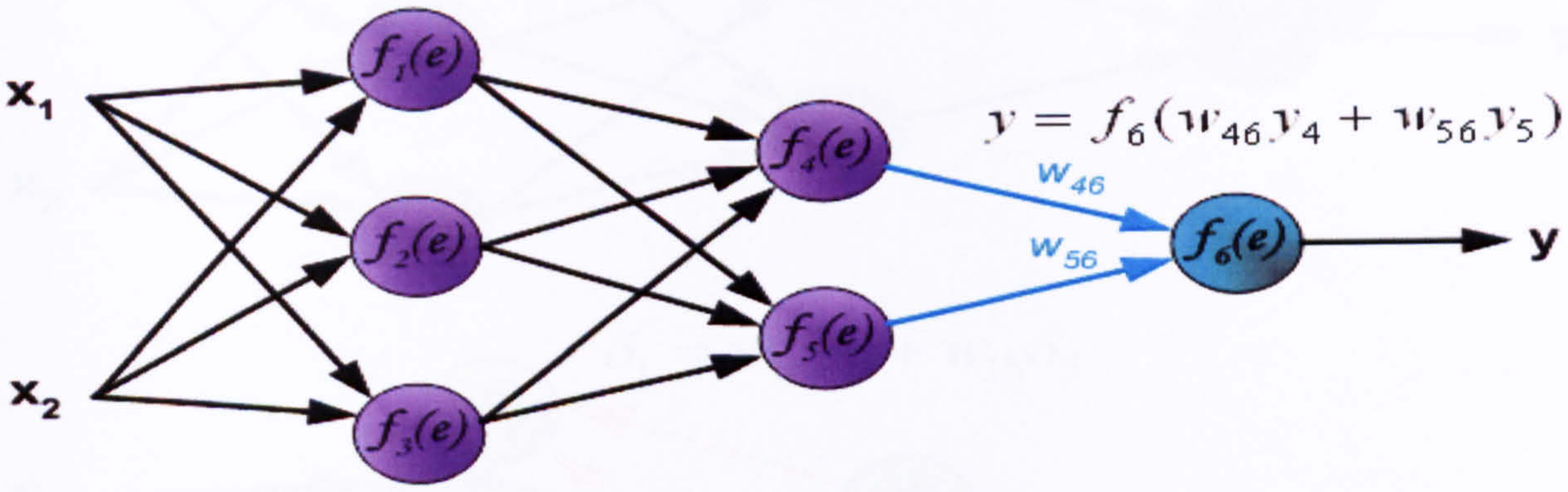

Figure 7.7 Third step: Propagation of data through the output layer

Fourth Step: In the next algorithm step the output signal of the network y is compared with the desired output value z (the actual output), which is found in the training data set. The difference is called the error signal δ of the output layer neuron.

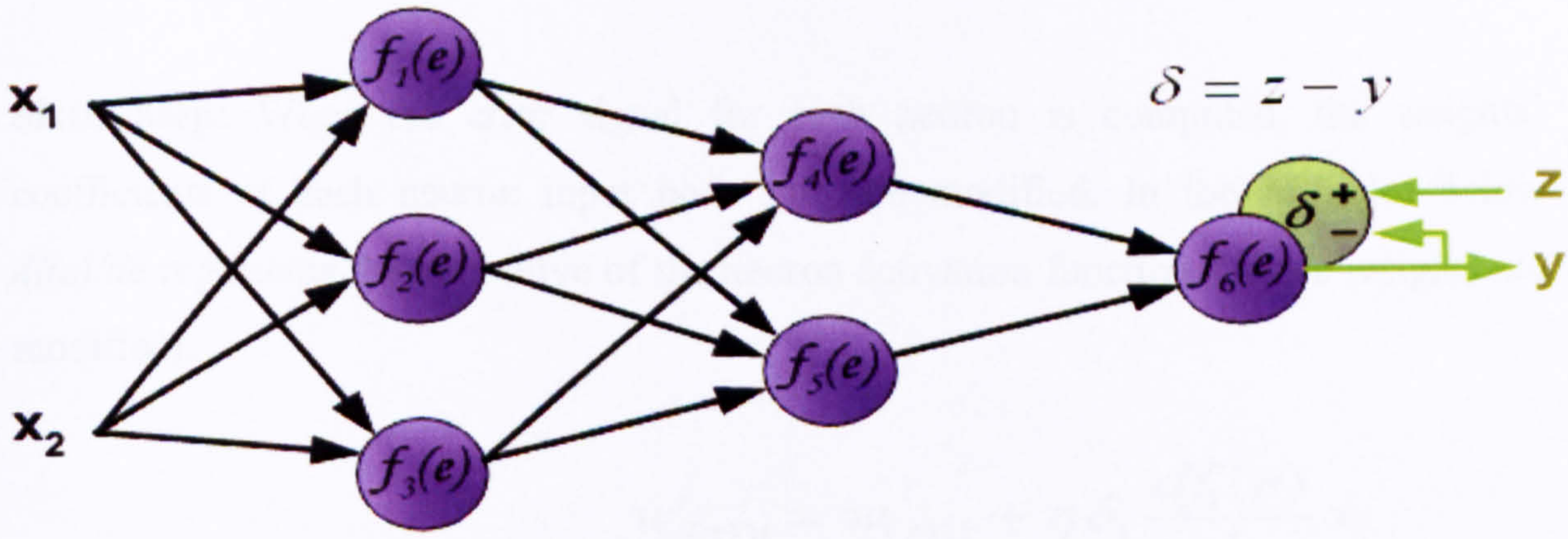

Figure 7.8 Fourth step: Calculation of the error for all the outputs

Fifth Step: It is impossible to compute error signals for internal neurons directly, because the output values of these neurons are unknown. The idea is to propagate error signal δ (computed in a single teaching step) back to all neurons, whith output signals input for the neuron discussed. The weights' coefficients w_{mn} used to propagate errors back are equal to those used during computational of the output value. Only the direction of data flow is changed (signals are propagated from outputs to inputs one after the other). This technique is used for all network layers. If propagated errors come from few neurons they are added, as illustrated below:

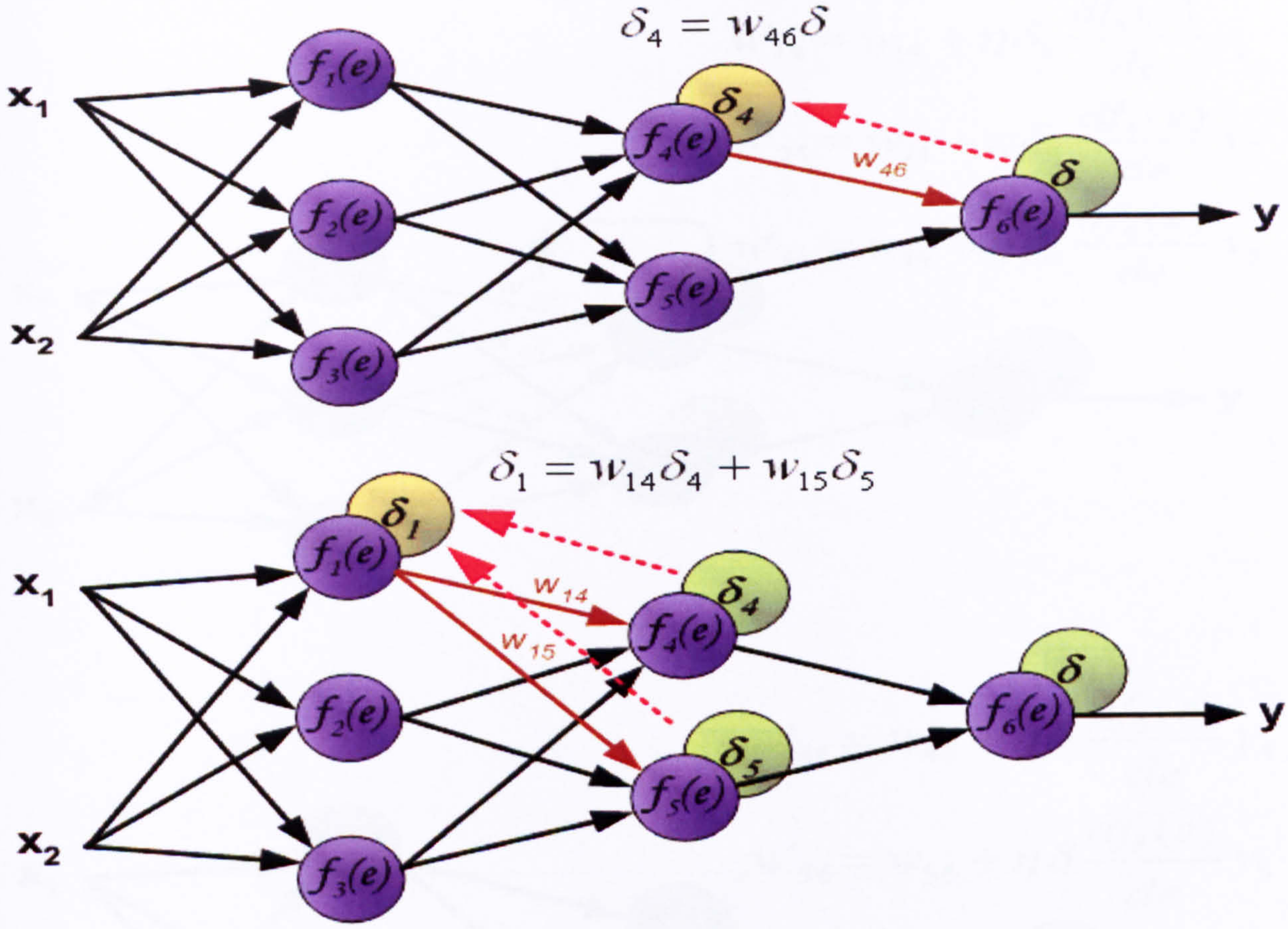

Figure 7.9 Fifth step: Propagation of the error signal back to all neurons

Sixth Step: When the error signal for each neuron is computed, the weights' coefficients of each neuron input node may be modified. In the formulas below *df(e)/de* represents the derivative of the neuron activation function (whose weights are modified).

$$w'_{(x1)1} = w_{(x1)1} + \eta\delta_1 \frac{df_1(e)}{de} x_1$$

$$w'_{(x2)1} = w_{(x2)1} + \eta\delta_1 \frac{df_1(e)}{de} x_2$$

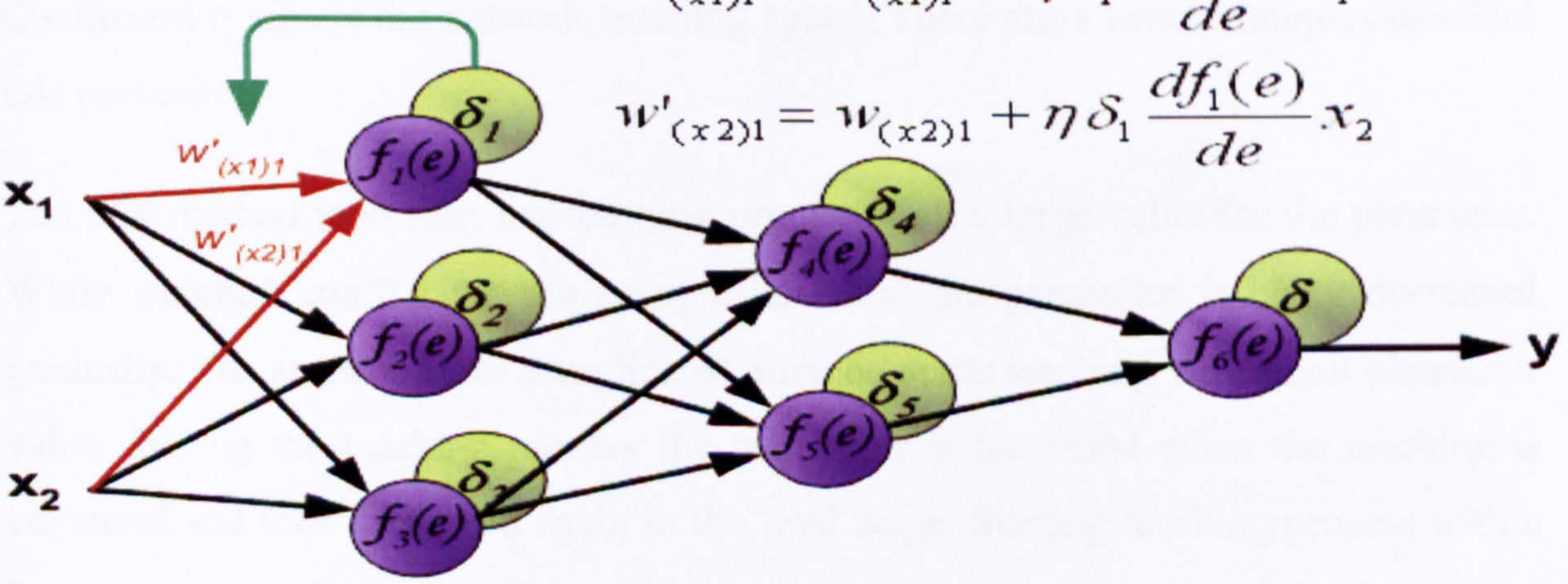

$$w'_{14} = w_{14} + \eta\delta_4 \frac{df_4(e)}{de} y_1$$

$$w'_{24} = w_{24} + \eta\delta_4 \frac{df_4(e)}{de} y_2$$

$$w'_{34} = w_{34} + \eta\delta_4 \frac{df_4(e)}{de} y_3$$

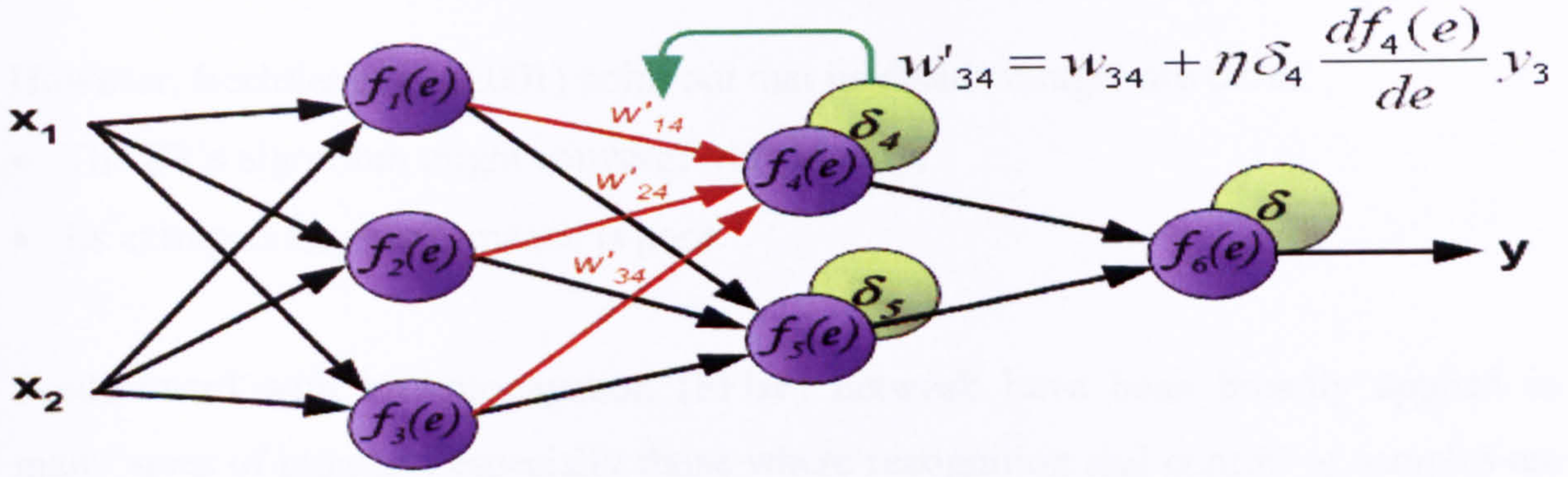

$$w'_{46} = w_{46} + \eta\delta \frac{df_6(e)}{de} y_4$$

$$w'_{56} = w_{56} + \eta\delta \frac{df_6(e)}{de} y_5$$

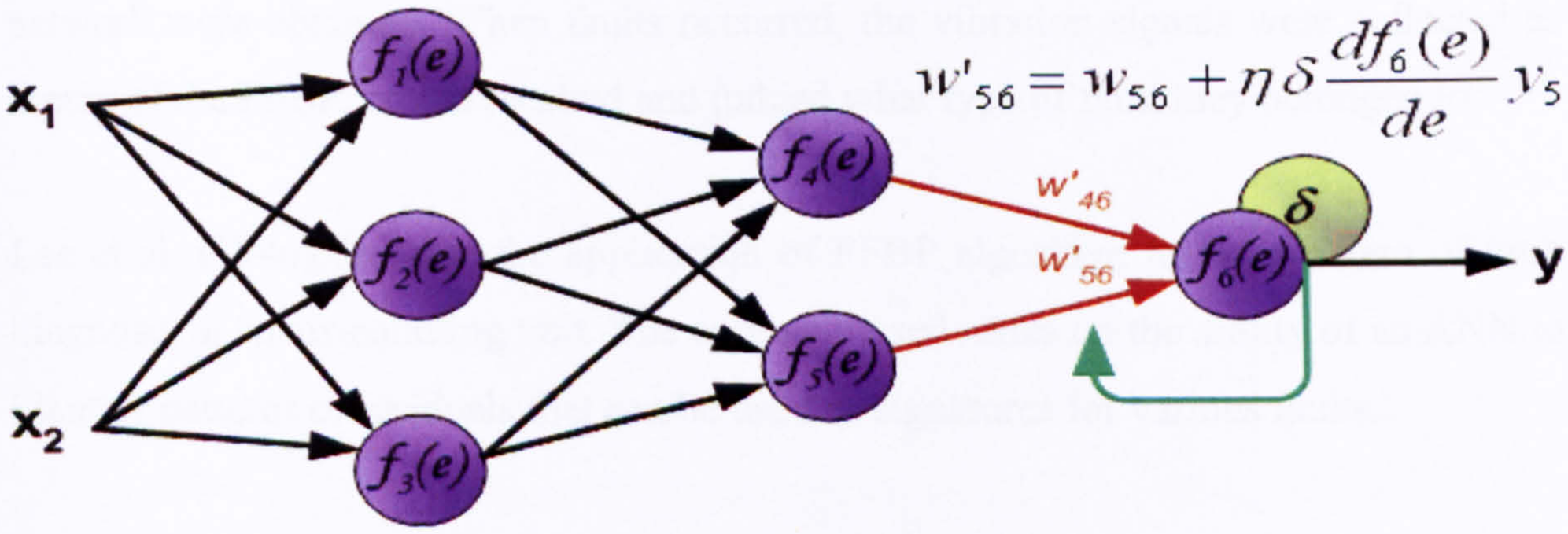

Figure 7.10 Sixth step: Weights coefficients of each neuron input node may be modified

Coefficient η affects the network teaching speed. There are a few techniques to select this parameter.

The first method is to start the teaching process with a large value for the parameter. While weights' coefficients are being established the parameter is being decreased gradually. The second, more complicated, method starts teaching with small parameter value. During the teaching process the parameter is increased when the teaching is advanced and then decreased again in the final stage. Starting teaching process with a low parameter value enables the weights' coefficients signs, to be determined.

Braun and Li (2001) state that the advantage of a BP algorithm it is very good at interpolating performance.

However, Bechtler et al. (2001) point out that its disadvantages are those:

- The BP's algorithm might converge very slowly.
- Its extrapolating performance is poor.

Feedforward with backpropagation (FFBP) network have been broadly applied in many areas of industry, especially those where recognition and control of samples are required. Kuo et al. (2002) applied FFBP to fault diagnosis of a marine propulsion shaft system. By applying a combination of the FFBP and fuzzy logic methods, an optimal propagation neural network and an optimal learning coefficient for the neural network were obtained. When faults occurred, the vibration signals were collected as inputs of the FFBP, which recalled and judged what type of fault they belonged to.

Lee et al. (1996) describe the application of FFBP algorithm to the problem of fault diagnosis in an air-handling unit. The approach used relies on the ability of an ANN to identify patterns of residuals that can be used as signatures for various faults.

A FFBP algorithm with Levenberg-Marquardt approximation has been used as a training algorithm for ANNs for FDD in a variable volume air handling unit. Here, the model method consists of comparing the real behaviour of the AHU plant with the normal behaviour given by the ANN trained during a preliminary phase. By this means Morisot and Marchio (1999) detected faults in the residual variation of temperature and relative humidity. Li et al. (1996) applied an ANN for fault diagnosis in a complex heating system. Here, a two-level ANN was constructed and simulated data were used to train and test it.

Furthermore, Li et al. (1997) developed an ANN prototype using the simulation data of a reference heating system. The ANN was trained using commercial software with an improved BP algorithm. They demonstrated the feasibility of using ANNs for detecting and diagnosing faults in heating systems.

7.2.2 Nonlinear Autoregressive Network with Exogenous Inputs NARX

The nonlinear autoregressive network with exogenous inputs (NARX) is a recurrent dynamic network, with feedback connections enclosing several layers of the network. The NARX model is based on the linear ARX model, which is commonly used in time-series modelling. The defining equation for the NARX model is (7.6) (Ljung, 1999):

$$y(n)=f(y(t-1),y(t-2),.....,y(t-n_y),u(t-1),u(t-2),.....u(t-n_u)) \tag{7.6}$$

Two types of NARX networks, NARX parallel and series-parallel arrangements will now be discussed in turn.

NARX parallel arrangement

An NARX parallel arrangement is where the next value of the dependent signal *y(n)* (equation 7.6) is regressed on previous values of the output signal and previous values of an independent (exogenous) input signal. Consequently, the output of the NARX network is an estimate of the output of some linear dynamic system that we are trying to model. The NARX model can be implemented, using a feedforward neural network to approximate the function f in equation 7.6. Fig. 7.11 show a schematic representation of the NARX parallel arrangement. Equation (7.6) can be represented in detail by (7.7) (Ljung, 1999):

$$y(n)=\sum_{i=0}^{P}a(i)u(n-i)+\sum_{j=1}^{Q}b(i)y(n-j)+\sum_{i=0}^{P}\sum_{j=0}^{P}a(i,j)u(n-i)u(n-j)+\sum_{i=1}^{Q}\sum_{j=1}^{Q}b(i,j)y(n-i)y(n-j)+ \tag{7.7}$$
$$\sum_{i=1}^{P}\sum_{j=1}^{Q}c(i,j)u(n-i)y(n-j)+.....+e(n)$$

where *y(t)* is the system output signal; *u(t)* is the input signal; *e(t)* is the error; *P* and *Q* represent the model order of the exogenous (linear and nonlinear) and the autoregressive terms, respectively; *a(i)* and *a(i,j)* are the coefficients of the linear and nonlinear exogenous terms; *b(i)* and *b(i,j)* are the coefficients of the linear and nonlinear autoregressive terms; and *c(i,j)* are the coefficients of the non linear cross in term.

If all the coefficients of the nonlinear terms are zero, equation (7.7) will give a linear ARX model.

Defining of the components of (7.7):

$$u = [u(t) \;\; u(t-1) \;\; .....u(t-P) \;\;]^T ; \; y = [y(t-1) \;\; y(t-2) \;\; .....y(t-Q) \;\;]^T$$

$$a = [a(1) \;\; a(2) \;\; .....a(P)]^T ; \; b = [b(1) \;\; b(2) \;\; .....b(Q)]^T$$

$$A_{NN} = \begin{bmatrix} a(0,0) & a(0,1) & .....a(0,P) \\ a(1,0) & a(1,1) & .....a(1,P) \\ & & \\ a(P,1) & a(P,2) & .....a(P,P) \end{bmatrix}; B_{NN} = \begin{bmatrix} b(0,0) & b(0,1) & .....b(0,Q) \\ b(1,0) & b(1,1) & .....b(1,Q) \\ & & \\ b(Q,1) & b(Q,2) & .....b(Q,P) \end{bmatrix};$$

$$C_{NN} = \begin{bmatrix} c(0,0) & c(0,1) & .....c(0,Q) \\ c(1,0) & c(1,1) & .....c(1,Q) \\ & & \\ c(Q,1) & c(Q,2) & .....c(Q,P) \end{bmatrix}$$

Thus, equation (7.7) can be expressed as follows:

$$y(n) = a^T u + b^T y + u^T A_{NN} u + y^T B_{NN} y + u^T C_{NN} y + ... + e(t) \qquad (7.8)$$

The main advantage of a NARX parallel arrangement network is that they perform better than conventional recurrent neural networks in long term dependency problems (Tsungnan et al., 1998; Benigo et al., 1994 and Lin et al., 1996).

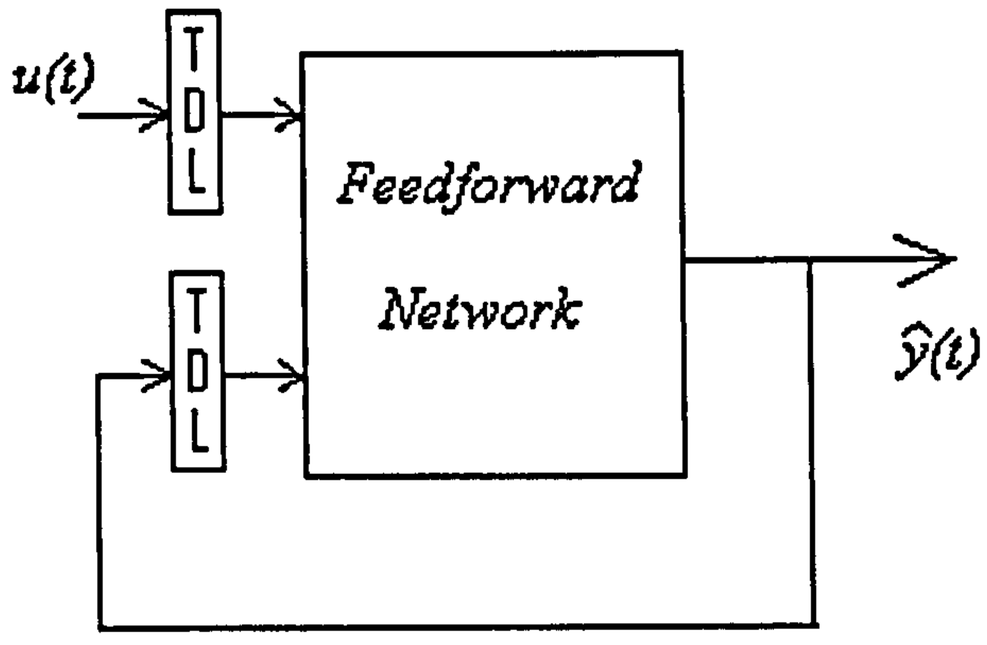

Figure 7.11 NARX with parallel architecture (Demuth et al., 2008)

NARX series-parallel arrangement

Unlike an NARX parallel arrangement, where the output estimated is fed back to the input of the feedforward network, an NARX series-parallel arrangement uses true output instead of estimated output (see Fig. 7.12).

NARX series-parallel arrangements have two advantages over NARX parallel arrangements.

The first is that the input to the feedforward network is more accurate. The second is that the resulting network has a purely feedforward architecture, and static BP algorithm can be used for training (Demuth et al., 2008).

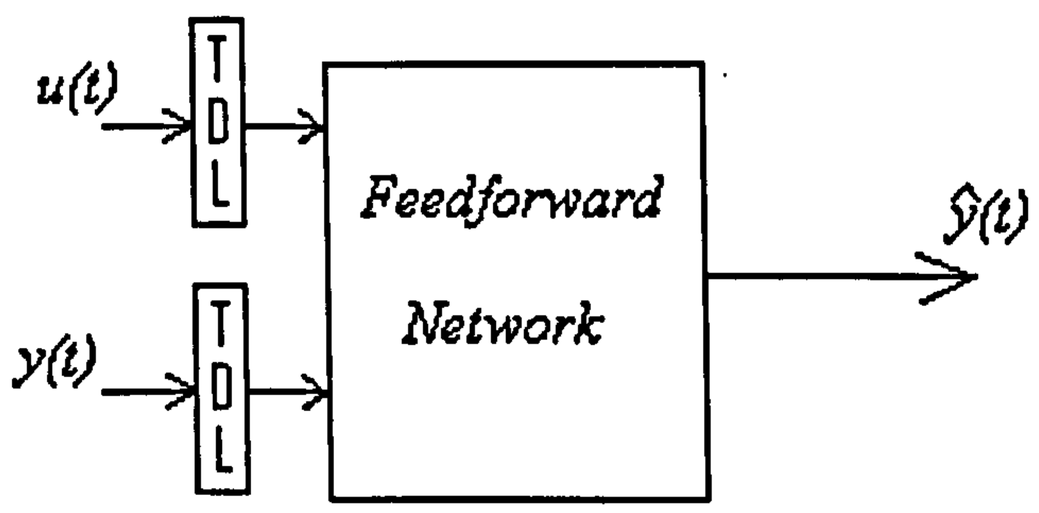

Figure 7.12 NARX with series-parallel architecture (Demuth et al., 2008)

The NARX series-parallel arrangements used in this project and from the results analysis it gives good approximation of the thermal behaviours in the three buildings throughout the year.

There are many applications for the NARX; some of which are reported successively. The NARX method is applied to model the three-way catalyst, based on measurements of the upstream and downstream air-fuel ratios. It is shown that the NARX models describe the process in great detail and they are valid over a very wide range of operating conditions. Thus, the efficiencies of exhaust gas conversion have been improved (Soumelidis and Stobart, 2006). Furthermore, NARX method is well suited for modelling non-linear systems such as heat exchanger (Chen et al., 1990), wastewater treatment plants, catalytic reforming systems in a petroleum refinery (Su and McAvoy, 1991 and Su et al., 1992).

Finally, Yu et al. (2005) investigated the use of NARX networks for fault control in chemical and biological processes, where the control scheme is composed of two parts. In the first part, NARX was used to model the process, where the model was made adaptive on-line to catch the dynamic changes caused by faults, while the second part included auto-tuning the PID controller to be adapted to compensate for the degradation of the system's stability and performance. They demonstrated the applicability of the developed scheme to industrial processes.

7.3 Neural Network Data Analysis and Model Development

In this chapter, neural networks are applied to the data obtained from Portman House, Visa building and Rockefeller building with particular NARX networks (feedforward parallel and series-parallel arrangements) and feedforward backpropagation (FFBP) types being used throughout the project to build the models for one year (2005). In contrast to the linear analysis in chapters 4, 5 and 6, the NARXSP, FFBP and NARX networks can have the same properties throughout the seasons. The schematic flowchart shown in Fig. 7.13 summarises the system identification procedure for the non-linear mathematical models.

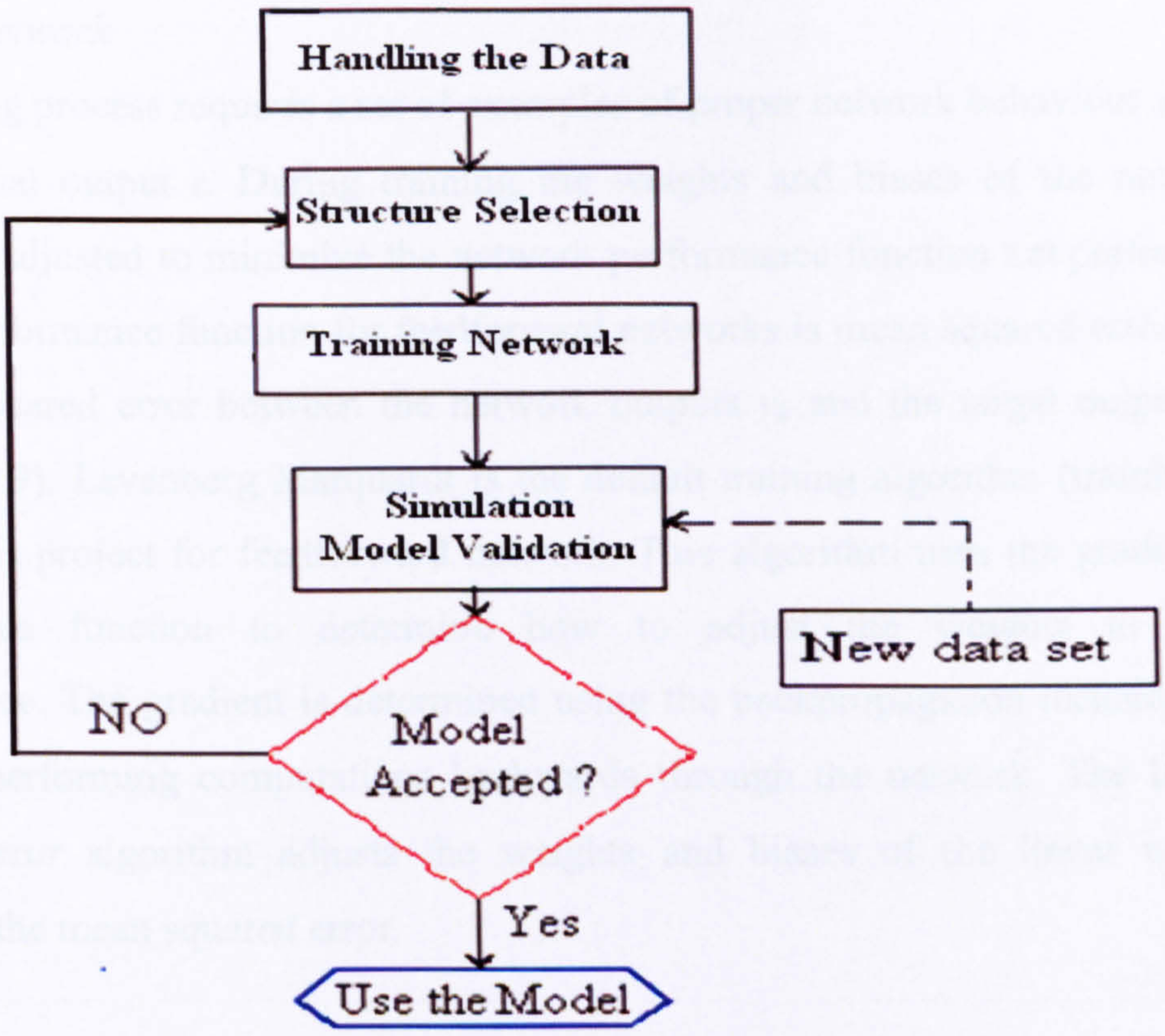

Figure 7.13 Neural network modeling basic steps (Demuth et al., 2008)

All stages of the schematic flowchart (Fig. 7.13) are listed below (Demuth et al., 2008):

Handling the data

A set of input-output data is presented for model development with non-linear mathematical models. The inputs selected are the same as those for linear parametric mathematical analysis (see chapters 4, 5 and 6).

Structure selection

A choice should be made between FFBP, NARX and NARXSP mathematical models that can be used to represent the system. The first step in structure selection is to create the network object. The function newff creates a feedforward network. It requires four inputs and returns the network object. The first input is the minimum and maximum of each row of the matrix which contains the inputs and outputs. The second input is an array containing the sizes of each layer. The third input is a cell array containing the sizes of the transfer functions to be used in each layer. The final input contains the name of the training function to be used

Training network

The training process requires a set of examples of proper network behaviour with input u and actual output t. During training the weights and biases of the network are iteratively adjusted to minimize the network performance function net.perforFcn. The default performance function for feedforward networks is mean squared error mse (the average squared error between the network outputs y_k and the target outputs t) (see equation 7.9). Levenberg Marquardt is the default training algorithm (trainlm) that is used in this project for feedforward network. This algorithm uses the gradient of the performance function to determine how to adjust the weights to minimize performance. The gradient is determined using the backpropagation technique, which involves performing computations backwards through the network. The least mean squared error algorithm adjusts the weights and biases of the linear network to minimize the mean squared error.

$$mse = \frac{1}{N}\sum_{p=1}^{N} e^2(p) = \frac{1}{N}\sum_{p=1}^{N}(t(p) - y_k(p))^2 \tag{7.9}$$

where,

- N is the number of input-target (output) pairs $(u(1)t(1), u(2)t(2), ...u(N), t(N))$
- $y_k(p)$ simulated model output at time $t = p$
- $t(p)$ actual output at time $t = p$ (measurements)

Finally, $mse \approx 2 * FPE$ (final prediction error for linear parametric models, see section 3.4.2)

Simulation and model validation

With a trained network, simulation is a way of testing the network to see if it meets our expectation. Simulation takes the network input u and the network object *net.* and returns the network output $y_k(p)$. Finally, for model validation a comparison is made between target and network output.

The next sections present the inputs and some of the results obtained for each season, while the properties of the networks used throughout the entire year and for each building are as follows:

NARX series parallel arrangement (NARXSP)

- Definition of the network: net = newnarxsp (minmax (m), ID, OD, [S1 S2], {'TF1','TF2'}, BTF , PF);

where,

- minmax (m) is the minimum and maximum of each row of the matrix 'm' which contains the inputs and outputs
- ID and OD is the input and output delay vector respectively. The values of ID and OD that have been used throughout this analysis with good results are:
- ID = [1:1] - [1:4]
- OD = [1:1]
- S1 and S2 are the sizes of the first and second layer (number of neurons in the first and second layer), where their values are (see Fig. 7.6, pg. 119):
- S1 = 3 - 20
- S2 = 2 (two outputs)
- TF1 and TF2 are the transfer functions of the first and second layer respectively (networks with two layers are used throughout the project)
- TF1 = 'tansig' (see section 7.1, pg. 118)
- TF2 = 'purelin' (see section 7.1, pg. 117)
- BTF backpropagation network training function (default = 'trainlm') (see section 7.2.1, pgs. 120 – 125)
- PF perfomance function (default = 'mse') (see section 7.3, pg. 131)

Feedforward backpropagation (FFBP)

- Definition of the network: net = newff (minmax (p), [S1 S2], {'TF1','TF2'}, BTF, PF);

where,

- p is the matrix that contains the inputs
- t is the matrix that contains the outputs

- minmax (p) is the minimum and maximum of each row of the matrix that contains the inputs
- S1 and S2 are the sizes of the first and second layer (number of neurons in the first and second layer)
- S1 = 3
- S2 = 2 (two outputs)
- TF1 and TF2 are the transfer functions of the first and second layer respectively (networks with two layers are used throughout the project)
- TF1 = 'tansig'
- TF2 = 'purelin'
- BTF backpropagation network training function (default = 'trainlm')
- PF perfomance function (default = 'mse')

NARX parallel arrangement (NARX)

- Definition of the network: net = newnarx (minmax (p), ID, OD, [S1 S2], {'TF1','TF2'}, BTF, PF);

where,

- p is the matrix that contains the inputs
- t is the matrix that contains the outputs
- minmax (p) is the minimum and maximum of each row of the matrix that contains the inputs
- ID and OD are the input and output delay vector respectively, where the values of ID and OD that are been used thruoghut this analysis with good results are:
- ID = [1:1] - [1:4]
- OD = [1:1]
- S1 and S2 are the sizes of the first and second layer (number of neurons in the first and second layer)
- S1 = 3
- S2 = 2 (two outputs)
- TF1 and TF2 are the transfer functions of the first and second layer respectively (networks with two layers are used throughout the project)
- TF1 = 'tansig'
- TF2 = 'purelin'

- BTF backpropagation network training function (default = 'trainlm')
- PF perfomance function (default = 'mse')

Finally, in the next sections the results of the analyses are:

- For two weeks respectively:
  - Week one (Monday Time 01:20 - Friday Time 19:00) sampled-data model estimation and
  - The following week, week two (Monday Time 01:20 to Friday Time 19:00) sampled-data model validation or alternatively
- The same week respectively for:
  - 900 sampled-data model estimation (75 hours) and 465 sampled-data model validation (39 hours)
  - 213 Sampled-data model estimation (18 hours in day 1 – Time 01:20-19:00) and 213 sampled-data model validation (18 hours in day 2 – Time 01:20-19:00)

7.3.1 Neural Network Data Analysis and Model Development in Portman House

In the following sections models with two layers are explored in terms of best fit with the real measurements of room temperature throughout the four seasons. The analysis in this section covers the entire room positioned on the second floor (zones 1 and 2). The inputs selected are the same as those for linear analysis (see chapter 5), but in addition, for analysing the entire room, supply air temperature AHU2 and supply air flow rate AHU1 are added as inputs and temperature zone 2 is added as an output (see Fig. 5.2).

Model development and validation for winter weekdays

Throughout the winter, the NARXSP model gave the best results for predicting room temperature for the second floor. Due to the similarities of the results for this season, only the weeks 16-20 January 2006 (model estimation) and 23-27 January 2006 (used to validate the model) are presented respectively in Figs. 7.14 and 7.15. Furthermore, the week 16-20 January 2006 was analysed with FFBP and NARXSP networks (Fig. 7.16).

The inputs that affect the results (room temperature zone 1 and zone 2) are: hot water temperature, supply air temperature AHU1, supply air flow rate AHU1, supply air temperature AHU2, supply air flow rate AHU2 and outside temperature, which are the same to linear models.

In addition, 16 and 17 January 2006 were analysed with NARXSP, FFBP and NARX networks and the model fits and errors are shown in Figs. 7.17 and 7.18. Throughout the winter NARXSP network (mse 10^{-4}) gives better fits than the FFBP and NARX networks (not presented). In Fig 7.18 the maximum error between measurements and model outputs is 0.6 degrees Celsius.

Finally, throughout the winter season mse ranged between 10^{-4} (NARXSP network for 1365 and 900 sampled data) and 10^{-3} (NARXSP network for 213 sampled data), while the errors between measurements and model outputs ranged between 0.2 (NARXSP network for 1365 and 900 sampled data) and 0.6 (NARXSP network for 213 sampled data) degrees Celsius.

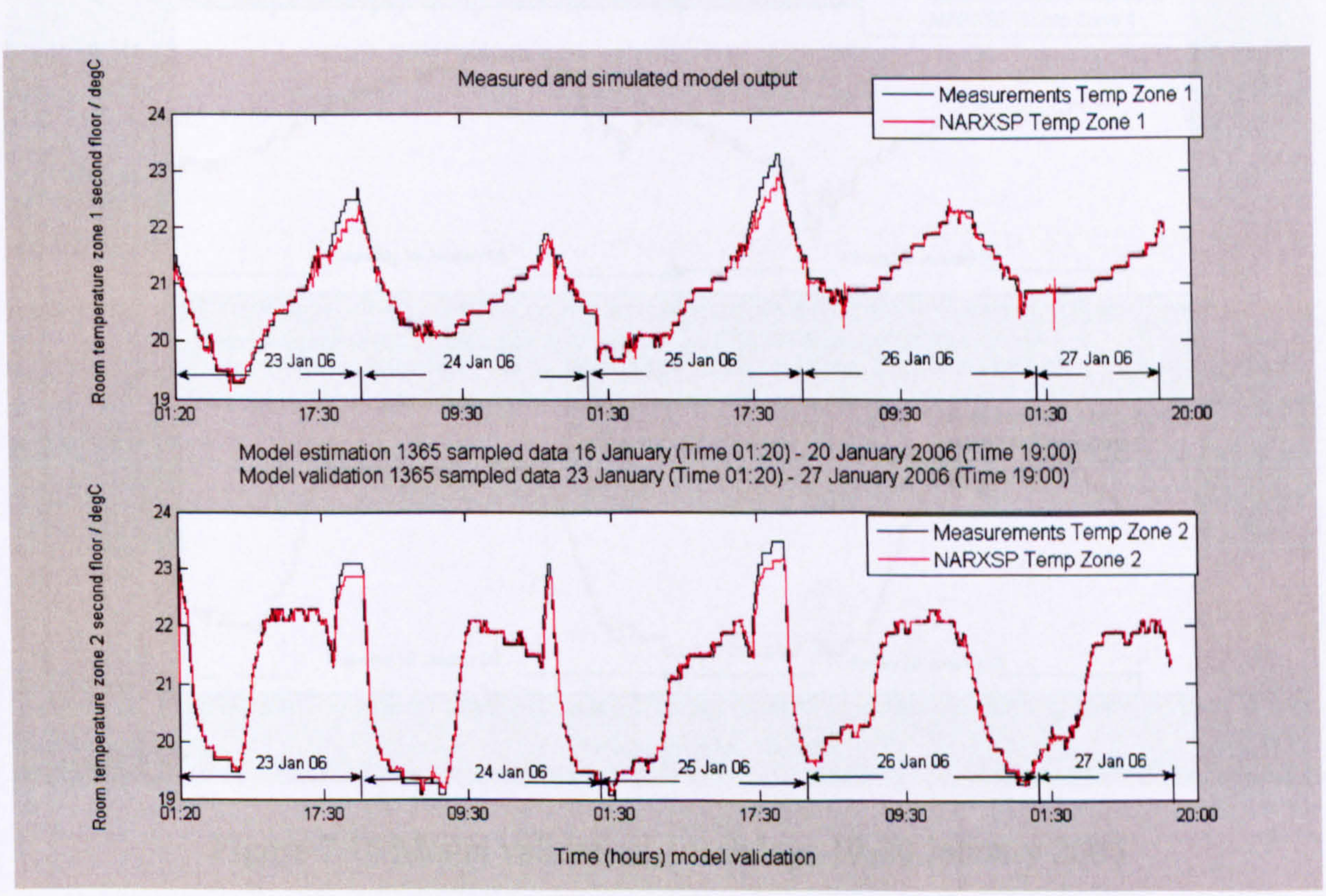

Figure 7.14 Model validation, weekdays 23-27 January 2006

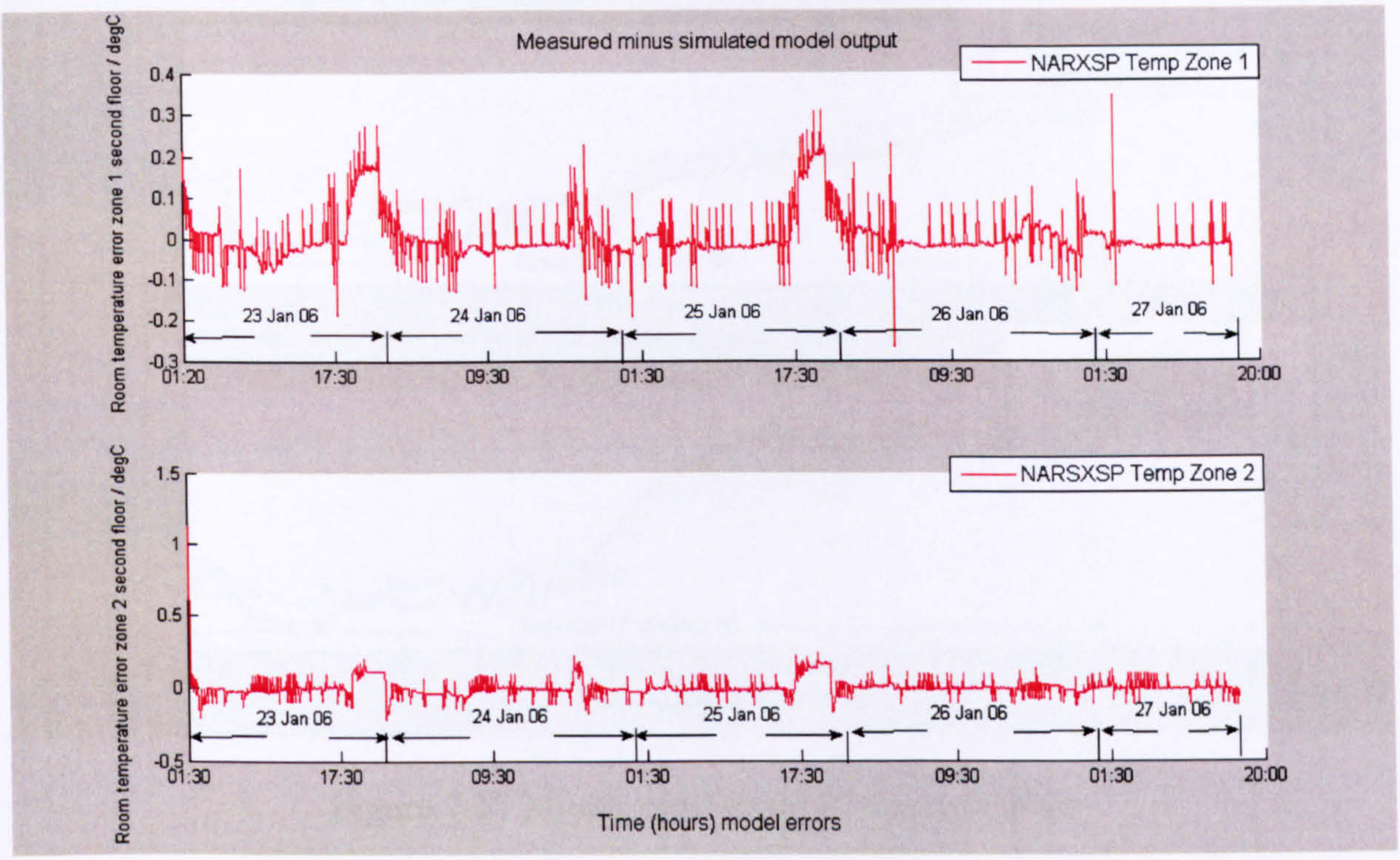

Figure 7.15 Model errors, weekdays 23-27 January 2006

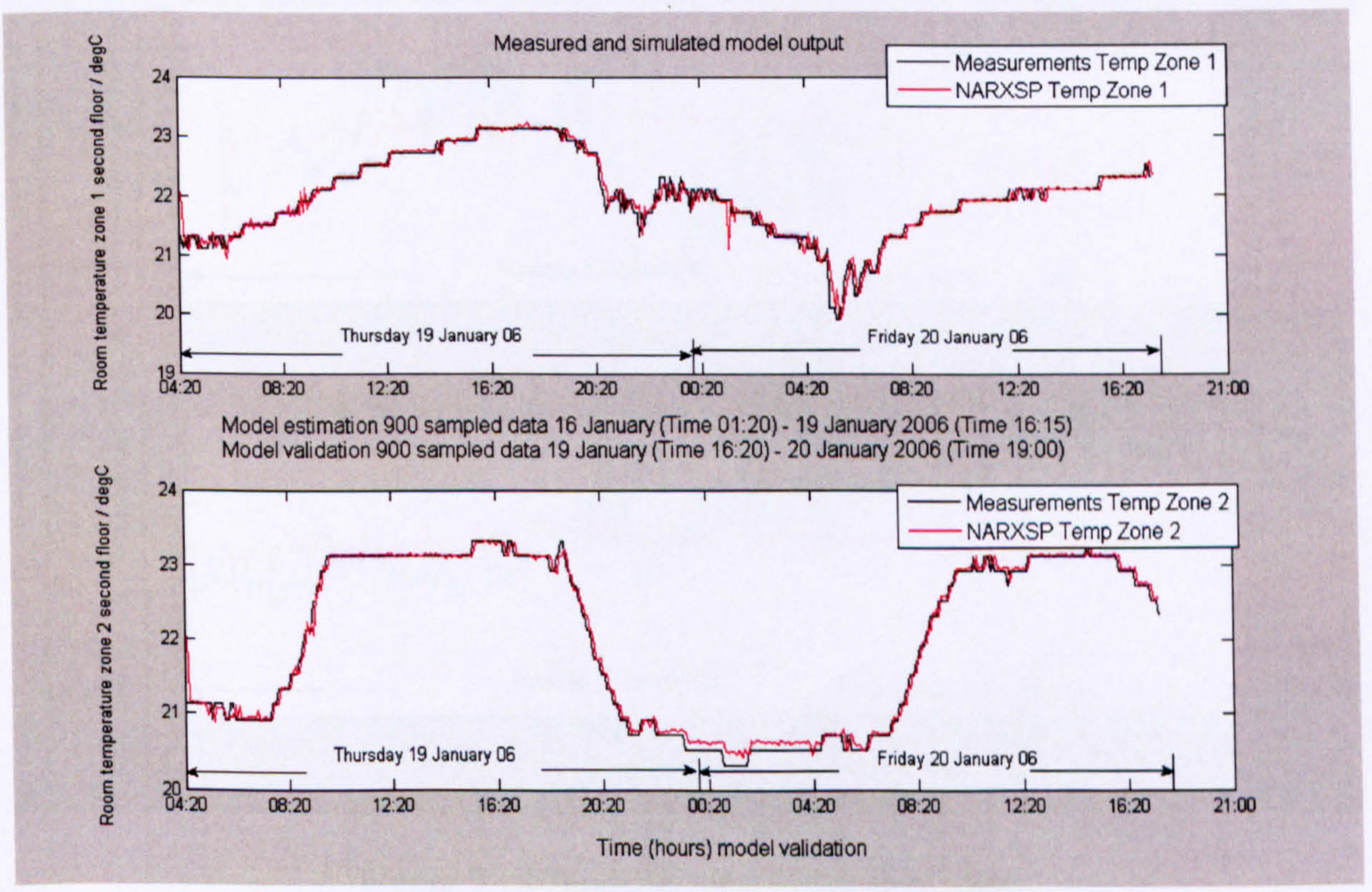

Figure 7.16 Model validation, weekdays 19-20 January 2006

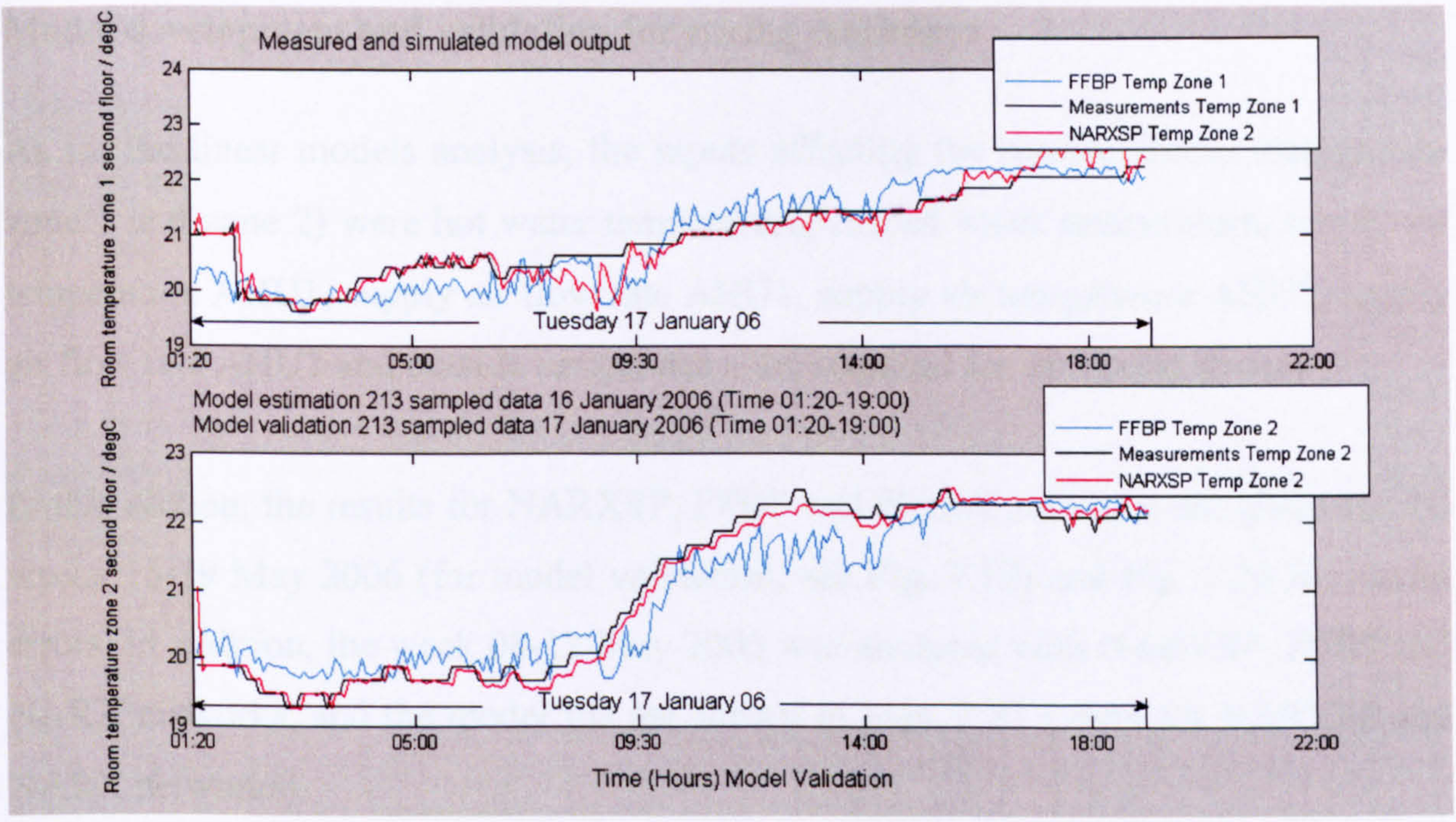

Figure 7.17 Model validation, 17 January 2006

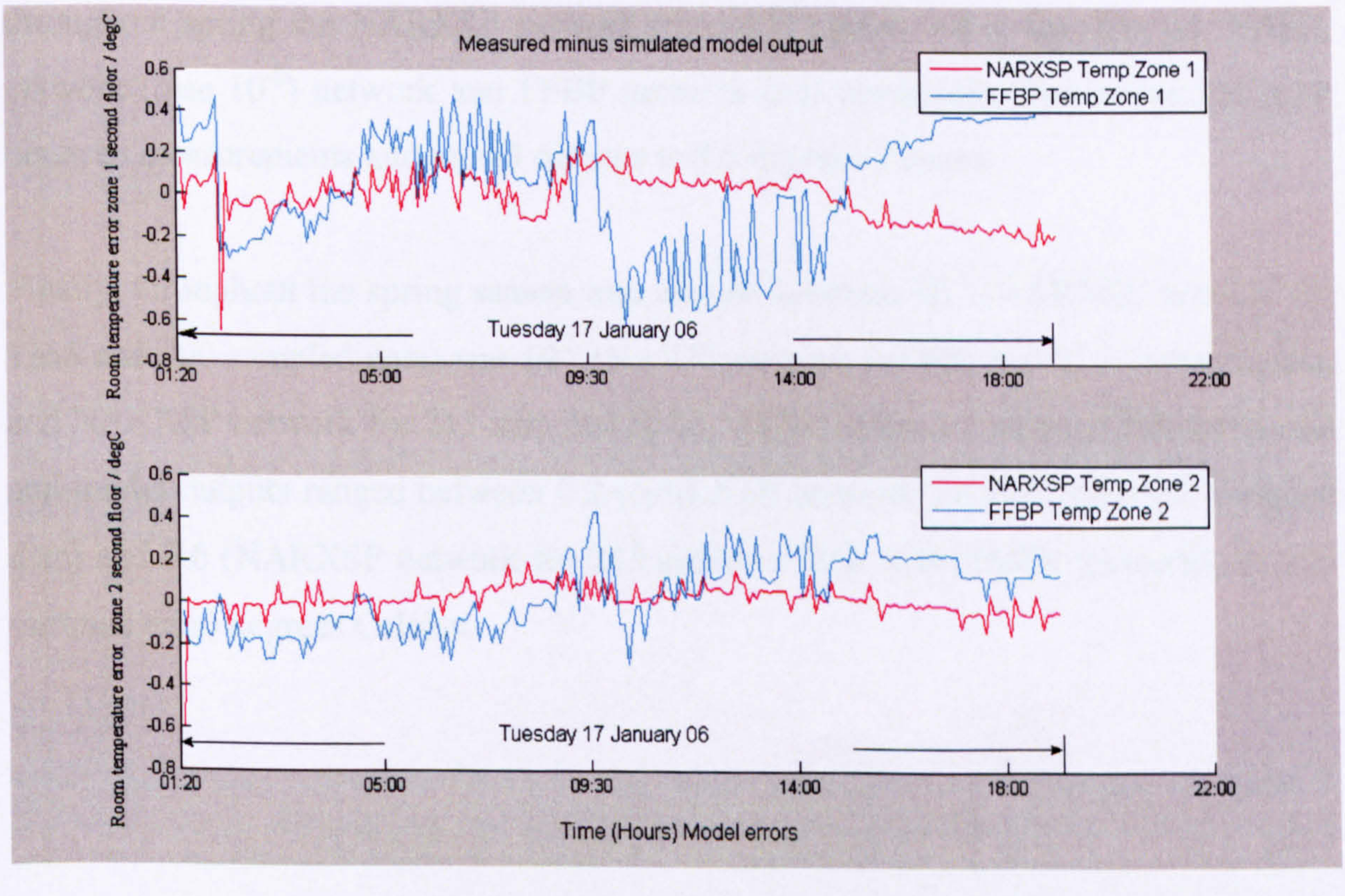

Figure 7.18 Model errors, 17 January 2006

Model development and validation for spring weekdays

As for the linear models analysis, the inputs affecting the results (Room temperature zone 1 and zone 2) were hot water temperature, chilled water temperature, supply air temperature AHU1, supply air flow rate AHU1, supply air temperature AHU2, supply air flow rate AHU2 and outside temperature, are required for the spring season.

In this section, the results for NARXSP, FFBP and NARX networks are given for the weeks 15-19 May 2006 (for model validation, see Fig. 7.19) and Fig. 7.20 for model errors. In addition, the week 08-12 May 2006 was analysed with NARXSP, FFBP and NARX networks, and the model fits are shown in Figs. 7.21 (only for NARXSP and NARX networks).

In addition, 08 and 09 May 2006 were analysed with NARXSP, FFBP and NARX networks and the model fits and errors are shown in Figs. 7.22 and 7.23. Finally, throughout spring the NARXSP network (mse 10^{-3}) gives better fits than the NARX network (mse 10^{-2}) network and FFBP network (not presented). The maximum error between measurements and model outputs is 0.6 degrees Celsius.

Finally, throughout the spring season mse ranged between 10^{-4} (NARXSP network for 1365 and 900 sampled data) and 10^{-2} (NARX network for 900 and 213 sampled data, and NARXSP network for 213 sampled data), while the errors between measurements and model outputs ranged between 0.2 (NARXSP network for 1365 and 900 sampled data) and 0.6 (NARXSP network for 213 sampled data, and NARX networks for 900 sampled data) degrees Celsius.

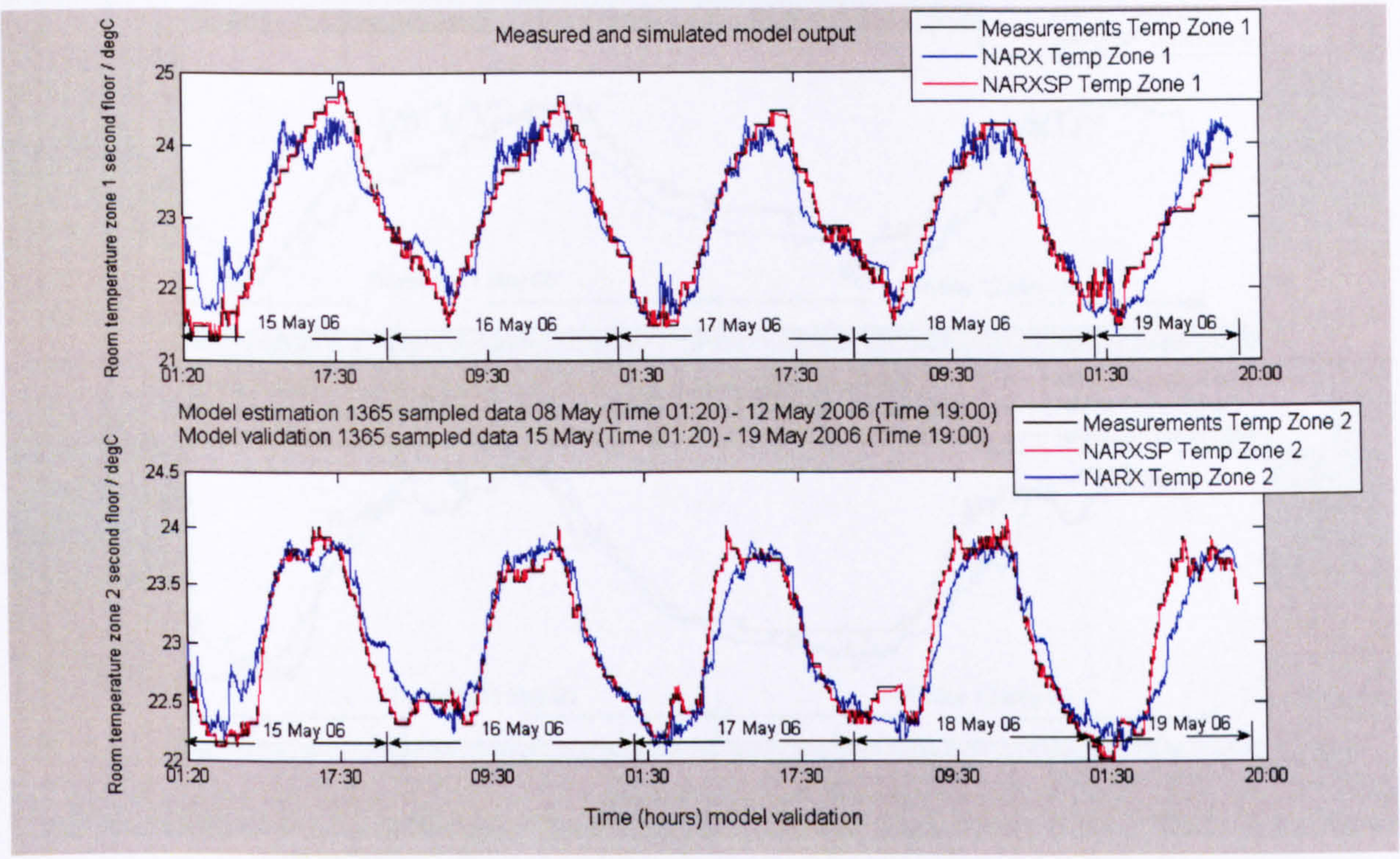

Figure 7.19 Model validation, weekdays 15-19 May 2006

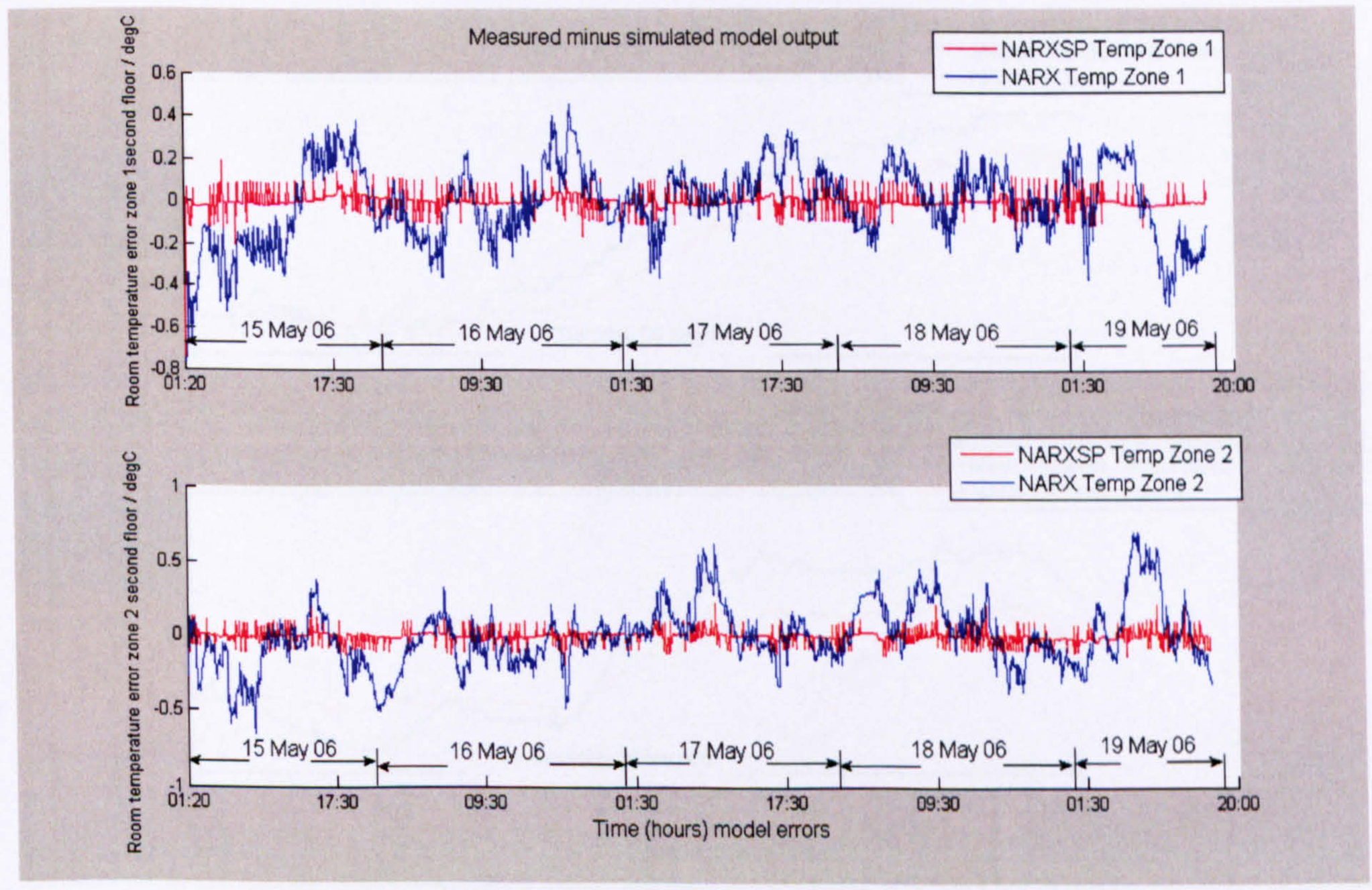

Figure 7.20 Model errors, weekdays 15-19 May 2006

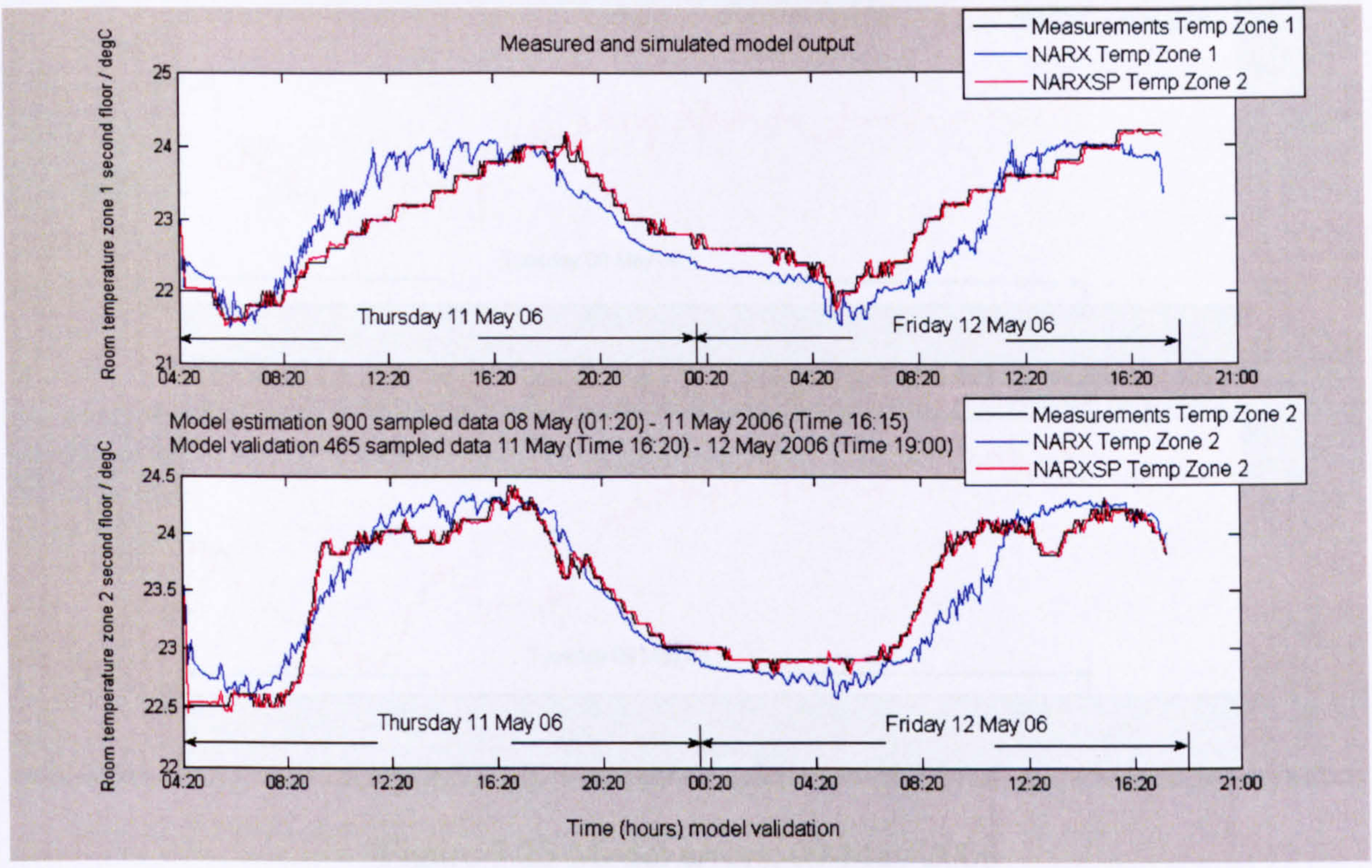

Figure 7.21 Model validation, weekdays 11-12 May 2006

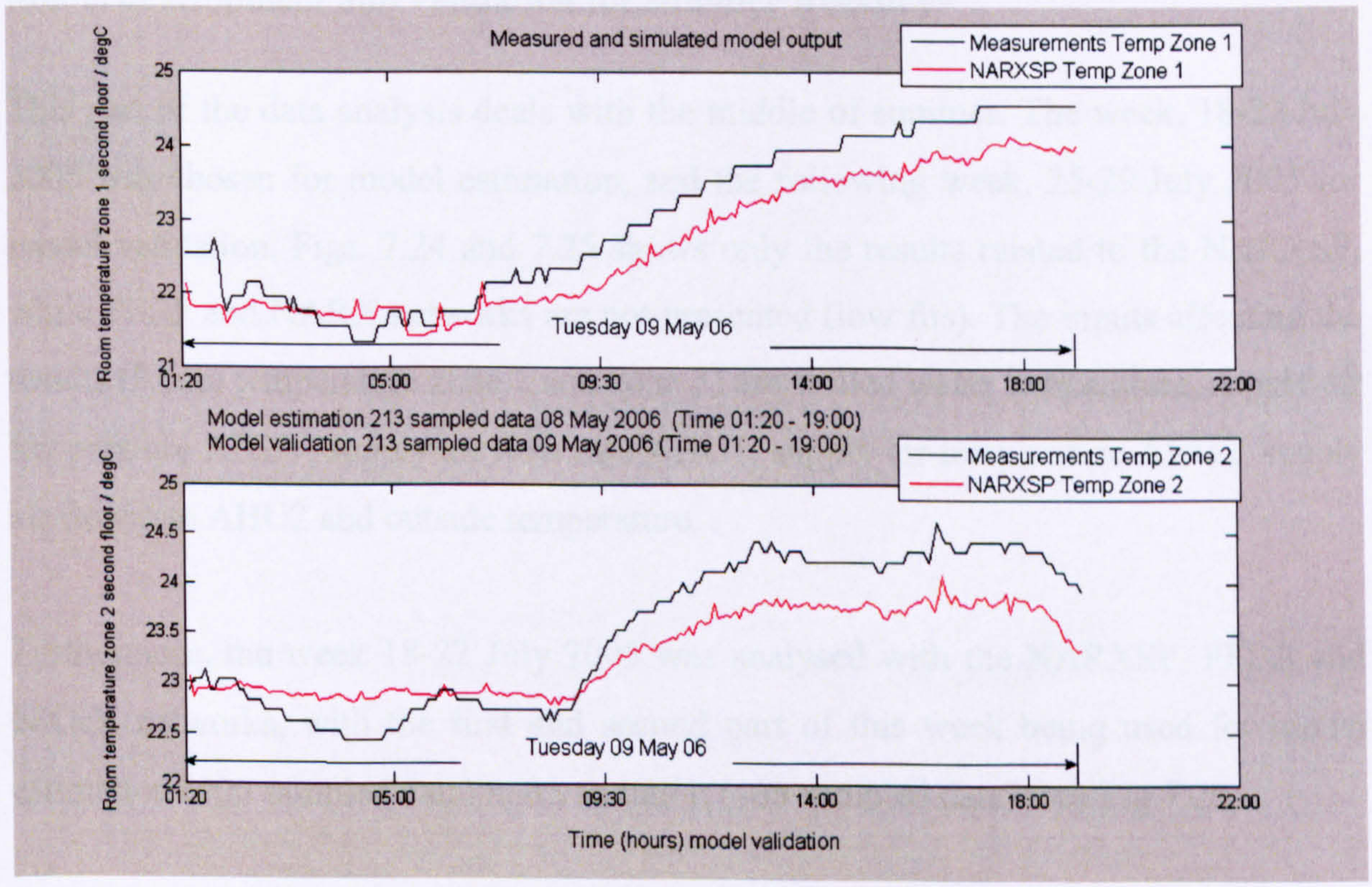

Figure 7.22 Model validation, 09 May 2006

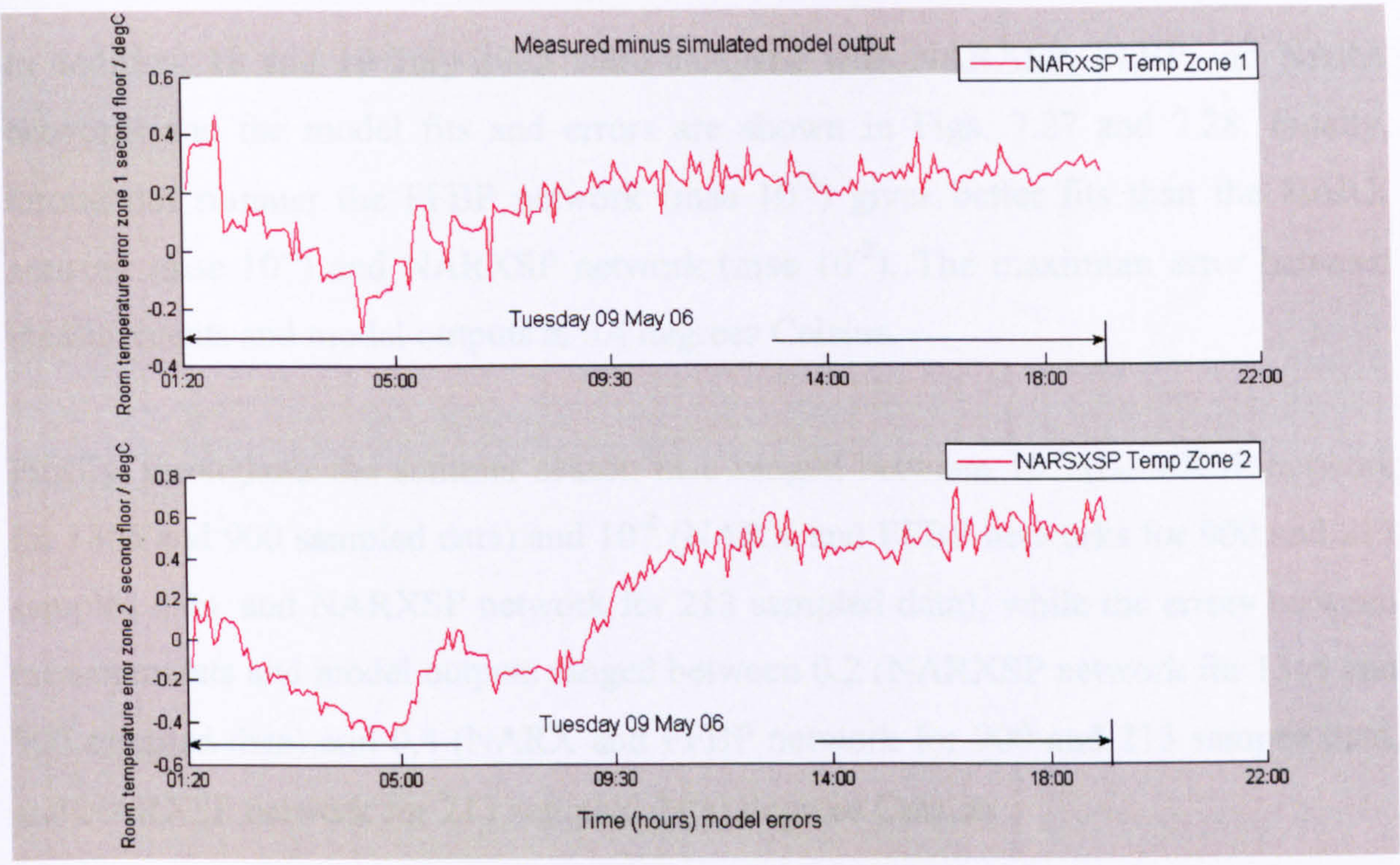

Figure 7.23 Model errors, 09 May 2006

Model development and validation for summer weekdays

This part of the data analysis deals with the middle of summer. The week, 18-22 July 2005 was chosen for model estimation, and the following week, 25-29 July 2005 for model validation. Figs. 7.24 and 7.25 shows only the results related to the NARXSP, while FFBP and NARX networks are not presented (low fits). The inputs affecting the results (Room temperature zone 1 and zone 2) are chilled water temperature, supply air temperature AHU1, supply air flow rate AHU1, supply air temperature AHU2, supply air flow rate AHU2 and outside temperature.

Furthermore, the week 18-22 July 2005 was analysed with the NARXSP, FFBB and NARX networks, with the first and second part of this week being used for model estimation (900 sampled data) and validation (465 sampled data) (see Fig 7.26).

In addition, 18 and 19 July 2005 were analysed with NARXSP, FFBP and NARX networks and the model fits and errors are shown in Figs. 7.27 and 7.28. Finally, throughout summer the FFBP network (mse 10^{-3}) gives better fits than the NARX network (mse 10^{-2}) and NARXSP network (mse 10^{-2}). The maximum error between measurements and model outputs is 0.4 degrees Celsius.

Finally, throughout the summer season mse ranged between 10^{-4} (NARXSP network for 1365 and 900 sampled data) and 10^{-2} (NARX and FFBP networks for 900 and 213 sampled data, and NARXSP network for 213 sampled data), while the errors between measurements and model outputs ranged between 0.2 (NARXSP network for 1365 and 900 sampled data) and 0.4 (NARX and FFBP network for 900 and 213 samped data, and NARXSP network for 213 sampled data) degrees Celsius.

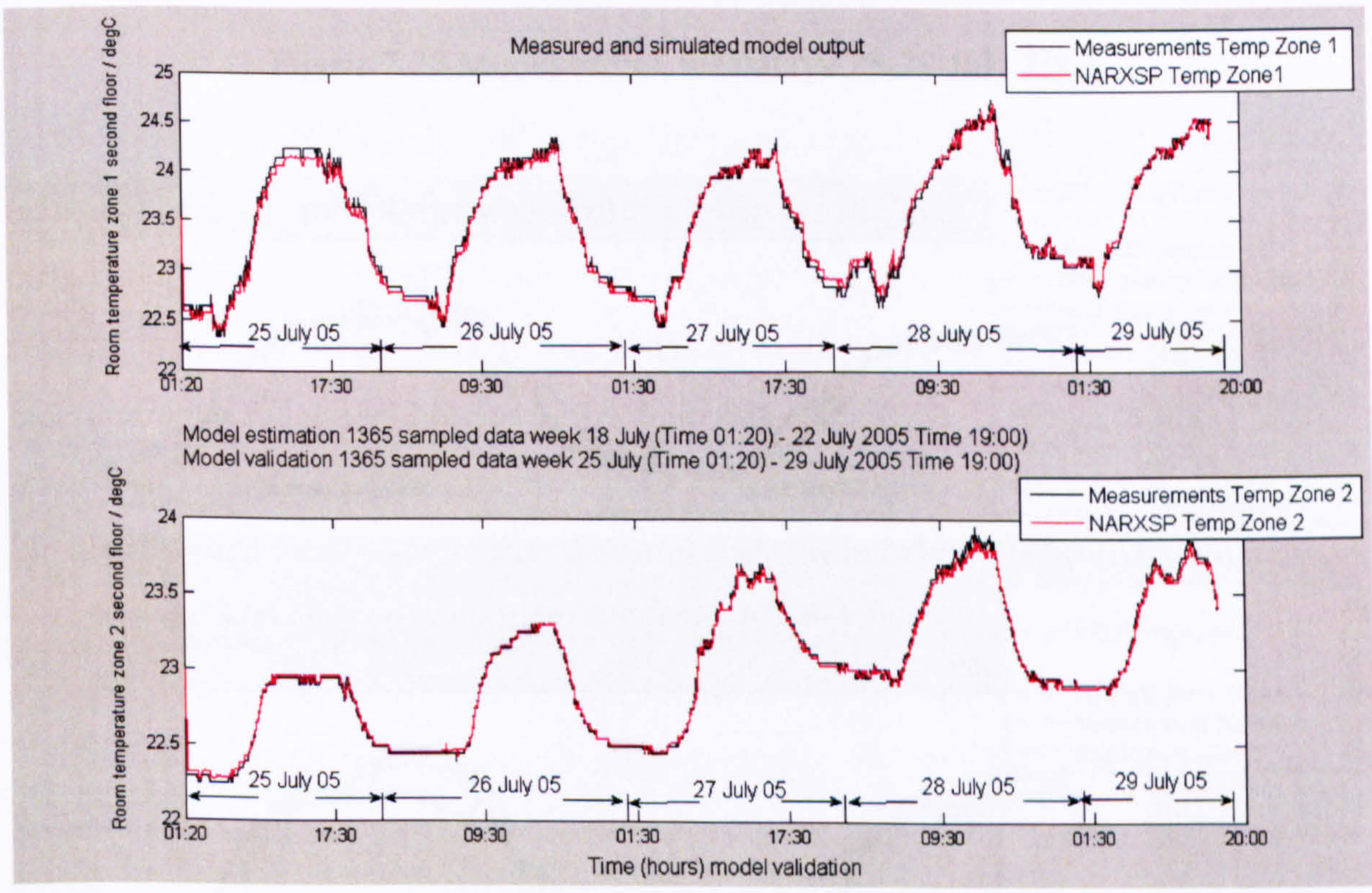

Figure 7.24 Model validation, weekdays 25-29 July 2005

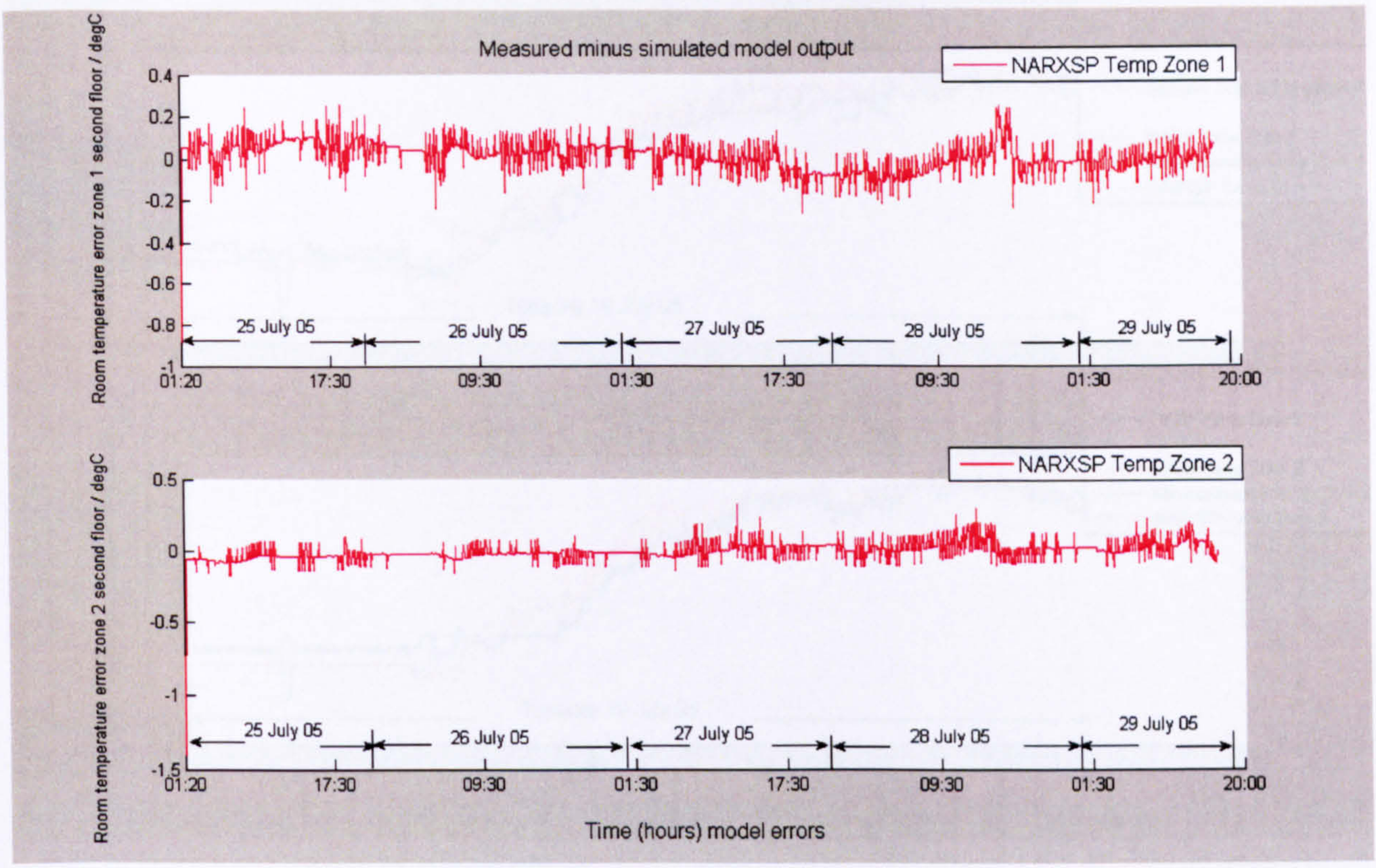

Figure 7.25 Model errors, weekdays 25-29 July 2005

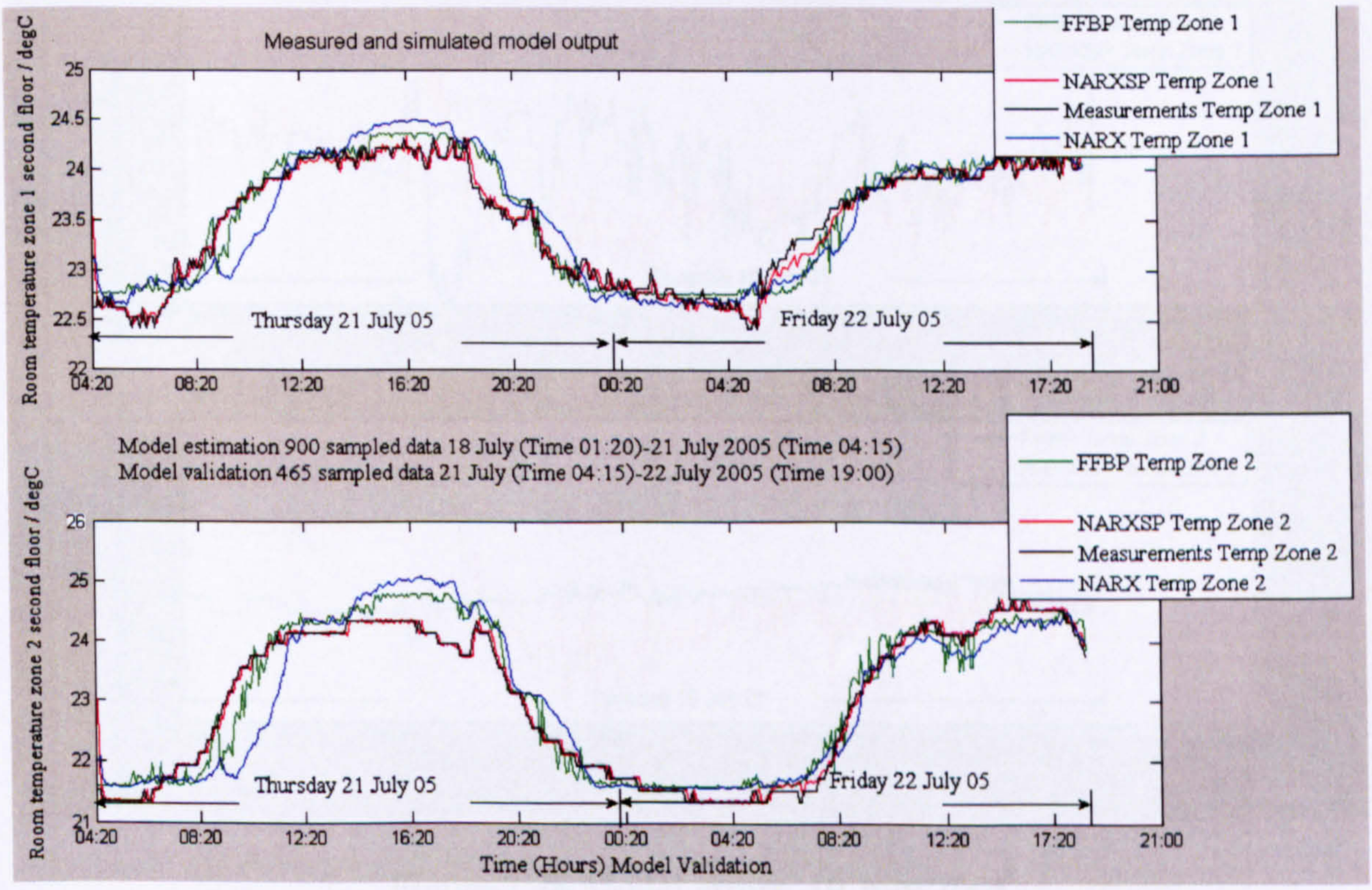

Figure 7.26 Model validation, weekdays 21-22 July 2005

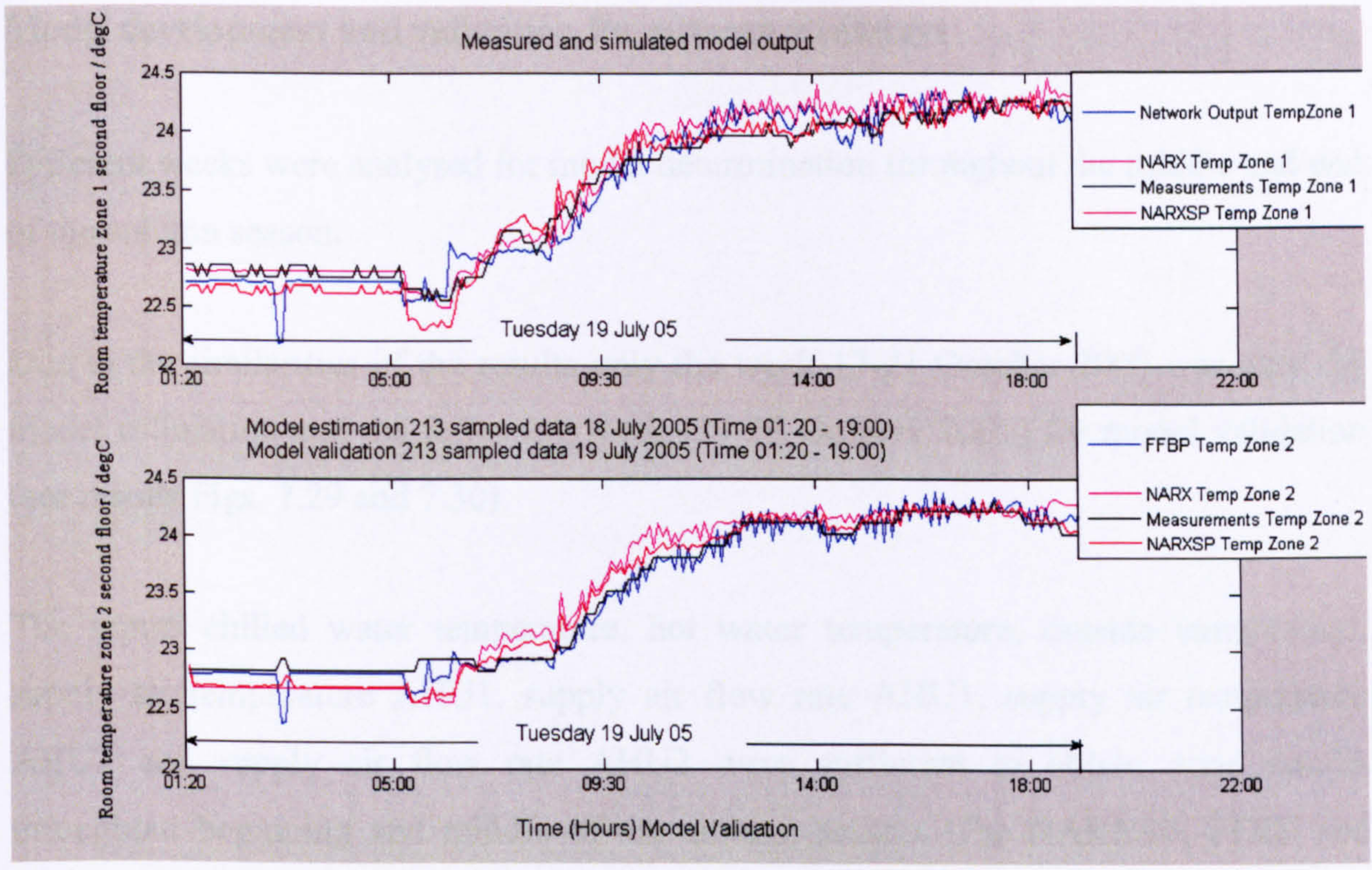

Figure 7.27 Model validation, 19 July 2005

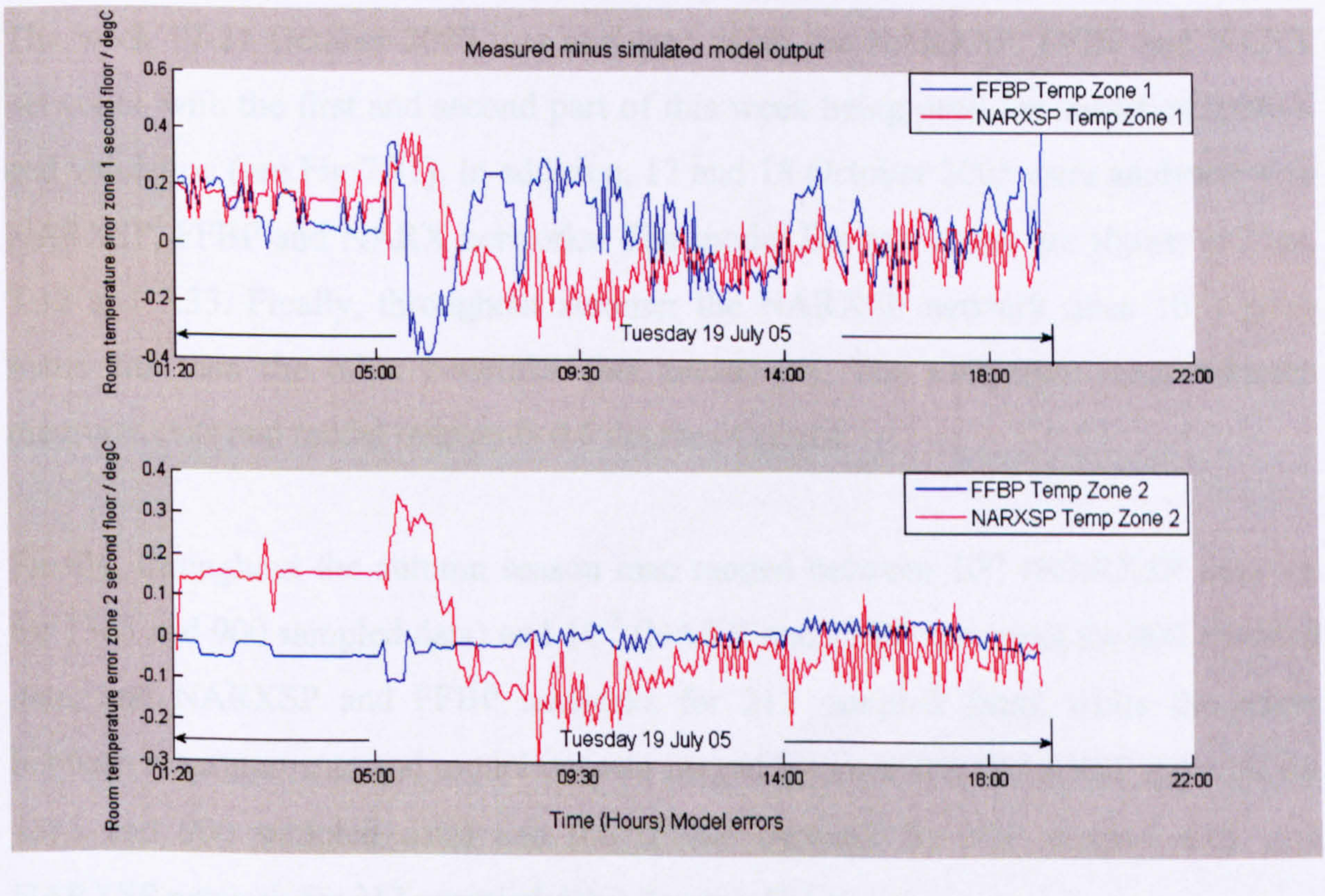

Figure 7.28 Model errors, 19 July 2005

Model development and validation for autumn weekdays

Different weeks were analysed for model determination throughout the middle and end of the autumn season.

Due to the similarities of the results only the week 17-21 October 2005 was used for model estimation and the following week (24-28 October 2005) for model validation (see results Figs. 7.29 and 7.30).

The inputs chilled water temperature, hot water temperature, outside temperature, supply air temperature AHU1, supply air flow rate AHU1, supply air temperature AHU2 and supply air flow rate AHU2 were sufficient to obtain good results throughout beginning and middle of the autumn season. The NARXSP, FFBP and NARX networks gave good results throughout autumn.

The week 17-21 October 2005 was analysed using the NARXSP, FFBP and NARX networks, with the first and second part of this week being used for model estimation and validation (see Fig 7.31). In addition, 17 and 18 October 2005 were analysed with NARXSP, FFBP and NARX networks. The model fits and errors are shown in Figs. 7.32 and 7.33. Finally, throughout summer the NARXSP network (mse 10^{-3}) gives better fits than the other networks (not presented). The maximum error between measurements and model outputs is 0.6 degrees Celsius.

Finally, throughout the autumn season mse ranged between 10^{-4} (NARXSP network for 1365 and 900 sampled data) and 10^{-3} (NARX and FFBP networks for 900 sampled data, and NARXSP and FFBP networks for 213 sampled data), while the errors between measurements and model outputs ranged between 0.2 (NARXSP network for 1365 and 900 sampled data) and 0.6 (FFBP network for 900 samped data, and NARXSP network for 213 sampled data) degrees Celsius.

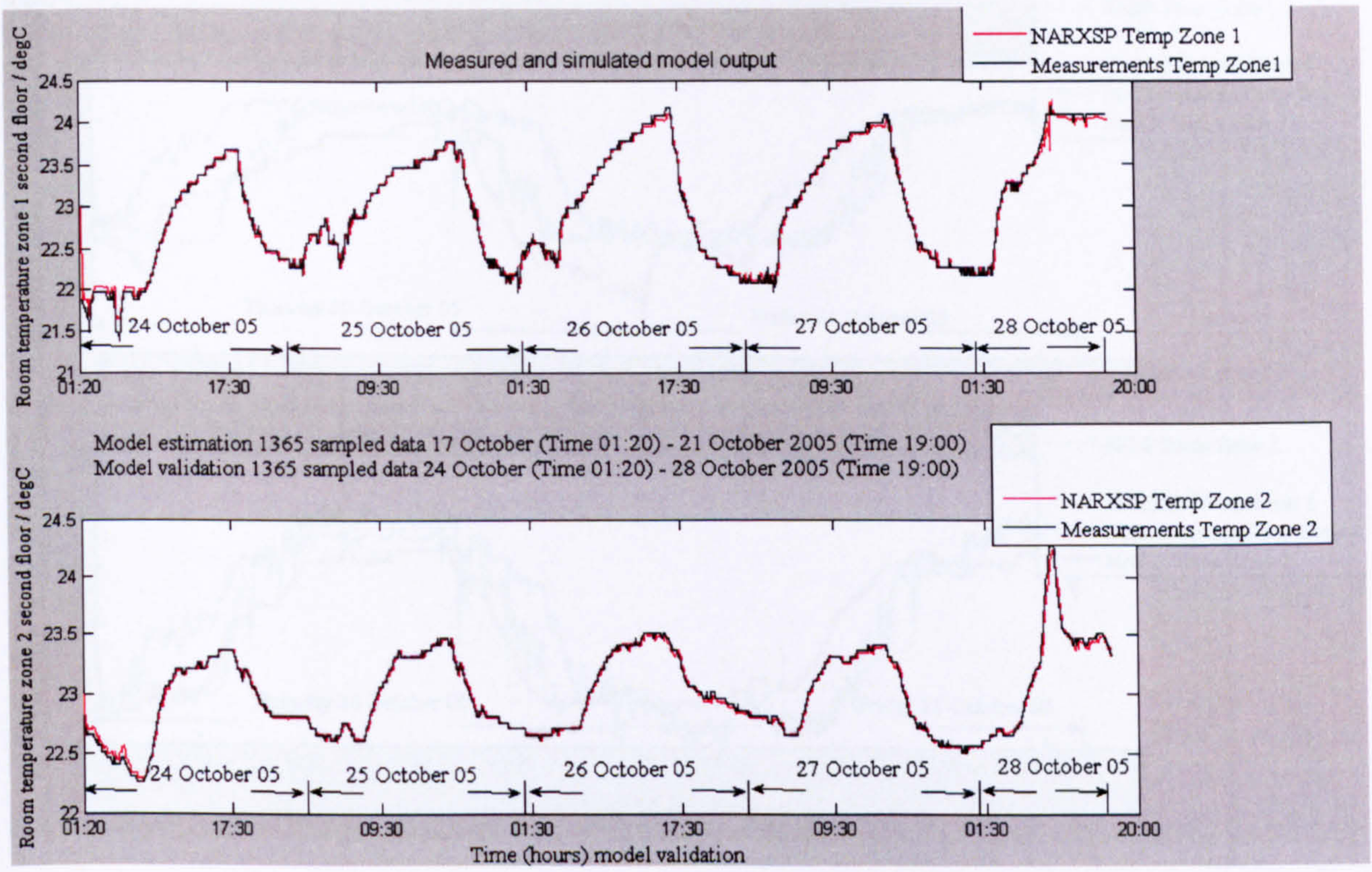

Figure 7.29 Model validation, weekdays 24-28 October 2005

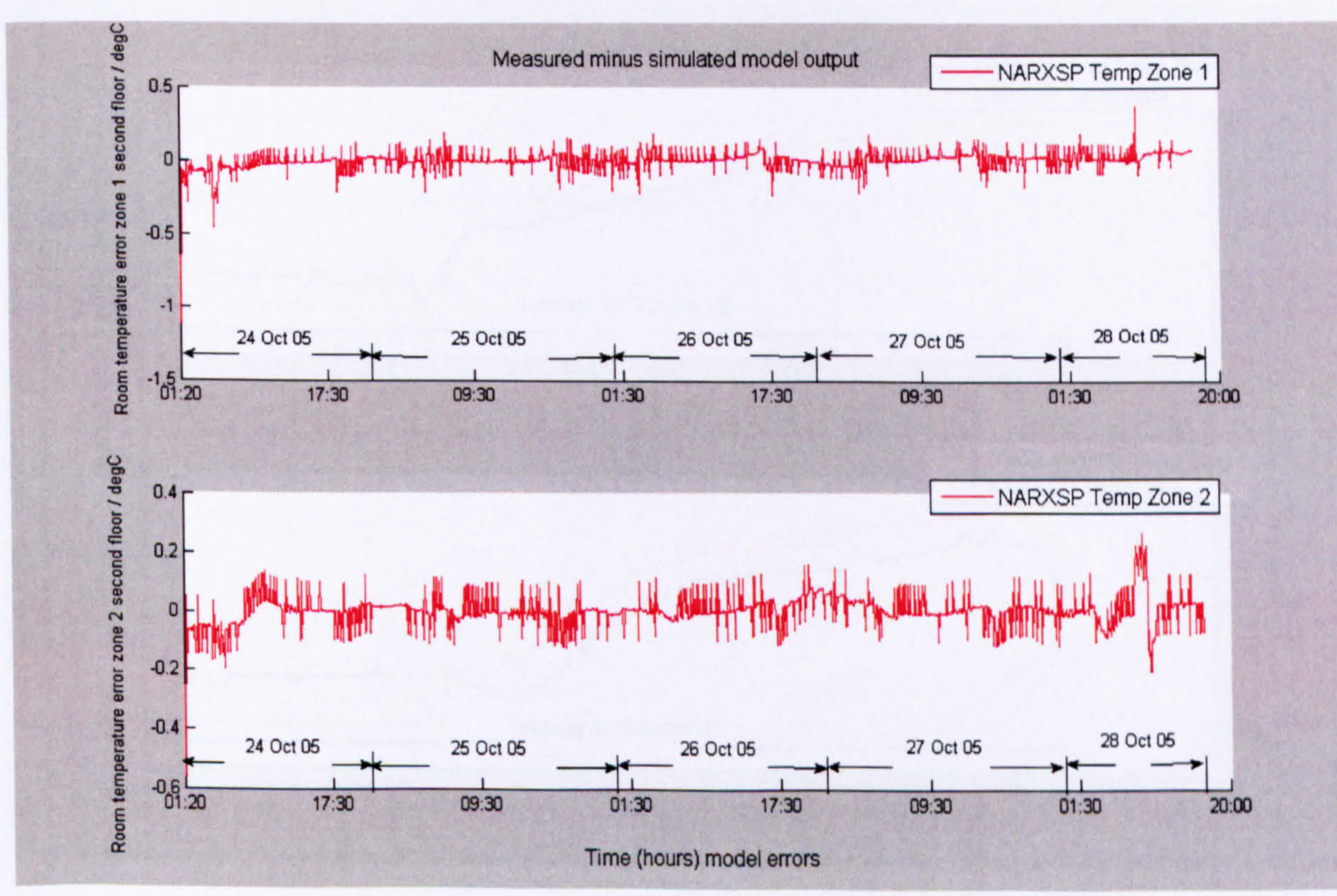

Figure 7.30 Model errors, weekdays 24-28 October 2005

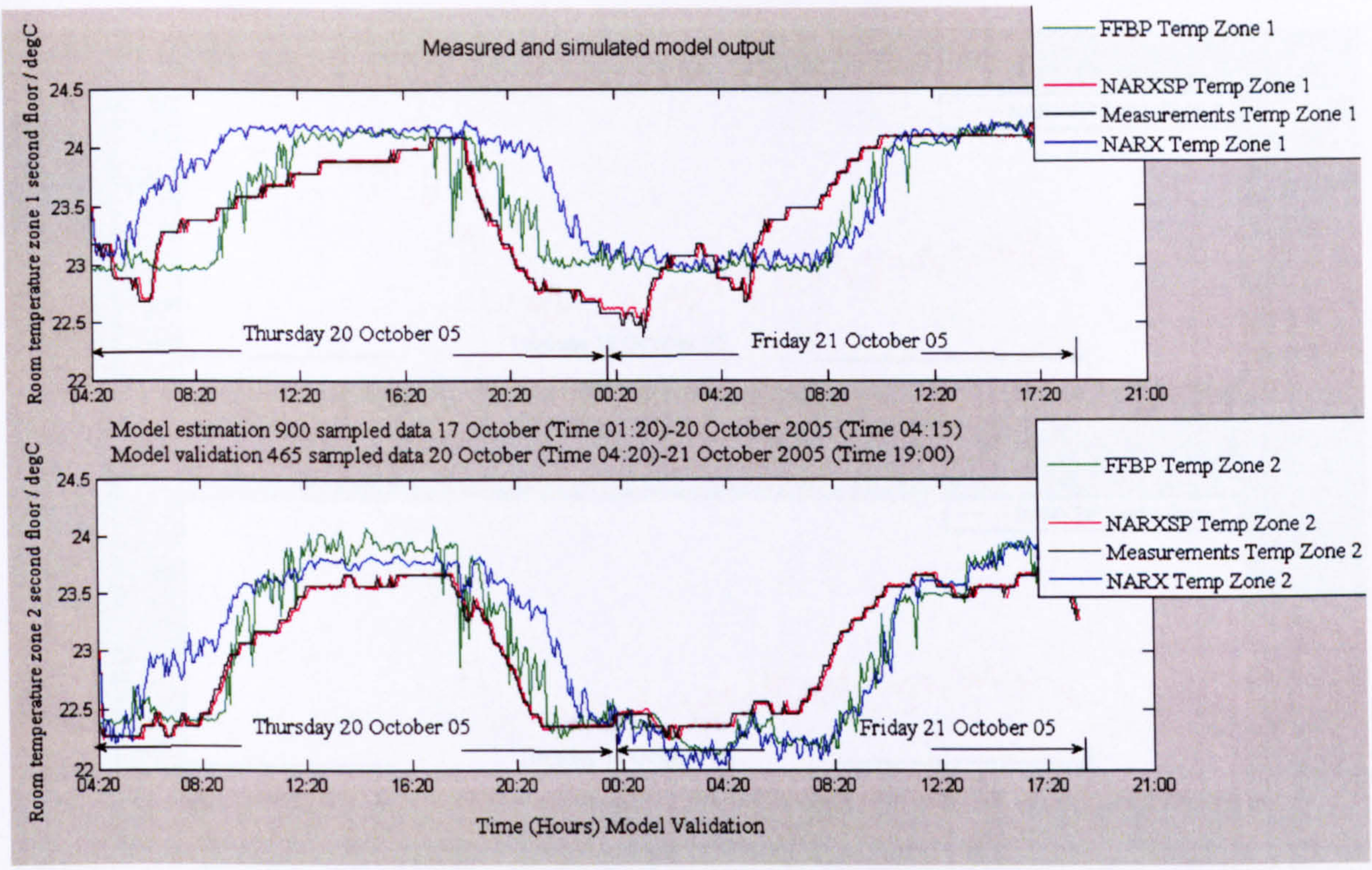

Figure 7.31 Model validation, weekdays 20-21 October 2005

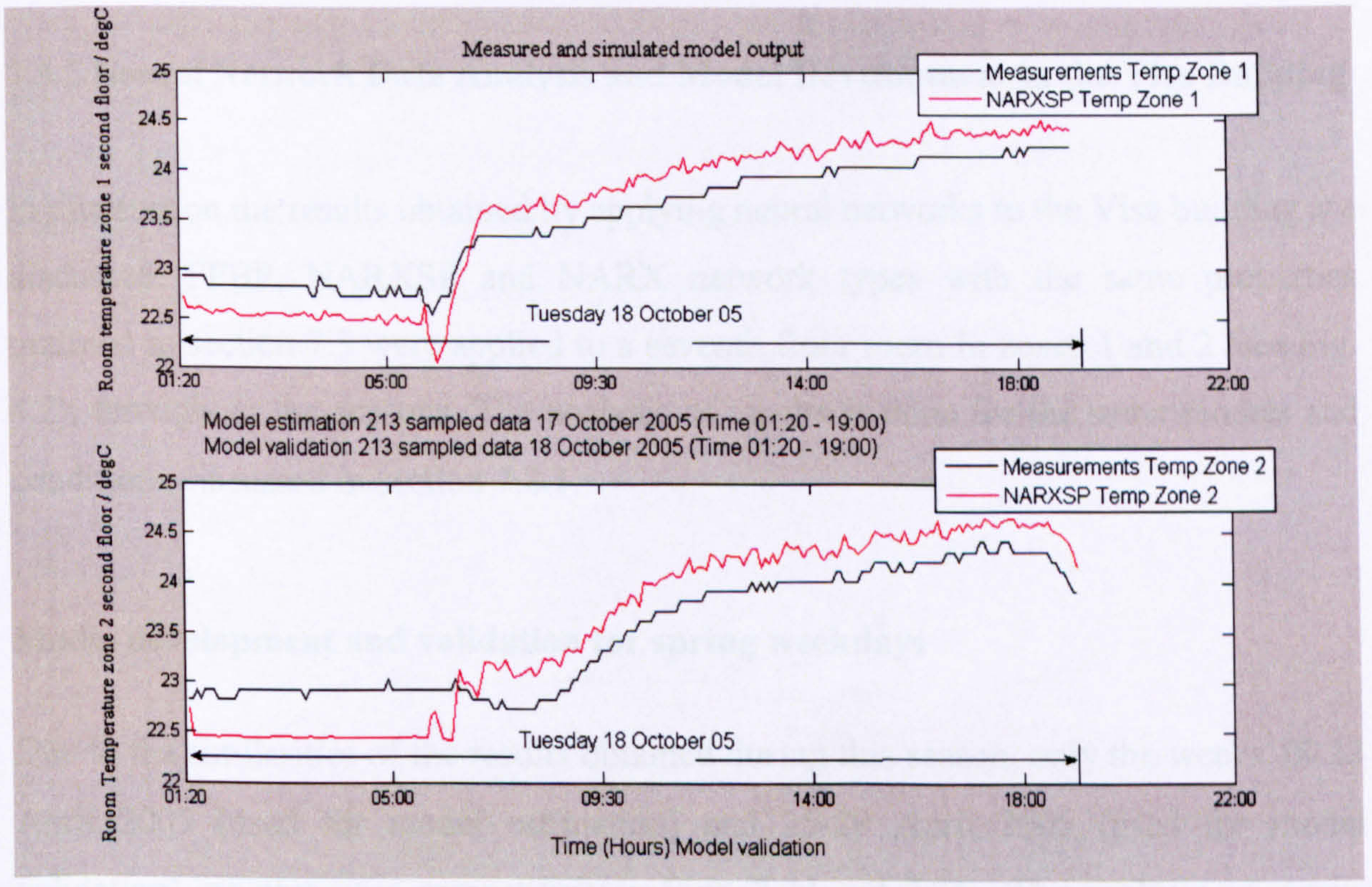

Figure 7.32 Model validation, 18 October 2005

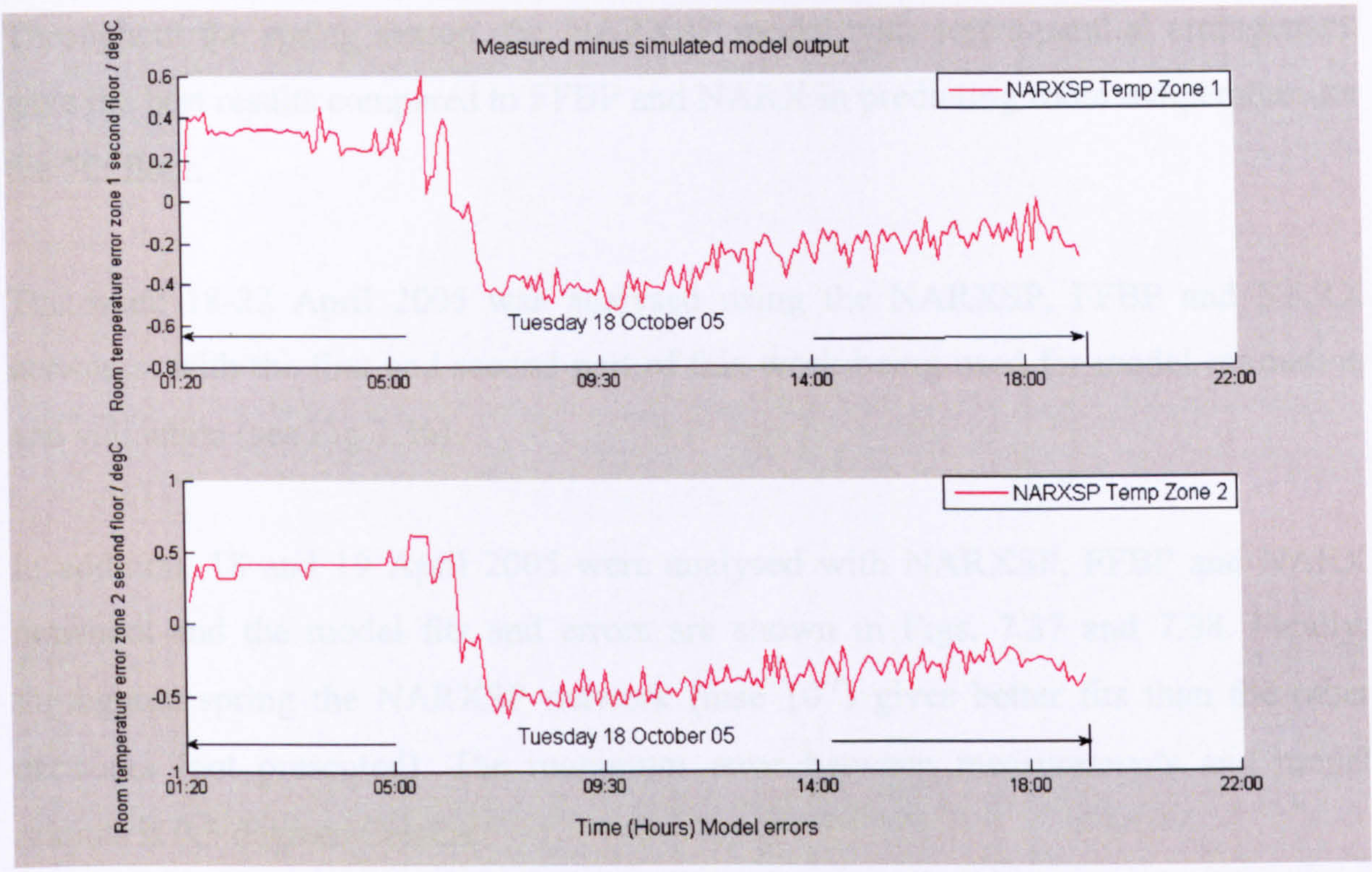

Figure 7.33 Model errors, 18 October 2005

7.3.2 Neural Network Data Analysis and Model Development in the Visa Building

In this section the results obtained by applying neural networks to the Visa building are discussed. FFBP, NARXSP and NARX network types with the same properties outlined in section 7.3 were applied to a seventh floor room in zones 1 and 2 (see Fig. 4.2), throughout the seasons. The analysis of results is done for the same models and conditions discussed in section 7.2.1.

Model development and validation for spring weekdays

Due to the similarities of the results obtained during this season, only the weeks 18-22 April 2005 (used for model estimation) and 25-29 April 2005 (used for model validation) are presented respectively in Figs. 7.34 and 7.35. The analysis of results reveals that the inputs affecting the results (room temperature zone 1 and 2, seventh floor) are outside temperature, hot water temperature, chilled water temperature, supply air temperature AHU1, supply air flow rate AHU1, supply air temperature AHU2 and supply air flow rate AHU2.

Throughout the spring season, the NARXSP model with series-parallel arrangement gave the best results compared to FFBP and NARX in predicting room temperature for the 7th floor.

The week 18-22 April 2005 was analysed using the NARXSP, FFBP and NARX networks, with the first and second part of this week being used for model estimation and validation (see Fig 7.36).

In addition, 18 and 19 April 2005 were analysed with NARXSP, FFBP and NARX networks and the model fits and errors are shown in Figs. 7.37 and 7.38. Finally, throughout spring the NARXSP network (mse 10^{-3}) gives better fits than the other networks (not presented). The maximum error between measurements and model outputs is 0.3 degrees Celsius.

Finally, throughout the spring season mse ranged between 10^{-4} (NARXSP network for 1365 and 900 sampled data) and 10^{-3} (NARX and FFBP networks for 900 sampled data, and NARXSP network for 213 sampled data), while the errors between measurements and model outputs ranged between 0.2 (NARXSP network for 1365 and 900 sampled data) and 0.3 (NARX and FFBP networks for 900 samped data, and NARXSP network for 213 sampled data) degrees Celsius.

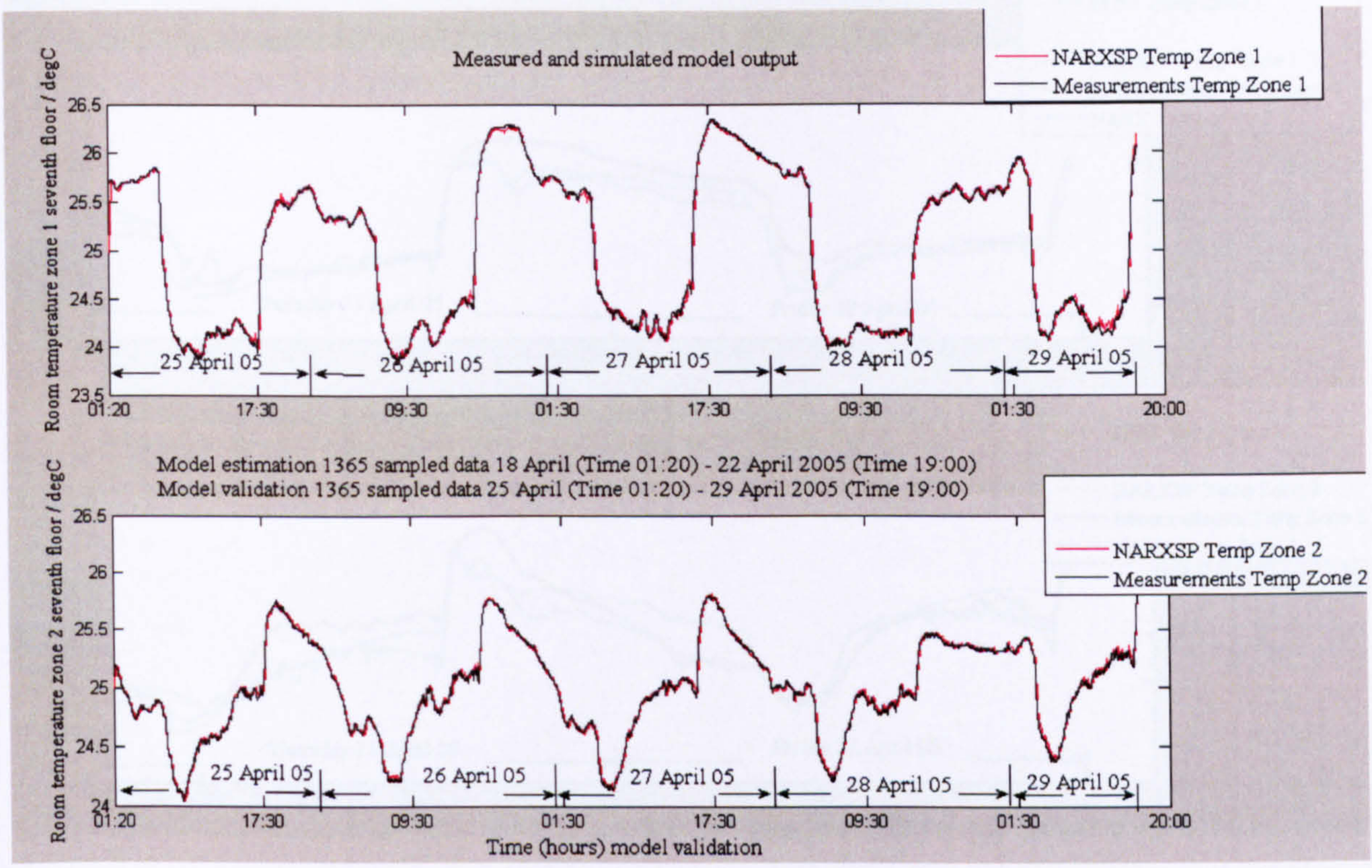

Figure 7.34 Model validation, weekdays 25-29 April 2005

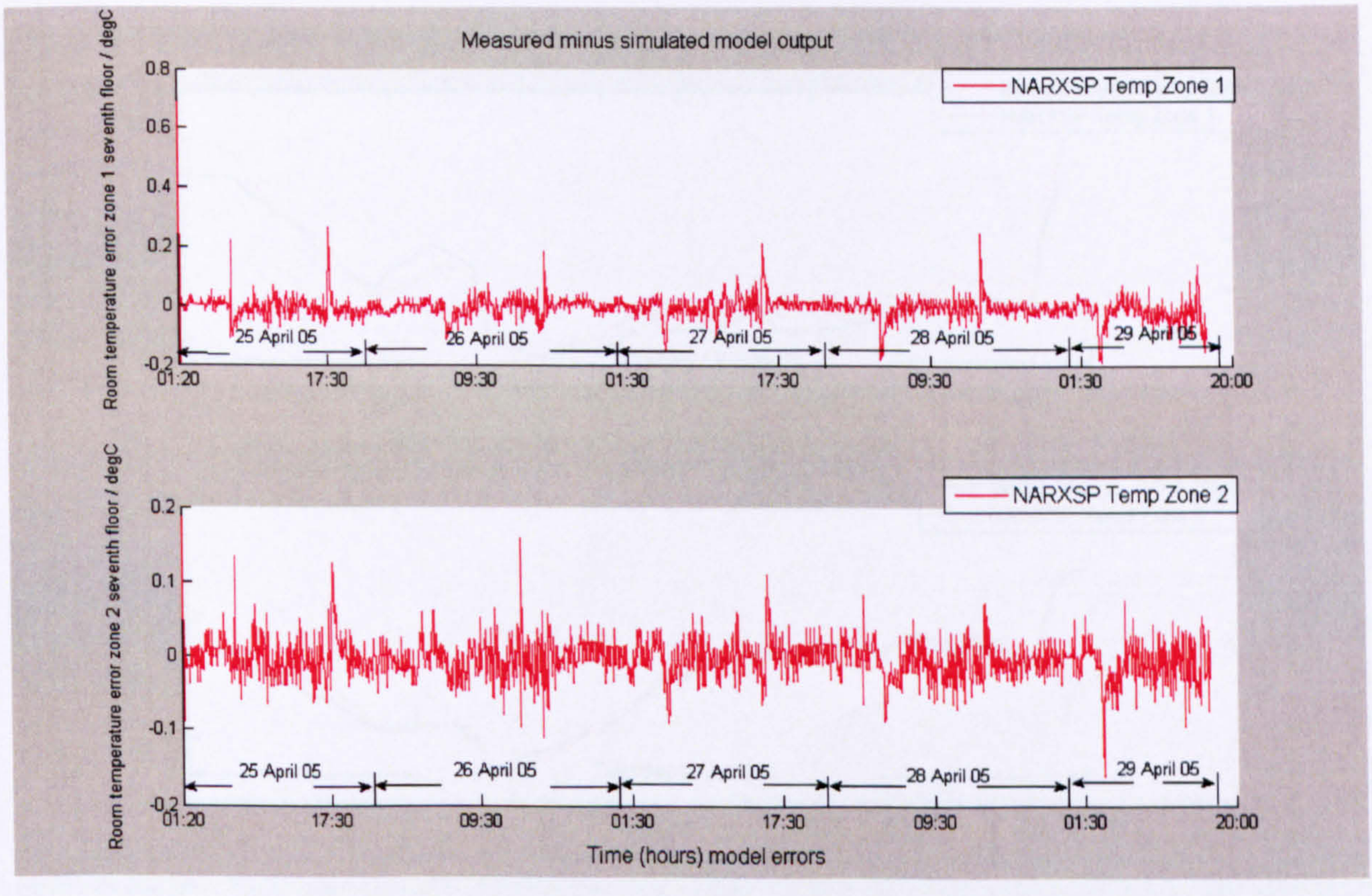

Figure 7.35 Model errors, weekdays 25-29 April 2005

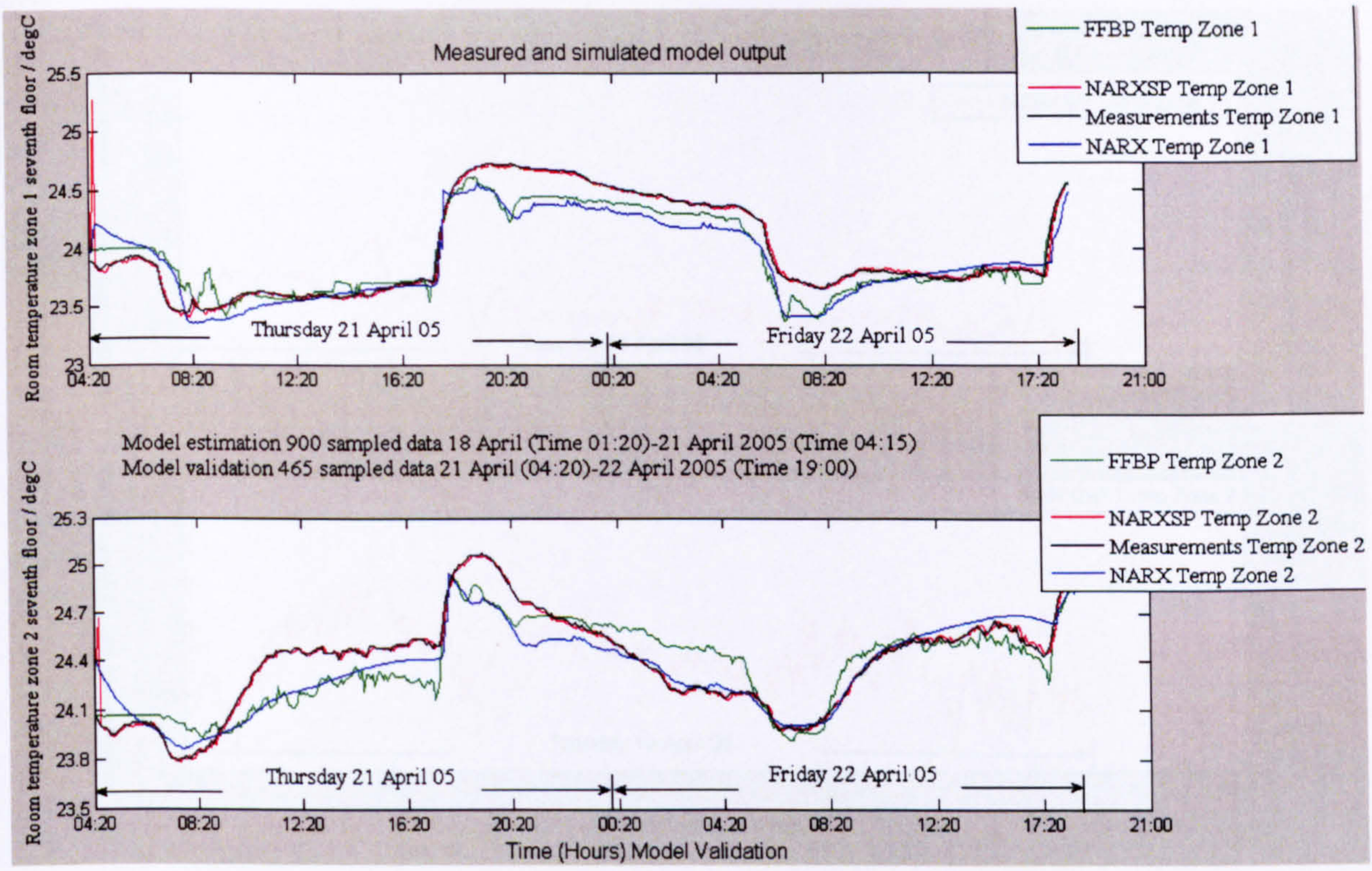

Figure 7.36 Model validation, weekdays 21-22 April 2005

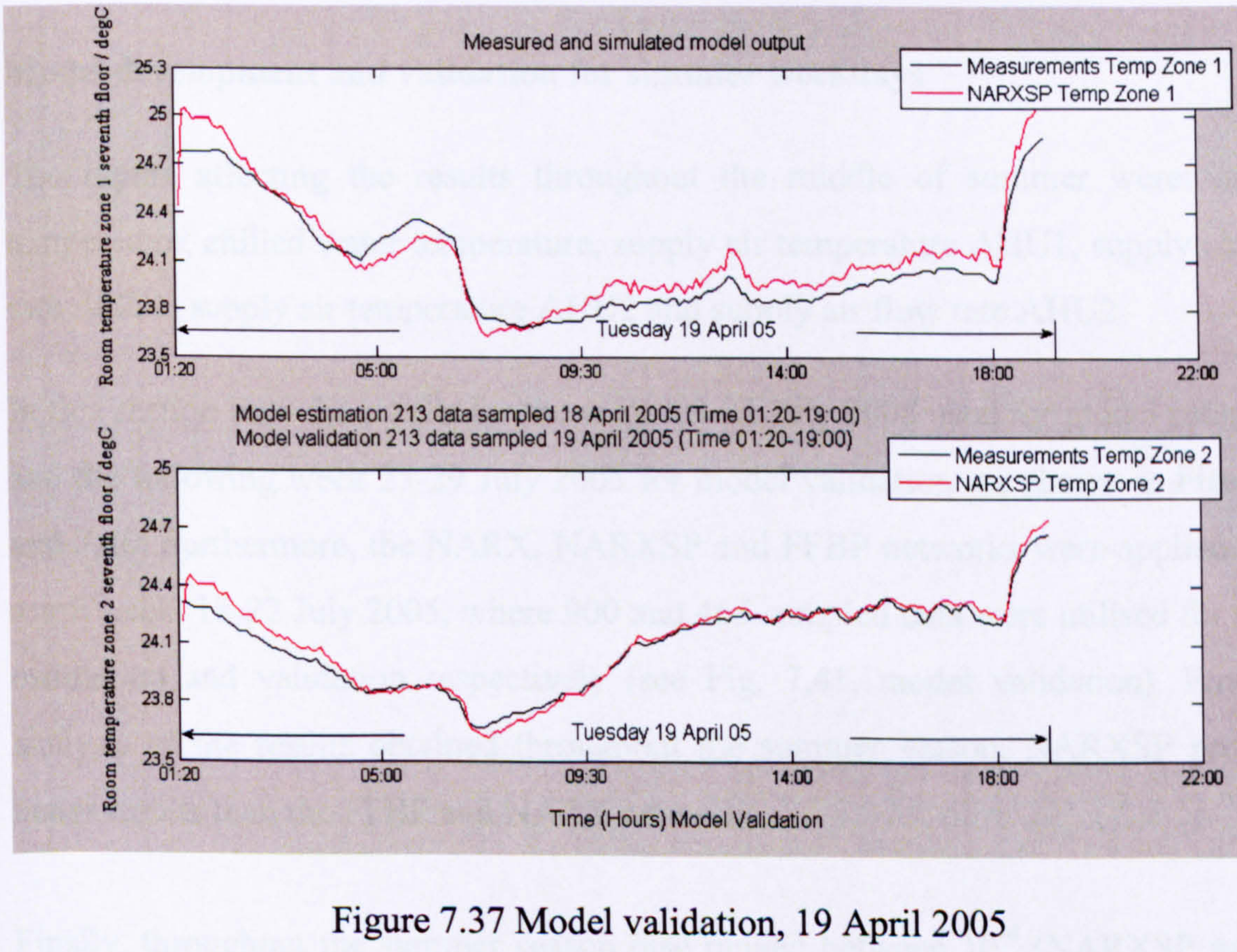

Figure 7.37 Model validation, 19 April 2005

Figure 7.38 Model errors, 19 April 2005

Model development and validation for summer weekdays

The inputs affecting the results throughout the middle of summer were: outside temperature, chilled water temperature, supply air temperature AHU1, supply air flow rate AHU1, supply air temperature AHU2 and supply air flow rate AHU2.

In this section only the results for the week 18-22 July 2005 used for model estimation and the following week 25-29 July 2005 for model validation are shown in Figs. 7.39 and 7.40. Furthermore, the NARX, NARXSP and FFBP networks were applied to the same week, 18-22 July 2005, where 900 and 465 sampled data were utilised for model estimation and validation respectively (see Fig. 7.41, model validation). From the analysis of the results obtained throughout the summer season, NARXSP produced better results than the FFBP and NARX networks.

Finally, throughout the summer season mse ranged between 10^{-4} (NARXSP network for 1365 and 900 sampled data) and 10^{-3} (NARX and FFBP networks for 900 sampled data), while the errors between measurements and model outputs ranged between 0.8 (NARXSP network for 1365 and 900 sampled data) and 1.5 (NARX and FFBP network for 900 samped data) degrees Celsius.

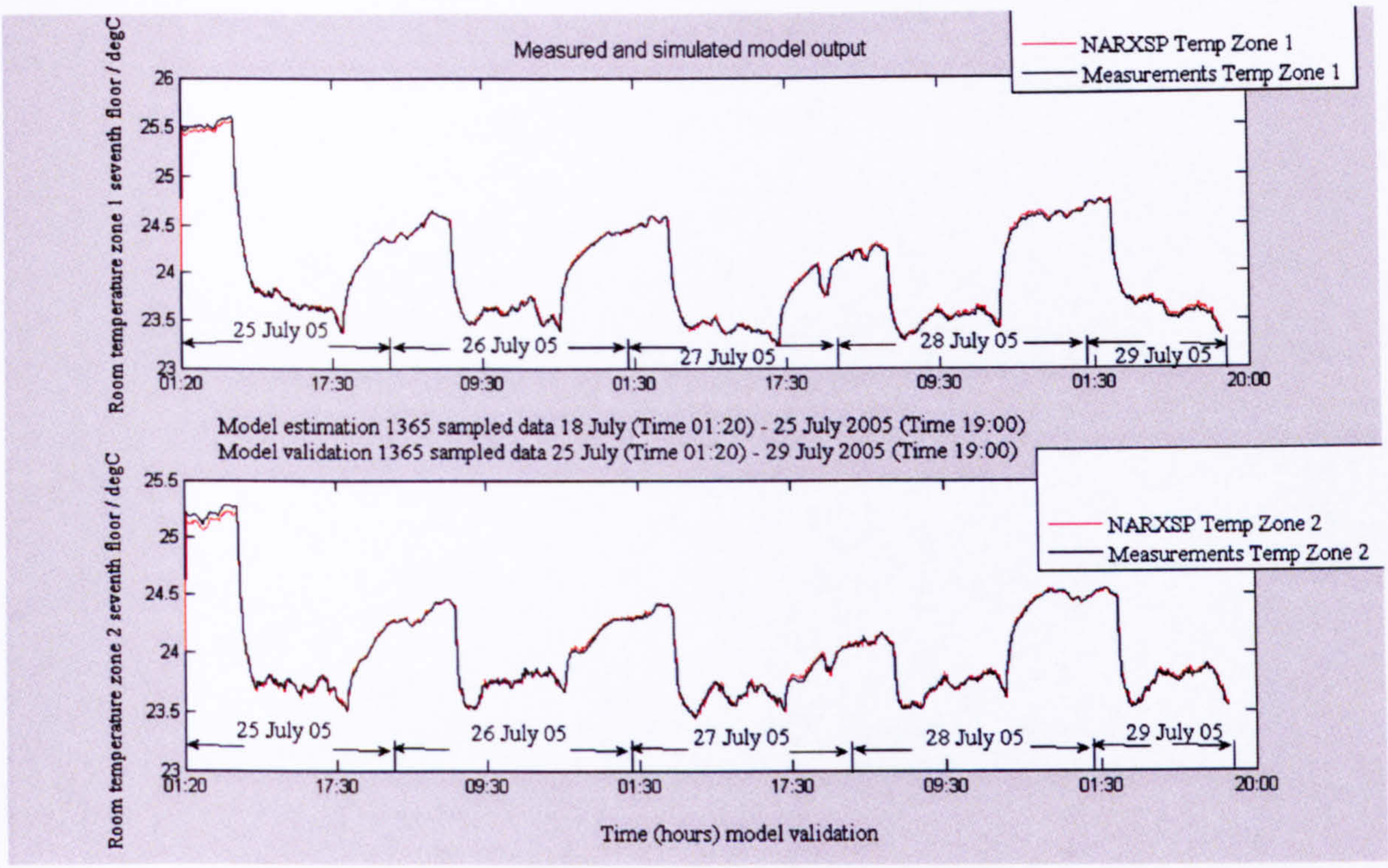

Figure 7.39 Model validation, weekdays 25-29 July 2005

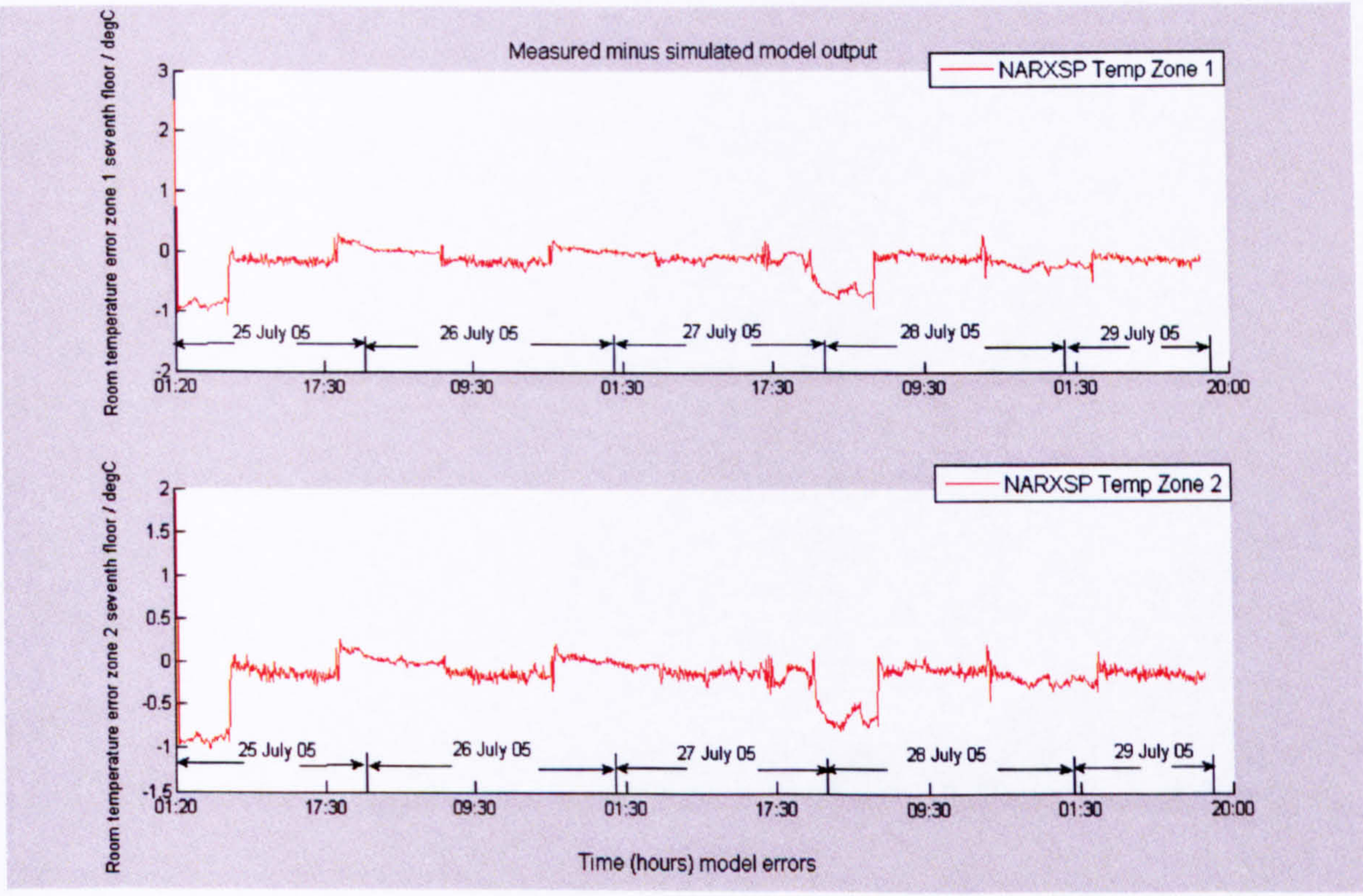

Figure 7.40 Model errors, weekdays 25-29 July 2005

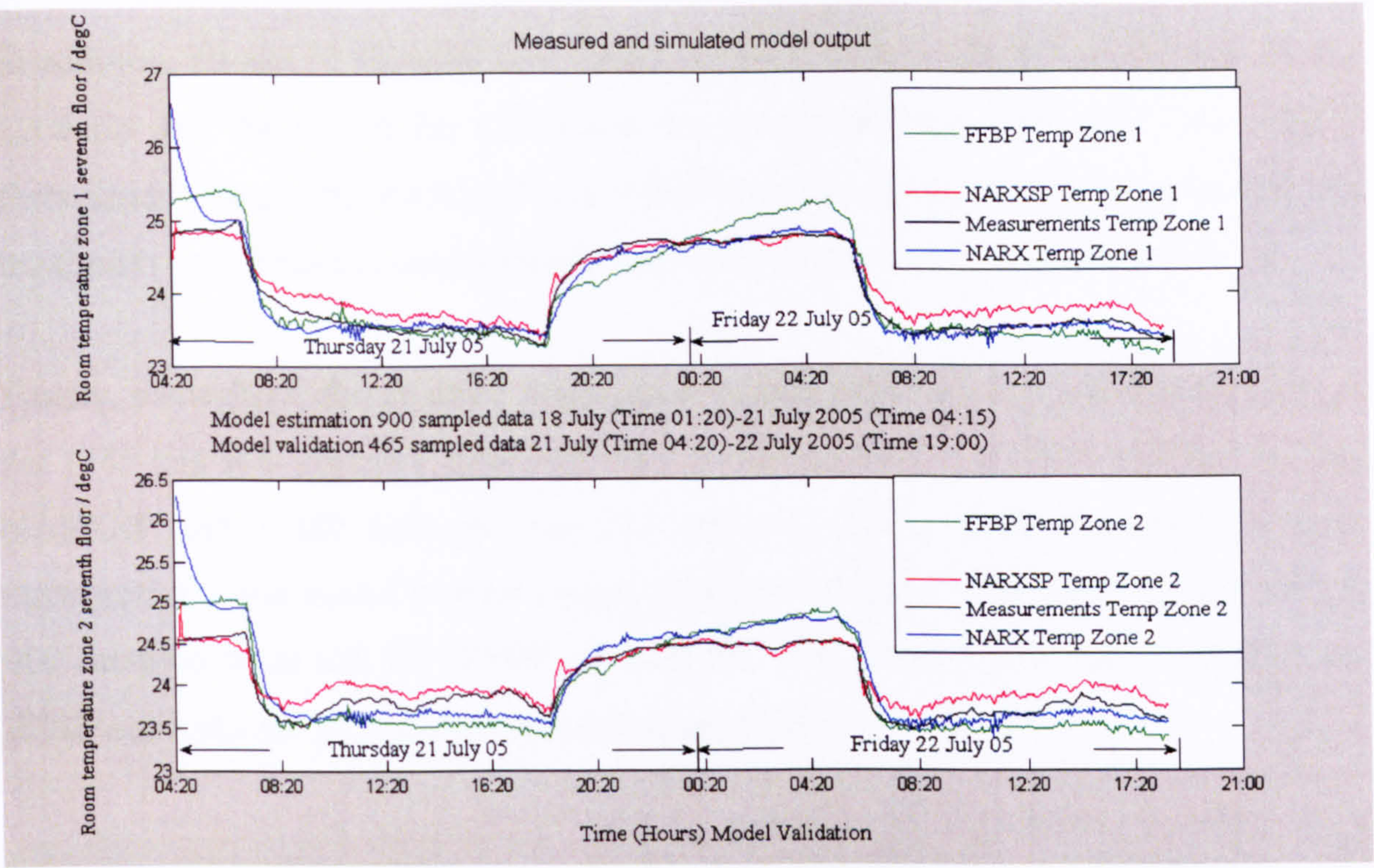

Figure 7.41 Model validation, weekdays 21-22 July 2005

Model development and validation for autumn weekdays

Throughout the middle of autumn, the inputs affecting the results were: chilled water temperature, hot water temperature, outside temperature, supply air temperature AHU1, supply air flow rate AHU1, supply air temperature AHU2 and supply air flow rate AHU2. In this section, only the results for the week 10-14 October 2005 used for model estimation and the following week 17-21 October 2005 for model validation are shown (see Figs. 7.42 and 7.43).

Furthermore, the same networks were applied to the same week, 10-14 October 2005, where 900 and 465 sampled data were utilised for model estimation and validation respectively (see Fig. 7.44, model validation). The NARXSP network gave better fits than the FFBP and NARX networks throughout the middle of the autumn season (1365 and 900 sampled data model development).

In addition, 10 and 11 October 2005 were analysed with NARXSP, FFBP and NARX networks and the model fits and errors are shown in Figs. 7.45 and 7.46. Finally, throughout autumn the NARXSP and FFBP networks (mse 10^{-3}) give good fits. The maximum error between measurements and model outputs is 0.6 degrees Celsius.

Finally, throughout the autumn season mse ranged between 10^{-4} (NARXSP network for 1365 and 900 sampled data) and 10^{-3} (FFBP network for 900 sampled data, and NARXSP and FFBP networks for 213 sampled data), while the errors between measurements and model outputs ranged between 0.3 (NARXSP network for 1365 and 900 sampled data) and 0.6 (FFBP network for 900 samped data, and NARXSP and FFBP networks for 213 sampled data) degrees Celsius.

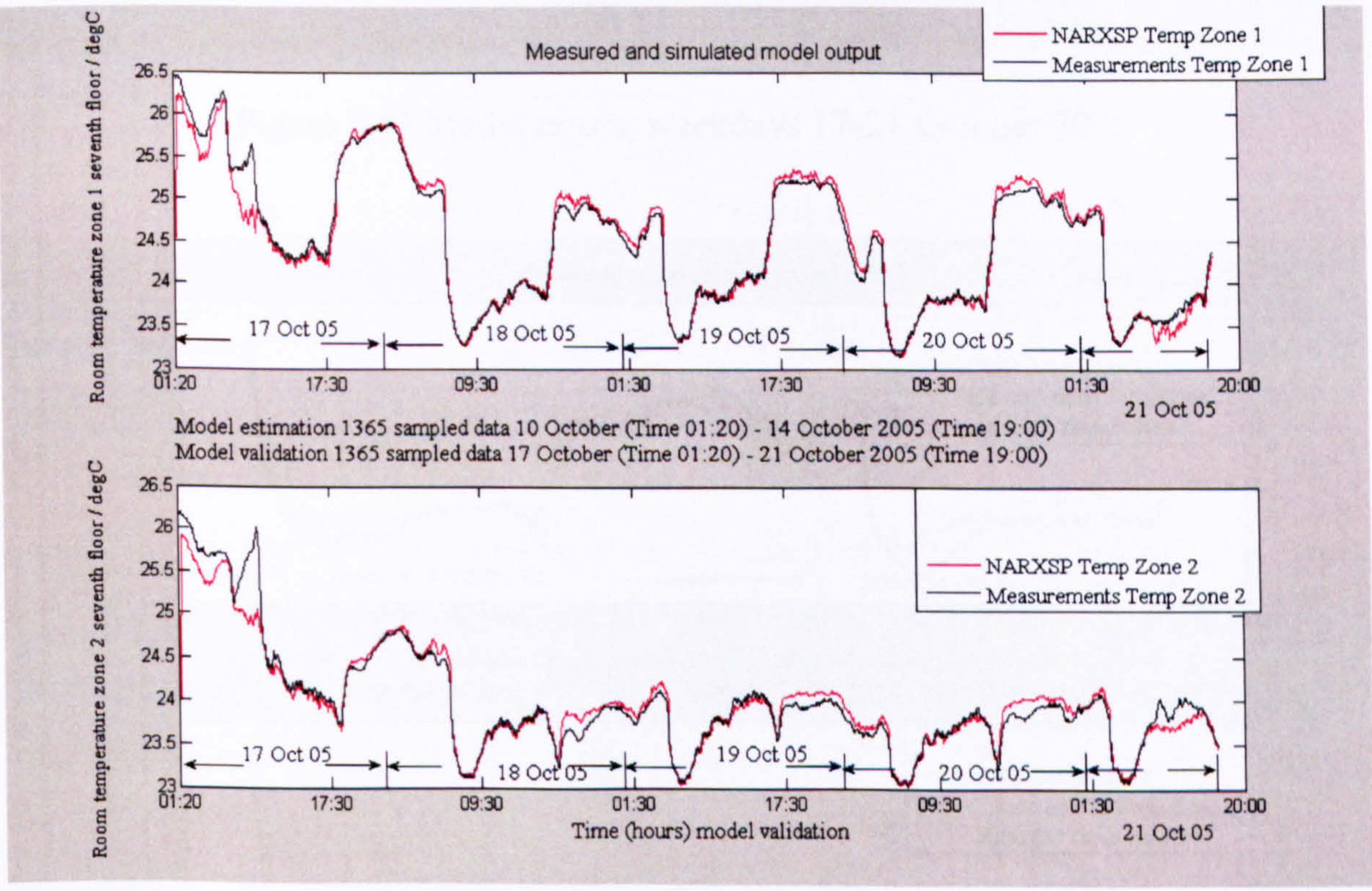

Figure 7.42 Model validation, weekdays 17-21 October 2005

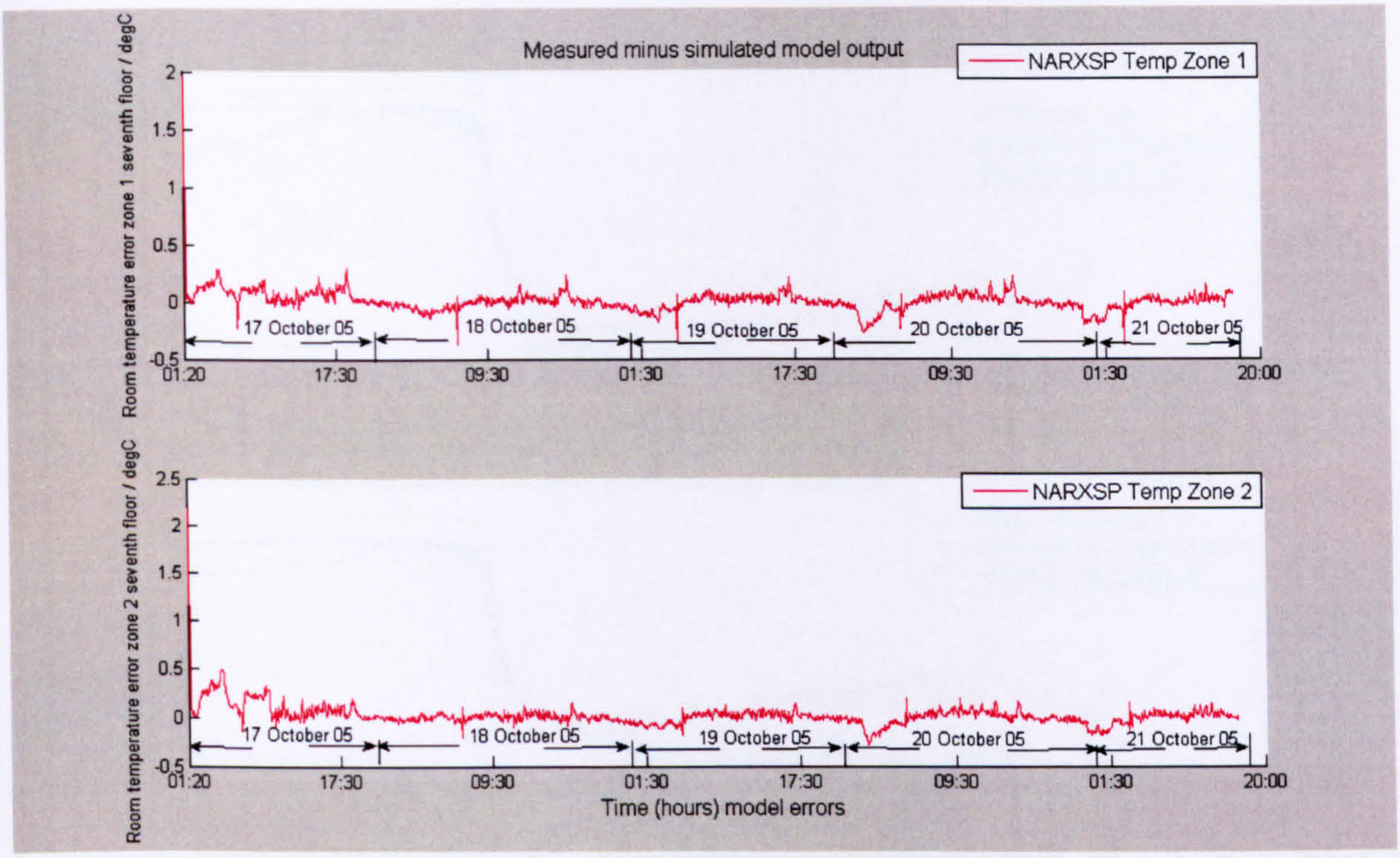

Figure 7.43 Model errors, weekdays 17-21 October 2005

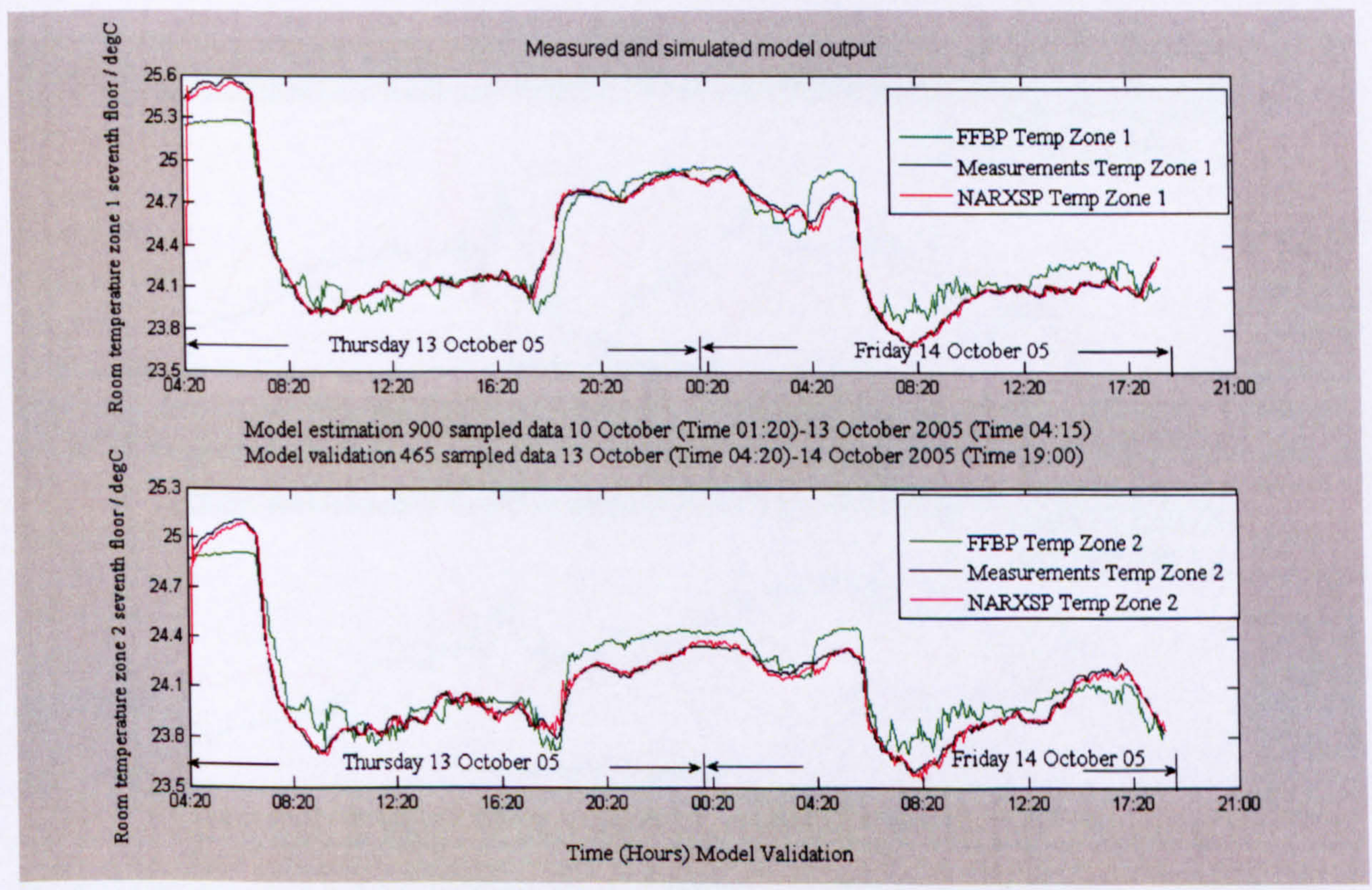

Figure 7.44 Model validation, weekdays 13-14 October 2005

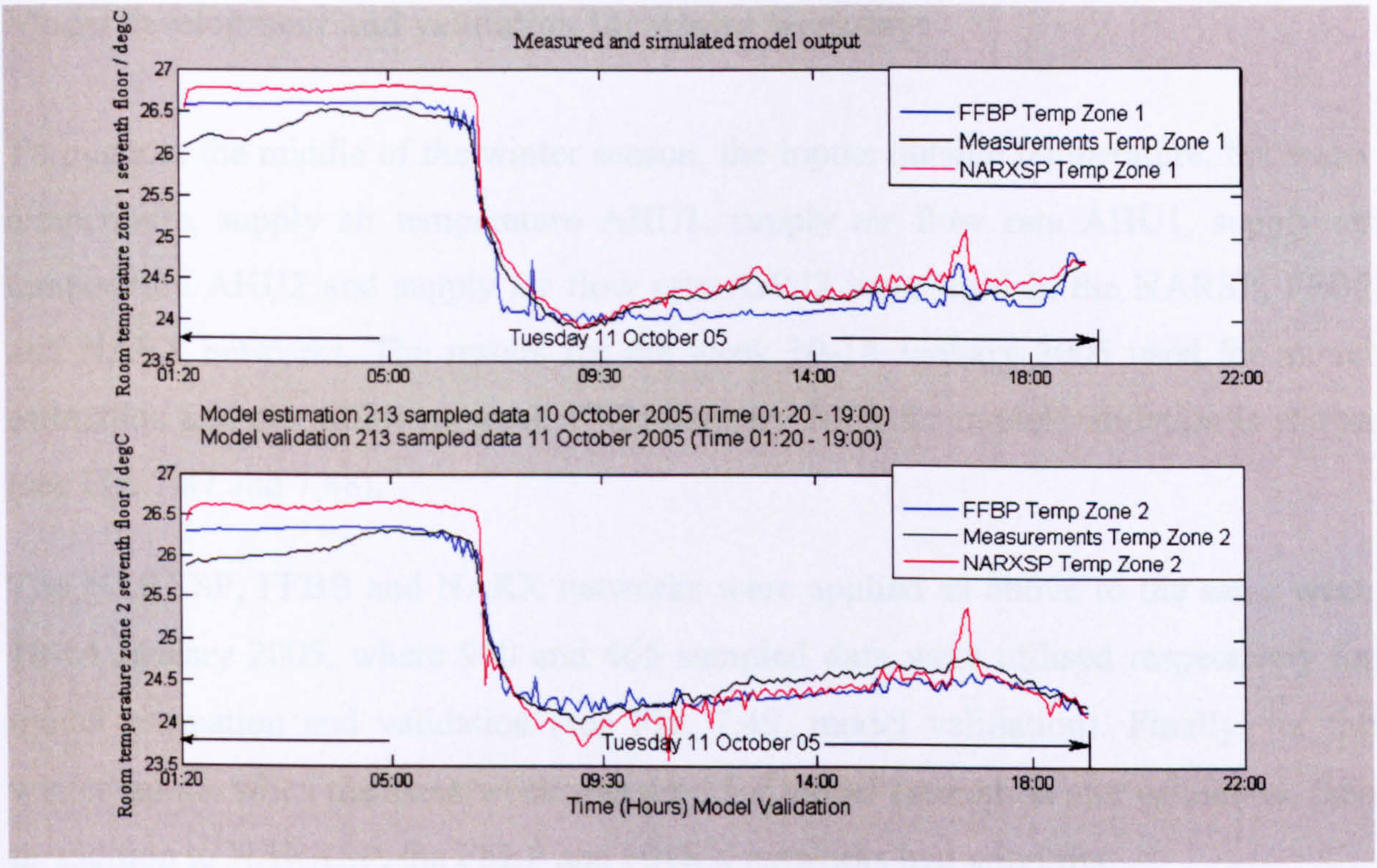

Figure 7.45 Model validation, 11 October 2005

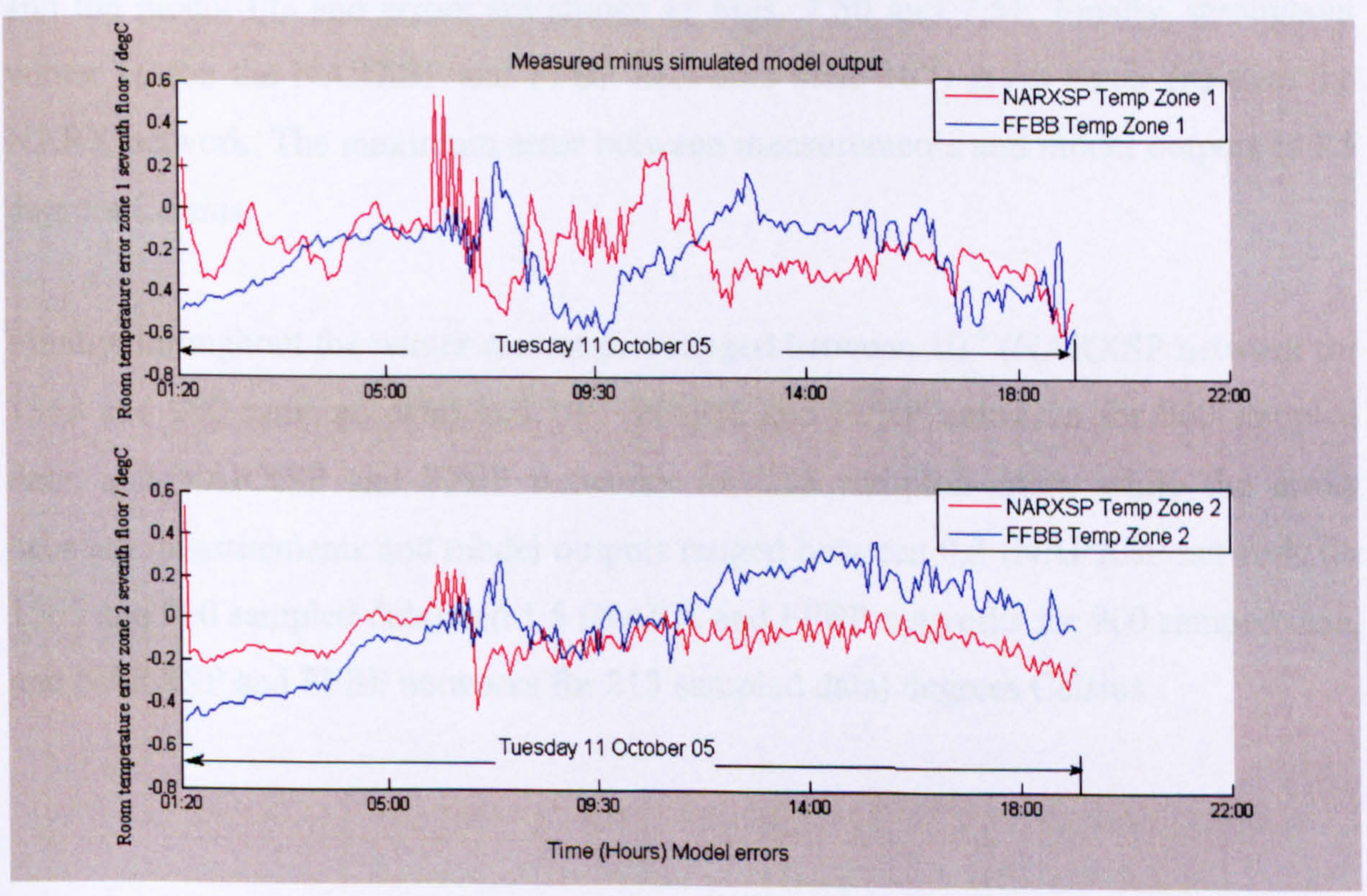

Figure 7.46 Model errors, 11 October 2005

Model development and validation for winter weekdays

Throughout the middle of the winter season, the inputs outside temperature, hot water temperature, supply air temperature AHU1, supply air flow rate AHU1, supply air temperature AHU2 and supply air flow rate AHU2 were used in the NARSP, FFBP and NARX networks. The results for the week 10-14 January 2005 used for model estimation and the following week 17-21 January 2005 for model validation is shown (see Fig. 7.47 and 7.48).

The NARXSP, FFBB and NARX networks were applied as above to the same week 10-14 January 2005, where 900 and 465 sampled data were utilised respectively for model estimation and validation (see Fig. 7.49, model validation). Finally, for the winter season when the same week was used for model estimation and validation, then in addition to NARXSP, the FFBP and NARX networks had good fits.

In addition, 10 and 11 January 2005 were analysed with NARXSP and FFBP networks and the model fits and errors are shown in Figs. 7.50 and 7.51. Finally, throughout winter season the NARXSP and FFBP networks (mse 10^{-3}) gives better fits than the NARX network. The maximum error between measurements and model outputs is 1.5 degrees Celsius.

Finally, throughout the winter season mse ranged between 10^{-4} (NARXSP network for 1365 and 900 sampled data) and 10^{-3} (NARX and FFBP networks for 900 sampled data, and NARXSP and FFBP networks for 213 sampled data), while the errors between measurements and model outputs ranged between 0.3 (NARXSP network for 1365 and 900 sampled data) and 1.5 (NARX and FFBP networks for 900 samped data, and NARXSP and FFBP networks for 213 sampled data) degrees Celsius.

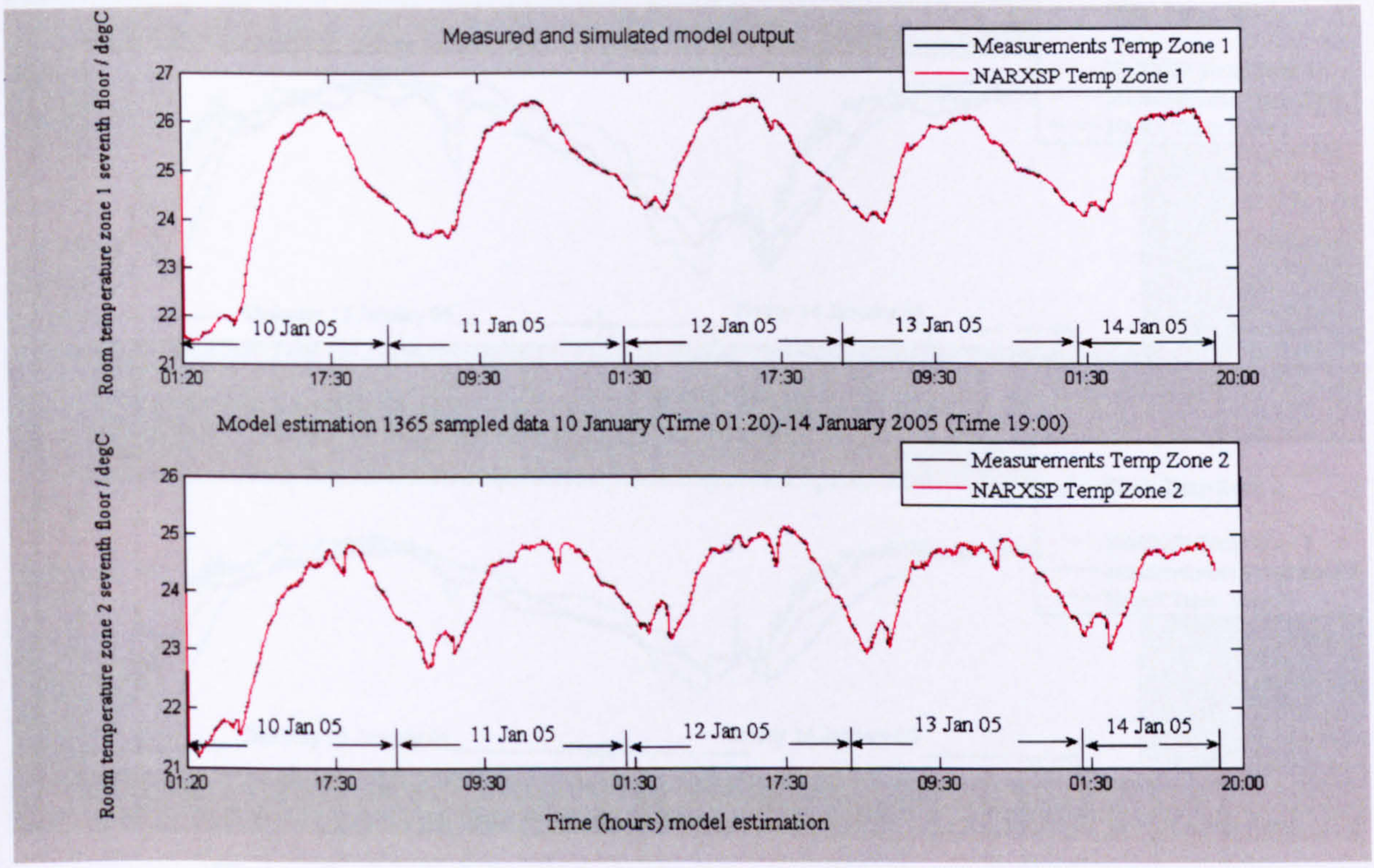

Figure 7.47 Model estimation, weekdays 10-14 January 2005

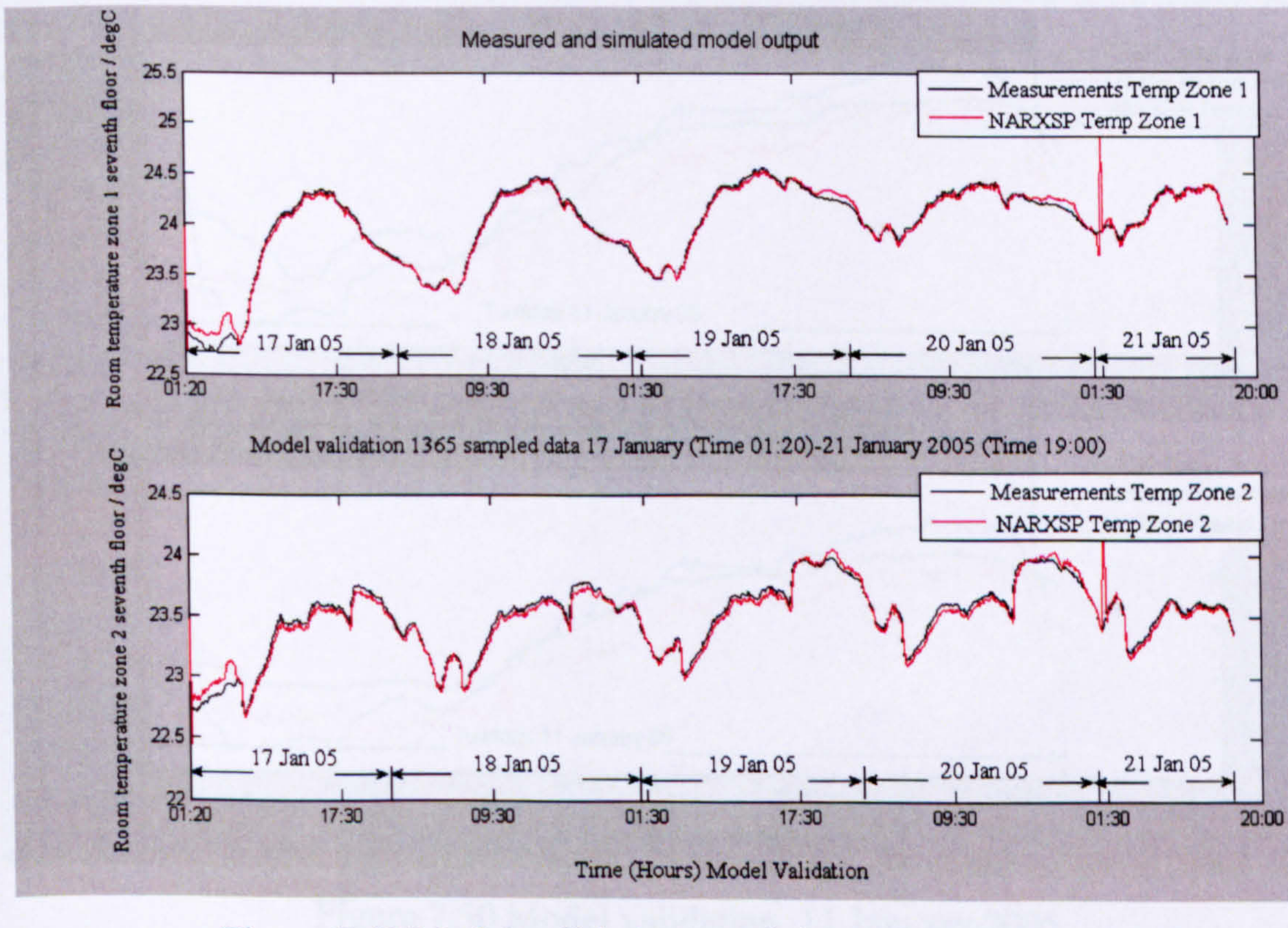

Figure 7.48 Model validation, weekdays 17-21 January 2005

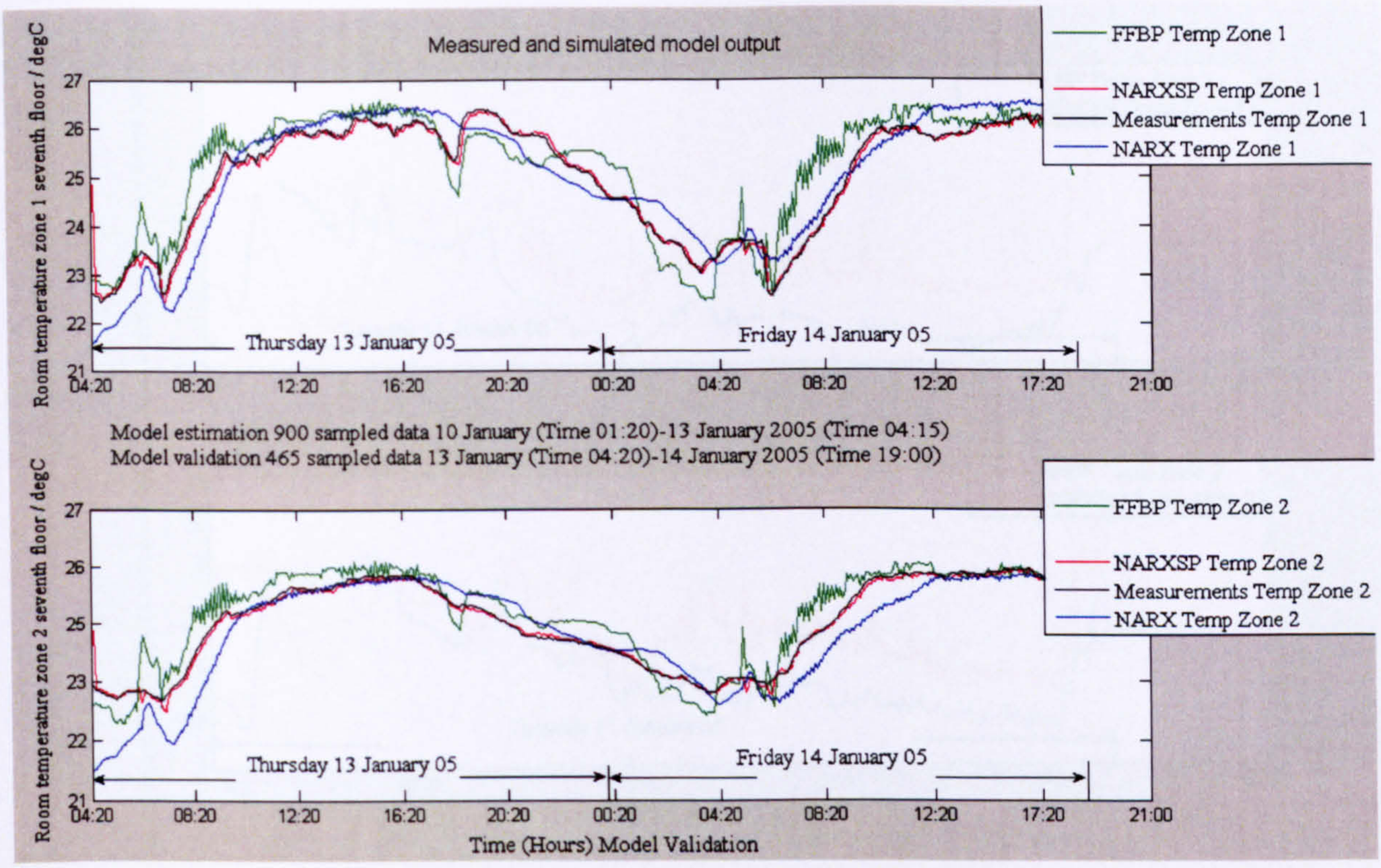

Figure 7.49 Model validation, weekdays 13-14 January 2005

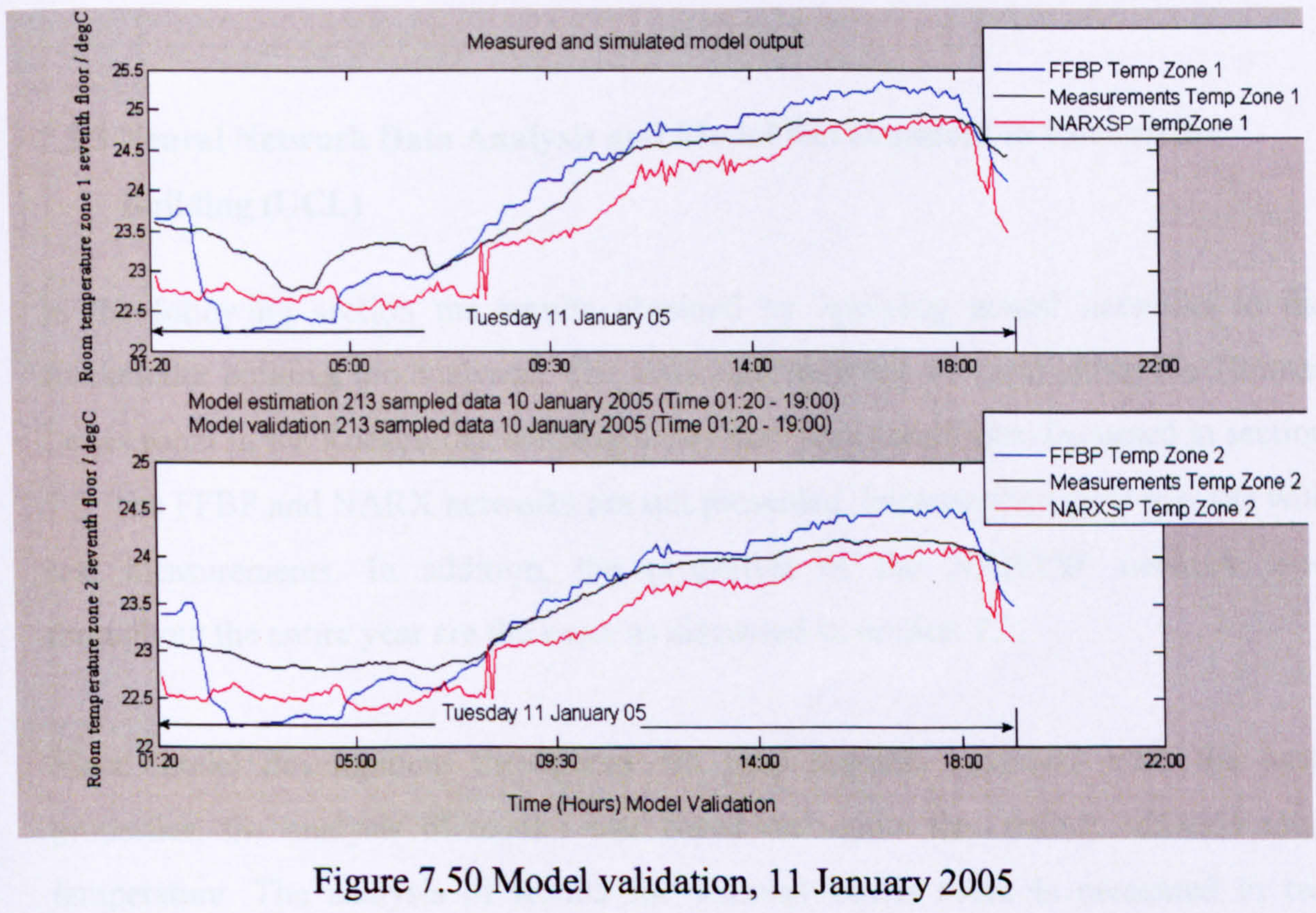

Figure 7.50 Model validation, 11 January 2005

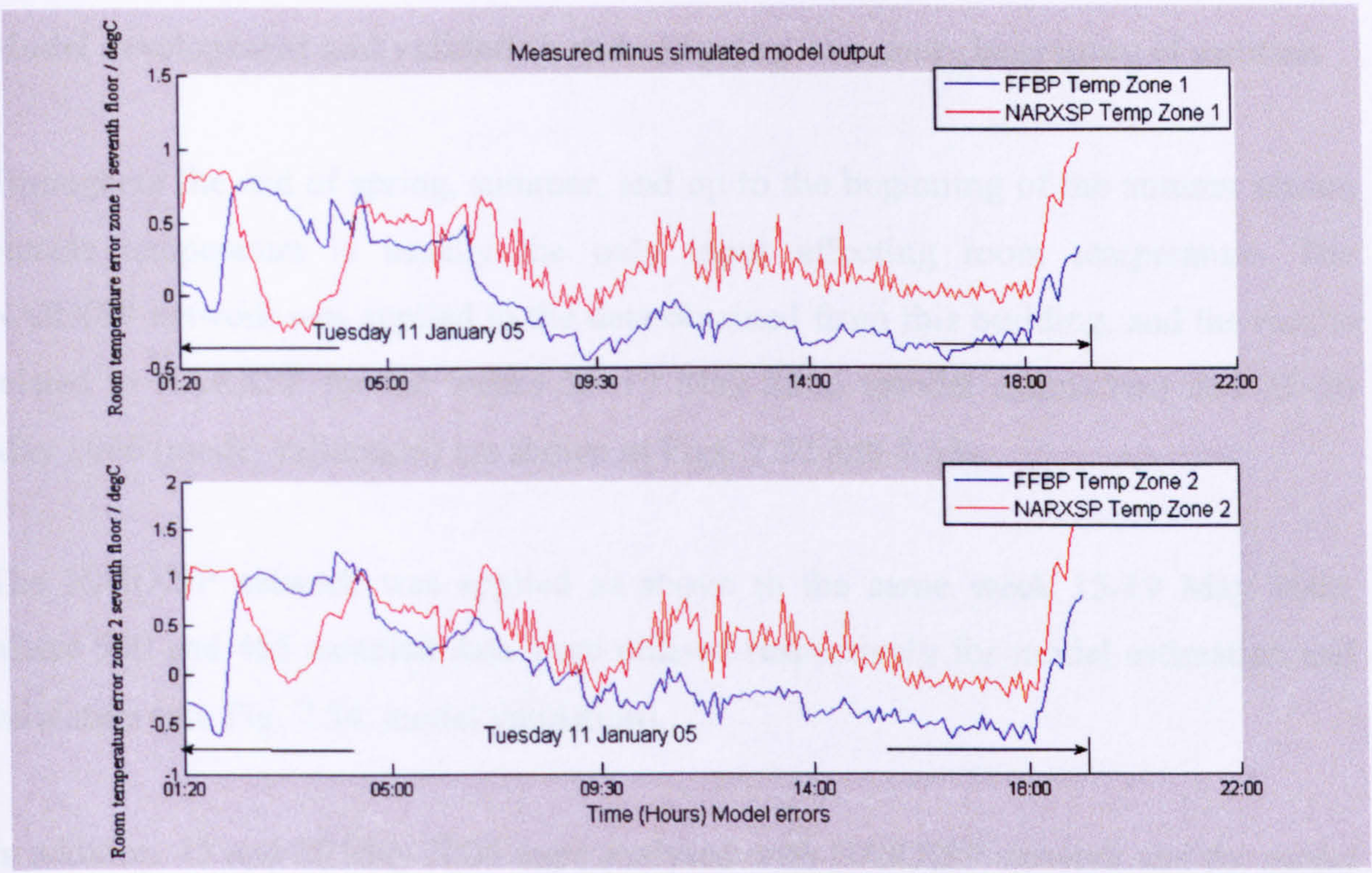

Figure 7.51 Model errors, 11 January 2005

7.3.3 Neural Network Data Analysis and Model Development in Rockefeller Building (UCL)

In the following section the results obtained by applying neural networks to the Rockefeller building are analysed. The NARXSP network was applied to the Thomas Lewis room in the Rockefeller building under the same conditions discussed in section 7.2. The FFBP and NARX networks are not presented, because they gave low fits with real measurements. In addition, the properties of the NARXSP network used throughout the entire year are the same as discussed in section 7.2.

Since model development throughout the year requires networks with the same properties, the analysis of results was based on inputs that mainly affected room temperature. The analysis of results for Thomas Lewis room is presented in two sections, the first one discussing present development models, for the end of spring and summer and the middle of autumn (where outside temperature is the input) and the second, giving the results for autumn, winter and the middle of spring (where the inputs are outside temperature and hot water temperature).

Model development and validation end of spring–summer- beginning of autumn

Throughout the end of spring, summer, and up to the beginning of the autumn season outside temperature is usually the only input affecting room temperature. The NARXSP network was applied to the data obtained from this building, and the results related to NARXSP for the weeks 15–19 May 2006 (model estimation) and 22–26 May 2006 (model validation) are shown in Figs. 7.52 and 7.53.

The NARXSP network was applied as above to the same week 15-19 May 2006, where 900 and 465 sampled data were utilised respectively for model estimation and validation (see Fig. 7.54, model validation).

In addition, 15 and 16 May 2006 were analysed with NARXSP network and the model fits and errors are shown in Figs. 7.55 and 7.56. Throughout the winter season NARXSP network (mse 10^{-3}) gives good fits. The maximum error between measurements and model outputs is 0.5 degrees Celsius.

Finally, throughout the end of spring-summer-beginning of autumn seasons mse ranged between 10^{-4} (NARXSP network for 1365 and 900 sampled data) and 10^{-3} (NARXSP network for 213 sampled data), while the errors between measurements and model outputs ranged between 0.5 (NARXSP network for 1365 and 900 sampled data) and 0.3 (NARXSP network for 213 sampled data) degrees Celsius.

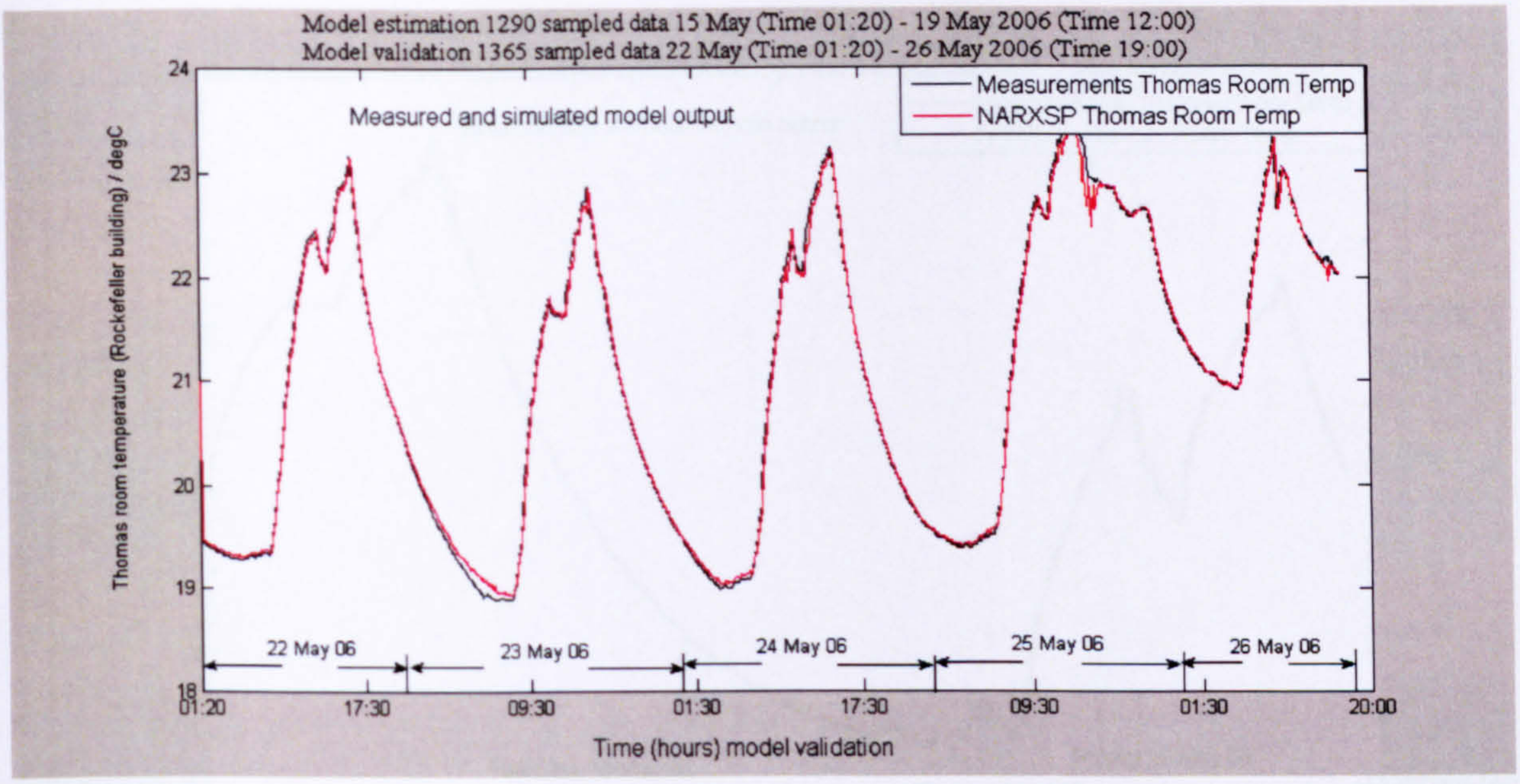

Figure 7.52 Model validation, weekdays 22-26 May 2006

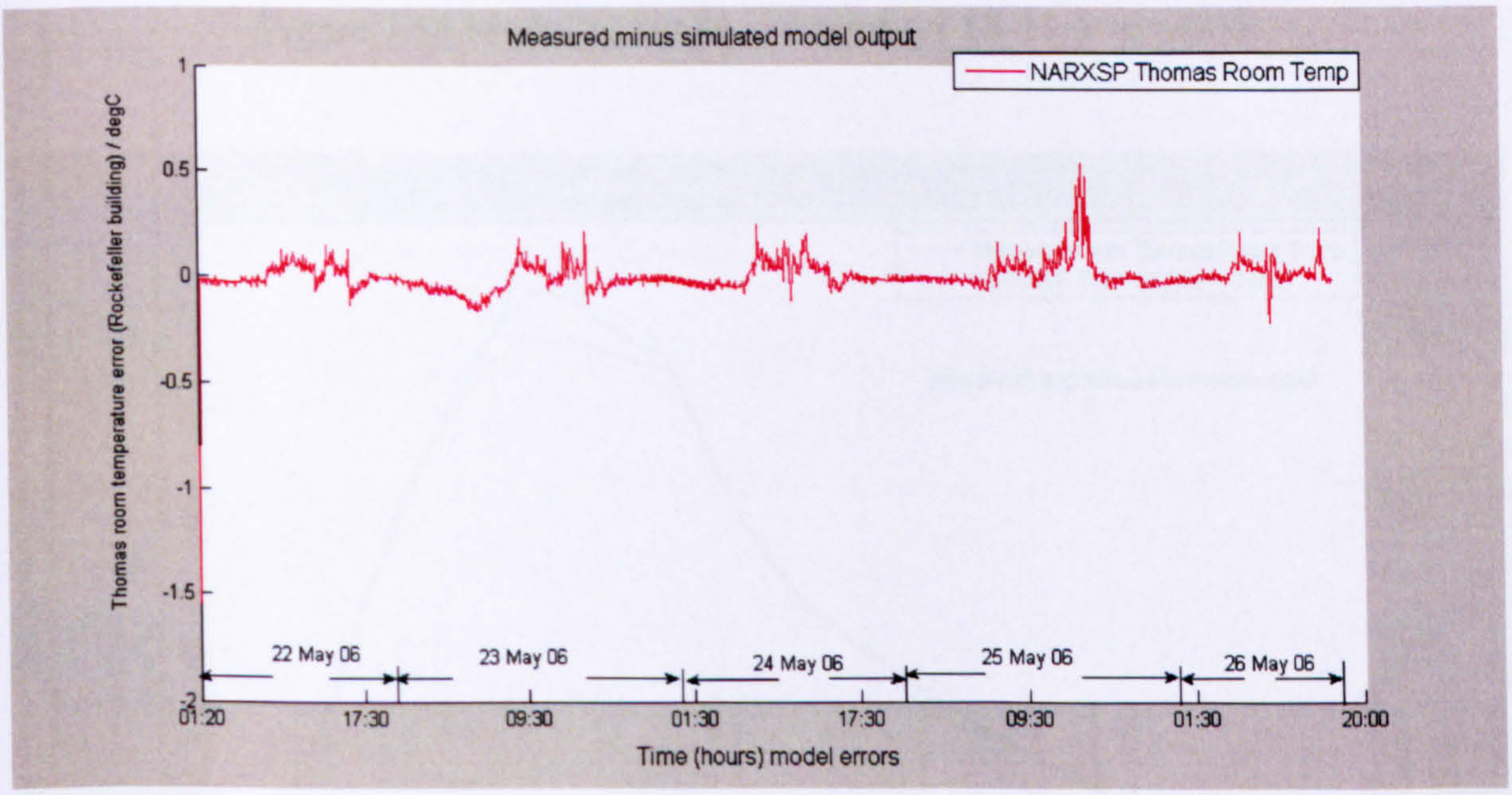

Figure 7.53 Model errors, weekdays 22-26 May 2006

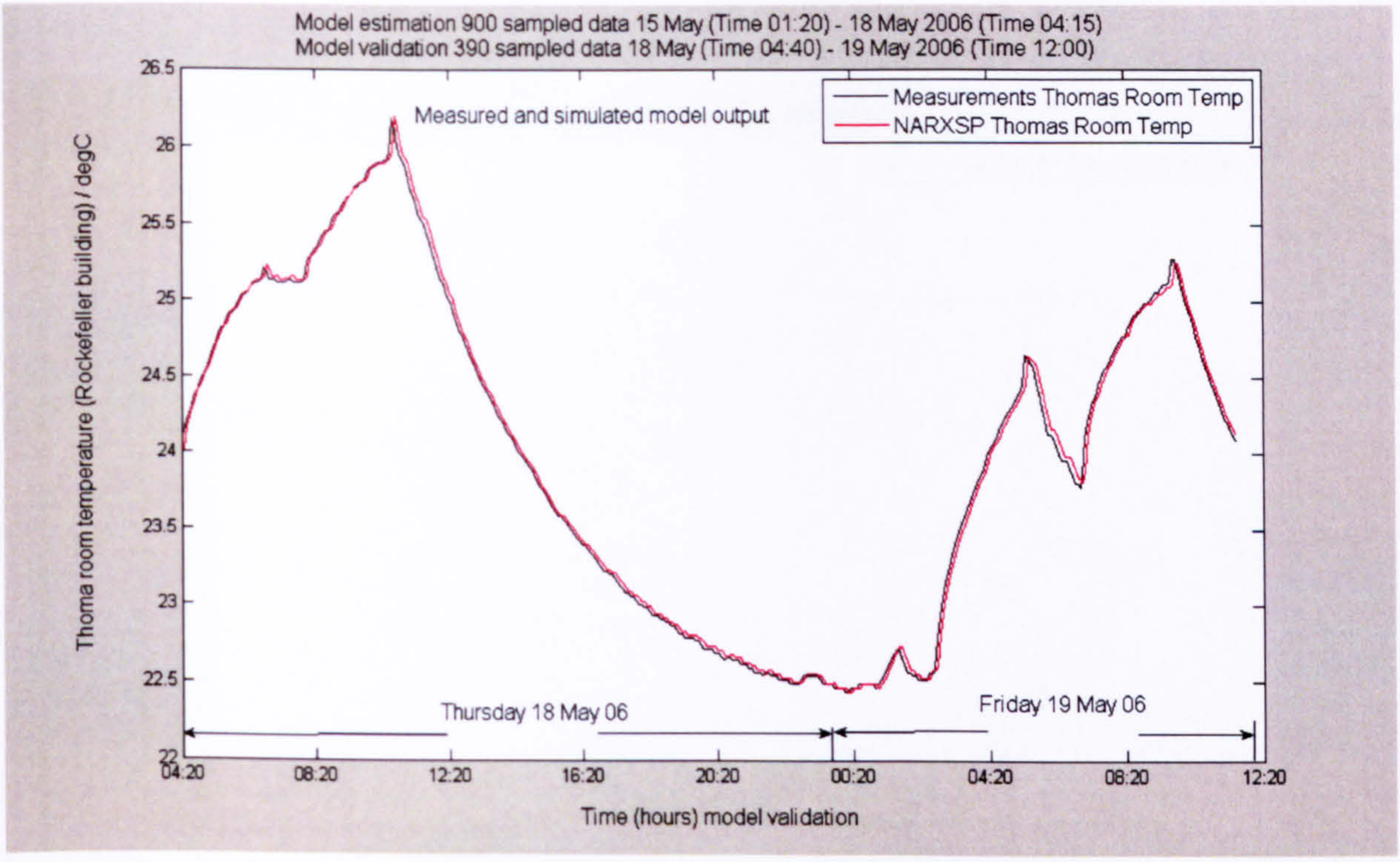

Figure 7.54 Model validation, weekdays 18-19 May 2006

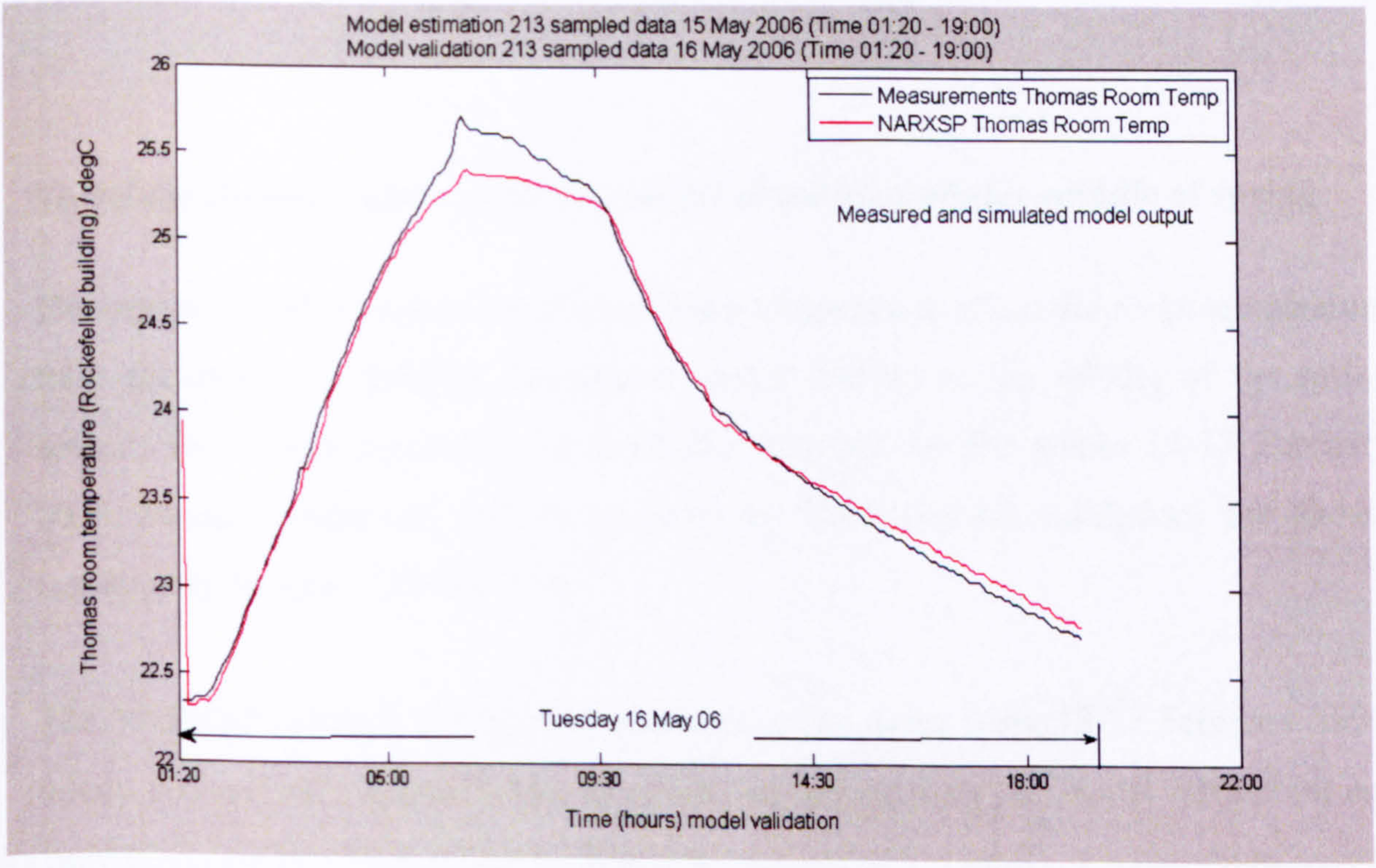

Figure 7.55 Model validation, 16 May 2006

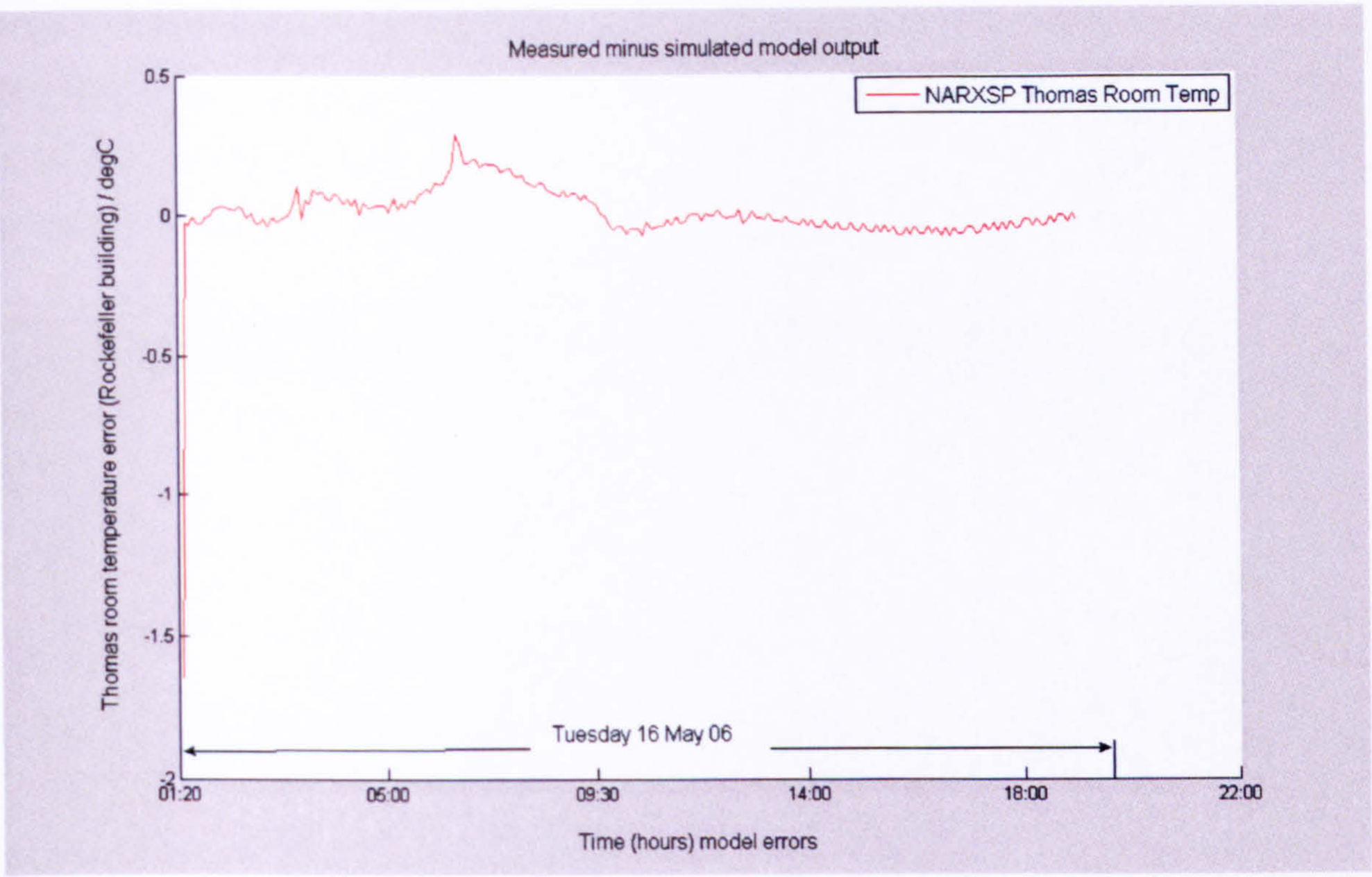

Figure 7.56 Model errors, 16 May 2006

Model development and validation middle of autumn-winter-middle of spring

The inputs, outside temperature and hot water temperature affect the room temperature from the middle of autumn, throughout winter and up to the middle of the spring season. The results related to the NARXSP network for the weeks 13-17 February 2006 (model estimation) and 20-24 February 2006 (model validation) are shown respectively in Figs. 7.57 and 7.58.

The NARXSP network was applied as above to the same week 13-17 February 2006, where 900 and 465 sampled data were utilised respectively for model estimation and validation (see Fig. 7.59, model validation).

In addition, 13 and 17 February 2006 were analysed with NARXSP network and the model fits and errors are shown in Figs. 7.60 and 7.61. Throughout the winter season the NARXSP network (mse 10^{-3}) gives good fit. The maximum error between measurements and model outputs is 0.9 degrees Celsius.

Finally, throughout the middle of autumn – winter – middle of the spring seasons mse ranged between 10^{-4} (NARXSP network for 1365 and 900 sampled data) and 10^{-3} (NARXSP network for 213 sampled data), while the errors between measurements and model outputs ranged between 0.1 (NARXSP network for 1365 and 900 sampled data) and 0.9 (NARXSP network for 213 sampled data) degrees Celsius.

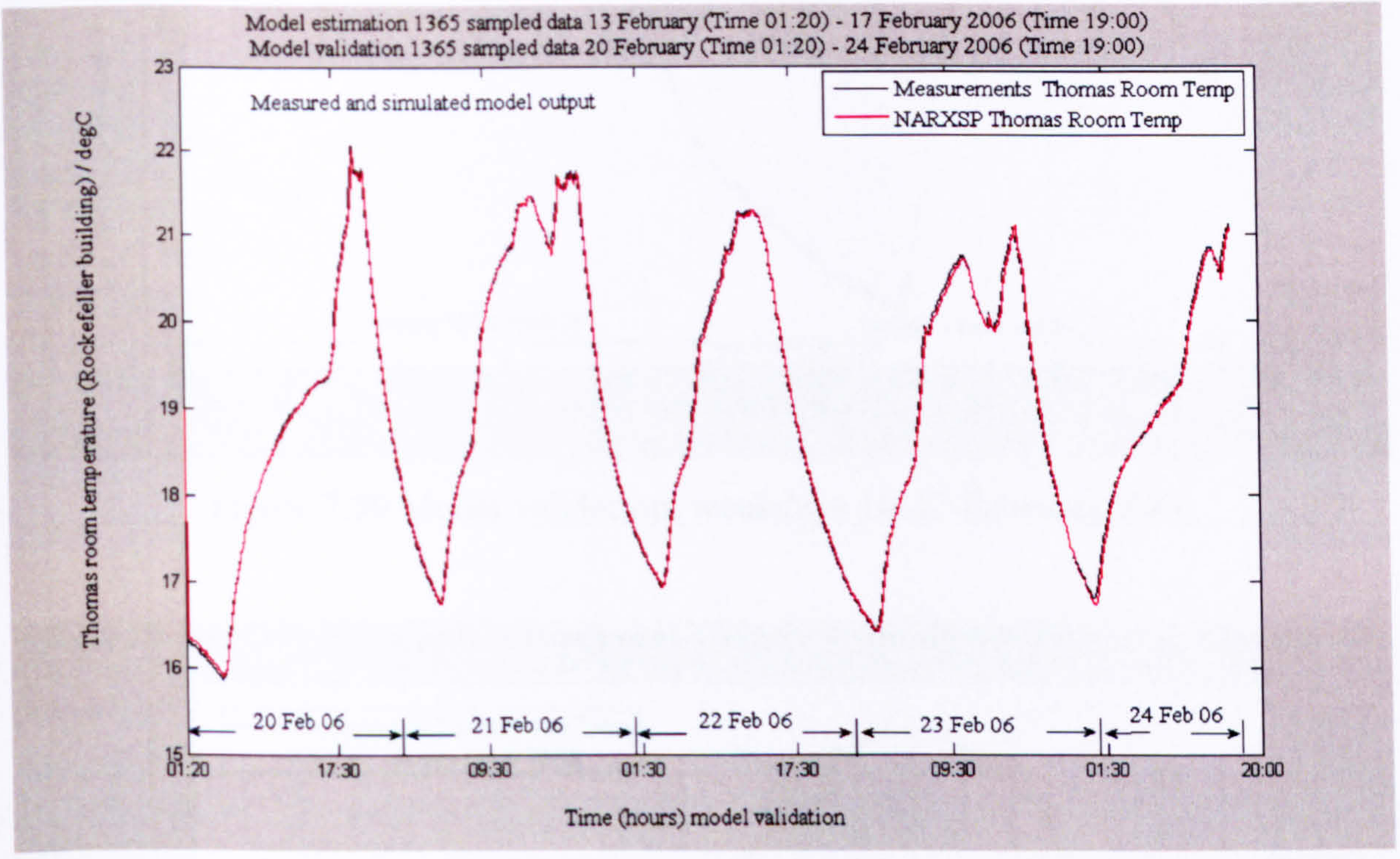

Figure 7.57 Model validation, weekdays 20-24 February 2006

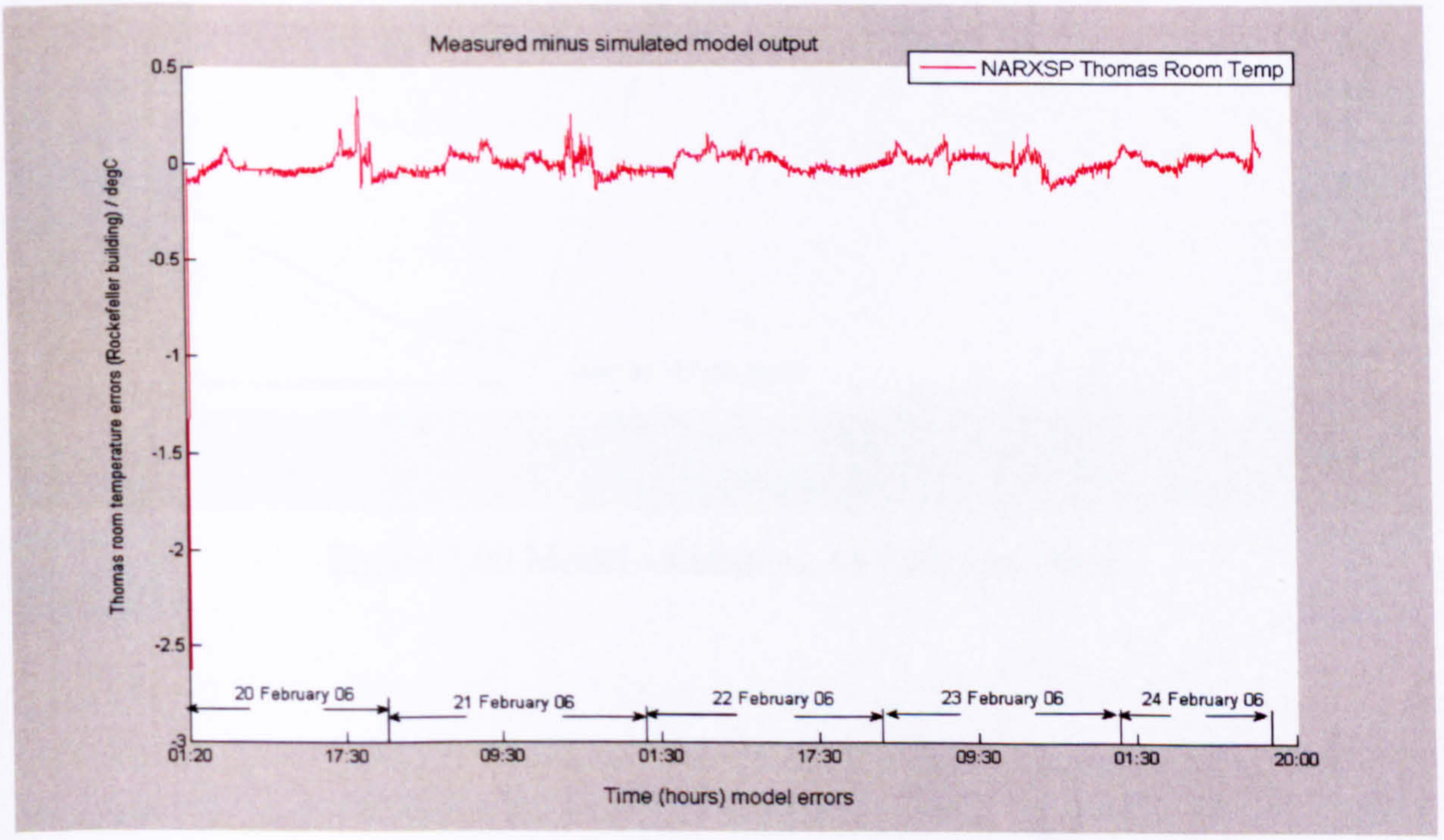

Figure 7.58 Model errors, weekdays 20-24 February 2006

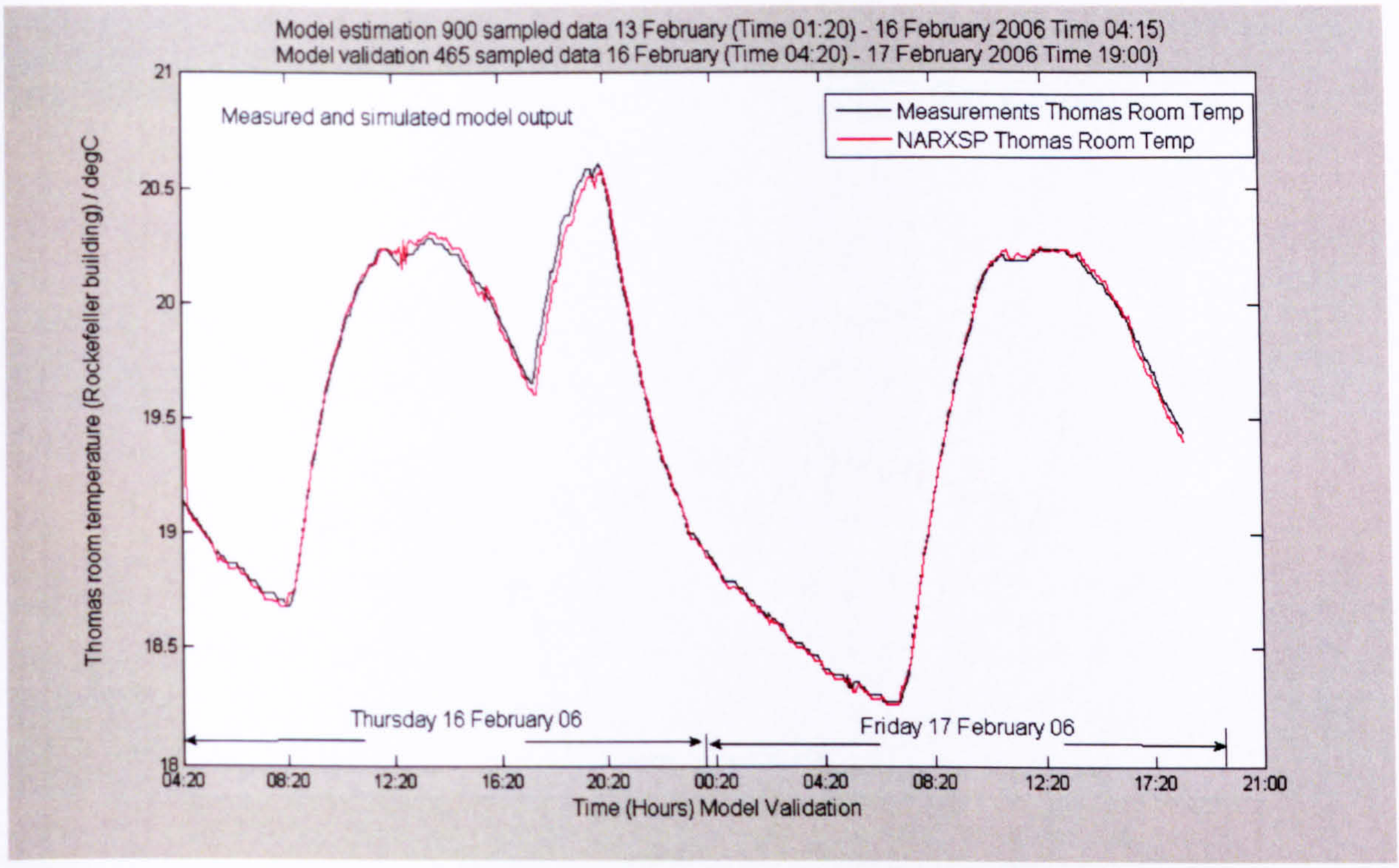

Figure 7.59 Model validation, weekdays 16-17 February 2006

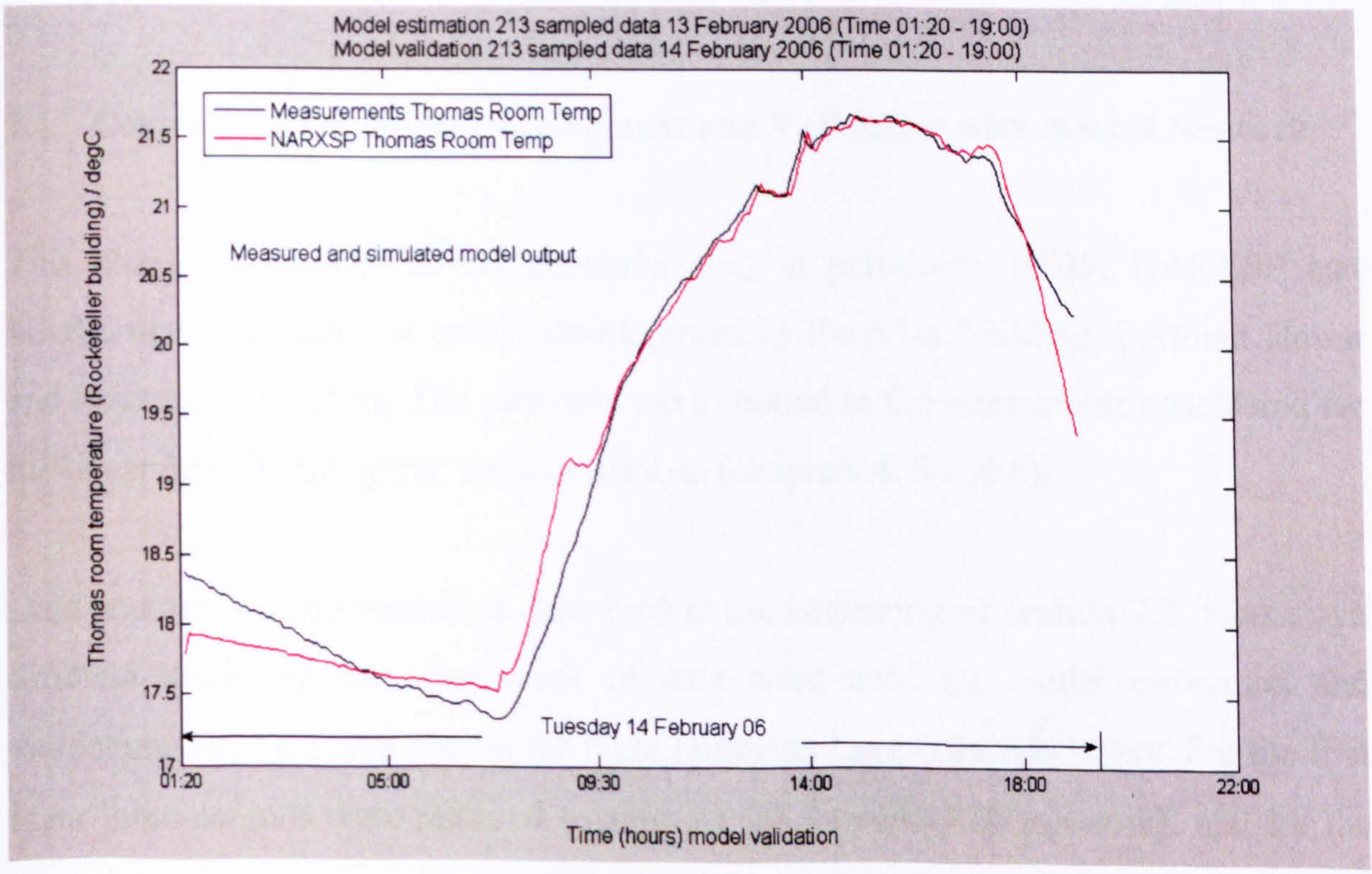

Figure 7.60 Model validation, 14 February 2006

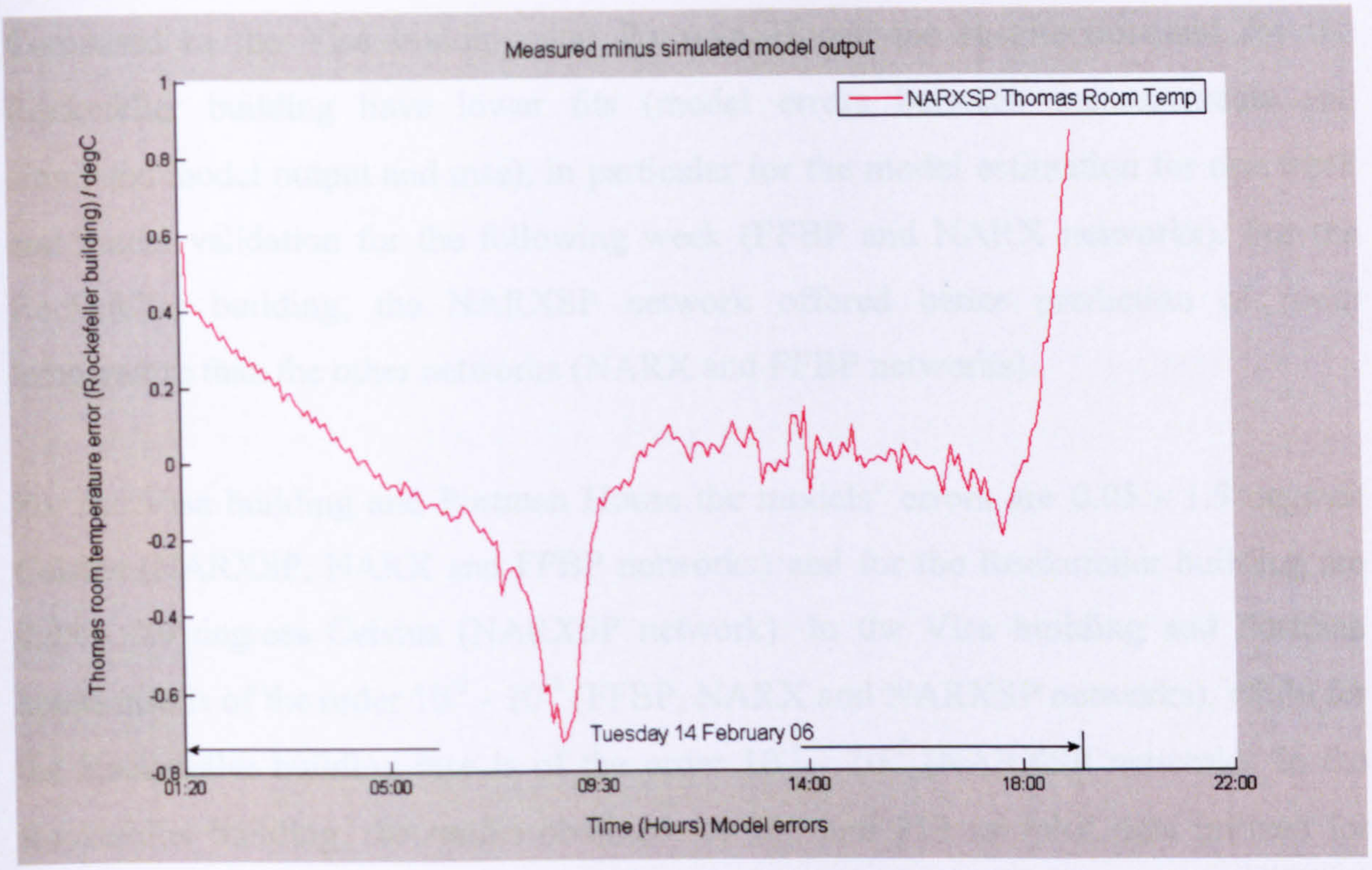

Figure 7.61 Model errors, 14 February 2006

7.4 Conclusions for Model Development and Validation with Neural Networks

This chapter dealt with neural networks and, in particular, FFBP, NARXSP and NARX networks used for model development in the Visa building, Portman House and Rockefeller building. The networks were applied to the same inputs considered for the linear models throughout the four seasons (chapters 4, 5 and 6).

Data analysis was performed as described at the beginning of section 7.3, where two different weeks or the same week of data were used for model estimation and validation. The networks chosen for these buildings have only two layers. For the first layer three neurons were required (maximum 20 for NARXSP network), and for the second layer, which was the output layer (room temperature zone 1 and 2), two neurons were required. If the number of neurons in the first layer increased above three (or maximum 20 for NARXSP network), the model validation on the other piece of data did not improve and for values above twenty neurons the solution got worse (over parameterization).

Compared to the Visa building and Portman House the results obtained for the Rockefeller building have lower fits (model errors between measurements and simulated model output and mse), in particular for the model estimation for one week and model validation for the following week (FFBP and NARX networks). For the Rockefeller building, the NARXSP network offered better prediction of room temperature than the other networks (NARX and FFBP networks).

For the Visa building and Portman House the models' errors are 0.05 - 1.5 degrees Celsius (NARXSP, NARX and FFBP networks) and for the Rockefeller building are 0.05 - 0.9 degrees Celsius (NARXSP network). In the Visa building and Portman house mse is of the order 10^{-2} - 10^{-4} (FFBP, NARX and NARXSP networks), while for the Rockefeller building mse is of the order 10^{-3} - 10^{-4} (NARXSP network). In the Rockefeller building, the results obtained for 900 and 213 sampled data utilized for model development with the NARXSP model are better compare than those obtained with the same network and sampled data for the other two buildings. Finally, overall comparing the year of data obtained from the three buildings the results obtained with the NARXSP network are better than those obtained with the other networks (NARX and FFBP). As the number of sampled data for model development increased from 213 to 1365 the NARXSP and NARX networks gave good results, because, the increased number of sampled data enabled the inclusion of past inputs and outputs.

The advantages of applying neural networks instead of linear models were:

- The same networks with the same properties as presented in section 7.3 could be used throughout the entire year and for the three buildings, with good results obtained for predicting room temperature.
- There was no limit on the number of outputs that could be used for model development with the FFBP, NARXSP and NARX networks
- With neural networks, the amount of time required for model development and validation throughout the year was less than that for linear models.
- The results obtained with non-linear models are better than those obtained with linear models because (see Table 7.1):
    - For non-linear models the values obtained for mse (10^{-2} - 10^{-4}) are less than those obtained with FPE (10^{-1} - 10^{-3}) with linear models ($mse \approx 2 * FPE$) and

- models' errors between measurements and simulated model output for non-linear models (0.05 - 1.5 degrees Celsius) are less than those obtained from linear models (0.1 - 2.5 degrees Celsius).

From the analysis of the results with non-linear mathematical models, as the number of sampling data for model development increased from one day (213 sampled data) to one week (900 to 1365 sampled data). The performance of these models in predicting room temperature improved significantly. The above conclusion can be verified by comparing the models errors between measurements and simulated model output for these networks, where for 900 and 1365 sampled data, they are very small (within 0.05 - 0.8 degrees Celsius), while for 213 sampled data, they increased to 1.5 degrees Celsius. This is because the non-linear mathematical models require vast amount of data to be included for model development to give good prediction of room temperature (Annex 34, 2001). Contrary to non-linear models, the linear models improved their prediction of room temperature as the number of sampled data decreased from 1365 to 213 model development. This is because in physics the equations for energy conservation of the heat transfer are non-linear (Rosenberg and Karnopp, 1983).

Sampled data model development (estimation)	Linear parametric mathematical models	ANNs (Non-linear models)
Model errors (degC) 1365 FPE / mse	0.6 – 2.5 FPE ≈ 10^{-1} - 10^{-2}	0.05 - 0.8 mse ≈ 10^{-3} - 10^{-4}
Model errors (degC) 900 FPE / mse	0.3 – 1.0 FPE ≈ 10^{-2} - 10^{-3}	0.1 – 0.8 mse ≈ 10^{-2} - 10^{-3}
Model errors (degC) 213 FPE / mse	0.1 – 0.8 FPE ≈ 10^{-2} - 10^{-3}	0.1 – 1.5 mse ≈ 10^{-2} - 10^{-3}

Table 7.1 Model errors (Measured minus simulated model output) – FPE / mse

CHAPTER 8 Conclusions and Future Work

8.1 Conclusions

This study has investigated the thermal behaviour of three different buildings built in different periods, one academic institute built in 1920 and two modern commercial buildings in London. Black–box linear (parametric mathematical models) and non-linear mathematical models (neural networks) were used to obtain the models from the data collected. This is because of the lack of available specific information related to the structure of the buildings such as windows, doors and building dimensions and the complexity of such details for a real case. In the Visa building and Portman House the input selection for one year was a long process because the same inputs gave a good prediction of the room's temperature only for a number of weeks at a time. In contrast, in the Rockefeller building, outside temperature and hot water temperature were the only inputs and room temperature was the only output provided by the BMS throughout the year.

In this project, the models were developed for different seasons and each season was subdivided into three parts: beginning, middle and end. The reasons for these subdivisions are listed below:

- Some inputs gave good models for a limited period of time (several weeks). Consequently, as reported below, the process of input selection and the period of validity in obtaining models that gave good thermal prediction (within the same period) were the first reasons for the subdivision. This criterion was applied throughout the analysis with linear and non-linear mathematical models.
- Another reason was that these models are linear and this was a disadvantage that affected the period of validity of some models. Sometimes it was even lower than that of the validity of the inputs selected for that period.

The primary assumption of the model development in the Visa building and Portman House was that the internal temperature variation is directly in part influenced by variations in external temperature and the internal air coming from the air handling units.

Although occupancy, computers, printers etc cause an additional internal heat gain, their impact is strongly correlated with the internal energy exchanged between the incoming air from AHUs, that flows inside the room from the fan coil units, and the circulating water (flows inside fan coil units and AHU) that is heated up and cooled down by the boiler and chiller plants respectively. As such, the effects of occupancy, computers, printers etc were indirectly in part included in the model. Contrary to the Visa building and Portman House, in the Rockefeller building the effects of additional internal heat gain caused by occupancy, computers and printers were not included in part in the model because their effect was small compared to the external temperature and hot water temperature throughout the cold season.

The model development and then validation using linear models followed the procedures discussed in chapter 3. Firstly, the same week or different days were utilized for model development and validation, where the first part (213, 900 or 800 sampled data) for model estimation and the second part (213, 465 or 565 sampled data) were utilized for model validation. Secondly, two weeks were utilized, where the first week (1365 sampled data) was used for model estimation and the following week (1365 sampled data) was used for model validation. The analyses were pursued for sampled-data model validation for one of the following weekdays in which inputs and model validity remained unchanged.

From the analysis of the results obtained with linear models (chapters 4, 5 and 6), the BJ models (bj [1 1 1 1 2], bj [1 1 1 1 3], bj [1 1 1 1 4] and bj [1 1 1 1 5]), OE models (oe [1 1 2], oe [1 1 3], oe [1 1 4] and oe [1 1 5]) and ARMAX models (amx [2 2 2 1], amx [2 2 2 2], amx [2 2 2 3], amx[2 2 2 4] and amx [2 2 2 5]) gave good results for a certain period, ranging from four to twelve weeks. The period of validity changed from one season to another, and sometimes within the same season and from one building to another, depending on the BMS. Furthermore, in the Visa building and Portman House throughout the year FPE varied between 10^{-1} and 10^{-3}, while model errors varied between 0.3 and 1.5 degrees Celsius. Finally, for the Rockefeller building the FPE is of the order 10^{-3} and model errors are within 0.6 and 2.5 degrees Celsius.

Chapter 7 deals with non-linear mathematical models (neural networks). NARX, FFBP and NARXSP networks were applied to the three buildings for one year.

As for the linear analysis, the same inputs selected for each season were used for these networks. In contrast to applying linear models, NARX, FFBP and NARXSP networks, with the same properties (section 7.3), gave good results for Portman House and the Visa building throughout the year.

Furthermore, for the Visa building and Portman House the models' errors are 0.05 - 1.5 degrees Celsius (NARXSP, NARX and FFBP networks) and for the Rockefeller building are 0.05 - 0.9 degrees Celsius (NARXSP network). In the Visa building and Portman house mse is of the order 10^{-2} - 10^{-4} (FFBP, NARX and NARXSP networks), while for the Rockefeller building mse is of the order 10^{-3} - 10^{-4} (NARXSP network). In the Rockefeller building, the results obtained for 900 and 213 sampled data utilized for model development with the NARXSP model are better compare than those obtained with the same network and sampled data for the other two buildings. Finally, the results obtained with non-linear models are better than those obtained with linear models (section 7.4).

8.2 Future Work

The following recommendations are made for future work:

First, this study could be extended to other offices in the three buildings to, obtain an overall analysis for each building. Modelling with black box linear and non-linear mathematical models and with the actual BMS could also be extended to

Second, HVAC plants' thermal behaviour could be analysed for one year. This is very important, because it would allow us to use these models for control purposes of these plants.

Third, the building's thermal models and HVAC plants could be installed together with the actual BMS detecting any changes in thermal behaviour, which use model and design advanced controller other than PI and PID.

Finally, this study could be extended to the other types of buildings like hospitals, supermarkets, airports and schools.

References

Abdullatif, E., Ben, N., and Mahmoud, M. A., (2004). *Cooling load prediction for buildings using general regression neural networks*. Energy Conversion and Management, vol. 45, pp. 2127–2141.

Albert, T. P. S., Chen, W. L., Chow, T. T., and Tse, W. L., (1995). *New HVAC Control by system identification*. Building and Environment, vol. 30, pp. 349-357.

Andersen, K. K., Madsen, H., and Hansen. L. H., (2000). *Modelling the heat dynamics of a building using stochastic differential equations*. Energy and Buildings, vol, 31, pp. 13-24.

Bechtler, H., Browne, M. W., Bansal, P. K., and Kecman, V., (2001). *Neural networks a new approach to model vapour-compression heat pumps*. International Journal of Energy Research, vol. 25, pp. 591- 599.

Benigo, Y., Simard, P and Fiasconi, P., (1994). *Learning long-term dependencies with gradient descent is difficult*. IEEE Trans. Neural Networks, vol. 5, no. 2, pp. 157–166.

Bosch, P. P. J., and van den Klauw A. C., (1994). *Modelling, identification and simulation of dynamical systems*. CRC Press, Inc. ISBN 0849391814.

Boulesteix, A. L., and Strimmer, K., (2005). *Partial Least Squares: A Versatile Tool for the Analysis of High-Dimensional Genomic Data*. Seminar for Applied Stochastics, Department of Statistics, University of Munich, Akademiestrasse 1, D-80799 Munich, Germany.

Braun, J., and Li, H., (2001). *Description of FDD modeling approach for normal performance expectaction*. Progress Report submitted by: Purdue University.

Chen, S., Billings, S., and Grant, P., (1990). *Non-linear system identification using neural networks*. Int. J. Control, vol. 51, no. 6, pp. 1191–1214.

Chiang, C. T., and Lin, C. S., (1996). *CMAC with general basis functions*. Neural Networks, vol. 9, pp. 1199–1211.

Cunningham, J., (2001). *Inferring ventilation and moisture release rates from field psychometric data only using system identification techniques*. Building and Environment, vol. 36, pp.129-138.

Dan, W., Lum, K. Y., and Guanghong, Y., (2002). *Parameter estimation of ARX/NARX model: a neural network based method.* Proceedings of the 9th International Conference on Neural Information Processing (ICONIP'02), vol 3, pp 1109-1113.

Datta, D., and Tassou, S. A., (1997). *Energy management in supermarkets through electrical load prediction*. In: Proc of the First Int Conf on Energy and Environment, Limassol, Cyprus, vol. 2. pp. 587-593.

De Moor, M., and Berckmans, D., (1996). *Building a grey box model to model the energy and mass transfer in an imperfectly mixed fluid by using experimental data.* Mathematics and Computers in Simulation, vol. 42, pp. 233-244.

Deque, F., Ollivier, F., and Poblador, A., (2000). *Grey boxes used to represent buildings with a minimum number of geometric and thermal parameters*. Energy and Buildings, vol. 31, pp. 29–35.

Demuth, H., Mark, B., and Hagan, M., (2008). *Neural Network Toolbox 6, User's Guide*. The MathWorks.

Dewson, T., Day, B., and Irving, A. D., (1993). *Least squares parameter estimation of a reduced order thermal model of an experimental building*. Building and Environment, vol. 28, pp. 127-137.

Dunteman, G. H., (1989). *Principal Components Analysis (Sage University Paper Series on Quantitative Applications in the Social Sciences)*. Sage Pubblications Inc. ISBN: 0803931042. pp. 7-10.

Earl. C., (1994). *The Fuzzy Systems Handbook : A Practitioner's Guide to Building, Using, and Maintaining Fuzzy Systems*. Book&Disk Edition, Paperback, Published by Ap Professional, ISBN: 0121942708.

Eykhoff, P., (1974). *System Identification: Parameter and State Estimation*. John Wiley & Sons, NY, ISBN 0471 249807.

Fan, J., and Gijbels, I., (1997). *Local Polynomial Modelling and Its Applications*. Monographs on Statistics and Applied Probability 66. London, Chapman and Hall.

Flores, S., Merts, E. I., Ketelaere, B. D., and Lammertyn, J., (2006). *Development and validation of "grey-box" models for refrigeration applications: a review of key concepts*. International Journal of Refrigeration, vol. 29, pp. 931-946.

Frank, I. E., and Friedman, J. H., (1993). *A statistical view of some chemometrics regression tools*. Technometrics, vol. 35, pp. 109–135.

Ghiaus, C., Chicinas, A., and Inard, C., (2006). *Grey-box identification of air-handling unit elements*. Control Engineering Practice. doi:10.1016/j.conengprac.2006.08.005.

Gilles, F., Christelle, V., Olivier, L., and Gilbert, A (2002). *Development of a simplified and accurate building model based on electrical analogy*. Energy and Buildings. vol 34, Issue 10, pp. 1017-1031.

Gordon, K. L., and Campagna, D., (1990). *A Summary Comparison of CMAC Neural Network and Traditional Adaptive Control Systems*. Neural Network for Control. Miller et al.eds. MIT press: Cambridge, MA. 143-69.

Goudaa, M. M., Danahera, S., and Underwood, C. P., (2002). *Building thermal model reduction using nonlinear constrained optimization*. Building and Environment, vol. 37, Issue 12, pp. 1255-1265.

Guglielmi, G., Parigini, T., and Rossi, G. K., (1995). *Paper: fault diagnosis and neural networks: A power plant application.* Control Eng. Practice, vol. 3, no. 5, pp. 601-620.

Hao, X., Zhang, G., and Chen, Y., (2005). *Fault-tolerant control and data recovery in HVAC monitoring system.* Energy and Buildings, vol 37, pp. 175–180.

Hardle, W. (1989). *Applied Nonparametric Regression.* Cambridge University Press.

Harunori, Y., Sanjay, K., and Yasunori, M., (2001). *Online fault detection and diagnosis in VAV air handling unit by RARX modeling.* Department of Global Environmental Engineering, Faculty of Engineering, Kyoto University, Sakyo-ku, Kyoto 606-01, Japan. Energy and Buildings, vol. 33, pp. 391-401.

Hassoun, M. H., (1995). *Fundamentals of Artificial Neural Networks.* The MIT Press.

Hornik, K., (1991). *Approximation capabilities of Multilayer Feedforward Networks.* Neural Networks, vol. 4, pp. 251–257.

Hornik, K., Stinchcombe, M., and White, H., (1989). *Multilayer Feedforward Networks are Universal Approximators.* Neural Networks, vol. 2, pp. 359–366.

IEA Annex 25., (1996). *Building Optimization and Fault Diagnosis Source Book.* Eds.J. Hyvfirinen and S. Karki. Technical Research Centre of Finland.

IEA Annex 34., (2001). *Demonstrating fault detection and diagnosis methods in real building.* Eds. A. Dexter and J. Pakanen. Technical Research Centre of Finland.

Jian, S., Guangfa, T., Ling, Z., and Nianping, L., (2004). *An efficient solution method for predicting indoor environment of buildings with complex geometric configuration.* Building and Environment, vol. 39, Issue 5, pp. 495-504.

Kalogirou, S., Eftekhari, M., and Marjanovic, L., (2003). *Predicting the pressure coefficients in a naturally ventilated test room using artificial neural networks.* Building and Environment, vol. 38, pp. 399 – 407.

Kanjilal, P. P., (1995). *Adaptive Prediction and Predictive Control.* IEE Control Engineering Series 52, Peter Peregrinus Ltd, UK, ISBN 0-86341-193-2.

Karri, V., (2000). *Drilling Performance Prediction Using General Regression Neural Networks*. Lecture Notes in Computer Science. IEA/AIE 2000, LNAI 1821, pp. 67-73.

Katipamula, S., and Brambley, M. R., (2005). *Methods for Fault Detection, Diagnostics, and Prognostics for Building Systems - A Review.* Part I, vol 11, no 1, HVAC&R RESEARCH.

Klir, G. J., Clair, St., Ute, H., and Yuan, B., (1997). *Fuzzy set theory: foundations and applications*. Englewood Cliffs, NJ: Prentice Hall. ISBN 0133410587.

Kontoleon, K. J., and Bikas, D. K., (2002). *Modelling the influence of glazed openings percentage and type of glazing on the thermal zone behaviour*. Energy and Buildings, vol. 34, pp. 389-399.

Kukolj, D. D., Berko, M. T., and Atlagic, B., (2001). *Experimental design of supervisory control functions based on multilayer perceptrons*. Artificial Intelligence for Engineering Design, Analysis and Manufacturing, vol.15, pp. 425–431.

Kumar, S., Kojima, T., and Yoshida, H., (2001). *Development of parameter based fault detection and diagnosis technique for energy efficient building management system*. Energy Conversion and Management vol, 42, pp. 833-854 (7).

Kuo, H. C., Wu, L. J., and Chen, J. H., (2002). *Neural Fuzzy fault diagnosis in a marine propulsion shaft system*. Jurnals of Material Processing Technology, vol, 122, pp. 12-22.

Laurene, F., (1994). *Fundamentals of Neural Networks. Architectures, Algorithms, and Applications*. Prentice-Hall. New Jersey.

Lee, W. Y., House, J. M., and Kyong, N.H., (2004). *Subsystem level fault diagnosis of a building's air-handling unit using general regression neural networks*. Applied Energy, vol. 77, pp. 153–170.

Lee, W. Y., House, J. M., Park, C., and Kelly, G. E., (1996). *Fault Diagnosis of an Air-Handling Unit Using Artificial Neural Networks*. ASHRAE Transactions, vol. 102, Pt. 1, pp. 540-549 (Pg 570-A).

Lee, W.Y., Park, C., and Kelly, G. E., (1996a). *Fault Detection in an Air Handling Unit using Residual and Recursive Parameter Identification Methods*. Ashrae Transactions, vol. 102, No 1, pp. 528-539.

Li, J. Q., Liu, J. Z., and Niu, Y. G., (2004). *Application of Cerebellar Model Articulation Control in Reheated-Steam System*. Tencon. 2004 IEEE Region 10 Conference, vol. 4, pp. 578- 580. ISBN: 0-7803-8560-8.

Li, X., Hossein, V., and Visier, J., (1996). *Development of a Fault Diagnosis Method for Heating Systems Using Neural Networks*. ASHRAE Transactions, vol. 102, Pt. 1, pp. 607-614 (Pg 47-C).

Li, X., Visier, J., and Vaezi, H. N., (1997). *A Neural Network Prototype for Fault Detection and Diagnosis of Heating Systems*. ASHRAE Transactions, vol. 103, Pt. 1, pp. 634-644 (Pg11-A).

Liddament, M.W., (1999). *Real Time Simulation of HVAC Systems for Building Optimisation, Fault Detection and Diagnostics*. IEA ECBCS Annex 25, Technical Synthesis Report based on Building and Optimisation Source Book.

Lin, T., Horne, B., Tino, P and Giles, C., (1996). Learning long-term dependencies is not as difficult with NARX recurrent neural networks. IEEE Trans. Neural Networks, vol. 7, no. 6.

Ljung, L., (1999). *System identification: theory for user 2nd Edition-cased.* Prentice Hall. Englewood Cliff. ISBN 9780136566953.

Ljung, L., (1987). *System Identification: Theory for user.* Prentice-Hall, Englewood Cliffs. ISBN 0-13-881640-9.

Ljung, L., and Glad, T., (1994). *Modelling of Dynamic Systems.* Prentice-Hall, Englewood Cliffs. ISBN 013-597097-0.

Lowry, G. and Lee, M. W., (2004). *Modelling the passive thermal response of a building using sparse BMS data.* Applied Energy, vol. 78, pp. 53–62.

MacGregor, J. F., and Kourti, T., (1995). *Statistical Process Control of Multivariate Processes.* Control Eng. Practice, vol 3, no. 3, pp. 403-414.

Madsen, H., and Holst, J., (1995). *Estimation of continuous – time models for the heat dynamics of a building.* Energy and Buildings, vol. 22, pp. 67-79.

Madsen, H., and Holst, J., (1993). *Estimation of continuous time models for the heat dynamics of a building.* Building and Environment, vol. 28, pp. 127-137.

Mahdi, J. K., and Araabi, B. N., (2004). *Neural Network based predictive control of a heat exchanger nonlinear process.* Journal of Electrical & Electronics Engineering, vol. 4, no 2, pp. 1219-1226.

Majors, M., Stori, J., and Cho, D., (1994). *Neural network control of automotive fuel-injection systems.* IEEE Contr. Syst. Mag., vol. 14, pp. 31–36.

Miller, W. T., (1989). *Real-time application of neural networks for sensor based control of robots with vision.* IEEE Trans. Syst., Man, Cybern., vol. 19, pp. 825–831.

Morisot, O., and Marchio, D., (1999). *Fault detection and diagnosis on HVAC variable air volume system using artificial neural network.* Proc. IBPSA Building Simulation, Kyoto, Japan (Pg 195-D).

Namburu, S. M., Luo, J., Azam, M., Choi, K., and Pattipati, K. R., (2005). *Fault detection diagnosis and data driven modelling in HVAC chillers*. SPIE - The International Society for Optical Engineering. Signal Processing, Sensor Fusion, and Target Recognition XIV, Ivan Kadar, Editor, vol. 5809, pp. 143-154.

Nguyen, D., and Rocke, D. M., (2002). *Tumor classification by partial least squares using microarray gene expression data*. Bioinformatics, vol. 18, pp. 39–50.

Nielsen, H. A., and Madsen, H., (2006). *Modelling the heat consumption in district heating systems using a grey-box approach*. Energy and Buildings, vol. 38, pp. 63–71.

Parlos, A. G., Chong, K. T., and Atiya, A. F., (1994). *Application of the recurrent multilayer perceptron in modeling complex process dynamics*. IEEE Transactions on Neural Networks, pp. 255–266.

Patterson, D. W., (1996). *Artificial Neural Network. Theory and Applications*. Prentice Hall. Singapore.

Peitsman, H. C., and Soethout, L. L., (1997). *ARX models and real-time model-based diagnosis*. ASHRAE Transaction, vol. 103 (1), pp. 657-671.

Peitsman, H.C., and Bakker, V., (1996). *Application of black-box models to HVAC systems for fault detection*. ASHRAE Transactions, vol. 102 (1), pp. 628-640.

Penman, J. M., (1990). *Second Order System Identification in the Thermal Response of a Working School*. Building and Environment, vol. 25, pp. 105-110.

Qin, J., and Wang, S., (2005). *A fault detection and diagnosis strategy of VAV air-conditioning systems for improved energy and control performances*. Energy and Buildings, vol. 37, pp. 1035-1048.

Roger, J. S., and Sun, C. T., (1995). *Neuro-Fuzzy Modeling and Control*. The Proceedings of the IEEE, vol. 83, no. 3, pp 378-406.

Roger, J., and Jang, S., (1993). *ANFIS: Adaptive-Network-Based Fuzzy Inference Systems*. IEEE Transactions on Systems, Man, and Cybernetics, vol. 23, no. 03, pp. 665-685.

Rojas, R., (1996). *Neural Networks. A Systematic Introduction*. Springer-Verlag, Berlin.

Rosenberg, R., and Karnopp, D., (1983). *Introduction to Physical System Dynamics*. McGraw-Hill, New York.

Rumelhart, D. E., Hinton, G. E., and Williams, R. J., (1986). *Learning internal representations by error propagation*. In Parallel Distributed Processin, vol. 1, chapter 8. The MIT Press.

Samanta, B., Balushi, K. R., and Araimi, S. A., (2006). *Artificial neural networks and genetic algorithm for bearing fault detection*. Soft Comput, vol. 10, pp. 264–271.

Schwenker, F., Kestler, H. A., and Palm, G., (2001). *Three learning phases for radial-basis-function networks*. Neural Networks, vol. 14, pp. 439-458.

Shiraishi, H., Ipri, S. L., and Cho, D. D., (1995). *CMAC neural network controller for fuel-injection systems*. IEEE Trans. Contr. Syst. Technol., vol. 3, pp. 32–38.

Soumelidis, M. I., and Stobart R. K., (2006). *Dynamic modelling of thee way catalyst using non-linear identification technique*. Proc. Imech Part I. Journal of System and Control Engineering, vol 220, no 7, pp. 596-605.

Specht, D. F., (1991). *A General regression neural-network*. IEEE Transactions on Neural Networks, vol. 2, no. 6, pp. 568–76.

Srinivas, K., and Brambley, M. R., (2005). *Methods for Fault Detection, Diagnostics, and Prognostics for Building Systems a Review*. Part I. HVAC & R Research, vol 11, no. 1.

Stone, M., and Brooks, R. J., (1990). *Continuum regression: cross-validated sequentially constructed prediction embracing ordinary least squares, partial least squares and principal component regression.* Journal of the Royal Statistical Society B, vol. 52, pp. 237– 269.

Su, H. T., and McAvoy, T., (1991). *Identification of chemical processes using recurrent networks*. Proc. American Controls Conf., vol. 3, pp. 2314–2319.

Su, H. T., McAvoy, T., and Werbos, P., (1992). *Long-term predictions of chemical processes using recurrent neural networks: A parallel training approach*. Industrial Engineering and Chemical Research, vol. 31, pp. 1338–1352.

Swider, D.J., Browne, M.W., Bansal, P.K., and Kecman, V., (2001). *Modelling of vapour-compression liquid chillers with neural Networks*. Applied Thermal Engineering, vol. 21, pp. 311-329.

The MathWorks., (2003). *System Identification Toolbox* 6. www.mathworks

Tsungnan, L., Horne B. G and Giles, C. L., (1998). *How embedded memory in recurrent neural network architectures helps learning long-term temporal dependences*. Neural Networks, vol. 11, pp. 861-868.

Underwood, C. P., (1999). *HVAC Control Systems: Modelling, Analysis and Design*. E & FN Spon, London ISBN 0-419–20980-8.

Venkatasubramanian, V., Rengaswamy, R., Yin, K., and Kavuri, S. N., (2003c). *A review of process fault detection and diagnosis*. Part III: Qualitative models and search strategies. Computers in Chemical Engineering, vol. 27, pp. 327-346.

Wang, J., Liao, X., and Yi, Z., (2005). *Fault Detection for Plasma Etching Processes using RBF Neural Networks*. (Eds.): ISNN 2005, LNCS 3498, pp. 538.543. Springer-Verlag Berlin Heidelberg.

Wang, S., and Chen, Y., (2004). *Sensor validation and reconstruction for building central chilling systems based on principal component analysis*. Energy Conversion and Management, vol. 45, pp. 673–695.

Wang, S., and Cui, J., (2005). *Sensor-fault detection, diagnosis and estimation for centrifugal chiller systems using principal-component analysis method*. Applied Energy, vol. 82, pp. 197–213.

Weyer, E., Szederkenyi, G., and Hangos, K., (2000). *Grey box fault detection of heat exchangers*. Control Engineering Practice, vol. 8, pp. 121-131.

Wong, Y., and Sideris, A., (1992). *Learning Convergence in the Cerebellar Model Articulation Controller*. IEEE Trans. Neural Networks, vol. 3, pp. 115-121.

Yoshida, H., and Kumar. S., (1999). *ARX an AFMM model-based on-line and real-time data base diagnoses of sudden fault in AHU of VAV system*. Energy Conversion & Management, vol. 40, pp. 1191-1206.

Yu, B., and Van Paassen, D. H. C., (2003). *Fuzzy Neural Networks model for Building Energy Diagnosis*. Eighth International IBPSA Conference Eindhoven, Netherlands, pp. 11-14.

Yu, D. L., and Zhai, Y. J., (2007). *A Neural Network Model Based MPC of Engine AFR with Single-Dimensional Optimization*. Lecture Notes in Computer Science. ISNN, Part I, LNCS 4491, pp. 339-348. Springer-Verlag Berlin Heidelberg.

Yu, D. L., Chang, T. K., and Yu, D. W., (2005). *Fault Tolerant Control of Multivariable Processes Using Auto-Tuning PID Controller*. IEEE Transactions on Systems, Man, and Cybernetics-Part B: Cybernetics, vol. 35, no. 1.

Appendix 1A Weekdays Results - Visa Building

- One week (Monday Time 01:20 to Friday Time 19:00) sampled-data model estimation
- Following week (Monday Time 01:20 to Friday Time 19:00) sampled-data model validation

Spring season

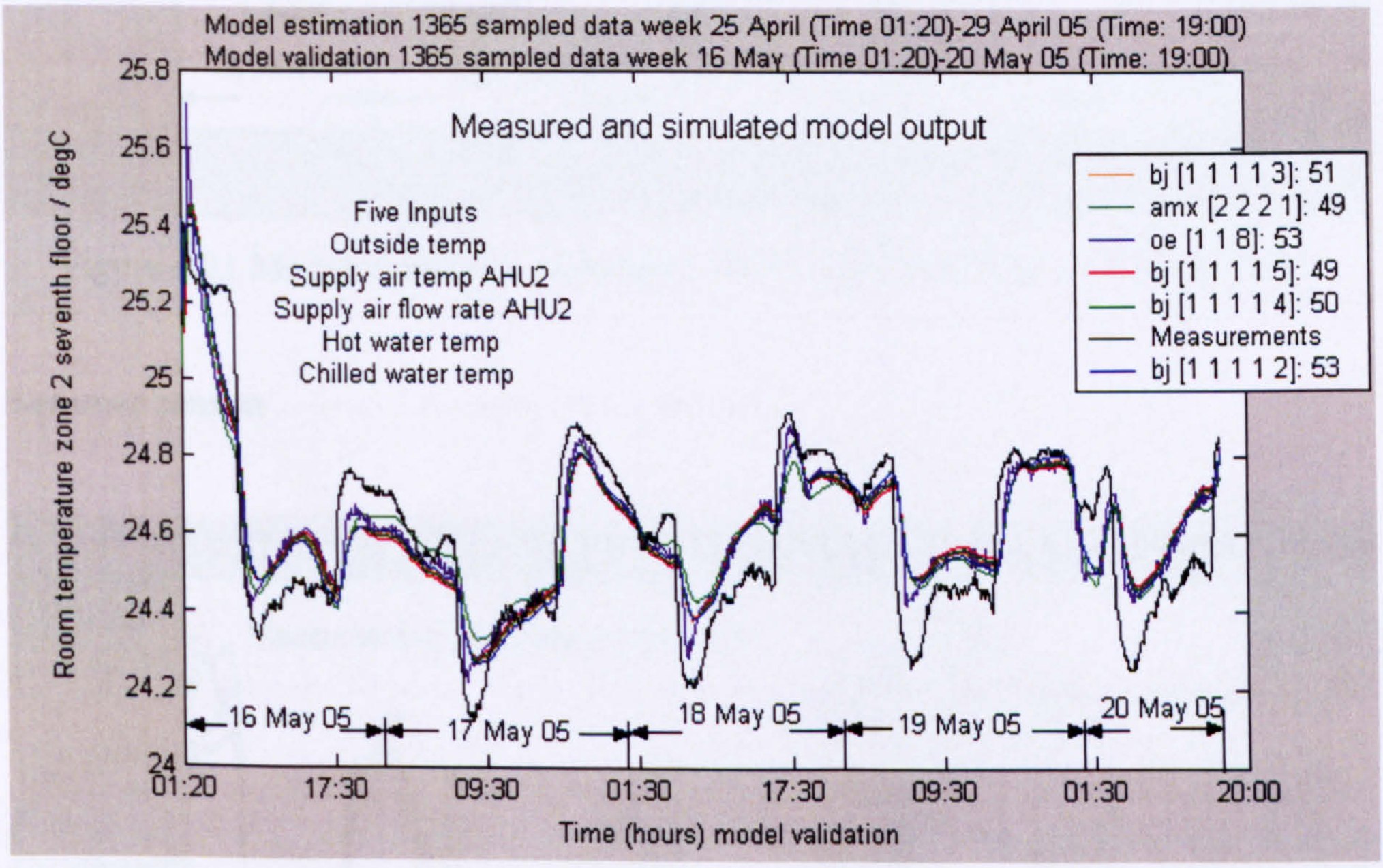

Figure 4.20 Model validation, weekdays 25-29 April 2005 and 16-20 May 2005

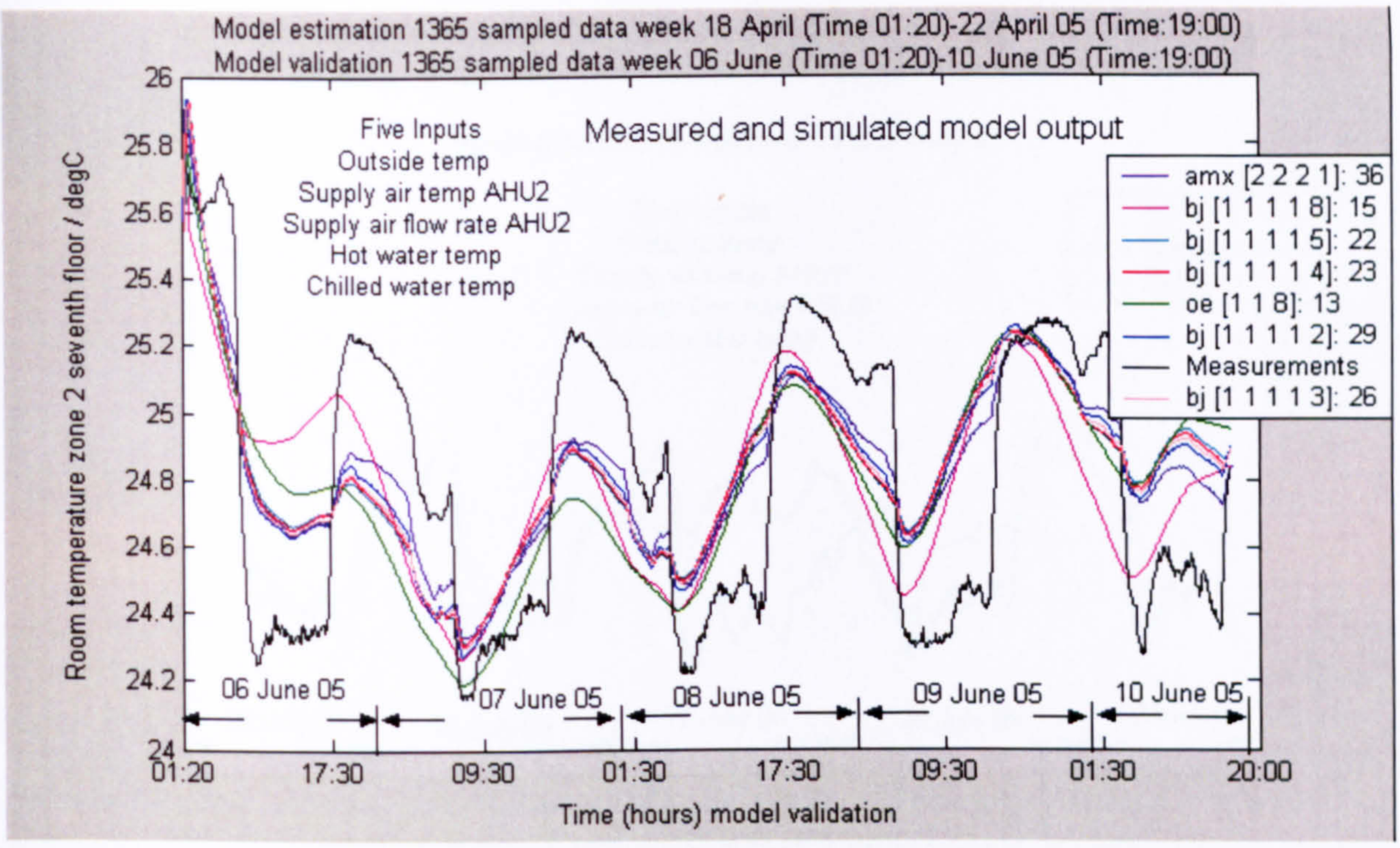

Figure 4.21 Model validation, weekdays 18-22 April 2005 and 06-10 June 2005

Summer season

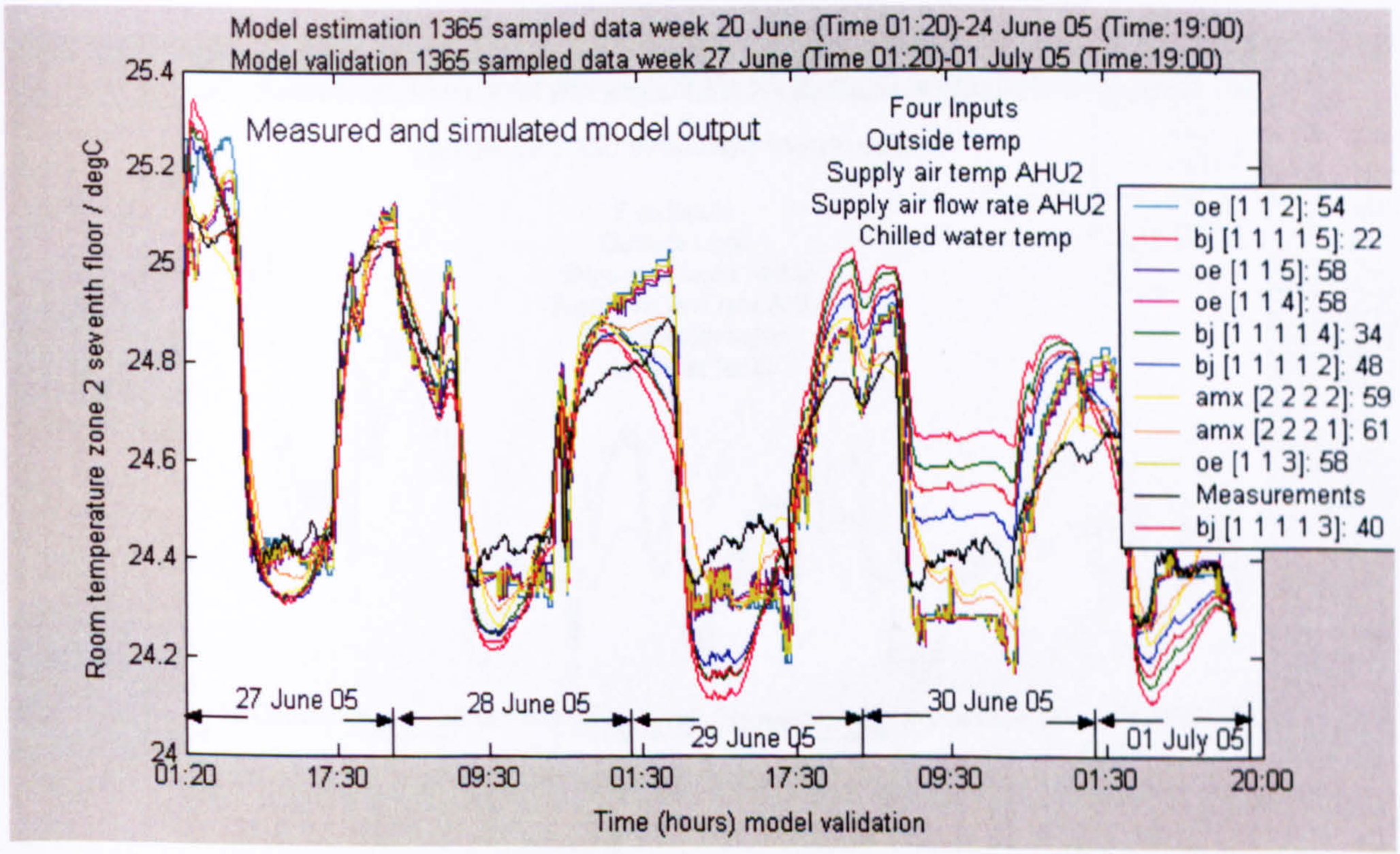

Figure 4.22 Model validation, weekdays 20-24 June 2005 and 27 June-01 July 2005

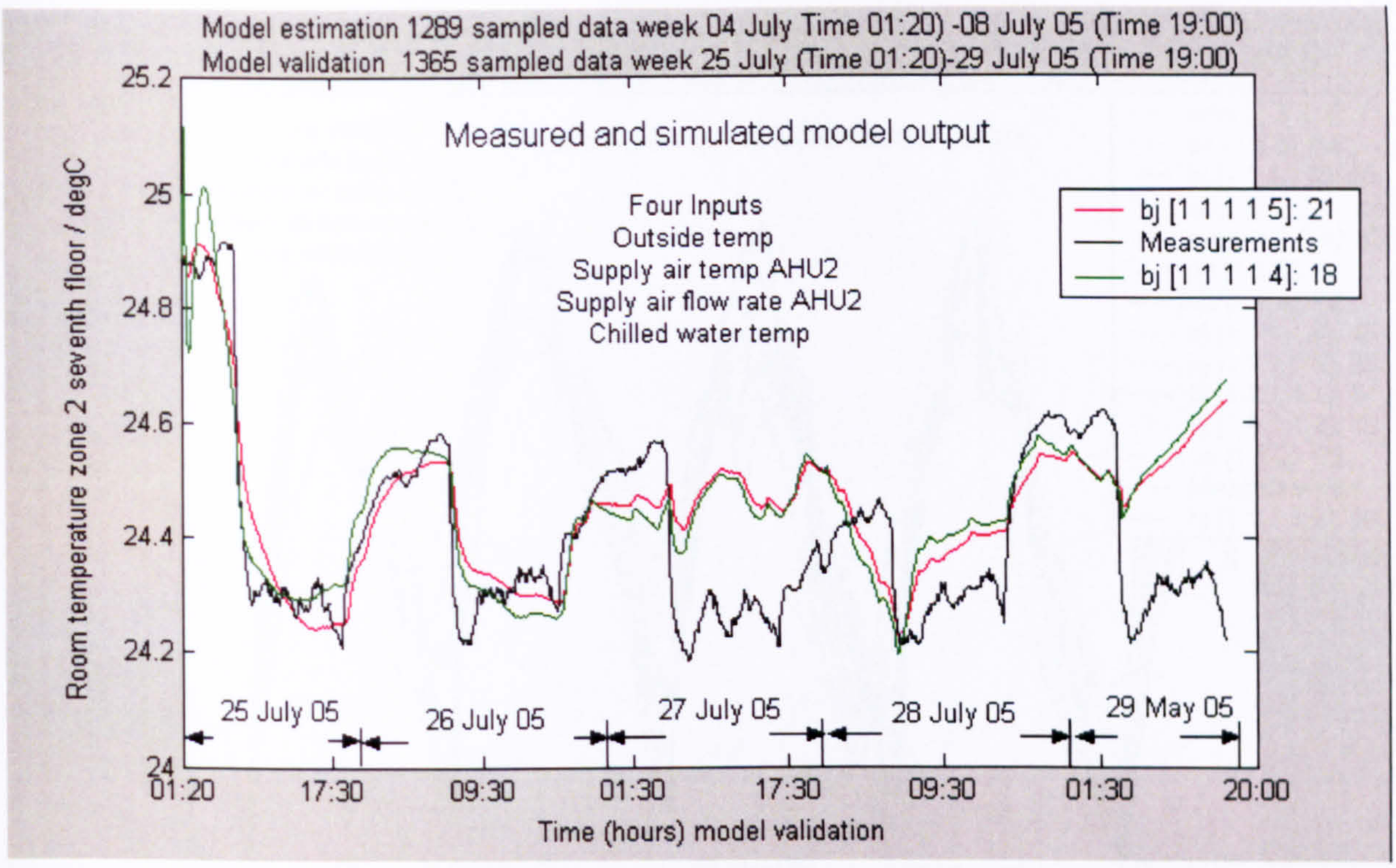

Figure 4.23 Model validation, weekdays 04-08 July 2005 and 25-29 July 2005

Autumn season

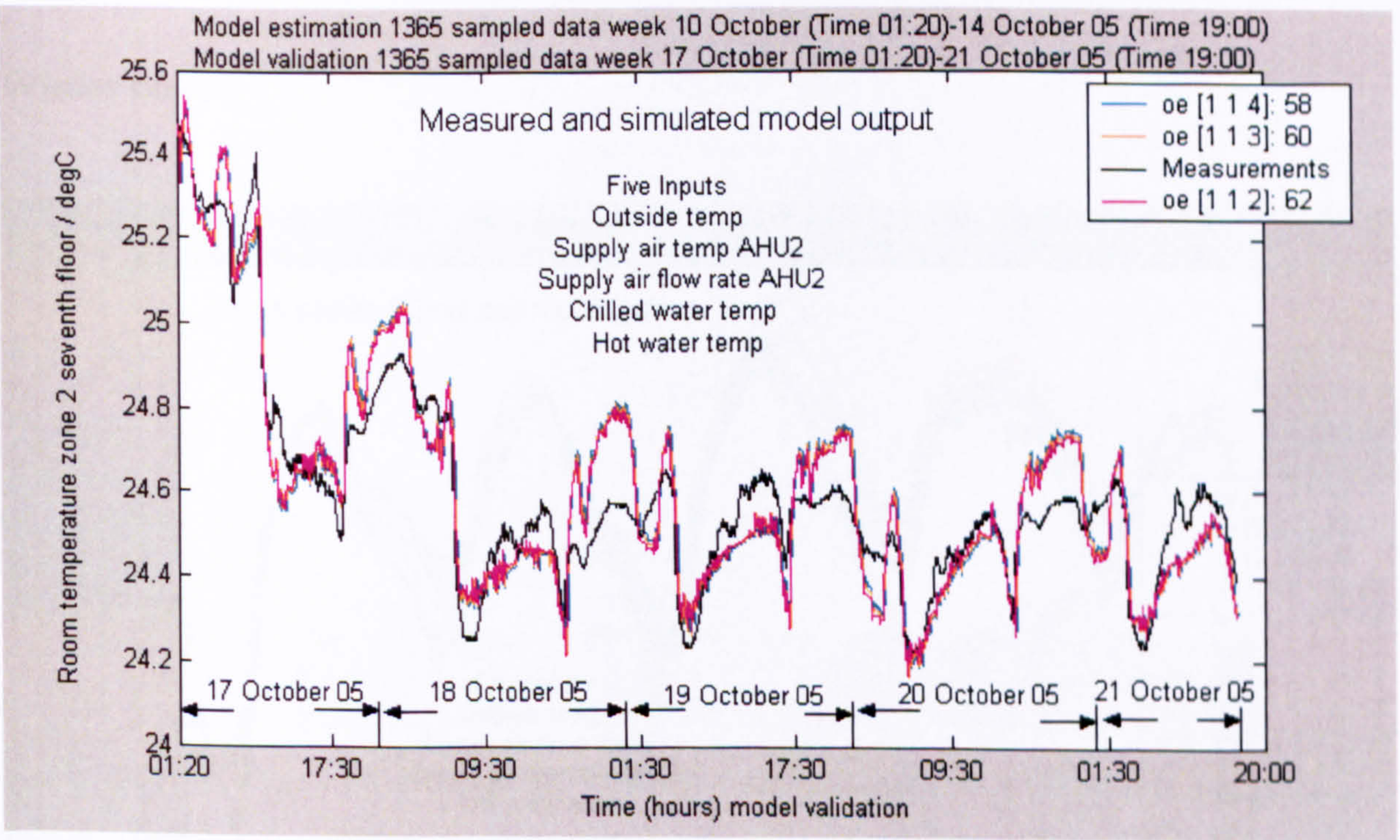

Figure 4.24 Model validation, weekdays 10-14 October 2005 and 17-21 October 2005

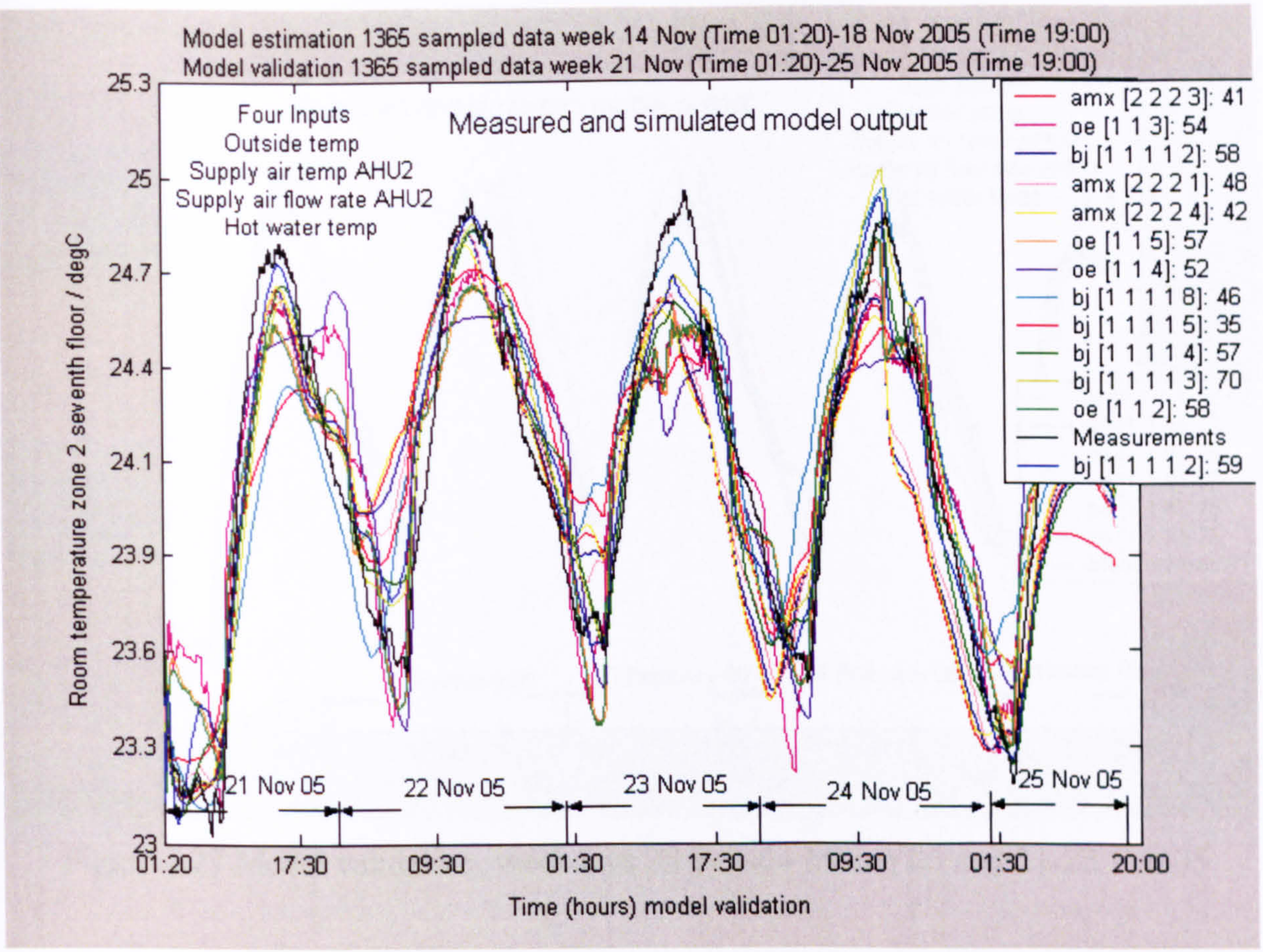

Figure 4.25 Model validation, weekdays 14-18 November 05 and 21-25 November 05

Winter season

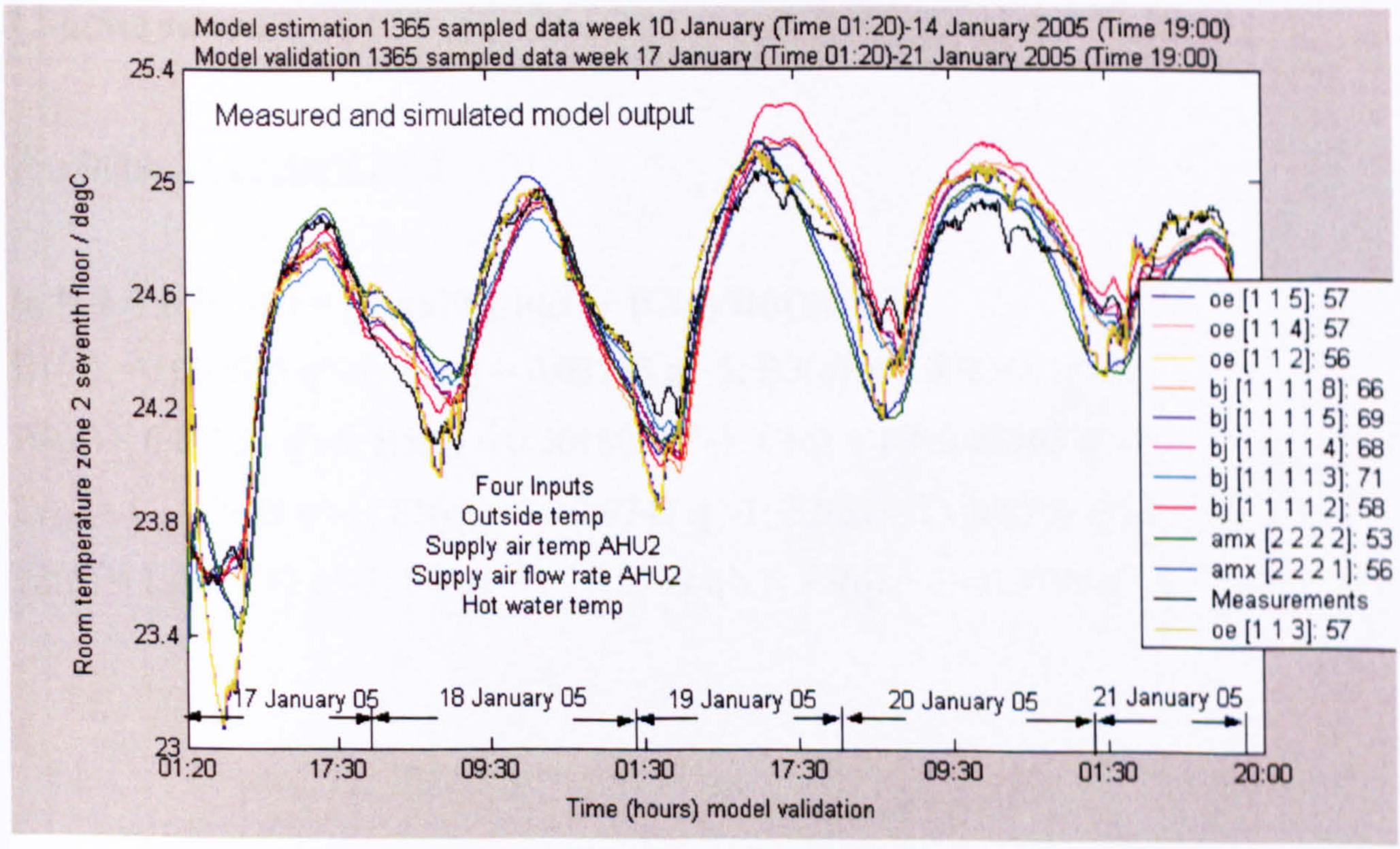

Figure 4.26 Model validation, weekdays 10-14 January 2005 and 17-21 January 2005

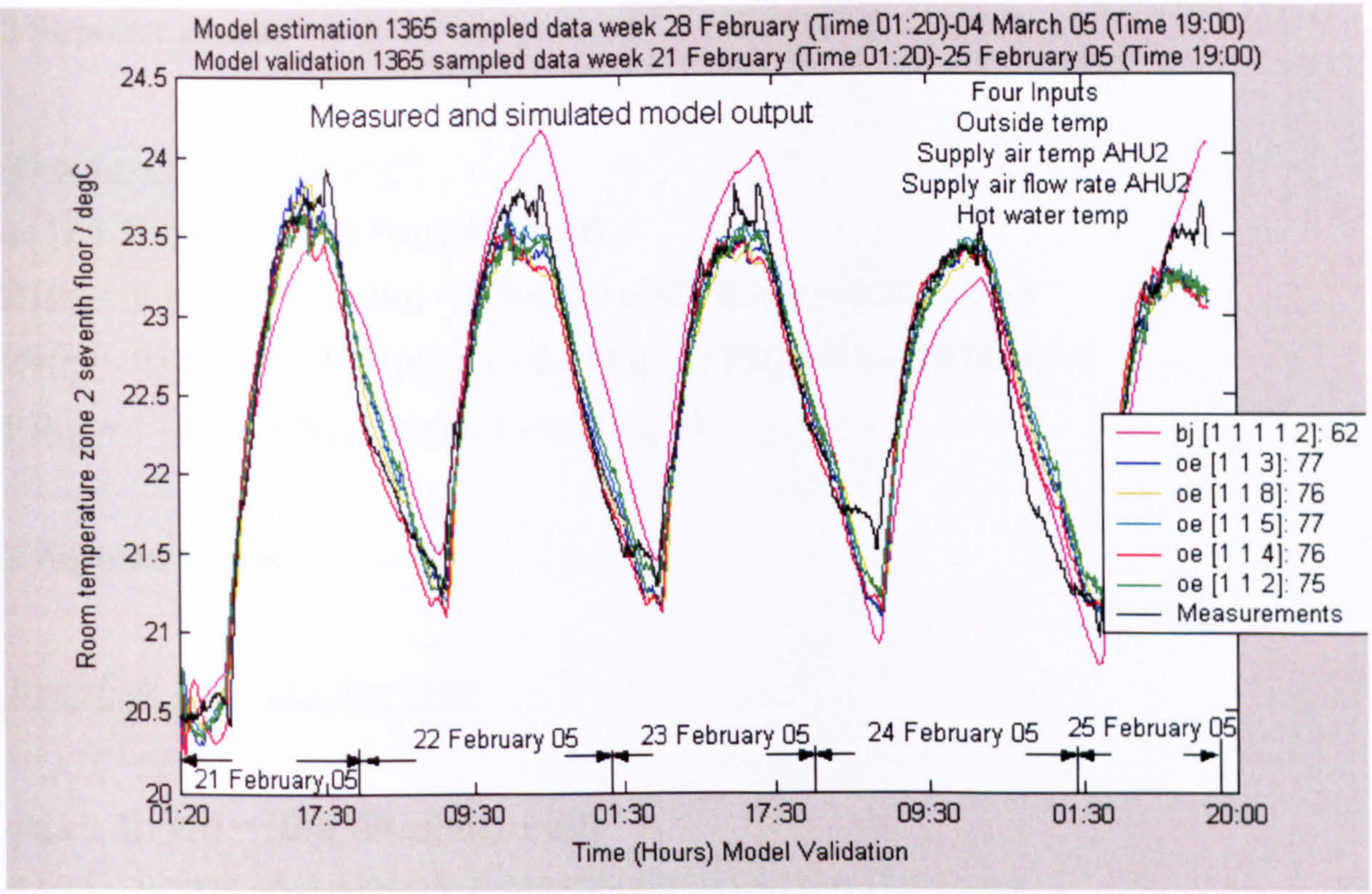

Figure 4.27 Model validation, weekdays 28 Feb-04 March 05 and 21-25 Feb 05

Appendix 1B Weekdays Results - Models Presentation Visa Building

Backward shift operator q (q ^ $-n$ * $u(t) = u$ (t-n), for n = 1,2,…..N, see Ljung, 1987)

1 Spring season

Weekdays 25-29 April 2005

bj [1 1 1 1 5]: y(t) = [B(q)/F(q)]u(t) + [C(q)/D(q)]e(t)

B1(q) = 0.002505 q^-5; B2(q) = 0.03758 q^-5; B3(q) = 0.002505 q^-5

B4(q) = 0.02758 q^-5; B5(q) = 0.001505 q^-5; C(q) = 1 + 0.09265 q^-1

D(q) = 1 - 0.9849 q^-1; F1(q) = 1 - 0.9747 q^-1; F2(q) = 1 - 0.8799 q^-1

F3(q) = 1 - 0.7747 q^-1; F4(q) = 1 - 0.5799 q^-1; F5(q) = 1 - 0.3799 q^-1

2 Summer season

Weekdays 13-17 June 2005

oe [1 1 3]: y(t) = [B(q)/F(q)]u(t) + e(t)

B1(q) = 0.4079 q^-3; B2(q) = 0.001359 q^-3; B3(q) = 0.2079 q^-3

B4(q) = 0.02359 q^-3; F1(q) = 1 - 0.419 q^-1; F2(q) = 1 - 0.9744 q^-1

F3(q) = 1 - 0.219 q^-1; F4(q) = 1 - 0.744 q^-1

3 Autumn season

Weekdays 17-21 October 2005

oe[1 1 2]: y(t) = [B(q)/F(q)]u(t) + e(t)

B1(q) = 0.2275 q^-2; B2(q) = 0.01353 q^-2; B3(q) = 0.1071 q^-2

B4(q) = 0.01356 q^-2; F1(q) = 1 - 0.113 q^-1; F2(q) = 1 - 0.7143 q^-1

F3(q) = 1 - 0.117 q^-1; F4(q) = 1 - 0.324 q^-1

Weekdays 14-18 November 2005

bj [1 1 1 1 3]: y(t) = [B(q)/F(q)]u(t) + [C(q)/D(q)]e(t)

B1(q) = 0.0155 q^-3; B2(q) = 0.001297 q^-3; B3(q) = -0.01358 q^-3

B3(q) = -0.01358 q^-3; C(q) = 1 + 0.2044 q^-1; D(q) = 1 - 0.9989 q^-1

F1(q) = 1 - 0.9226 q^-1; F2(q) = 1 - 0.01025 q^-1; F3(q) = 1 - 1.009 q^-1

F4(q) = 1 - 0.03 q^-1

amx [2 2 2 1]: A(q)y(t) = B(q)u(t) + C(q)e(t)

A(q) = 1 - 1.858 q^-1 + 0.8587 q^-2;

B1(q) = 0.02581 q^-1 - 0.02576 q^-2; B2(q) = 0.0003755 q^-1 - 0.000354 q^-2

B3(q) = 0.006878 q^-2 - 0.008425 q^-2; B4(q) = 0.001338 q^-2 - 0.002225 q^-2

C(q) = 1 - 0.7898 q^-1 + 0.1913 q^-2

4 Winter season

Weekdays 10-14 January 2005

bj [1 1 1 1 4]: y(t) = [B(q)/F(q)]u(t) + [C(q)/D(q)]e(t)

B1(q) = -0.0003127 q^-4; B2(q) = 0.002565 q^-4; B3(q) = 0.03768 q^-4

B4(q) = 0.01057 q^-4; C(q) = 1 + 0.1433 q^-1; D(q) = 1 - 0.9989 q^-1

F1(q) = 1 - 1.001 q^-1; F2(q) = 1 - 0.9706 q^-1

F3(q) = 1 - 0.4979 q^-1; F4(q) = 1 - 0.9338 q^-1

oe [1 1 2]: y(t) = [B(q)/F(q)]u(t) + e(t)

B1(q) = 0.001889 q^-2; B2(q) = 0.01142 q^-2; B3(q) = 0.2938 q^-2

B4(q) = 0.5032 q^-2; F1(q) = 1 - 0.9609 q^-1; F2(q) = 1 - 0.1532 q^-1

F3(q) = 1 + 0.5423 q^-1; F4(q) = 1 + 0.03903 q^-1

Weekdays 28 February-04 March 2005

bj [1 1 1 1 2]: y(t) = [B(q)/F(q)]u(t) + [C(q)/D(q)]e(t)

B1(q) = 0.004019 q^-2; B2(q) = 0.0003863 q^-2; B3(q) = 0.0003626 q^-2

B4(q) = -0.0249 q^-2; C(q) = 1 + 0.2078 q^-1; D(q) = 1 - 0.9995 q^-1

F1(q) = 1 - 0.976 q^-1; F2(q) = 1 - 0.8594 q^-1; F3(q) = 1 - 0.984 q^-1

F4(q) = 1 - 1.001 q^-1

Appendix 2A Weekdays Results - Portman House Building

- One week (Monday Time 01:20 to Friday Time 19:00) sampled-data model estimation
- Following week (Monday Time 01:20 to Friday Time 19:00) sampled-data model validation

Winter season

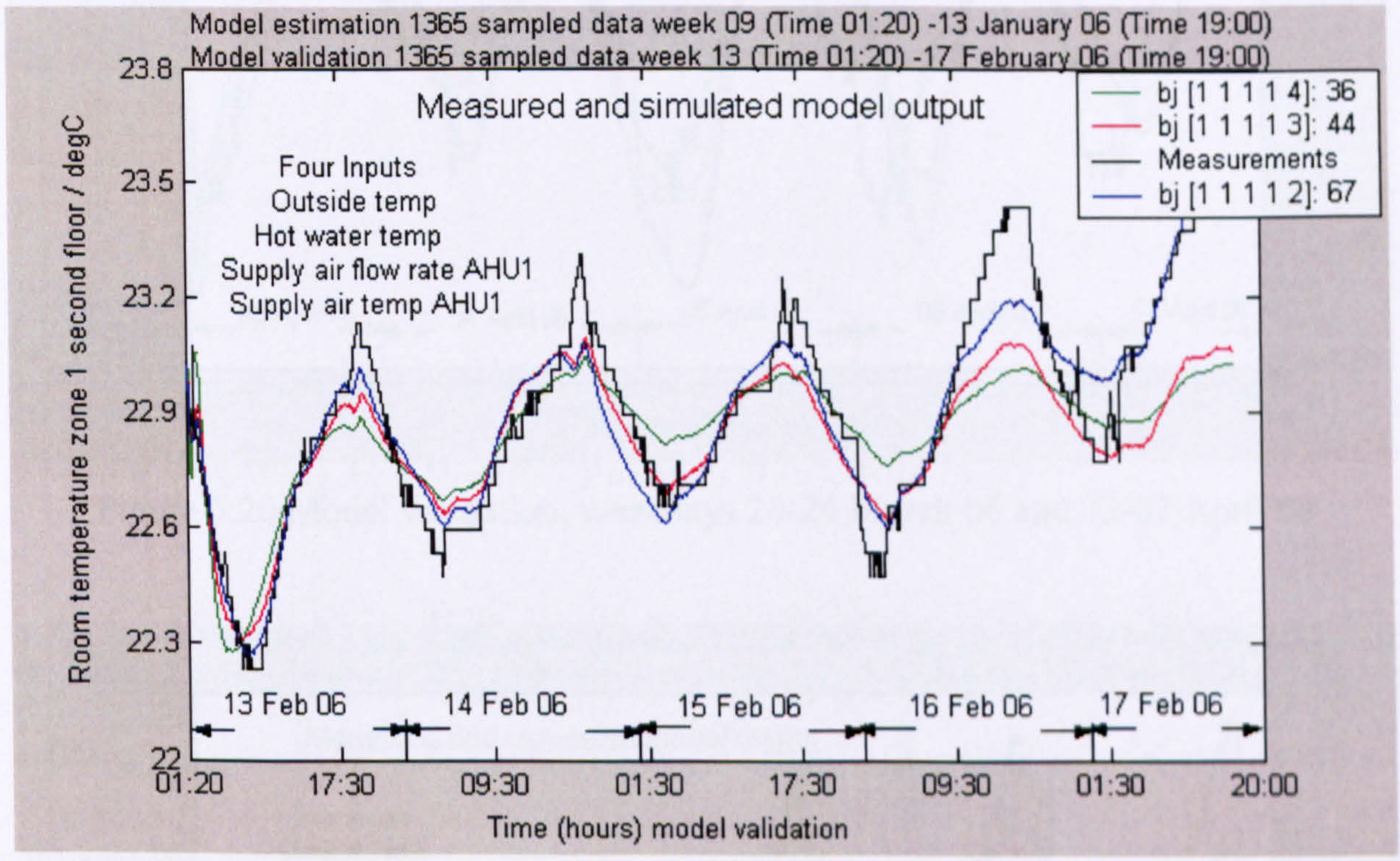

Figure 5.19 Model validation, weekdays 09-13 January 06 and 13-17 February 06

Spring season

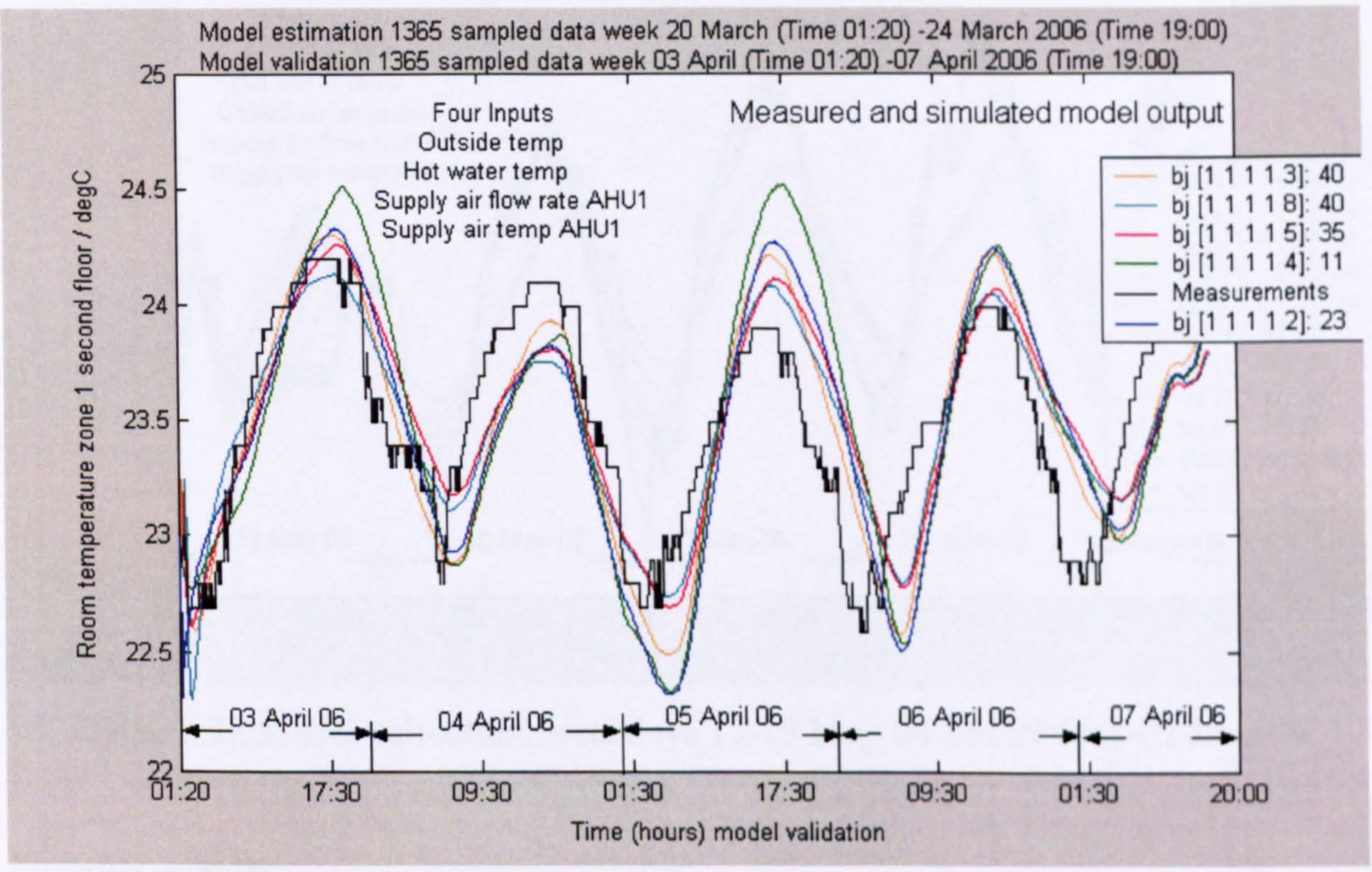

Figure 5.20 Model validation, weekdays 20-24 March 06 and 03-07 April 06

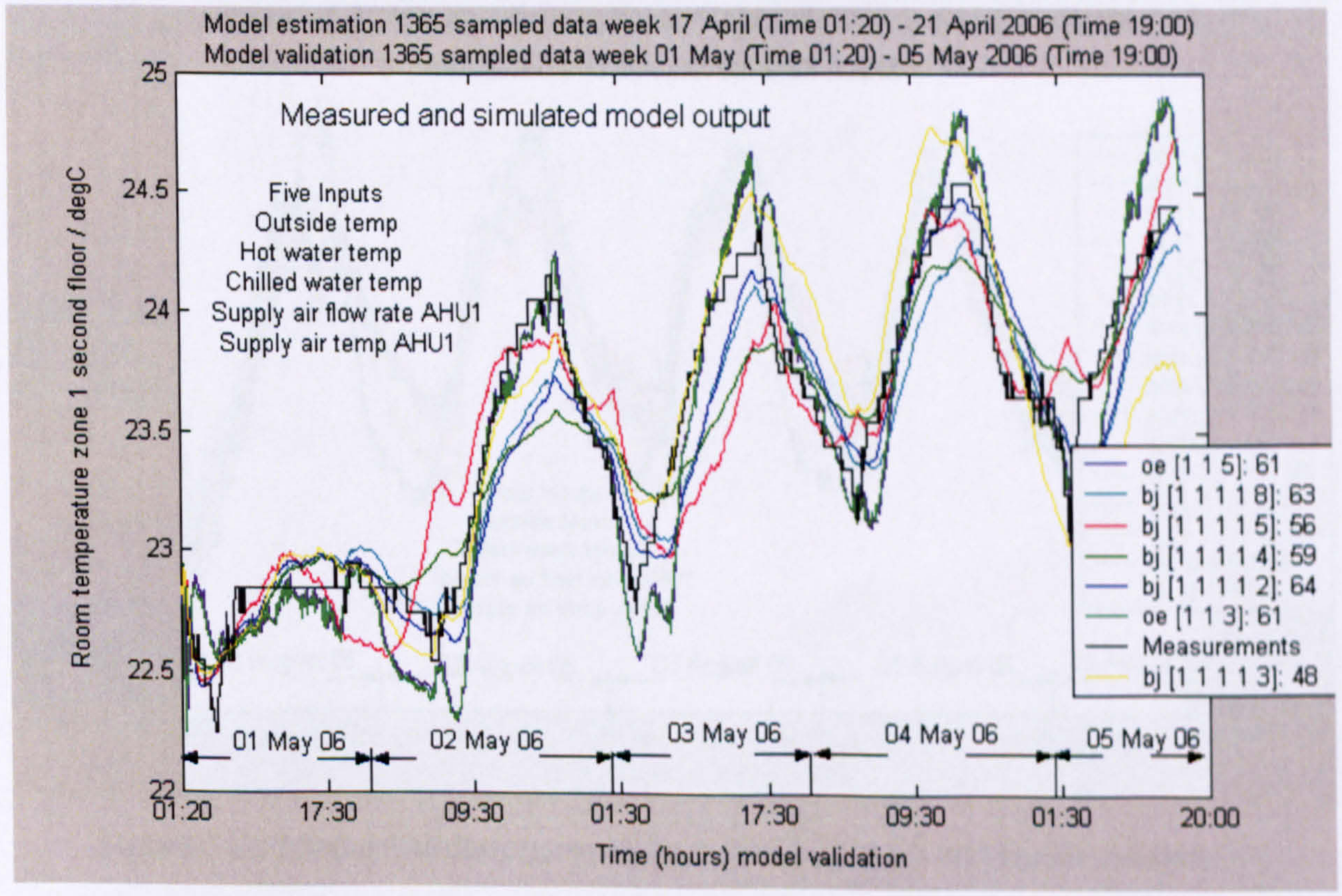

Figure 5.21 Model validation, weekdays 17-21 April 06 and 01-05 May 06

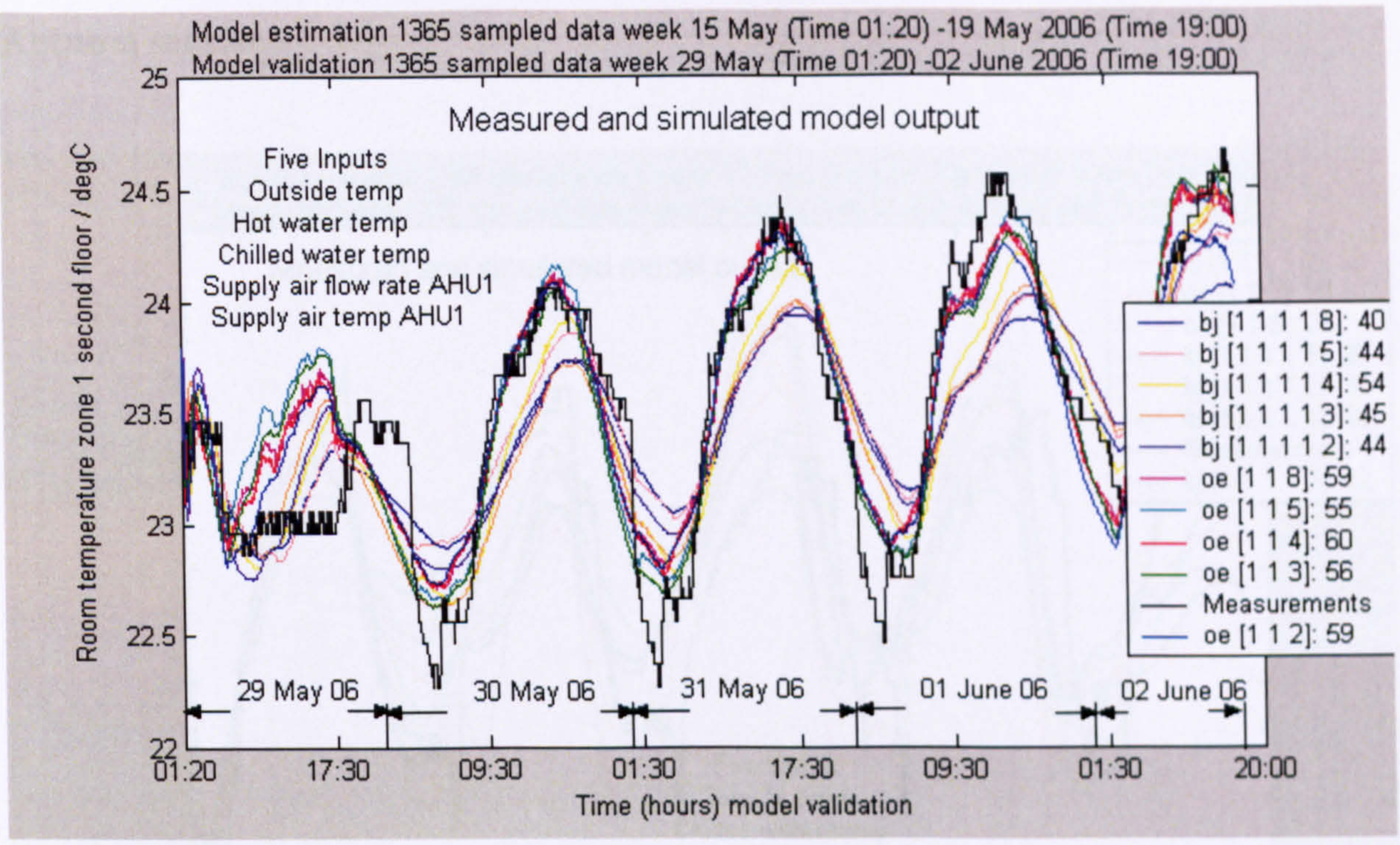

Figure 5.22 Model validation, weekdays 15-19 May 06 and 29 May-02 June 06

Summer season

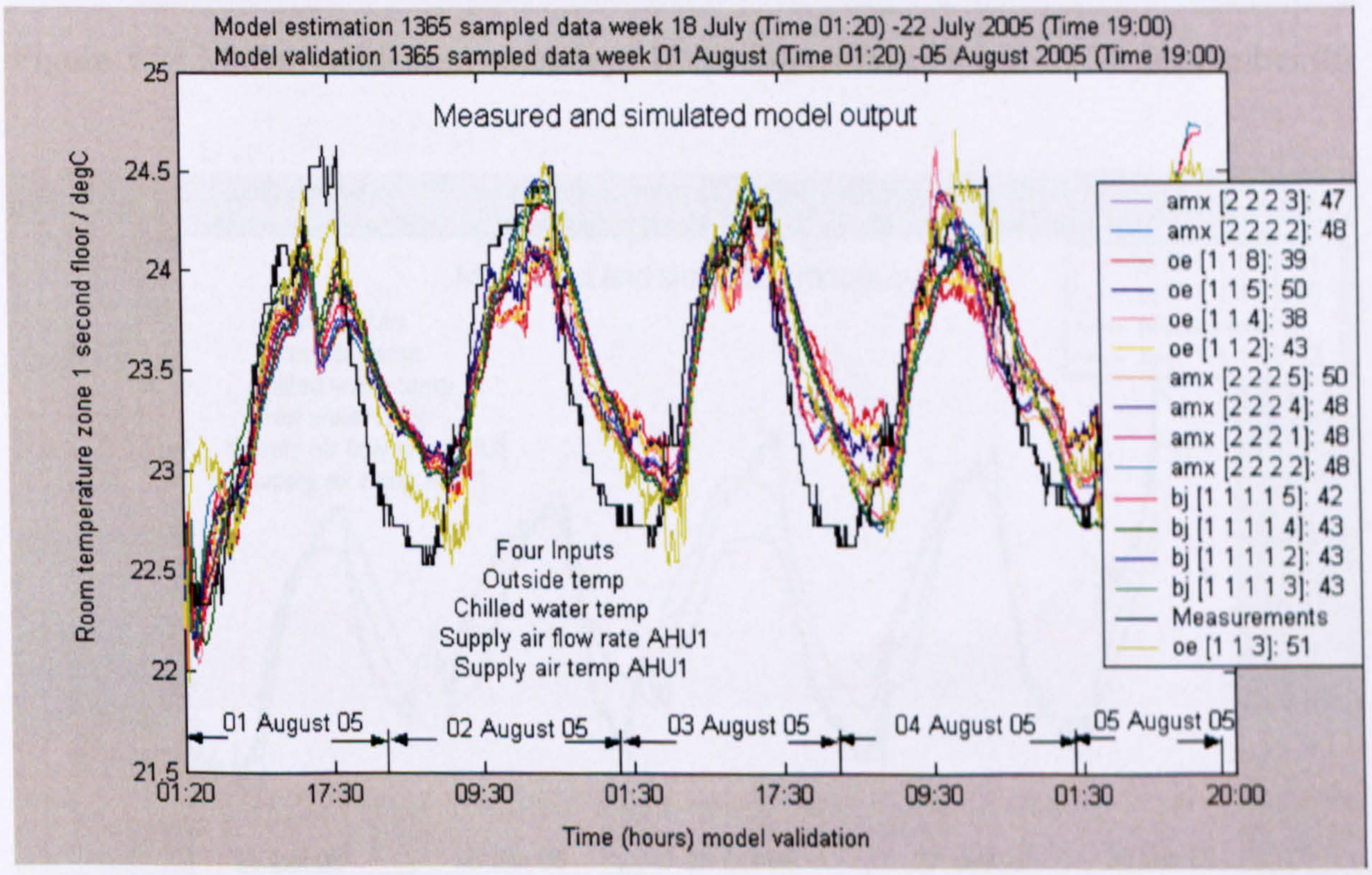

Figure 5.23 Model validation, weekdays 18-22 July 05 and 01-05 August 05

Autumn season

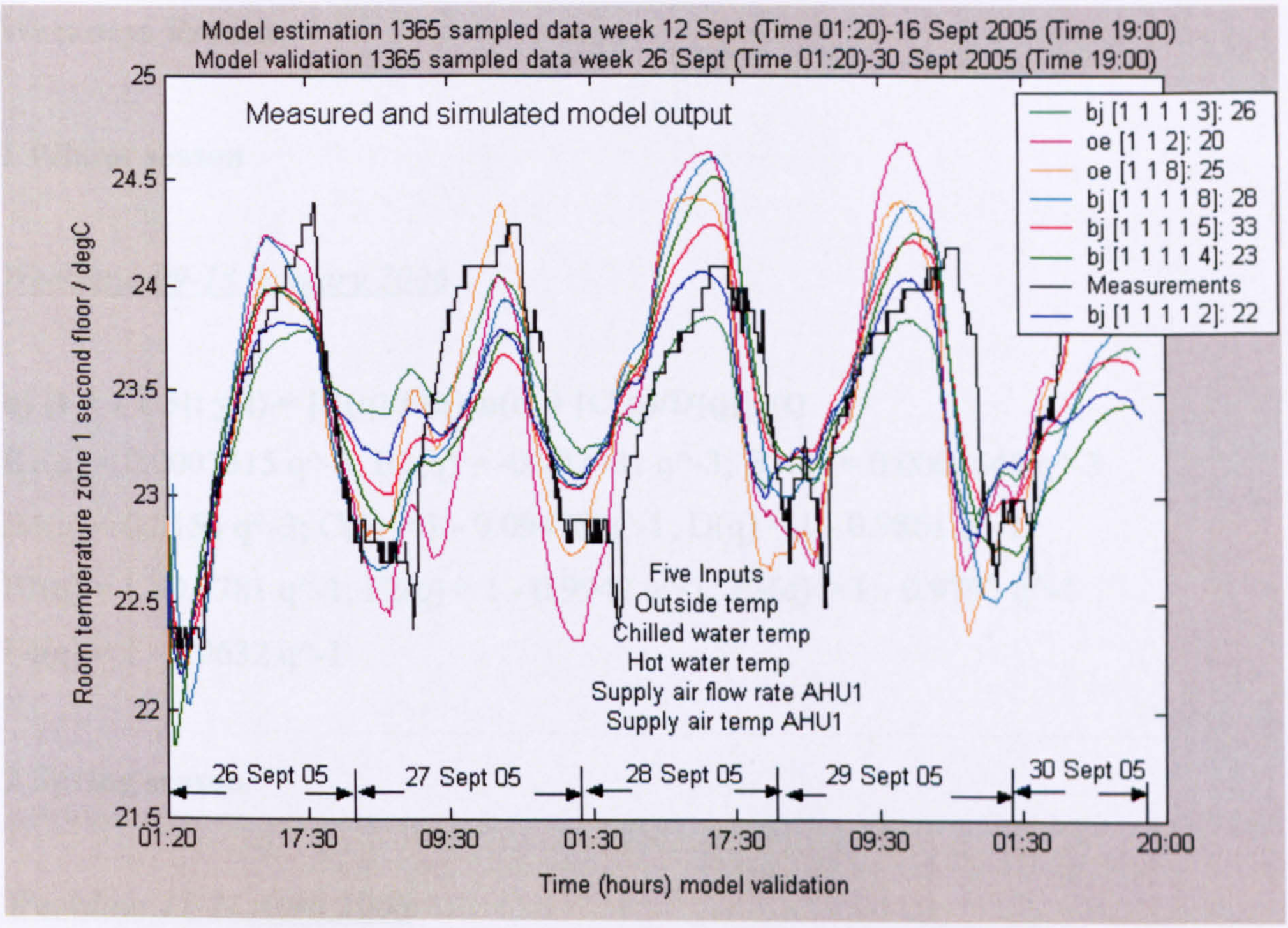

Figure 5.24 Model validation, weekdays 12-16 September 05 and 26-30 September 05

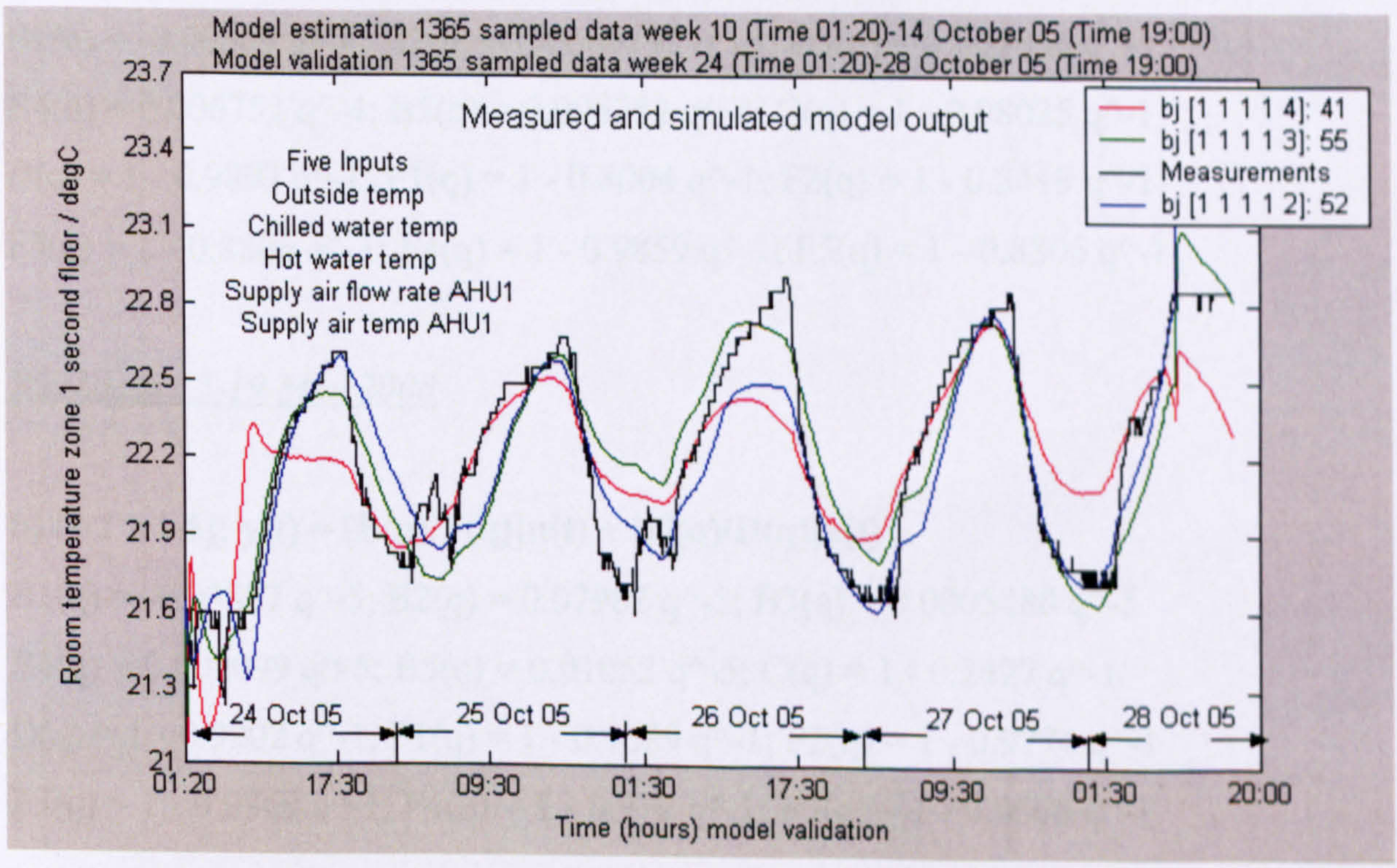

Figure 5.25 Model validation, weekdays 10-14 October 05 and 24-28 October 05

Appendix 2B Weekdays Results - Models Presentation Portman House Building

Weekdays Results

1 Winter season

Weekdays 09-13 January 2006

bj [1 1 1 1 3]: y(t) = [B(q)/F(q)]u(t) + [C(q)/D(q)]e(t)

B1(q) = 0.0007315 q^-3; B2(q) = -0.002481 q^-3; B3(q) = 0.0008548 q^-3

B4(q) = 0.0154 q^-3; C(q) = 1 - 0.09478 q^-1; D(q) = 1 - 0.9861 q^-1

F1(q) = 1 - 0.7781 q^-1; F2(q) = 1 - 0.9942 q^-1; F3(q) = 1 - 0.9793 q^-1

F4(q) = 1 - 0.9632 q^-1

2 Spring season

Weekdays 17-21 April 2006

bj [1 1 1 1 4]: y(t) = [B(q)/F(q)]u(t) + [C(q)/D(q)]e(t)

B1(q) = -0.00569 q^-4; B2(q) = 0.0009799 q^-4; B3(q) = 0.006836 q^-4

B4(q) = 0.006752 q^-4; B5(q) = 0.006752 q^-4; C(q) = 1 - 0.08025 q^-1

D(q) = 1 - 0.9892 q^-1; F1(q) = 1 - 0.8004 q^-1; F2(q) = 1 - 0.5419 q^-1

F3(q) = 1 - 0.8806 q^-1; F4(q) = 1 - 0.9859 q^-1; F5(q) = 1 - 0.8806 q^-1

Weekdays 15-19 May 2006

bj [1 1 1 1 5]: y(t) = [B(q)/F(q)]u(t) + [C(q)/D(q)]e(t)

B1(q) = -0.03887 q^-5; B2(q) = 0.07982 q^-5; B3(q) = 0.0005488 q^-5

B4(q) = 0.002099 q^-5; B5(q) = 0.01052 q^-5; C(q) = 1 - 0.2427 q^-1

D(q) = 1 - 0.9902 q^-1; F1(q) = 1 - 0.7089 q^-1; F2(q) = 1 - 0.9774 q^-1

F3(q) = 1 - 0.9869 q^-1; F4(q) = 1 - 0.972 q^-1; F5(q) = 1 - 0.9666 q^-1

3 Summer season

Weekdays 13-17 June 2005

bj [1 1 1 1 2]: y(t) = [B(q)/F(q)]u(t) + [C(q)/D(q)]e(t)

B1(q) = -0.03682 q^-2; B2(q) = -0.009268 q^-2; B3(q) = 6.073e-005 q^-2

B4(q) = 0.007348 q^-2; C(q) = 1 - 0.1457 q^-1; D(q) = 1 - 0.996 q^-1

F1(q) = 1 - 0.9165 q^-1; F2(q) = 1 - 1.001 q^-1

F3(q) = 1 - 1.007 q^-1; F4(q) = 1 - 0.916 q^-1

oe [1 1 2]: y(t) = [B(q)/F(q)]u(t) + e(t)

B1(q) = -0.02526 q^-2; B2(q) = 0.01979 q^-2; B3(q) = -0.02455 q^-2

B4(q) = 0.02721 q^-2; F1(q) = 1 - 0.985 q^-1; F2(q) = 1 + 0.8677 q^-1

F3(q) = 1 - 0.9152 q^-1; F4(q) = 1 - 0.6921 q^-1

4 Autumn season

Weekdays 24-28 October 2005

bj [1 1 1 1 5]: y(t) = [B(q)/F(q)]u(t) + [C(q)/D(q)]e(t)

B1(q) = 0.03861 q^-5; B2(q) = -0.0003461 q^-5 B3(q) = -0.000928 q^-5

B4(q) = -0.002189 q^-5; B5(q) = -0.00123 q^- 5; C(q) = 1 - 0.06846 q^-1

D(q) = 1 - 0.995 q^-1; F1(q) = 1 - 0.9842 q^-1

F2(q) = 1 - 0.9765 q^-1; F3(q) = 1 - 0.9962 q^-1

F4(q) = 1 - 0.9975 q^-1; F5(q) = 1 - 0.3572 q^-1

Appendix 3A Weekdays Results – Rockefeller Building

- One week (Monday Time 01:20 to Friday Time 19:00) sampled-data model estimation
- Following week (Monday Time 01:20 to Friday Time 19:00) sampled-data model validation

Summer season

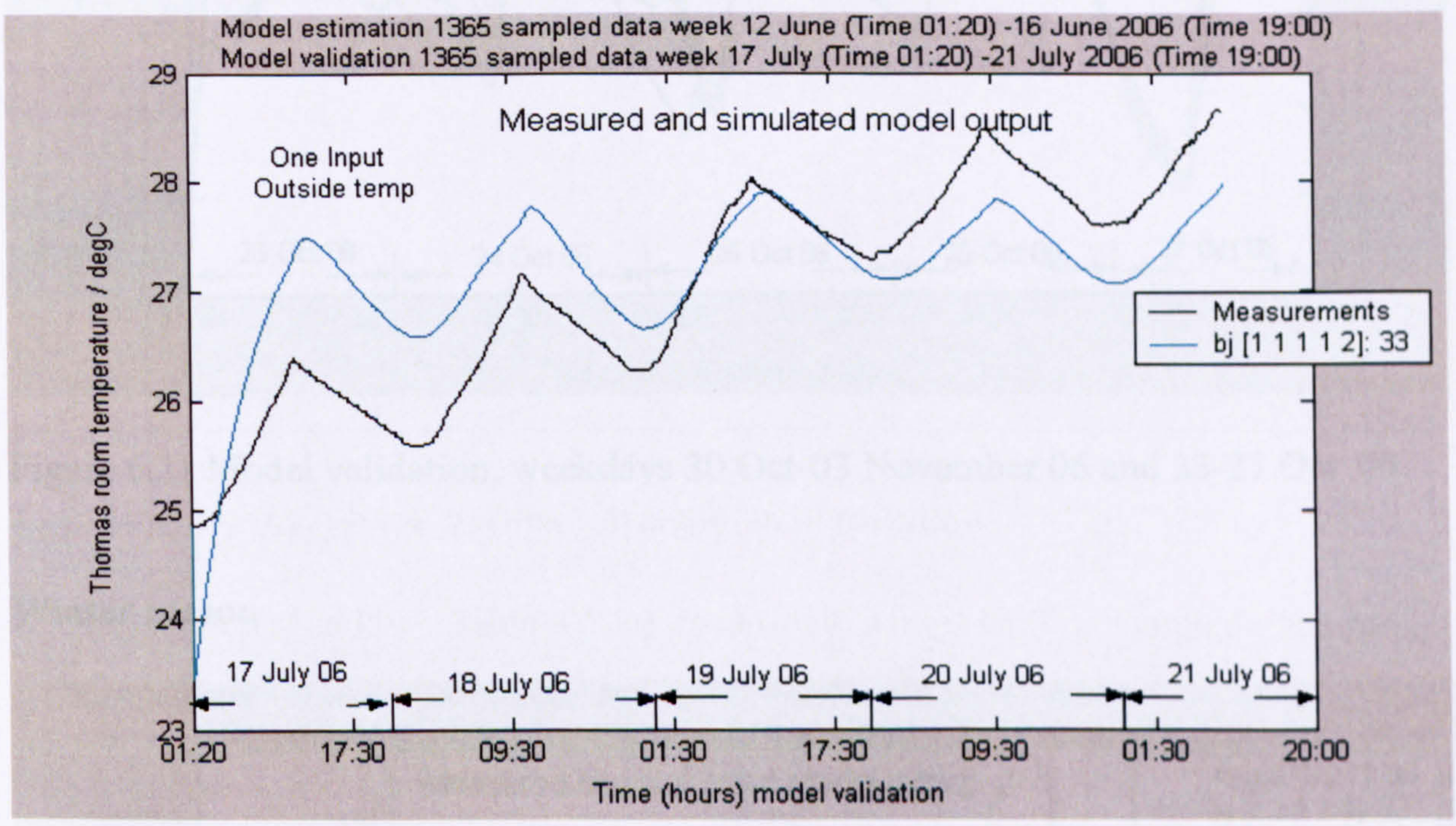

Figure 6.19 Model validation, weekdays 12-16 June 2006 and 17-21 July 2006

Autumn season

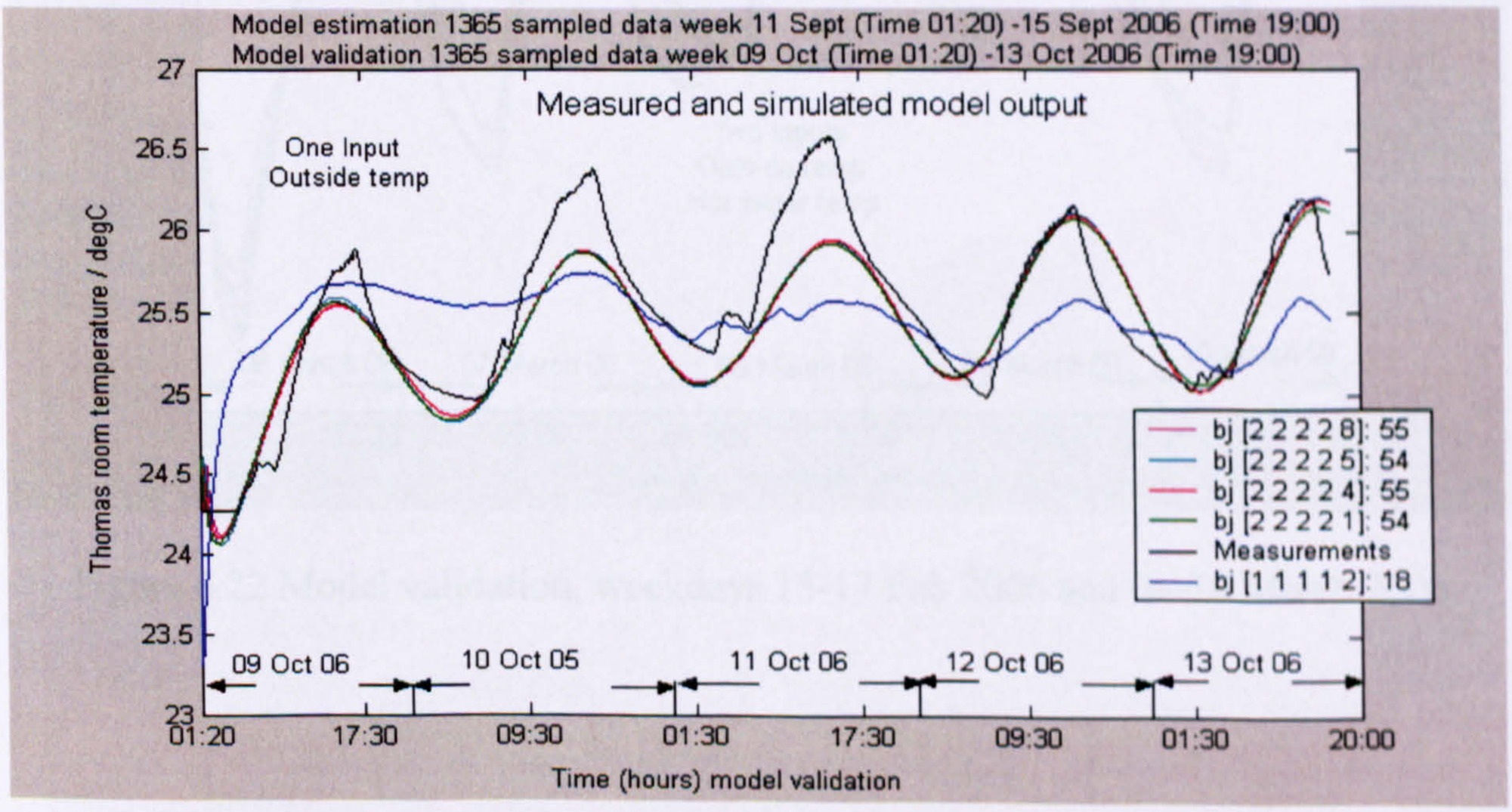

Figure 6.20 Model validation, weekdays 11-15 September 06 and 09-13 October 06

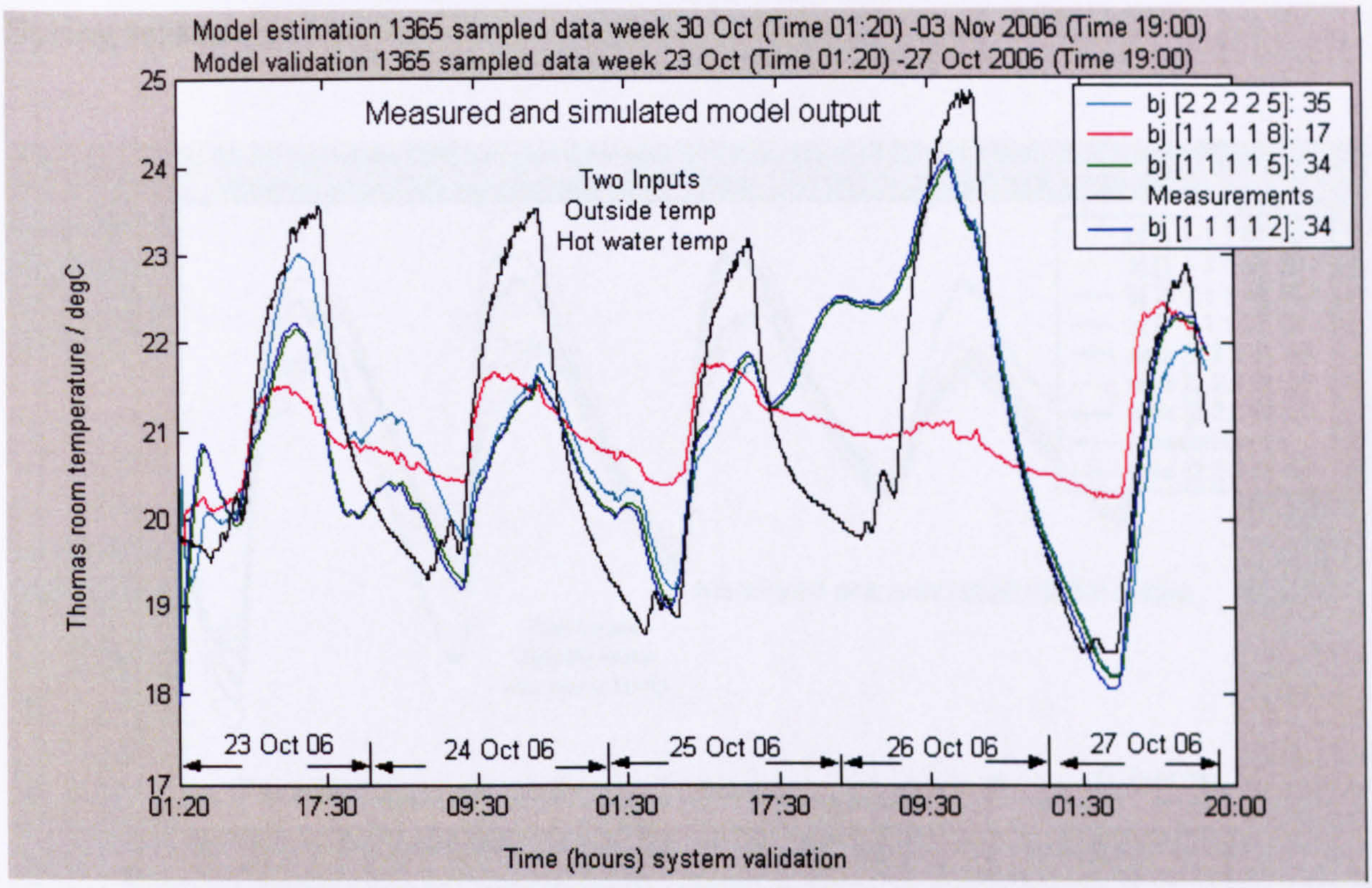

Figure 6.21 Model validation, weekdays 30 Oct-03 November 06 and 23-27 Oct 06

Winter season

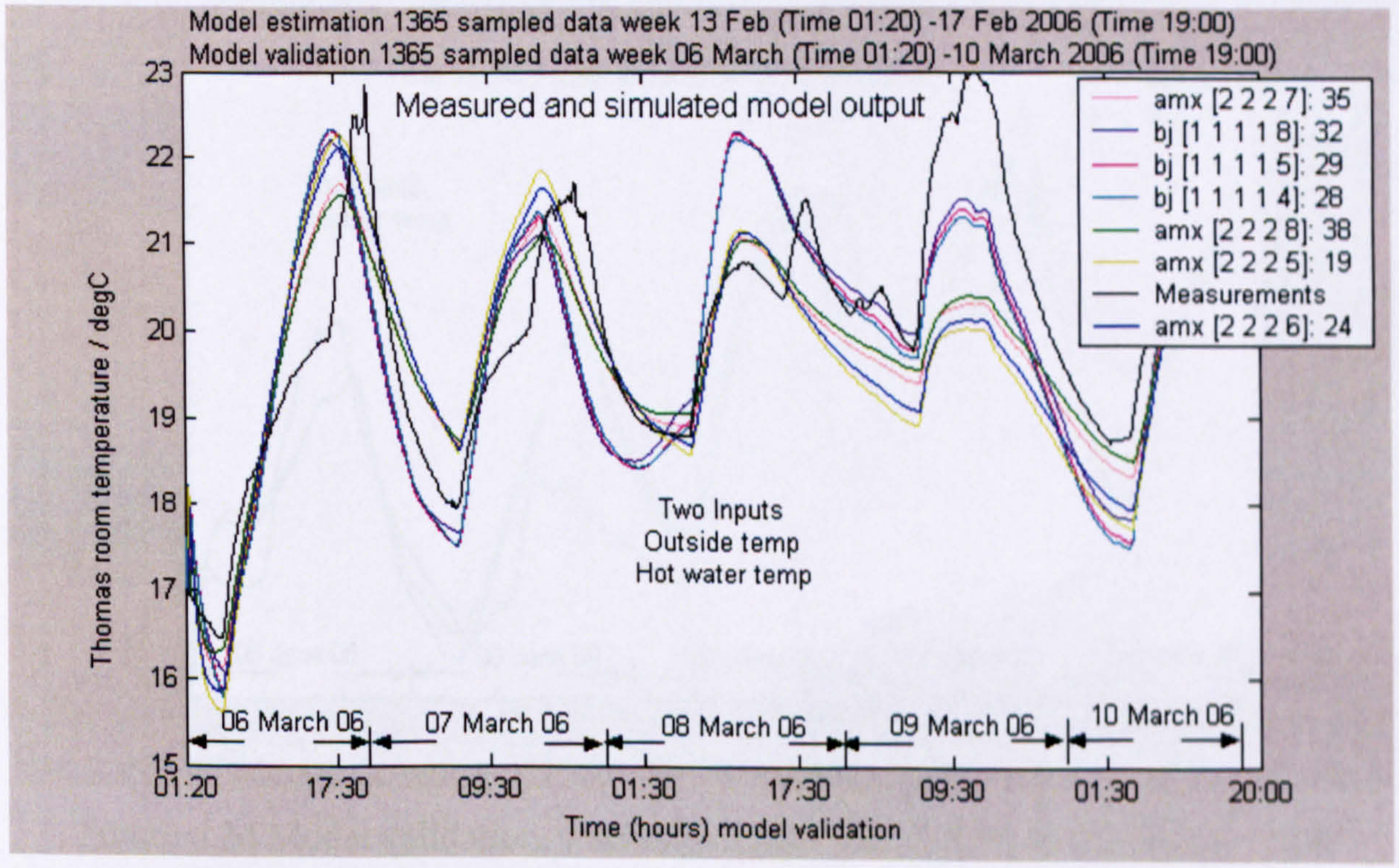

Figure 6.22 Model validation, weekdays 13-17 Feb 2006 and 06-10 March 2006

Spring season

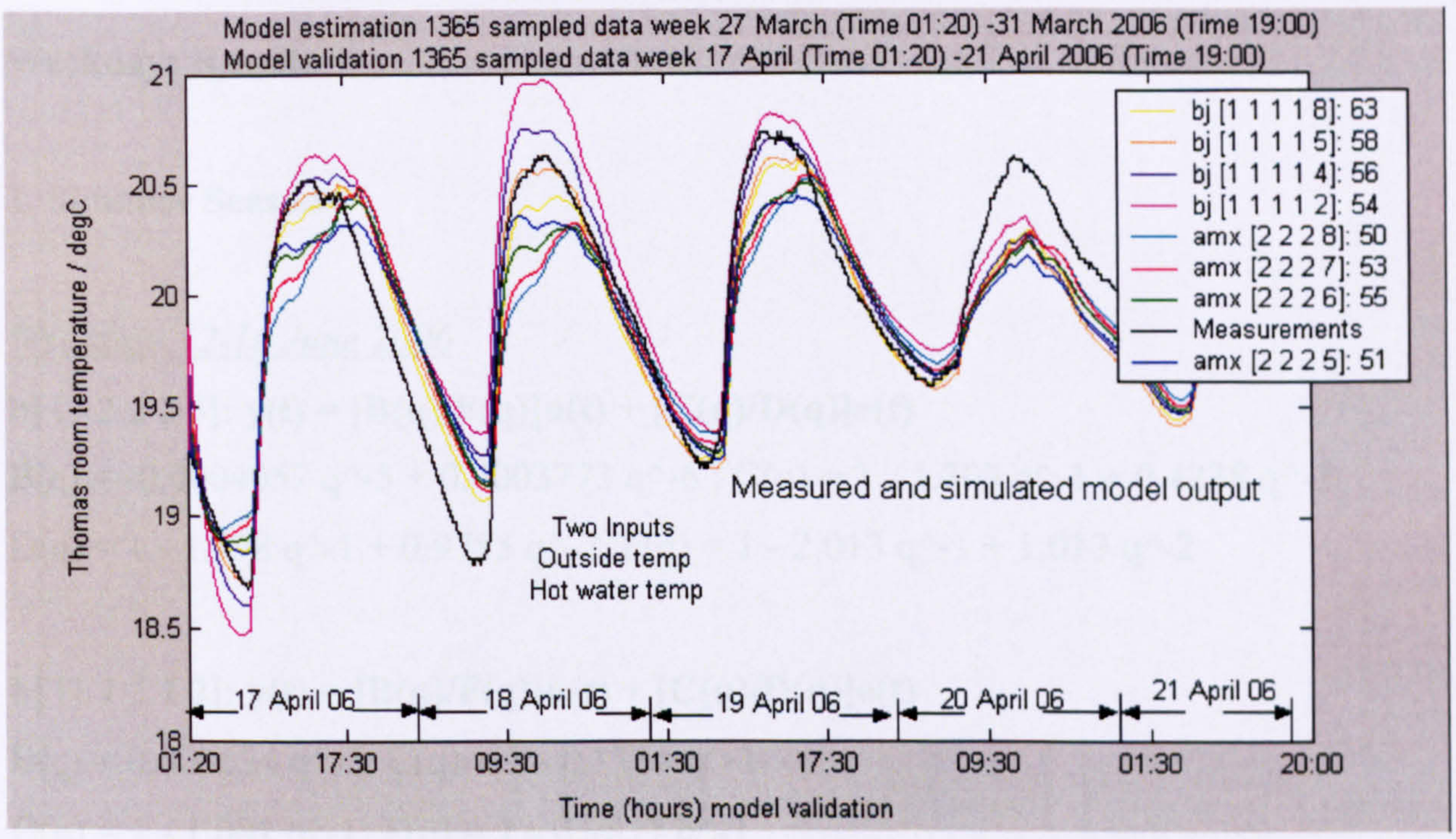

Figure 6.23 Model validation, weekdays 27-31 March 2006 and 17-21 April 2006

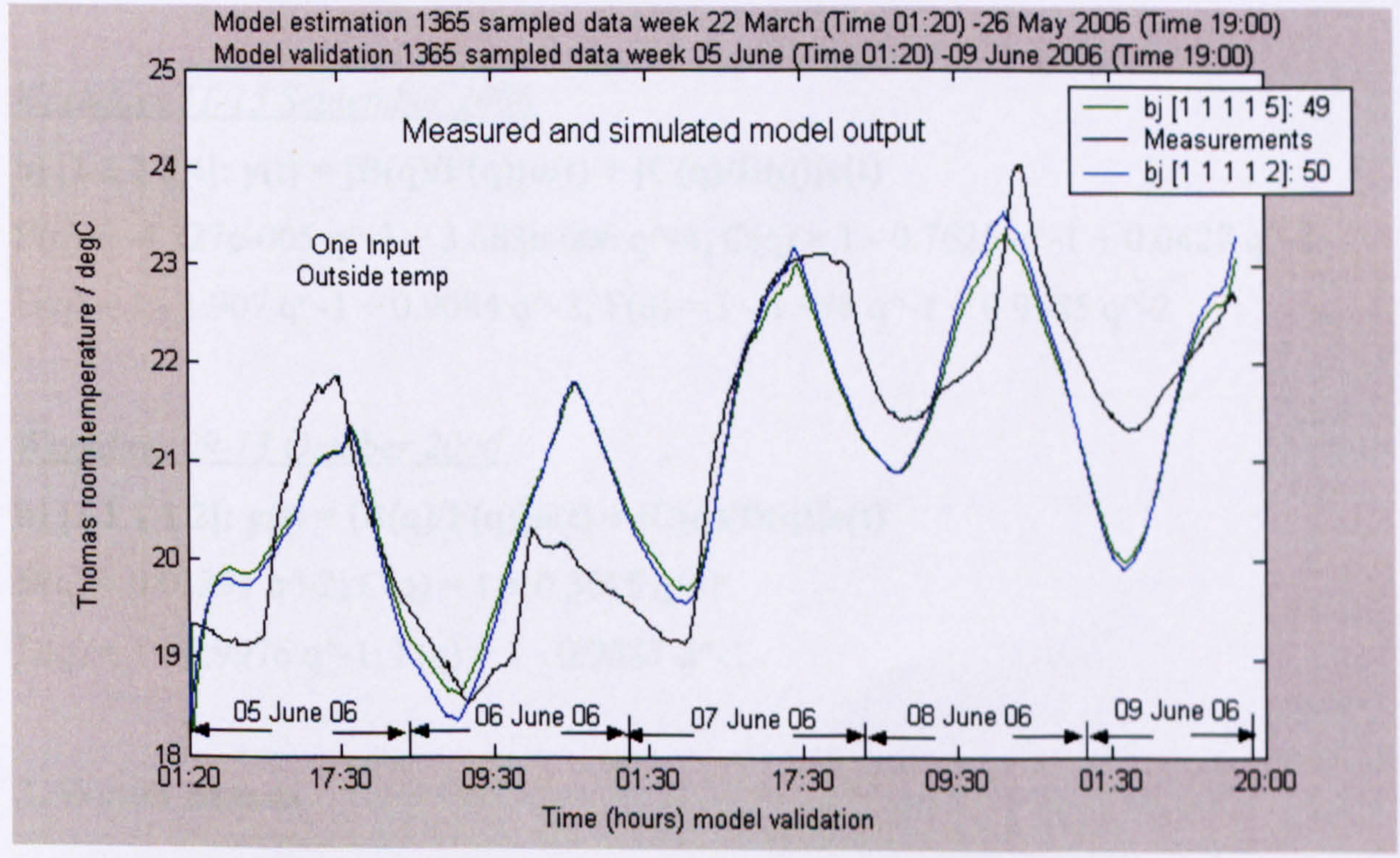

Figure 6.24 Model validation, weekdays 22-26 May 2006 and 05-09 June 2006

Appendix 3B Weekdays Results - Models Presentation Rockefeller Building

Weekdays Results

1. Summer Season

Weekdays 12-16 June 2006

bj [2 2 2 2 5]: y(t) = [B(q)/F(q)]u(t) + [C(q)/D(q)]e(t)

B(q) = -0.0004057 q^-5 + 0.0003773 q^-6 ; C(q) = 1 - 1.303 q^-1 + 0.4238 q^-2

D(q) = 1 - 1.978 q^-1 + 0.9785 q^-2, F(q) = 1 - 2.013 q^-1 + 1.013 q^-2

bj [1 1 1 1 2]: y(t) = [B(q)/F(q)]u(t) + [C(q)/D(q)]e(t)

B(q) = 0.001634 q^-2; C(q) = 1 - 0.1154 q^-1

D(q) = 1 - 1.001 q^-1; F(q) = 1 - 0.9877 q^-1

2. Autumn Season

Weekdays 11-15 September 2006

bj [2 2 2 2 4]: y(t) = [B(q)/F(q)]u(t) + [C(q)/D(q)]e(t)

B(q) = -4.227e-005 q^-3 + 3.683e-006 q^-4; C(q) = 1 - 0.7625 q^-1 + 0.0427 q^-2

D(q) = 1 - 1.907 q^-1 + 0.9084 q^-2; F(q) = 1 - 1.998 q^-1 + 0.9985 q^-2

Weekdays 09-13 October 2006

bj [1 1 1 1 2]: y(t) = [B(q)/F(q)]u(t) + [C(q)/D(q)]e(t)

B(q) = 0.01291 q^-2; C(q) = 1 + 0.3015 q^-1

D(q) = 1 - 0.9976 q^-1; F(q) = 1 - 0.9587 q^-1

3. Winter Season

Weekdays 13-17 February 2006

amx [2 2 2 8]: A(q)y(t) = B(q)u(t) + C(q)e(t)

A(q) = 1 - 1.903 q^-1 + 0.9036 q^-2; B1(q) = 0.009897 q^-8 - 0.00979 q^-9

B2(q) = 0.0008419 q^-8 - 0.0007356 q^-9; C(q) = 1 - 0.5634 q^-1 + 0.03532 q^-2

4. Spring Season

Weekdays 27-31 March 2006

amx [2 2 2 8]: A(q)y(t) = B(q)u(t) + C(q)e(t)

A(q) = 1 - 1.898 q^-1 + 0.899 q^-2; B1(q) = 0.003587 q^-8 - 0.003319 q^-9

B2(q) = 0.001143 q^-8 - 0.001082 q^-9; C(q) = 1 - 0.9978 q^-1 + 0.2371 q^-2

bj [1 1 1 1 3]: y(t) = [B(q)/F(q)]u(t) + [C(q)/D(q)]e(t)

B1(q) = 0.00483 q^-3; B2(q) = 0.001389 q^-3

C(q) = 1 - 0.1261 q^-1; D(q) = 1 - 0.9989 q^-1

F1(q) = 1 + 0.755 q^-1; F2(q) = 1 - 0.992 q^-1

Weekdays 01-05 May 2006

bj [1 1 1 1 5]: y(t) = [B(q)/F(q)]u(t) + [C(q)/D(q)]e(t)

B1(q) = 0.01129 q^-5; B2(q) = 0.002186 q^-5

C(q) = 1 + 0.2754 q^-1; D(q) = 1 - 0.999 q^-1

F1(q) = 1 - 0.9445 q^-1; F2(q) = 1 - 0.9708 q^-1

Black-box linear parametric mathematical models - orders and delays description

ARMAX models

- Four inputs
  - amx[2 2 2 1]: $na = 2$, $nb = [2\ 2\ 2\ 2]$, $nc = 2$, $nk = [1\ 1\ 1\ 1]$
- Two inputs
  - amx2226: $na = 2$, $nb = [2\ 2]$, $nc = 2$, $nk = [6\ 6]$
  - amx2227: $na = 2$, $nb = [2\ 2]$, $nc = 2$, $nk = [7\ 7]$
  - amx2228: $na = 2$, $nb = [2\ 2]$, $nc = 2$, $nk = [8\ 8]$
- One input
  - amx[2 2 2 1]: $na = 2$, $nb = 2$, $nc = 2$, $nk = 1$
  - amx[1 1 1 2]: $na = 1$, $nb = 1$, $nc = 1$, $nk = 2$

BJ models

- Five inputs
  - bj[1 1 1 1 2]: $nb = [1\ 1\ 1\ 1\ 1]$, $nc = 1$, $nd = 1$, $nf = [1\ 1\ 1\ 1\ 1]$, $nk = [2\ 2\ 2\ 2\ 2]$
  - bj[1 1 1 1 3]: $nb = [1\ 1\ 1\ 1\ 1]$, $nc = 1$, $nd = 1$, $nf = [1\ 1\ 1\ 1\ 1]$, $nk = [3\ 3\ 3\ 3\ 3]$
  - bj[1 1 1 1 4]: $nb = [1\ 1\ 1\ 1\ 1]$, $nc = 1$, $nd = 1$, $nf = [1\ 1\ 1\ 1\ 1]$, $nk = [4\ 4\ 4\ 4\ 4]$
  - bj[1 1 1 1 5]: $nb = [1\ 1\ 1\ 1\ 1]$, $nc = 1$, $nd = 1$, $nf = [1\ 1\ 1\ 1\ 1]$, $nk = [5\ 5\ 5\ 5\ 5]$
- Four inputs
  - bj[1 1 1 1 2]: $nb = [1\ 1\ 1\ 1]$, $nc = 1$, $nd = 1$, $nf = [1\ 1\ 1\ 1]$, $nk = [2\ 2\ 2\ 2]$
  - bj[1 1 1 1 3]: $nb = [1\ 1\ 1\ 1]$, $nc = 1$, $nd = 1$, $nf = [1\ 1\ 1\ 1]$, $nk = [3\ 3\ 3\ 3]$
  - bj[1 1 1 1 4]: $nb = [1\ 1\ 1\ 1]$, $nc = 1$, $nd = 1$, $nf = [1\ 1\ 1\ 1]$, $nk = [4\ 4\ 4\ 4]$
  - bj[1 1 1 1 5]: $nb = [1\ 1\ 1\ 1]$, $nc = 1$, $nd = 1$, $nf = [1\ 1\ 1\ 1]$, $nk = [5\ 5\ 5\ 5]$
  - bj[1 1 1 1 8]: $nb = [1\ 1\ 1\ 1]$, $nc = 1$, $nd = 1$, $nf = [1\ 1\ 1\ 1]$, $nk = [5\ 5\ 5\ 8]$
- Two inputs
  - bj[2 2 2 2 4]: $nb = [2\ 2]$, $nc = 2$, $nd = 2$, $nf = [2\ 2]$, $nk = [4\ 4]$
  - bj[1 1 1 1 2]: $nb = [1\ 1]$, $nc = 1$, $nd = 1$, $nf = [1\ 1]$, $nk = [2\ 2]$
  - bj[1 1 1 1 3]: $nb = [1\ 1]$, $nc = 1$, $nd = 1$, $nf = [1\ 1]$, $nk = [3\ 3]$
  - bj[1 1 1 1 4]: $nb = [1\ 1]$, $nc = 1$, $nd = 1$, $nf = [1\ 1]$, $nk = [4\ 4]$
  - bj[1 1 1 1 5]: $nb = [1\ 1]$, $nc = 1$, $nd = 1$, $nf = [1\ 1]$, $nk = [5\ 5]$
  - bj[1 1 1 1 7]: $nb = [1\ 1]$, $nc = 1$, $nd = 1$, $nf = [1\ 1]$, $nk = [7\ 7]$
  - bj[1 1 1 1 8]: $nb = [1\ 1]$, $nc = 1$, $nd = 1$, $nf = [1\ 1]$, $nk = [8\ 8]$

- One input
  - bj[2 2 2 2 5]: $nb = 2, nc = 2, nd = 2, nf = 2, nk = 5$
  - bj[2 2 2 2 4]: $nb = 2, nc = 2, nd = 2, nf = 2, nk = 4$
  - bj[2 2 2 2 1]: $nb = 2, nc = 2, nd = 2, nf = 2, nk = 1$
  - bj[1 1 1 1 2]: $nb = 1, nc = 1, nd = 1, nf = 1, nk = 2$
  - bj[1 1 1 1 5]: $nb = 1, nc = 1, nd = 1, nf = 1, nk = 5$
  - bj[1 1 1 1 6]: $nb = 1, nc = 1, nd = 1, nf = 1, nk = 6$
  - bj[1 1 1 1 7]: $nb = 1, nc = 1, nd = 1, nf = 1, nk = 7$
  - bj[1 1 1 1 8]: $nb = 1, nc = 1, nd = 1, nf = 1, nk = 8$

OE models

- Five inputs
  - oe[1 1 2]: $nb = [1\ 1\ 1\ 1\ 1], nf = [1\ 1\ 1\ 1\ 1], nk = [2\ 2\ 2\ 2\ 2]$
  - oe[1 1 3]: $nb = [1\ 1\ 1\ 1\ 1], nf = [1\ 1\ 1\ 1\ 1], nk = [3\ 3\ 3\ 3\ 3]$
- Four inputs
  - oe[1 1 2]: $nb = [1\ 1\ 1\ 1], nf = [1\ 1\ 1\ 1], nk = [2\ 2\ 2\ 2]$
  - oe[1 1 3]: $nb = [1\ 1\ 1\ 1], nf = [1\ 1\ 1\ 1], nk = [3\ 3\ 3\ 3]$
  - oe[1 1 3]: $nb = [1\ 1\ 1\ 1], nf = [1\ 1\ 1\ 1], nk = [3\ 3\ 3\ 3]$
  - oe[1 1 4]: $nb = [1\ 1\ 1\ 1], nf = [1\ 1\ 1\ 1], nk = [4\ 4\ 4\ 4]$
  - oe[1 1 5]: $nb = [1\ 1\ 1\ 1], nf = [1\ 1\ 1\ 1], nk = [5\ 5\ 5\ 5]$